Online ISSN: 1920-3853

Vol. 6, No. 1, Feb 2012

Print ISSN : 1715-9997

Canadian Journal of pure & applied sciences

an International Journal

SENRA

Academic Publishers

Burnaby, British Columbia

The Canadian Journal of Pure and Applied Sciences (CJPAS-ISSN 1715-9997) is a peer reviewed multi-disciplinary specialist journal aimed at promoting research worldwide in Agricultural Sciences, Biological Sciences, Chemical Sciences, Computer and Mathematical Sciences, Engineering, Environmental Sciences, Medicine and Physics (all subjects).

CJPAS is Abstracted/Indexed in:
EBSCO, Ulrich's Periodicals Directory, Scirus, CiteSeerX, Index Copernicus, Directory of Open Access Journals, Google Scholar, CABI, Chemical Abstracts, Zoological Records, Biblioteca Central, The Intute Consortium, WorldCat. CJPAS has received Index Copernicus Journals Evaluation for 2010 = 4.98

Editorial Office
E-mail: editor@cjpas.ca
: editor@cjpas.net

SENRA Academic Publishers
7845 15th Street Burnaby
British Columbia V3N 3A3 Canada
www.cjpas.net
E-mail: senra@cjpas.ca

Print ISSN 1715-9997
Online ISSN 1920-3853

Volume 6, Number 1
Feb 2012

CANADIAN JOURNAL OF PURE AND APPLIED SCIENCES

Board of Editorial Advisors

Canadian Journal of pure&applied sciences

Volume 6, Number 1
February 2012

CONTENTS

SHORT COMMUNICATIONS

SENRA Academic Publishers, Burnaby, British Columbia
Vol. 6, No. 1, pp. 1733-1737, Feb 2012
Online ISSN: 1920-3853; Print ISSN: 1715-9997

Canadian Journal of pure&applied sciences

FLUORESCENT COMPOUND FORMED IN AND EFFLUX FROM YEAST CELLS STUDIED ON A FLOW CYTOMETRY MICROCHIP

Wilson Chim, Michael CK Wong and *Paul CH Li
Department of Chemistry, Simon Fraser University
8888 University Drive, Burnaby, BC V5A 1S6, Canada

ABSTRACT

This paper describes an easy and simple method to perform yeast cell experiment on a flow cytometry chip. We are able to observe the influx-hydrolysis-efflux phenomenon of a fluorogenic substrate on yeast cells. As a study model, the fluorogenic substrate fluorescein diacetate (FDA) diffused into the yeast cell, and FDA was hydrolyzed in the cytosol to produce fluorescein. Then, fluorescein was effluxed from the yeast cell.

Keywords: Microfluidic Flow Assay Chip, Flow cytometry, Baker's Yeast, Fluorescein Acetate.

INTRODUCTION

In recent years, microfluidic lab-on-a-chip has widely been applied for biochemical analysis (Auroux *et al*., 2002; Landers, 2003; Li, 2010). In particular, various microchip techniques for cellular biochemical analysis have been developed recently (Gao *et al*., 2004; Li *et al*., 2008). For example, microchips have been used to study the intracellular activities of cancer cells (Li *et al*., 2009; Li *et al*., 2011).

Most cell studies were performed on groups of cells and only few studies were performed on a single cell (Roper *et al*., 2003; Li and Li, 2005a; Li and Li, 2005b; Li *et al*., 2007). Although it is useful to conduct single-cell experiments to elucidate cellular variations, it is easier to study a group of cells and when there is a need to understand cell-to-cell interactions.

For on-chip experiments, transport and selection of cells have been mainly achieved by liquid flow (Wheeler *et al*., 2003; Li *et al*., 2004). The flow cytometry chip is used to measure the selected characteristics of individual cells by determining fluorescence emission at wavelengths of interest (Breeuwer *et al*., 1995; Wittrup and Bailey, 1990).

In this study, a microfluidic cell chip (Fig. 1) is used in a commercial Bioanalyzer to perform a simple and fast flow cytometry experiment on yeast cells. The use of the chip saves money because less reagents and samples are used (Mitchell, 2011). Furthermore, it is easy to prepare the chip for experiments, and the results can quickly (in less than 30 minutes) and clearly are seen.

As a study model of a yeast metabolic process, a cell-permeable fluorogenic substrate fluorescein diacetate (FDA), normally used to determine cell viability (Jones and Senft, 1985), diffused into the yeast cell (Fig. 2A). FDA was then metabolized by a carboxylesterase (Degrassi *et al*., 1999) intracellularly to produce fluorescein (Fig. 2B). Then, fluorescein effluxed from the cell (Figs. 2C and 2D).

The movement of cells in the cell chip is controlled by a pressure-driven flow inside the interconnected networks of microfluidic channels. Cells are hydrodynamically focused in these channels before passing the fluorescence detector in single file.

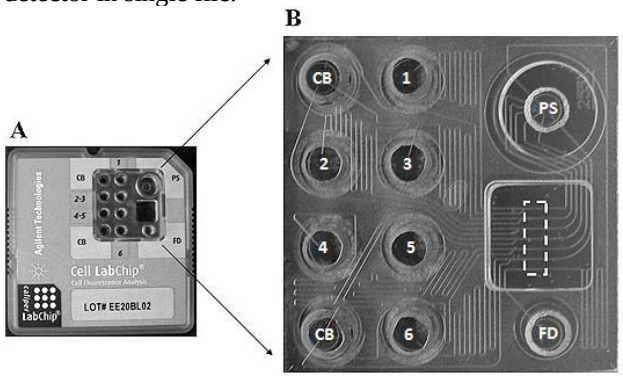

Fig. 1. Microfluidic cell chip is fixed in a plastic caddy for use in a commercial Bioanalyzer. The chip contains six sample wells (1-6), two cell buffer wells (CB), one well for a reference dye (FD), and one well for a vacuum interface and collection of the fluid waste (PS). A common buffer channel joins each sample channel in close proximity to the detection area (broken line box). Reprinted with permission from Elsevier Science (Kataoka *et al*., 2005).

The chip allows up to six cell samples to be analyzed and the cells are measured sequentially for 4 minutes each. For each event, the intensities of the red and blue

*Corresponding author email: paulli@sfu.ca

fluorescent signals are recorded. The red light excitation is at 630 nm and emission is at 680 nm. The blue light excitation is at 470 nm and green emission is at 525 nm. The intensity of the fluorescent signal depends on the amount of fluorescent molecules present in the cell. The detector will collect the data and present them as dot plots and histograms (Nitsche, 2001).

MATERIALS AND METHODS

Preparation of FDA solution

2.5 mg of fluorescein diacetate (Sigma-Aldrich) was mixed with 500 µL of DMSO (Sigma-Aldrich, mol. biology grade) to make a stock solution of FDA. This solution was stored at -20°C and protected from light, as reported previously (Peng and Li, 2004a; Peng and Li, 2004b). A working FDA solution of 12 µM was prepared when needed.

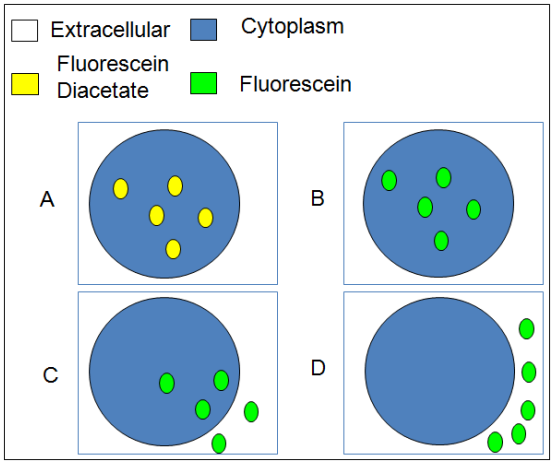

Fig. 2. A schematic diagram showing the fluorescent compound formed in a yeast cell and effluxed from it. A) fluorescein diacetate in the cell. B) fluorescein formed in the cell. C) Continuous efflux of fluorescein from the cell. D) Complete efflux of all fluorescein molecules.

Preparation of chip reagents

According to the vendor's protocol, the Cell Kit which contained the priming solution, the focusing dye, the cell buffer, and bead sample and FDA solution, were protected from light and equilibrated at room temperature for 30 min. before use. The bead vial was then vortexed for 15 s to resuspend the beads. Then, 95 µL of cell buffer were mixed with 5 µL of beads in a 0.5 mL microcentrifuge tube.

Preparation of the Cell Chip

On the glass cell chip, 10 µL of priming solution was added first in the well labelled PS. The priming solution filled the entire channel and displaced all the air in the microchannels after 1 min. The yeast solution and yeast-FDA solution were then quickly prepared (as described in detail in the next section) for sample wells 1-5. Yeast solution B (10 µL) was added to well sample 5 as the negative control. Then, 10 µL of yeast-FDA solution C was pipetted each to wells 1-4.

Then, 10 µL of focusing dye was added to the well labelled FC. This solution was used by the instrument to optically focus the detector on the channel. Buffer solution (30 µL) was then added to each of the wells labelled CB. This solution was used to hydrodynamically focus and align the cells before they passed the detection point. Lastly, 10 µL of bead solution (positive control) was pipetted to well sample 6. The chip was loaded onto the Bioanalyzer to initiate the flow cytometry experiment. After ~25 min., the experiment was completed and the results were presented either as dot plots or histograms. If the chip is needed to be reused, it will be cleaned as described previously (Chim and Li, 2012).

Preparation of Yeast and Yeast-FDA Solution

Baker's yeast (0.001 g) was mixed with 1000 µL of distilled water (solution A). 100 µL of solution A was diluted with 900 µL distilled water to give solution B (yeast-only solution), which was pipetted to sample well 5. Then, solution B was mixed with 1 µL of FDA solution to make solution C (yeast-FDA solution), which was pipetted to sample wells 1-4. Cell density for each of the solution B and C was ~1.25 x 10^6 cells per mL. All solutions were prepared at room temperature right after the channel priming step was completed.

RESULTS AND DISCUSSION

In figure 3, there are 2 dot plots on the left (a, c) which show red fluorescence intensity vs. the blue fluorescence intensity of the 2 types of particles (yeast cells and beads). The beads show high fluorescent intensity in the level of 10^2-10^3. The unstained yeast cells show the intensity below 10^0. As no red fluorescent molecules were present in the beads and cells, the intensities were all below 10^{-1}. There are 2 histograms on the right (b, d) which show the number of particles (events) vs. the fluorescence intensity. When there are fluorescein molecules inside the cell, the data from the cell would have fluorescence intensity greater than 10^0. An increase in the number of fluorescein molecules inside the cell would increase the fluorescence intensity.

Figures 3a and b are negative controls which are yeast cells without FDA. Both figures show there are no data above the fluorescent intensity of 10^0 which means there is no fluorescein molecule inside the cell. Figure 3c and d are positive controls which are the beads. Both figures show there are data above the fluorescent intensity of 10^0 which means there are fluorescein molecules inside the cell.

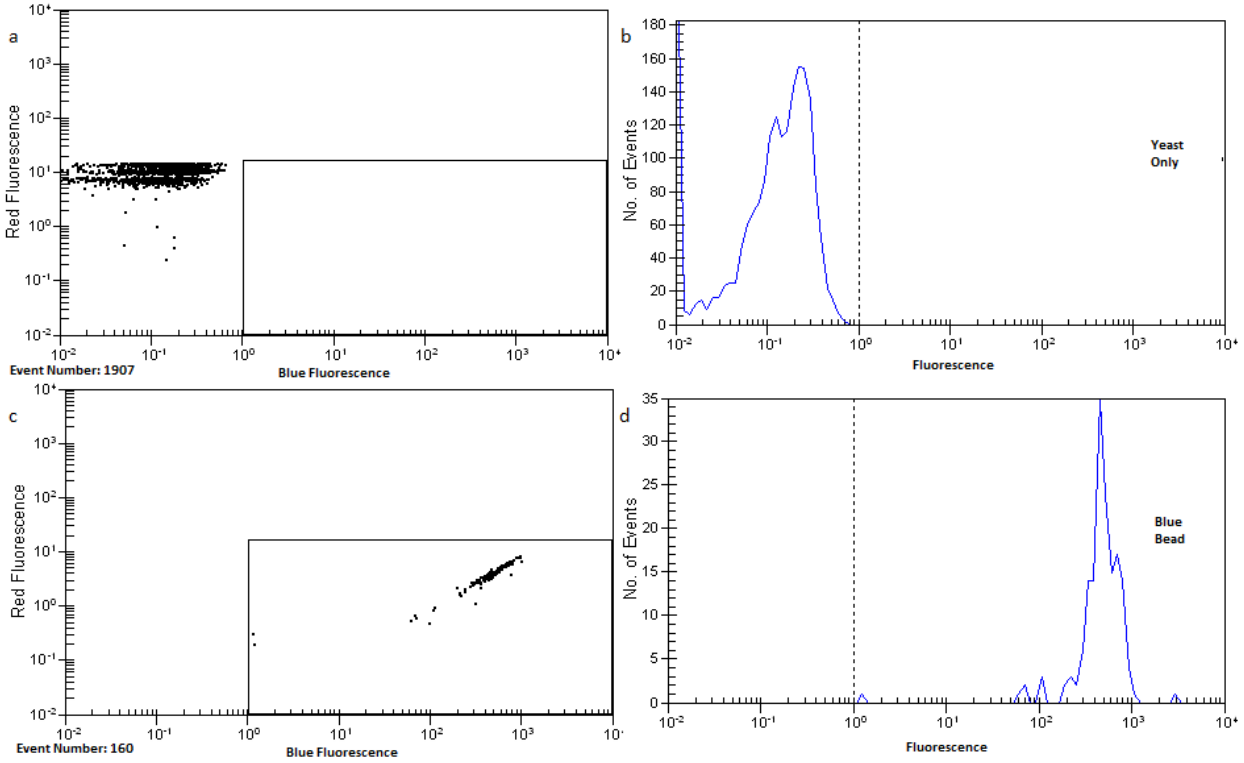

Fig. 3. Data of the negative control (unstained yeast cells) in (a) dot plot and (b) histogram, and the positive control (blue beads) in (c) dot plot and (d) histogram. The dot plots show the red fluorescence versus the blue fluorescence (should be green emission when excited in blue). The histograms show the number of events or cells versus the level of fluorescent emission only excited in blue.

The Bioanalyzer detected cells from each sample wells consecutively for 4 min. while a constant flow of cells was maintained in all channels. In figure 4, it shows the histogram of FDA-yeast cell collected consecutively every 4 min. In the cases of (a) 0-4 min. and (b) 4-8 min., the fluorescent intensity is higher than 10^0. When compared with the unstained cells, we know these cells are stained. However, from 8-12 min. (c) we begin to see fluorescent intensity lower than 10^0 which indicate the presence of an increasing number of unstained cells. Then from 12-16 min. (d), we only see unstained cells with fluorescent intensity lower than 10^0.

In order for the yeast cells to hydrolyze FDA to give fluorescein, the cell must have activated carboxylesterase. This intracellular enzyme broke the ester bond in FDA and released fluorescein, however, after a few min., some of the yeast cells started to pump fluorescein out of the cell. Moreover, some yeast cells produced more fluorescein as seen at 8-12 min. After a few minutes, all of the fluorescein inside the cells was pumped out by efflux as seen at 12-16 min. This is consistent with the time scale reported previously (Peng and Li, 2004b).

Results are also summarized in figure 5. There was no staining in the negative control and there was 100% staining in the positive control. At 0-4 min. and 4-8 min., the % stained cells are similar to that of the positive control, which indicates all the yeast cells are stained. At 8-12 min. there are both stained cells and unstained cells, resulting from the efflux of fluorescein from yeast cells. At 12-16 min., the histogram is similar to that of the negative control, which is resulted from complete fluorescein efflux .

CONCLUSION

This paper shows a simple flow cytometry experiment using readily obtained Baker's yeast. We also observed the influx-hydrolysis-efflux phenomenon of the fluorogenic substrate on yeast cells. This experiment can be completed in less than an hour, which saves time. Furthermore, it requires less samples and reagents, which save money. These experiments can be extended to measure multidrug resistance in cancer cells due to efflux, with proper biosafety precautions of working with cancer cell samples.

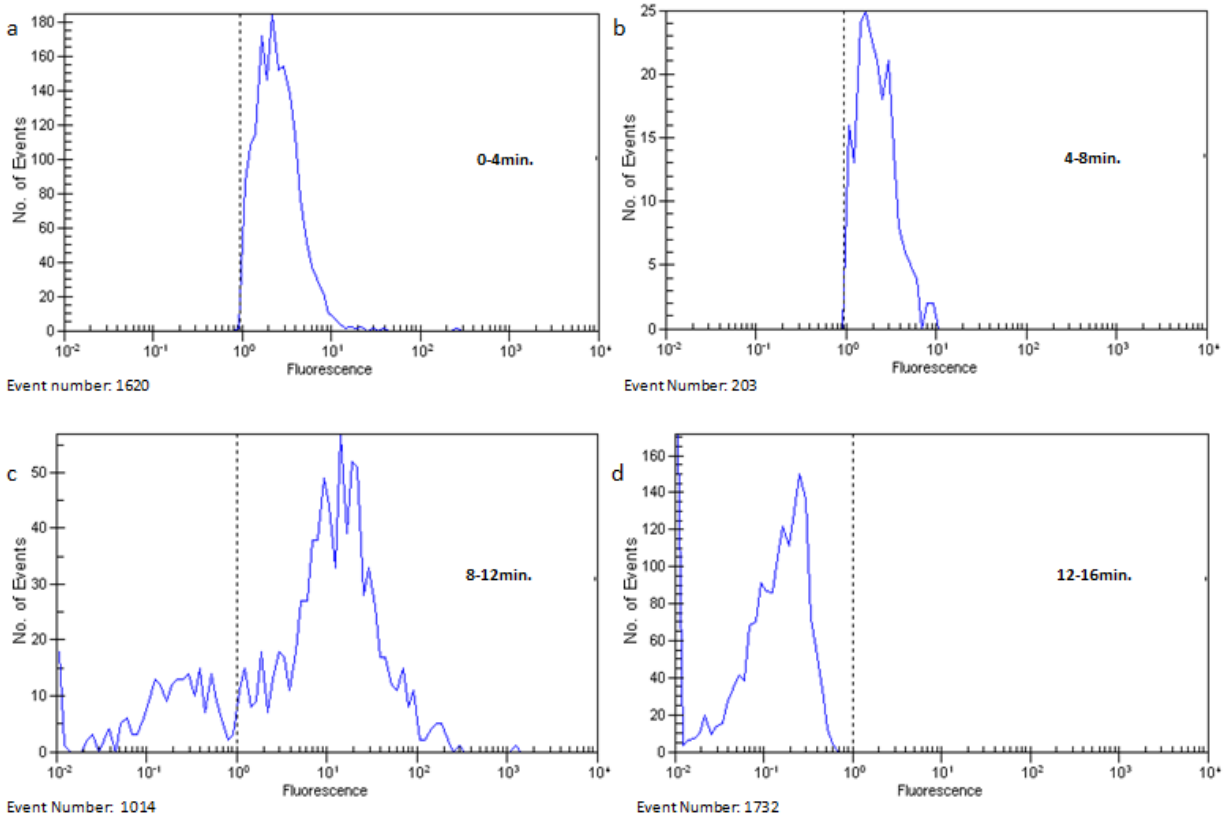

Fig. 4. The histograms of the influx-hydrolysis-efflux process in yeast cells. The data show the number of events versus the fluorescence intensity. The dotted line at 10^0 indicates the threshold level for stained cells to be recorded.

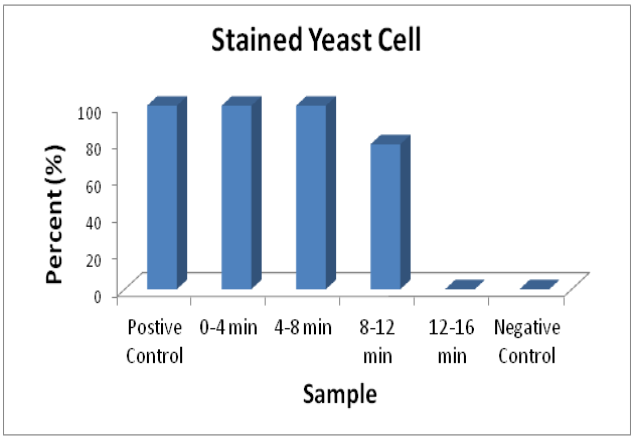

Fig. 5. The graph shows the percentage of stained yeast cells, as compared to the positive (beads) and negative (yeast cell only) control.

ACKNOWLEDGEMENT

We are grateful to Stephanie Howes (K' Technologies) for instrument training. Moreover, funding from NSERC URA is gratefully acknowledged.

REFERENCES

Auroux, PA., Lossifidis, D., Reyes, DR. and Manz, A. 2002. Micro Total Analysis Systems. 2. Analytical Standard Operations and Applications. Analytical Chemistry. 74:2637-2652.

Breeuwer, P., Drocourt, JL., Bunschoten, N., Zwietering, MH., Rombouts, FM. and Abee, T. 1995. Characterization of uptake and hydrolysis of fluorescein diacetate and carboxyfluorescein diacetate by intracellular esterases in Saccharomyces cerevisiae, which result in accumulation of fluorescent product. Applied Environmental Microbiology. 61:1614-1619.

Chim, W. and Li, PCH. 2012. Repeated Capillary Electrophoresis Separations conducted on a commercial DNA Chip. Analytical Methods. (In press).

Degrassi, G., Uotila, L., Klima, R. and Venturi, V.1999. Purification and Properties of an Esterase from the Yeast Saccharomyces cerevisiae and Identification of the Encoding Gene. Applied Environmental Microbiology. 65:3470-3472.

Gao, J., Yin., XF. and Fang, ZL. 2004. Integration of single cell injection, cell lysis, separation and detection of intracellular constituents on a microfluidic chip. Lab Chip. 4:47-52.

Jones, KH. and Senft, JAJ. 1985. An improved method to determine cell viability by simultaneous staining with fluorescein diacetate-propidium iodide. Histochemistry and Cytochemistry. 33:77-79.

Kataoka, M., Fukura, Y., Shinohara, Y. and Baba, Y. 2005. Analysis of mitochondrial membrane potential in the cells by microchip flow cytometry. Electrophoresis. 26:3025–3031

Landers, JP. 2003. Molecular Diagnostics on Electrophoretic Microchips. Analytical Chemistry. 75:2919-2927.

Li, PCH., de Camprieu, L., Cai. J. and Sangar, M. 2004. Transport, retention and fluorescent measurement of single biological cells studied in microfluidic chips. Lab Chip. 4:174-180.

Li, XJ. and Li, PCH. 2005a. Microfluidic selection and retention of a single cardiac muscle cell, on-chip dye loading, cell contraction by chemical stimulation and quantitative fluorescent analysis of intracellular calcium. Analytical Chemistry. 77: 4315-4322.

Li, XJ. and Li, PCH. 2005b. Contraction study of single myocyte in the microfluidic chip, in Methods in Molecular Biology: Microfluidic techniques: Reviews and Protocol, Humana Press. 199-225.

Li, XJ., Huang, J., Tibbits, GF. and Li, PCH. 2007. Real-time monitoring of intracellular calcium of a single cardiomyocyte in a microfluidic chip pertaining to drug discovery. Electrophoresis. 28:4723-4733.

Li, XJ., Ling, V. and Li, PCH. 2008. Same-Single-Cell Approach (SASCA) for the Study of Drug Efflux Modulation of Multidrug Resistant Cells Using a Microfluidic Chip. Analytical Chemistry. 80:4095-4102.

Li, XJ., Xue, XY. and Li, PCH. 2009. Real-time detection of the early event of cytotoxicity of herbal ingredients on single leukemia cells studied in a microfluidic biochip. Integrative Biology. 1:90-98.

Li, PCH. 2010. Fundamentals of Microfluidics and Lab on a chip for Biological Analysis and Discovery. CRC Press.

Li, XJ., Chen, YC. and Li, PCH. 2011. A simple and fast microfluidic approach of same-single-cell analysis (SASCA) for the study of multidrug resistance modulation in cancer cells. Lab Chip. 11:1378-1384.

Mitchell, P. 2011. Microfluidics-downsizing large-scale biology. Nat Biotechnol. 19:717-721.

Nitsche, R. 2001. Cell fluorescence assays on the Agilent 2100 bioanalyzer – general use. Agilent Technologies Application Note. Publication Number 5988-4323EN.

Peng, XY. and Li, P. 2004[a]. A three-dimensional flow control concept for single-cell experiments on a microchip (I): cell selection, cell retention, cell culture, cell balancing and cell scanning. Anal. Chem. 76:5273-5281.

Peng, XY. and Li, P. 2004[b]. A three-dimensional flow control concept for single-cell experiments on a microchip (II): Fluorescein diacetate metabolism and calcium mobilization in a single yeast cell as stimulated by glucose and pH changes. Anal. Chem. 76:5282-5292.

Roper, MG., Culbertson, CT., Dahlgren, GM. and Kennedy, RT. 2003. Microfluidic Chip for Continuous Monitoring of Hormone Secretion from Live Cells Using an Electrophoresis-Based Immunoassay. Anal. Chem. 75:4711-4717.

Wittrup, KD. and Bailey, JE. 1990. Propagation of an amplifiable recombinant plasmid in Saccharomyces cerevisiae: flow cytometry studies and segregated modeling. Biotechnology and Bioengineering. 35:525-532.

Wheeler, AR., Throndset, WR., Whelan, R. J., Leach, AM., Zare, RN., Liao, YH., Farrell, K., Manger, ID. and Daridon, A. 2003. Microfluidic Device for Single-Cell Analysis. Analytical Chemistry. 75:3581-3586.

Received: Dec 30, 2011; Accepted: Jan 5, 2012

SENRA Academic Publishers, Burnaby, British Columbia
Vol. 6, No. 1, pp. 1739-1748, Feb 2012
Online ISSN: 1920-3853; Print ISSN: 1715-9997

Canadian Journal of pure&applied sciences

LINCOMYCIN ANTIBIOTIC BIOSYNTHESIS PRODUCED BY *STREPTOMYCES* SP. ISOLATED FROM SAUDI ARABIA SOIL: I-TAXONOMICAL, ANTIMICROBIAL AND INSECTICIDAL STUDIES ON THE PRODUCING ORGANISM

*Ibtisam M Ababutain[1], Zeinab K Abdul Aziz[2] and Nijla A AL-Meshhen[1]
[1]Department of Biology, Faculty of Science, University of Dammam, Kingdom of Saudi Arabia
[2]Department of Botany and Microbiology (Girl's branch), Faculty of Science
Al-Azhar University, Cairo, Egypt

ABSTRACT

The present study began with the isolation of 60 actinomycetes isolates from soil samples collected from different selected locations of Saudi Arabia. The purified actinomycetes isolates were subjected for screening program of antimicrobial and insecticidal activities. Isolate No. 4 isolated from Dammam governorate was found to be the most active actinomycetes isolate in which it produces an active substance belonging to lincomycin antibiotic against Gram positive, Gram negative bacteria and insects. The most active actinomycetes isolates No. 4 was selected for further studies concerning their identification. Morphological, physiological and phylogenetic analysis (16S rRNA); in addition to biochemical studies and culture characteristics as well as the chemical analysis of the cell wall, were carried out for the isolate under study. Based on the phenotypic and genotypic accumulated characteristics of the most active actinomycetes isolate and consulting the recommended International Key's of Bergey's Manual for identification of actinomycetes, it was found that this isolate matched with *Streptomyces* sp. MS-266 and was given the name *Streptomyces* sp. MS-266 Dm4.

Key words: Actinomycetes, diversity, biocontrol, identification, *streptomyces*.

INTRODUCTION

Aerobic actinomycetes are widely distributed in soil. Actinomycetes especially *Streptomyces* sp. are rich sources of bioactive natural products with potential applications as pharmaceuticals and agrochemicals (Atta, 2009; Atta *et al*., 2009; Manteca *et al*., 2008). They are prolific producers of secondary metabolites: antibiotics, herbicides, pesticides and anticancer agents (Atta and Ahmad, 2009; Osada, 1998; Saadoun and Gharaibeh, 2003). Actinomycetes play an important role in the biological control of insects through the production of insecticidal active compounds against the house fly *Musca domestica* (Hussain *et al*., 2002). More than 6000 compounds are produced by *Streptomyces* sp. and many of them have commercial importance as anti-infective (antibiotics, antiparasitic and antifungal agents) anticancer or immunosuppressant agents (Takahashi and Omura, 2003). For example, *S. aureofasies* considered one of important microbes in industrially because of their ability to produce chlortetracycline and tetracycline also; *S. rugosporus* produce pyrroindomycine (Abbanat *et al*., 1999). Antibiotic resistant pathogens have been widely and continuously reported. In consequence, novel antibiotics have been investigated intensively (Holtzel *et al*., 1998; Mukhopadhyay *et al*., 1999; Madigan *et al*., 2000; Aman, 2001; Kim *et al*., 2001; Lewis *et al*., 2003). The aim of this study is the isolation, identification and characterization of the *streptomyces* species isolated from Saudi soil. In addition, the insecticidal and inhibitory effects of these organisms were also investigated.

MATERIALS AND METHODS

Isolation of microorganisms

During the study, 13 soil samples were collected from different locations in Saudi Arabia. Soil samples were taken from a 15-20cm depth, after removing approximately 3cm of the soil surface. The samples were placed in polyethylene bags, closed tightly and stored in a refrigerator until used.

Preparation of Soil Samples

Soil samples were sieved to get rid of any unwanted materials and then dried in the air and mix with calcium carbonate (1%) and incubated at 28^{o}C for several days as the lead to reduce the numbers of vegetative bacterial cells and allowed to increase the numbers of actinomycetes as mentioned by Tsao *et al.* (1960). Dilution method Tsao *et al*. (1960) was used to isolate and purify the actinomycetes by using Starch-nitrate agar as a growth medium.

*Corresponding author email: dr.king2007@hotmail.com

Isolation and purification of the used microorganisms
This was conducted by using soil dilution plate technique according to the method described by Johnson *et al*. (1959).

The antimicrobial activity tests for actinomycetes isolates
Antimicrobial activity for actinomycetes isolates was tested by using the classical diffusion methods described by (Betina, 1983). The following microbial cultures were used for this tests: *Pseudomonas aeruginosa* ATCC 9027, *Escherichia coli* ATCC7839, *Bacillus cereus*, *Bacillus subtilis* ATCC 6633, *Candida albicans* ATCC 10231, *Aspergillus flavus* ATCC 16883, and *Aspergillus niger* ATCC 16404. The Petri dishes were maintained for 2h in a refrigerator at 5^{o}C to allow the diffusion of the bioactive compound. The diameter of complete inhibition zone was measured (in mm) after 24 h for the bacteria and up to 3 days for the fungi incubation at 30^{o}C. The strongest antimicrobial activities of the isolates were selected.

The isolates that gave the strongest antimicrobial activity were grown in submerged culture in 250 ml flasks containing 50ml of the yeast dextrose broth media. The flasks were incubated at 30^{o}C for three days with shaking at 200rpm. One milliliter of the previous culture were transferred to flasks contain 100ml of starch nitrate broth as a production medium which incubated in the same conditions. After growth, Analytical paper disks 740-E/2 diameter that soaked with the cell-free filtrate were placed on the surface of agar plates, which were previously inoculated with the test organisms. The dishes were maintained for 2h in a refrigerator at 5^{o}C to allow the diffusion of the bioactive compound. The diameter of complete inhibition zone was measured (in mm) after 24h for the bacteria and up to 3 days for the fungi incubation at 30°C.

The insecticidal activity tests for actinomycetes isolates:

Origin and rearing of the mosquitoes
Culex pipiens were collected and reared for several generations according to Rady *et al*. (1991) under controlled conditions at temperature of 27 ± 2^{o}C, relative humidity 75 ± 5% and 12- 12 light-dark regime. Adult mosquitoes were kept in (50×50×50cm) wooden cages and daily provided with sponge pieces soaked in 10% sucrose solution for a period of 3-4 days after emergence. After this period, the females were allowed to take a blood meal from a pigeon host, which is necessary for laying eggs (an autogeny). Plastic cup oviposition (15×15cm) containing dechlorinaed tap water was placed in the cage. The obtained egg rafts picked up from the plastic dish and transferred into plastic pans (25×30×15cm) containing 3 liters of tap water left for 24h. The hatching larvae were provided daily with fish food as a diet. This diet was found to be the most preferable food for the larval development and a well female fecundity (Kasap and Demirhan, 1992).

Insect treatment
Ten *C. pipiens* larvae were tested for each 50ml of actinomycetes filtrates in plastic cup. The control tubes were maintained as tap water (50ml) free from actinomycetes filtrate. The experiment was checked daily for recording the biological effects.

Larval mortality percent was estimated by using the Abbott′s formula: % Larval mortality = % A – % B / % A – 100×100, where A = number of controlled larvae and B = number of tested larva (Abbott, 1925).

Methods used for identifying actinomycetes isolates
The identification of genera includes morphological studies, which were done by cover slip culture technique (Kawato and Shinobu, 1959) and total cell hydrolysates analysis of the organisms to detect the meso or the LL-forms of diaminopimelic acid (DAP) according to (Becker *et al*., 1964; Lechevalier and Lechevalier, 1970).

Methods used for classification of the most potent actinomycetes
(a) Studies concerning the morphological characteristics
Determination of the spore-bearing hyphae and spore chains morphology were done by cover slip culture technique (Kawato and Shinobu, 1959) or by direct microscopically examination to the surface of the culture on the growth plates. Electron microscope study was done for spore chain morphology and spore surface.

(b) Studies concerning the cultural characteristics
Diaminopimelic acid (DAP) in the whole cell was analyzed according to Becker *et al*. (1964) and Yamaguchi (1965). Culture characteristics were observed on different kinds of media: Yeast extract-Malt extract agar (ISP2), Oatmeal agar (ISP3), Inorganic salt-starch agar (ISP4), Glycerol-Asparagine agar (ISP5). The color of sporulating aerial mycelium, substrate mycelium and soluble pigments in media were recorded in accordance with the guidelines established by the International Streptomyces Project (Shirling and Gottlieb, 1966) ISP methods. The incubation was carried out at 30^{o}C for 14 days. Colors were assessed on the scale developed by Kenneth (1976).

Growth on Czapek`s agar medium
Ability of the streptomycetes to show good or poor growth on Czapek`s agar medium was carried out by streaking the organism under study on plates of this medium and incubated at 30^{o}C for 14 days.

(c) Studies concerning the physiological properties
Melanoid pigments were observed on the following media: Peptone-Yeast extract- Iron- Agar (ISP 6) (Tresner

and Danga, 1958), Trypton- Yeast extract broth (ISP 1) (Pridham and Gottlieb, 1948) and Tyrosine agar (ISP 7) (Shinobu, 1958). Media were prepared in tubes and inoculated with the isolate No. (4) after sterilization. After incubated for 2- 4 days in 30^{o}C the results have been taken by naked eye the color grayish brown or brown black were considered as a positive result.

Utilization of Carbon Sources was examined by the method of Pridham and Gottlieb (1948). After (10-16 days) incubation, the growth was observed and compared with the positive control (basal medium with glucose) and the negative control (basal medium without carbon source). Sensitivity to streptomycin was carried out according to the method of Bauer *et al.* (1966).

(d) Studies concerning the Phylogenetic characteristics

Genomic DNA extraction was conducted in accordance with the methods described by Sambrook *et al*. (1989). PCR amplification of 16S rDNA gene of the local actinomycete strain was conducted using two primers, F27 with the sequence 5'-AGAGTTTGATCMTGGTCAG-3' and R1492 with the sequence 5'-TACGGYTACCTTGTTACGACTT-3', in accordance with the method described by Edwards *et al*. (1989). Purification of PCR products and sequencing of PCR products for the isolate under study; were preformed in the Genetic analyzer unite of Egyptian company for production of Vaccines, sera and drugs (Vacsera) El-Dokki, Egypt.

Sequence similarities and phylogenetic analysis

The BLAST program (www.ncbi.nlm.gov/blast) was employed in order to assess the degree of DNA similarity. Multiple sequence alignment and molecular phylogeny were evaluated using BioEdit software (Hall, 1999).

RESULTS

Isolation and Purification of Actinomycetes colonies from different habitats

Sixty actinomycetes colony were isolated from thirteen soil samples collected from various locations in Saudi Arabia (Table 1).

Screening for antimicrobial activity of the isolated actinomycetes cultures

Twenty-seven isolates out of sixty showed antimicrobial activity so only 45% of the isolate have antimicrobial activity. The less percentage was the isolates from Khobar (22%), only two out of nine isolates showed antimicrobial activity followed by isolates from Dammam-Riyadh road, three out of twelve (25%) where the isolates from Unaizah one out of two showed antimicrobial activity (50%). The highest percentage was the isolates from Dhahran (60%), three out of five then isolate from Dammam (55%), sixteen out of twenty nine showed antimicrobial activities. However, the isolate from Jubail had no antimicrobial activity (Table 2).

Studies on insecticidal activity of actinomycete isolate No. (4)

The effect of filtrate of isolate No. 4 on the vitality and activity of the larvae of mosquito *C. pipiens* (Culicidae-Diptera) as a vector for some diseases of man and animals, such as "Alfellria" was carried out.

a- Effect on the vitality of mosquito larvae

Table 3 shows the effect of different filtrate concentrations of isolate No. 4 used against mosquito larvae in the third age. It also shows that there is a moral correlation between fatality rates and the different concentrations. When drawing a linear relationship (regression line) between the rates of mortality and

Table 1. Location of the collected samples investigated for isolation of actinomycetes cultures.

Isolate No.	Location	Sample characteristics
1 to 12 (Dm)	Dammam	Sandy soil
13 (Dm)	Dammam	Clay soil
14 to 18 (Dm)	Dammam	Sandy soil
19 to 23 (Dm)	Dammam	Clay soil
24 to 32 (kh)	Khobar	Clay soil
33 to34 (Dm)	Dammam	Clay soil
35 to 39 (Dh)	Dhahran	Clay soil
40 to 42 (Ju)	Jubail	Clay soil
43 (Dm)	Dammam	Clay soil
44 to 46 (Dm)	Dammam	Clay soil
47 to 52 (Dm-Ri)	Dammam-Riyadh	Sandy soil
53 to 58 (Dm-Ri)	Dammam-Riyadh	Sandy soil
59 to 60 (Un)	Unaizah	Clay soil

concentrations, the lethal dose of half the tribe of larvae (LC_{50}) can be calculated ,which was 0.22 ml/L (Fig.1).

b- Effect on the external form of the mosquito larva

After treatment of a group of larva with different doses of isolate No. 4 filtrate, some treated larvae were photographed after 24hours. Figure 2 shows the normal structure of 3rd instars larva of the mosquito *C. pipiens* (Diptera). Figure 3 shows the effect of lower concentration (0.01 ml/L) of isolate No. 4 filtrate on the larvae and the effect will be almost unnoticeable, but from a simple laceration in some areas of the outer layer of the body of the larva (cuticle). Figures 4, 5 and 6 explaining the inhibitory effect of high concentrations of the same isolate on the hardening of cuticle in the body of larvae, where the larvae become transparent, it was possible to observe easily the digestive tract from outside the body.

Table 2**.** Selected actinomycete isolates producing antimicrobial activity.

Isolates No.	Test organisms						
	Ps. aerugina	*E. coli*	*B. cereus*	*B. subtilis*	*Candida albicans*	*Asper. flavus*	*Asper. niger*
1	-	-	-	-	-	-	-
2	-	-	-	- , +	-	-	-
3	-	-	-	+++	-	-	-
4	+++	++	+++++	+++++	+++++	-	-
5	-	-	-	- , +	-	-	-
6	-	-	+	-	-	+	-
8	- , +	-	+	+++	-	+	-
9	-	-	+	- , +	-	-	-
10	-	-	+	-	-	-	-
11	- , +	-	-	- , +	-	-	-
12	-	+	+	++	-	-	-
13	-	+	++	+	-	-	-
14	- , +	-	-	+	-	-	-
15 - 16	-	-	-	-	-	-	-
17	-	+	+	++	-	-	-
18	- , +	+++	++	++	-	- , +	-
19	-	-	-	-	-	-	-
20	-	+	-	+	-	-	-
21	-	+	++	++	-	-	-
22	-	++	-	++	-	+	++
23	-	+	-	+	-	-	-
24	-	-	-	-	-	-	-
25	- , +	- , +	-	- , +	-	-	-
26	-	+	++	+	-	-	-
27	-	-	++	+	-	-	-
28	-	-	-	- , +	-	-	-
29 – 30 -31	-	-	-	-	-	-	-
32	-	-	- , +	- , +	-	-	-
33	-	+	-	-	-	++	++
34	-	-	-	-	-	-	-
35	-	++	-	- , +	-	- , +	-
36	-	-	-	-	-	-	-
37	-,+	-	-	+	-	-	-
38	-	++	-	++	-	-	-
39	-	-	-	-	-	-	-
40	- , +	-	-	- , +	-	-	-
41	-	-	-	-	-	-	-
42	-	-	-	-	-	-	-
43	- , +	-	-	-	-	-	-
44	-	-	-	-	-	-	-
45	-	-	-	+	-	-	-
46-47-48-49	-	-	-	-	-	-	-
50	+	-	-	-	-	-	-
51	-	-	-	-	-	-	-
52	+	-	-	-	-	-	-
53-54-55-56	-	-	-	-	-	-	-
57	++	++	-	-	-	-	-
58	-	-	-	-	-	-	-
59	++	-	++	+	-	-	-
60	-	-	-	-	-	-	-

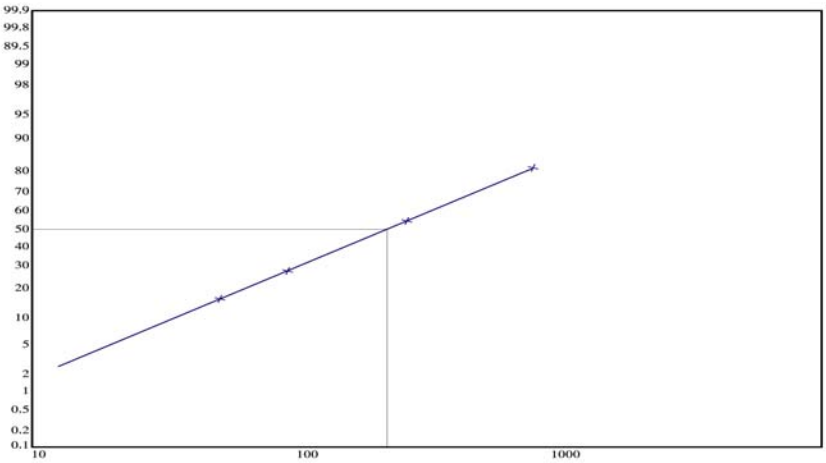

Fig. 1. LC_{50} value of isolate No. (4) filtrate against 3rd larval instars of *Culex pipiens*.

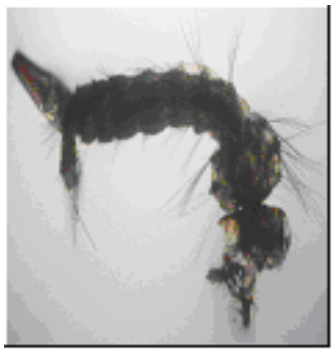

Fig. 2. Normal structure of 3rd instars larva of the mosquito *C. pipiens* (Diptera) (X40).

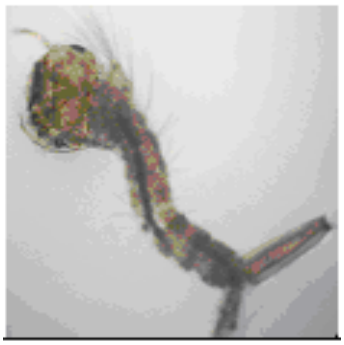

Fig. 3. 3rd instars larva of *C. pipiens* after treatment with (0.01ml/L) concentration (X40).

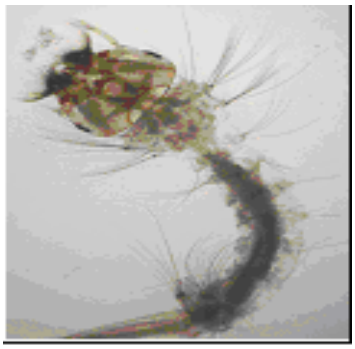

Fig. 4. 3rd instars larva of *C. pipiens* after treatment with (0.1ml/L) concentrations (X40).

Fig. 5. 3rd instars larva of *C. pipiens* after treatment with (0.25ml/L) concentrations (X40).

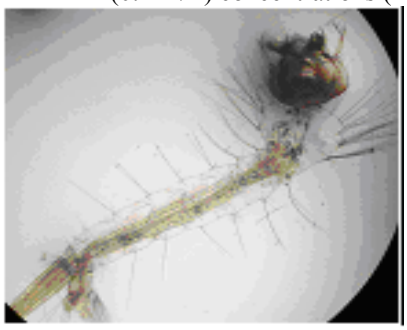

Fig. 6. 3rd instars larva of *C. pipiens* after treatment with (0.5ml/L) concentrations ((X40).

Table 3. The effect of isolate No. 4 filtrates against 3rd larval instars of *C. pipiens*.

Concentration of isolate (ml/L)	% Corrected mortality	LC_{50} value
0.5	90	0.22 ml/L
0.25	56.6	
0.1	26.6	
0.05	16.6	
0.01	13.3	
Control (0.0)	2	

Identification of the most active actinomycetes isolates

The morphological, physiological, cultural and biochemical characteristics for isolate No. 4 see tables 4, 5 and figures 7, 8.

16S rRNA gene sequencing

The 16S rRNA gene sequence was defined to the isolate No. 4 at pb 480 (Fig. 9). Table 6 show the multiple sequence alignment for isolate No. 4 which, showed that isolate No. (4) close to *Streptomyces* sp. MS– 266 by 91

Table 4. Cultural and physiological characteristics of the actinomycetes isolate No. 4.

Types of media	Growth	Aerial mycelium	Substrate mycelium	Diffusible pigments
Starch-nitrate agar	Good	Light Gray (ISCC-NBS 264)	Pale greenish yellow (ISCC-NBS 104)	Light orange yellow (ISCC-NBS 70)
Inorganic-trace salt- starch agar (ISP 4)	Good	Gray (ISCC-NBS 265)	Grayish yellow (ISCC-NBS 90)	Light orange yellow (ISCC-NBS 70)
Glycerol asparagine agar (ISP 5)	Good	Pale yellow (ISCC-NBS 89)	Slightly yellow (ISCC-NBS 84)	Light orange yellow (ISCC-NBS 70)
Yeast extract- malt extract agar (ISP 2)	Good	Gray (ISCC-NBS 265)	Grayish yellow (ISCC-NBS 90)	Light orange yellow (ISCC-NBS 70)
Oat meal agar (ISP 3)	Good	Light Gray (ISCC-NBS 264)	Dark yellow (ISCC-NBS 88)	Light orange yellow (ISCC-NBS 70)
Melanin pigment media 1-Tryptone yeast extract broth (ISP 1)	Weak	White (ISCC-NBS 263)	Slightly yellow (ISCC-NBS 84)	Deep yellowish brown (ISCC-NBS 78)
2- Peptone yeast extract iron agar (ISP 6)	Weak	Pale greenish yellow (ISCC-NBS 104)	Grayish yellow (ISCC-NBS 90)	Strong brown (ISCC-NBS 55)
3- Tyrosine agar (ISP 7)	No Growth	-	-	-

% and it was gave the name *Streptomyces* sp. MS– 266 Dm4.

Table 5. Morphological and biochemical characteristics of actinomycetes isolate No. 4.

Characters	Results
1. Morphological characteristics:	
Spore chain	Spiral
Spore mass	Gray
Spore surface	Smooth
Motility	Non motile
Color of substrate mycelium	Grayish yellow
Diffusible pigment	Light orange yellow
2. Chemotaxonomic analysis: Cell wall hydrolysis for:	
Diaminopimelic acid (DAP)	LL-DAP
Sugar pattern	ND

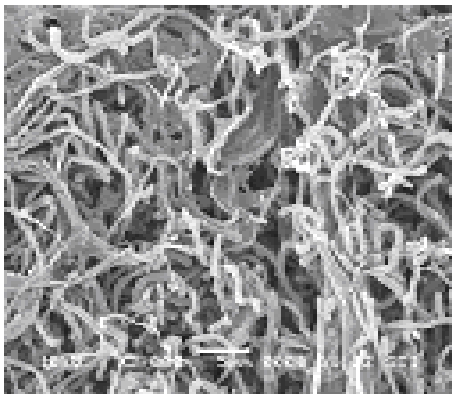

Fig. 7. Scanning electron micrograph of isolates No. 4 showing spiral shaped mycelium (X 3.000).

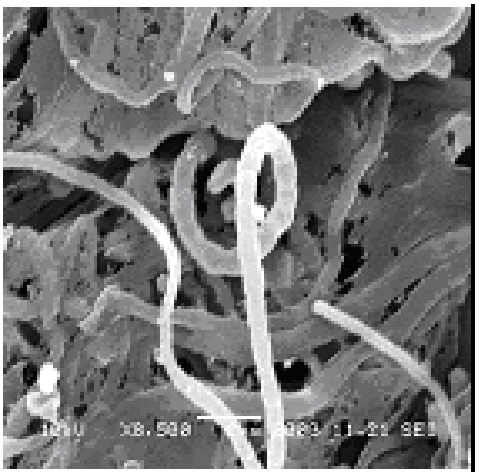

Fig. 8. Scanning electron micrograph of isolates No. 4 showing smooth spore surface (X 8.500).

DISCUSSION

The present study was started by isolation and purification of sixty actinomycetes isolates, which isolated from different regions of Saudi Arabian soil. The 60 isolates were tested for their ability to inhibit the growth of Gram-positive bacteria, Gram-negative bacteria, yeasts, fungi and as insecticide. According to many scientists, which isolate and purify the actinomycetes, Bream *et al*. (2001) isolated different actinomycetes strains from Saudi Arabia and Egypt soil. However, many researchers isolated actinomycetes strains from different places (Sahin and Ugur, 2002; Pandey *et al*., 2004; Ilić *et al*., 2005; Xie *et al*., 2007; Igarashi *et al*., 2008; Malik *et al*., 2008). Recently Dhanasekaran *et al*. (2010) isolated 64

Fig. 9. 16S rRNA gene sequencing for isolate No. 4.

Table 6. Sequences producing significant alignments for isolate No. 4.

Accession	Description	Maximum identities
AY645903.1	*Streptomyces* sp. MS-266	91%
FJ532407.1	*Streptomyces microflavus* strain HBUM174141	91%
FJ481053.1	*Streptomyces cavourensis* strain xsd08096	91%
FJ486354.1	*Streptomyces anulatus* strain HBUM174206	91%
AB184642.1	*Streptomyces cavourensis sub* sp. *washingtonensis* strain: NBRC 15391	91%
AF112162.1	*Streptomyces* sp. EF-41	91%
GU211900.1	*Streptomyces* sp. WZ57	91%
FJ481633.1	*Streptomyces microflavus* strain HBUM174884	91%
FJ486351.1	*Streptomyces microflavus* strain HBUM174178	91%
FJ486435.1	*Streptomyces microflavus* strain HBUM174246	91%

actinomycetes strains from coastal soil. From twenty-seven isolates showed antagonistic activity against test organisms, isolate No. 4 showed the strongest activity against Gram-positive and Gram- negative bacteria. The identification of isolate No. 4 was done according to Bergey`s Manual (Williams, 1989; Holt *et al*., 1994), in which the basis for the definition depends on the morphological characteristics and the pigments produced in addition to the physiological and genetic studies (amplification and sequencing of the 16S rRNA). Kim and Goodfellow (2002) explained that the basis for the definition of *streptomyces* depends on the characteristics of morphology and the production of dyes in addition to the physiological and biochemistry to gain access to the species, and therefore they were differed between the four species of *streptomyces* isolated from British soil. Also, Sahin and Ugur (2002) were identified three isolates belonging to *streptomyces* by following the information in Bergey`s Manual. Whereas, Pandey *et al*. (2004) used the morphology and biochemical methods to describe the actinomycetes isolated from Nepal, and compared the shape with Bergey`s Manual of Determinative Bacteriology Holt *et al*. (1994). Jayasuriye *et al*. (2007) was adopted in its definition of a species on morphological characteristics, as well as analysis of serial 16S rDNA. Ningthoujam *et al*. (2009) identified strain of *streptomyces* sp. LS1-128 as more relevant to *S. sindenensis* based on morphological- physiological–cultural as well as genetic traits. Therefore, it was found that isolate No. 4 matched with *streptomyces* sp. MS-266

and was given the name *Streptomyces* sp. MS- 266 Dm4 in which (Dm) refers to Dammam governorate.

When examining the insecticidal activity of actinomycetes isolates against insect pests, it was noted the existence of effects on the external shape of the larvae of mosquito *C. pipiens* when using filtrate of isolate No. (4), where it have an effect on the cuticle layer which consisting of Arthropod in proteins and "chitin" These compounds gave solidity to the larval body or adult stage (Figs. 2-6). Where the process of Sclerotization had disappeared which responsible for giving the dark color to the cuticle of larva or adult stage. The hardness of cuticle is done by the formation of chemical bonds between cuticle proteins and "Polyphenols" substance secreted from the skin cells layer. The present results are, however, in accordance with several results performed with actinomycetes and other insect species. Dhanasekaran *et al*. (2010) found actinomycetes isolate producing strong larvicidal activity against Anopheles mosquito larvae. Liu *et al*. (2008) obtained on quinomycin A compound isolated from *Streptomyces* sp. which has the effect of inhibiting the growth of many pathogen insects, including mosquito *Culex*.

Since the cuticle of insect species consists largely of chitin, it was postulated that chitinase produced by these isolates could be involved in insect control. Therefore, the production of chitinase was used as the criteria for the selection of potential biocontrol agents of insects. Microbial chitinolytic enzymes have been considered important in the biological control of many insects because of their ability to interfere with chitin deposition (Tripathi *et al*., 2002).

CONCLUSION

Actinomycetes metabolites exhibited its effect against mosquito *C. pipiens*, so based of our results it can be used as an alternative insecticide, because they are free from harmful effects on the environment.

REFERENCES

Abbot, WS. 1925. A method of computing the objectiveness of an insecticide. J. Econ. Entomol. 18:265-267.

Abbanat, D., Maiese, W. and Greenstein, M. 1999. Biosynthesis of the pyrroindomycins by *Streptomyces rugosporus* LL-42D005; Characterization of nutrient requirements. J. Antibiot. 52(2):117-126.

Aman, GZ. 2001. Studies on Some Actinomycete Isolates from Certain Desert Soil Samples. PhD thesis, Faculty of Science. Al-Azhar University, Egypt.

Atta, HM. 2009. An Antifungal agent produced by *Streptomyces olivaceiscleroticus* AZ-SH514. World Applied Sci. J. 6:1495-1505.

Atta, HM., Dabour, SM. and Desoukey, SG. 2009. Sprasomycin antibiotic production by *Streptomyces* sp. AZ-NIOFD1: Taxonomy, fermentation, purification and biological activities. Am-Euras J. Agric. Environ. Sci. 5(3):368-377.

Atta, MA. and Ahmad, MS. 2009. Antimycin-A antibiotic biosynthesis produced by *Streptomyces* sp. AZ-AR-262: Taxonomy, fermentation, purification and biological activities. Aust. J. Bas. Applied Sci. 3:126-135.

Bauer, AW., Kirby, WMM., Sherris, JC. and Truck, M. 1966. Antibiotic susceptibility testing by a standardized single disk method. Am. J. Clin. Pathol. 45:493-496.

Becker, B., Lechevalier, MP., Gordon, RE. and Lechevalier, HA. 1964. Rapid differentiation between *Nocardia* and *Streptomyces* by paper chromatography of whole cell hydrolysates. Appl. Microbiol. 12:421-423.

Betina, V. 1983. The chemistry and biology of antibiotics. Elsevier Scientific Publishing Company Inc, Amsterdam, New York, USA.

Bream, AS., Ghazal, SA., Abdul El-Aziz, ZK. and Ibrahim, SY. 2001. Insecticidal activity of selected actinomycete strains against the Egyptian cotton leaf worm *Soodoptera littoralis* (Lepidoptera: Noctuidae). Meded. Rijksuniv. Gent. Fak. Landbouwkd. Toegep. Biol. Wet. 66(2a):503-12.

Dhanasekaran, D., Thajuddin, N. and Panneerselvam, A. 2010. Herbicidal agents from actinomycetes against selected crop plants and weeds. Nat. Prod. Res. 24(6):521-529.

Edwards, U., Rogall, T., Bocker, H., Emade, M. and Bottger, E. 1989. Isolation and direct complete nucleotide determination of entire genes. Characterization of a gene coding for 16S ribosomal DNA. Nucleic Acid Res. 17:7843-7853.

Hall, TA. 1999. A user-friendly biological sequence alignment editor and analysis program for Windows 95/98/NT. Nucl. Acids Symp. Ser. 41:95-98.

Holt, JG., Krieg, NR., Sneath, PHA., Staley, JT. and Williams, ST. 1994. Bergey's Manual of Determinative Bacteriology (9th ed.). Williams & Wilkins, Maryland Baltimore, USA.

Holtzel, A., Kempter, C., Metzger, JM., Jung, G., Groth, I., Fritz, T. and Fiedler, HP. 1998. Spirofungin, a new antifungal. J. Antibiot. 51(8):699-707.

Hussain, AA., Mostafa, SA., Ghazal, SA. and Ibrahim, SY. 2002. Studies on antifungal antibiotic and

bioinsecticidal activities of some actinomycete isolates. African J. Mycol. Biotechnol. 10:63- 80.

Igarashi, M., Sawa, R., Kinoshita, N., Hashizume, H., Nakagawa, N., Homma, Y., Nishimura, Y. and Akamatsu, Y. 2008. Pargamycin A, a novel cyclic peptide antibiotic from *Amycolatopsis* sp. J. Antibiot. 61(6):387-393.

Ilic`, SB., Konstantinovic`, SS. and Todorvic, ZB. 2005. UV/VIS analysis and antimicrobial activity of *Streptomyces* isolates. Medicine and Biology. 12(1):44-46.

Jayasuriya, H., Herath, K., Ondeyka, JG., Zhang, C., Zink, DL., Brower, M., Gailliot, FP., Greene, J., Birdsall, G., Venugopal, J., Ushio, M., Burgess, B., Russotti, G., Walker, A., Hesse, M., Seeley, A., Junker, B., Connors, N., Salazar, O., Genilloud, O., Liu, K., Masurekar, P., Barrett, JF. and Singh, SHB. 2007. Isolation and structure elucidation of thiazomycin–Apotent thiazolyl peptide antibiotic from *Amycolatopsis fastidiosa*. J. Antibiot. 60(9):554-564.

Johnson, LF., Curl, EA., Bond, JH. and Fribourg, HA. 1959. Methods for studying soil Microflora plant disease relationships. Burgess publishing company, Minneapolis, Minnesota, USA.

Kasap, M. and Demirhan, L. 1992. The effect of various larval foods on the rate of adult emergence and fecundity of mosquitoes. Turkiye Parasitol Derg. 161:87-97.

Kawato, M. and Shinobu, R. 1959. On *S. herbaricolor* nov. sp. Supplement: A simple technique for the microscopical observation. Memoirs of Osaka Univ. Liberal Arts and Education. pp 114.

Kenneth, LK. 1976. The Universal Color Language. In Color: Universal Language and Dictionary of name. Eds. Kenneth, LK. and Deane, BJ. Nat. Bur. Stand (US) Spes. Pupl. 440:1-19.

Kim, SB. and Goodfellow, M. 2002. *Streptomyces avermitilis* sp. nov., nom. rev., a taxonomic home for the avermectin-producing streptpmycetes. IJSEM 52:2011-2014.

Kim, CJ., Chang, YK., Chun, GT., Teong, YH. and Lee, SJ. 2001. Continuous culture of immobilized *Streptomyces* cells for kasugamycin production. Biotechnol. Prog. 17(3):453- 461.

Lechevalier, MP. and Lechevalier, HA. 1970. Chemical composition as a criterion in the classification of aerobic actinomycetes. J. Syst. Bacteriol. 20 (4):435-443.

Lewis, EA., Adamek, TL., Vining, LC. and White, RL. 2003. Metabolites of a blocked chloramphenicol producer. J. Nat. Prod. 66(1):62-66.

Liu, H., Qin, S., Wang, Y., Li, W. and Zhang, J. 2008. Insecticidal action of Quinomycin A from *Streptomyces* sp. KN-0647, isolated from a forest soil. World J. Microbiol. Biotechnol. 24:2243-2248.

Madigan, M., Martinko, J. and Parker, J. 2000. Brock Biology of Microorganisms. Prentince Hall. International, Inc.

Malik, H., Sur, B., Singhal, N. and Bihari, V. 2008. Antimicrobial protein from *Streptomyces fulvissimus* inhibitory to methicillin resistant *Staphylococcus aureus*. Indian J. Exp. Biol. 46:254-257.

Manteca, A., Alvarez, R., Salazar, N., Yague, P. and Sanchez, J. 2008. Mycelium differentiation and antibiotic production in submerged culture of *Streptomyces coelicolor*. Appl. Environ. Microbiol. 74:3877-3886.

Mukhopadhyay, T., Nadkarni, SR., Bhat, RG., Gupte, SV., Ganguli, BN., Petry, S. and Kogler, H. 1999. Mathemycin B, a new antifungal macolactone from actinomycete species HIL Y-8620959. J. Nat. Prod. 62(6):889-890.

Ningthoujam, D., Sanasam, S. and Nimaichand, S. 2009. A *Streptomyces sindenensis* strain LS1-128 exhibiting broad spectrum antimicrobial activity. J. Biol. Sci. 4(10):1085-1091.

Osada, H. 1998. Actinomycetes: how fascinating microorganisms. Actinomycetologica 12:85-88.

Pandey, B., Ghimire, P. and Agrawal, VP. 2004. Studies on the antibacterial activity of the Actinomycetes isolated from the Khumbu Region of Nepal. J. Biol. Sci. 23:44-53.

Pridham, TG. and Gottlieb, D. 1948. The utilization of carbon compounds by some actinomycetes as an aid for species determination. J. Bacteriol. 56:107-114.

Rady, M., Merdan, A. and Salem, S. 1991. Water soluble toxins of *Bacillus thuringiensis* sero type H-14 demonstrating lethal action no *Culex pipiens* larvae. Egypt J. Microbiol. 26(2):147-156.

Saadoum, I. and Gharaibeh, R. 2003. The *Streptomyces* flora of Badia region of Jordan and its potential as a source of antibiotics active against antibiotic-resistant bacteria. J. Arid Environ. 53:365-371.

Sahin, N. and Ugur, A. 2002. Investigation of the antimicrobial activity of some *Streptomyces* isolates. Turk. J. Biology. 27:79-84.

Sambrook, J., Fritsch, EF. and Maniatis, T. 1989. Molecular cloning: a laboratory Manual (2^{nd} ed.). Cold Spring Harbor Laboratory, Cold Spring.

Shinobu, R. 1958. Physiological and cultural study for the identification of soil *Actinomycetes* species. Memoirs of Osaka Univ. Liberal Arts and Education. Ser. B 7:1-116.

Shirling, EB. and Gottlieb, D. 1966. Methods for characterization of *Streptomyces* species. Intern. J. Syst. Bacteriol. 16:313-340.

Takahashi, YO. and Mura, S. 2003. Isolation of new actinomycete strains for the screening of new bioactive compounds. J. Gen. Appl. Microbio. 49:141-154.

Tresner, HD. and Danga, F. 1958. Hydrogen sulfide production by *Streptomyces* as a criterion for species differentiation. J. Bacteriol. 76:329.

Tripathi, AK., Khanuja, SPS. and Kumar, S. 2002. Chitin synthesis inhibitors as insect pest control agents. J. Med. Arom. Plant Sci. 24:104-122.

Tsao, PH., Leben, C. and Keitt, GW. 1960. Medium constitution for isolation of actinomycetes. Phytopathology. 50:88-89.

Williams, ST. 1989. Bergey's Manual of Systematic Bacteriology (vol. 4). Williams and Wilkins Co, Baltimore, Hong Kong, London, Sydney.

Xie, Y., Chen, R., Si, S., Sun, CH. and Xu, H. 2007. A new nucleosidyl-peptide antibiotic, Sansanmycin. J. Antibiot. 60(2):158-161.

Yamaguchi., T. 1965. Comparison of the wall composition of morphologically distinct actinomycetes. J. Bacteriol. 89:444-453.

Received: Dec 8, 2011; Accepted: Jan 8, 2012

SENRA Academic Publishers, Burnaby, British Columbia
Vol. 6, No. 1, pp. 1749-1758, Feb 2012
Online ISSN: 1920-3853; Print ISSN: 1715-9997

Canadian Journal of pure&applied sciences

FIRE AND POPULATION DYNAMICS OF WOODY PLANT SPECIES IN A GUINEA SAVANNA VEGETATION IN MOLE NATIONAL PARK, GHANA: MATRIX MODEL PROJECTIONS

*I Sackey[1], WHG Hale[2] and A-WM Imoro[1]
[1]Department of Applied Biology, University for Development Studies, PO Box 24, Navrongo, Ghana
[2]Department of Geography and Environmental Science, University of Bradford, Bradford, BD7 1DP, United Kingdom

ABSTRACT

Recurrent fires have a considerable potential to influence the structure and composition of savanna vegetation. In Mole National Park in Ghana, the policy is to burn the vegetation annually, early in the dry season. This paper examines the likely effects of these regular fires on the population dynamics of five tree species in the park using matrix model projections. The matrix manipulations were programmed using the Microsoft Excel spreadsheet software. The model is based on analyses and data put forward in Sackey (2006), as well as data on fire impacts and seedling production and growth of woody species recently obtained by Sackey and Imoro (unpublished study) from a savanna vegetation near Mole National Park. The model results show that annual burns will lead to changes in the relative abundance, as well as a decline in the density of all five tree species. The results also show that Burkea africana and Terminalia spp. require a minimum fire-free interval of > 2 years for their persistence, while 2 years minimum burning interval is required for the maintenance of Acacia dudgeoni, Combretum adenogonium and Vitellaria paradoxa. A minimum fire-free interval of > 3 years on a rotational system is suggested for the persistence of the majority of the woody plant species in the park.

Keywords: Grupe camp, fire impacts, matrix models, vegetation transformation.

INTRODUCTION

Plants differ widely in their tolerance of fire and their capacity to recover afterwards. As a result, recurrent fires have considerable potential to influence the structure and composition of vegetation (Trapnell, 1959; Charter and Keay, 1960; Ramsay and Rose-Innes, 1963; Hopkins, 1965; Rose-Innes, 1972; Brookman-Amissah *et al*., 1980; Frost and Robertson, 1987; Swaine *et al*., 1992; Ben-Shahar, 1998; Sackey, 2006; Sackey and Hale, 2008). The extent to which this occurs depends not only on differences in the sensitivity of different species but also on the fire regime (type, frequency and intensity of fire) of the area, and on the physiological and developmental states of individual plants at the time of burning.

In Mole National Park, the policy is to burn the vegetation annually early in the dry season when the grass fuel is still moist, presumably to achieve low fire intensity and, thus, minimise its impact on the Park's vegetation. It is, however, certain that late dry season fires occur regularly over large areas of the Park. Sackey and Hale (2008) and Sackey (2006) in a recent study showed that these regular dry season fires are causing mortality and topkill to trees ≥ 2 m tall in the Guinea savanna near Grupe camp of the Park. A matrix population model is a valuable tool for predicting population response to burning (Silva *et al*., 1991; Hoffmann, 1999) and is used in the present study to predict the long-term effects of the regular fires on the population dynamics of five main tree species (*Acacia dudgeoni*, *Burkea africana*, *Combretum adenogonium*, *Terminalia* spp. and *Vitellaria paradoxa*) in the south-western section of the Mole National Park, Ghana, near Grupe camp. The model is based on analyses and data put forward in Sackey (2006), as well as data on fire impacts and seedling production and growth of woody species recently obtained by Sackey and Imoro (unpublished study) from a savanna vegetation near Mole National Park. The mathematical workability of the matrix model can be found in Lefkovitch (1965). Further description of matrix models can be found in Hartshorn (1975), Caswell (1982), Crouse *et al*. (1987), Enright and Watson (1991) and Desmet *et al*. (1996).

*Corresponding author email: isackey5@yahoo.com

MATERIALS AND METHODS

METHODS

Study Area

Mole National Park is situated in northern Ghana between 9º 12' - 10º 06' North and 1º 25' - 2º 17' West and covers an area of approximately 4840 km^2. The Mole and Lovi rivers are the most significant among the numerous rivers which cross or originate in the Park. A climatic diagram for the nearest meteorological station, Damongo, about 18 km south of Mole is shown in figure 1. More than 95% of the mean annual rain (1098.1 ± 78.3 mm) falls during the single rainy season from April to October, with maxima occurring in June and the prime peak in September. The

five consecutive months of the dry season (November – March) have a mean total rainfall of 49.7 ± 3.2 mm. The mean annual temperature of 27.7ºC varies little from month to month (25.7-31.0ºC), while the average diurnal range is 13.3ºC.

The Park lies in the Guinea savanna zone. The dominant vegetation type is the open savanna woodland with a grass layer that can reach up to 3 m tall during the rainy season and which is burnt annually. Hall and Jeník (1968) have recognised four savanna vegetation types in the West Gonja District, which includes the Park. These are the *Terminalia macroptera-Loudetiopsis thoroldi*-type in badly-drained and seasonally flooded plains, the *Mitragyna inermis-Andropogon gayanus var. gayanus*-type in valley bottoms along streams, the *Isoberlinia doka-Loudetiopsis scaethae-Hyperrhenia subplumosa*-type on gentle slopes and well-drained plains and the *Loudetiopsis kerstingii-Polycarpea tenuifolia*-type on iron stone plateaux.

There are about 94 species of mammals (including bats) and over 300 species of birds in the Park (Hossain and Hall, 1996). The distribution of large mammals, particularly elephants, is concentrated in the south-eastern section of the Park. This study was conducted in the south-western section of the Park where elephants as well as other large mammals are virtually absent for most of

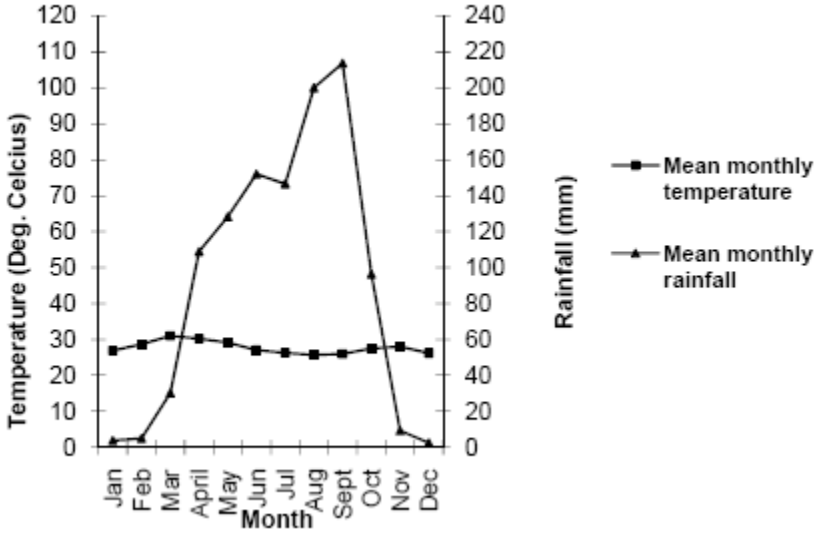

Fig. 1. Climatic diagram for Damongo, Ghana, based on rainfall data from 1985-2003 and temperature data from 1998-2003. Source of data: Ghana Meteorological Services.

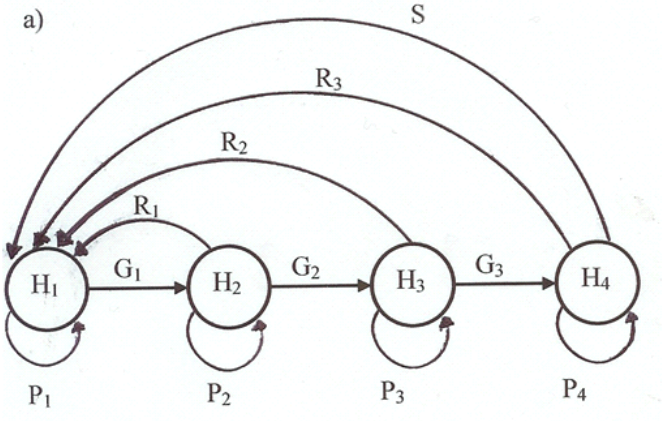

Fig. 2. Generalised life-stage graph of savanna tree species with arrows representing all the possible life-history transitions. H: height stages; *S*: seedling production; *R*: the probability of reversing to height stage H_1; *P*: the probability of remaining in the same height stage; and *G*: the probability of progressing to the next height stage within the time period of the model.

Table 1. Top-kill and mortality rates of the five tree species in one fire season according to height class.

Plant species	Top-kill (%)				Mortality (%)			
	< 1 m	1 – 2 m	2 – 5 m	> 5 m	< 1 m	1 – 2 m	2 – 5 m	> 5 m
Acacia dudgeoni	39.30	63.00	0.07	0.67	52.20	21.60	0.25	9.33
Burkea africana	37.50	59.70	0.10	0.50	60.50	32.50	1.38	5.35
Combretum adenogonium	31.10	67.30	0.32	0.14	65.30	19.40	0.37	1.02
Terminalia spp.	35.30	66.20	2.88	2.20	57.30	17.20	0.97	1.11
Vitellaria paradoxa	33.70	57.10	0.47	0.36	61.10	15.30	0.27	1.52

the year. The savanna vegetation in the area is largely the *Isoberlinia doka-Loudetiopsis scaethae-Hyperrhenia subplumosa* subtype of Hall and Jeník (1968). Further details of the Mole National Park are included in Sackey (2006).

The Matrix Models

The absence of large mammalian herbivores in the savanna near the Grupe camp makes fire the major factor directly influencing the population structure of the component woody species and, hence, the entire woody plant community structure. A stage-based matrix model was, therefore, developed to gain some quantitative insight into the effects of fire on the dynamics of five tree species' populations. A simple matrix based on the division of the life-history of the tree species into four height-classes (H: < 1 m, 1-2 m, 2-5 m and > 5 m) was used. Life-stage graph (Fig. 2) representing all the possible transitions (growth, stasis and reversal) an individual tree in any of the height classes (H) can make in any one time period, as well as seedling production by trees > 5 m tall, was drawn. The effect of climatic changes upon seedling production and tree survival and growth rates, as well as the density-dependent effects of tree numbers upon seedling survival (population-regulation mechanisms) and grass production and, hence, fire intensity has not been considered.

Fire was incorporated in the model in two ways: fire impact and burn frequency. Regarding fire impact, fire was programmed to operate at height-specific rates upon the four delineated height classes of the individual tree species (acting as a mortality or reversal agent), while burn frequency was incorporated as an annual event and as regular two- to four-year burn intervals. The model assumed that the population of a given height-class is exposed to either height-specific mortality rate or height-specific reversal rate (*R*) due to the impact of fire. Thus only two categories of fire damage were recognised, namely, tree totally killed, i.e., fire acting as a mortality agent, and tree top-killed, i.e., fire acting as a reversal agent reversing tree height. Field observations indicate that fire impact is most severe at tree bole bases (below 1.5 m in height) and re-sprouting of dead stems commonly occurs from root-collars or stumps below 1 m (Sackey, 2006). Thus the model assumed that all fire-induced height reversals were to the lowest height-class, that is, < 1 m. All living trees with moderate fire damage involving slight scorching of the lower canopy or bark were considered as survivors. The procedure by Desmet *et al*. (1996) was followed to estimate the proportion of these survivors that will progress to the next higher height class (*G*) and the proportion that will remain or persist in the same height class (Stasis or *P*) in one year time period. Seedling input (*S*) was modelled as 'viable seedlings produced per tree' rather than seed production and survival.

Model Parameterization

The following parameter estimates were used in deriving the transition probabilities for the construction of the matrix models for the tree species:

Mortality and top-kill rates of tree species

Top-kill and mortality rates used for the model are summarised in table 1. Data for height classes 2 – 5m and > 5m are derived from Sackey (2006), while data for height classes < 1 m and 1 – 2 m are derived from an unpublished study by I. Sackey and A-W. M. Imoro in savanna vegetation within the 20 km buffer zone of the Mole National Park. The methods used in the unpublished study involved tagging individual plants of height < 1 m and 1-2 m tall, belonging to the five study species in vegetation near Larabanga. The number of individual plants tagged ranged from 55 to 70, depending on their availability for the season, and the vegetation burnt annually in November for three consecutive years, from 2007 to 2009. Fourteen days after each burn, the growth condition of the individual plants were assessed as dead or top-killed or living. The data were analysed in the form of proportions and averaged over the three burning seasons.

Seedling production rates

Seedling production rates of the tree species are derived from an unpublished study by Sackey and Imoro (Table 2). In this study, three trees of reproductive height (> 5 m tall) were selected for each of the five study species.

Table 2. Annual seedling production per tree estimated over three years for the five tree species incorporated in the model. (Source: Unpublished study by Sackey and Imoro).

Plant species	№ of seedlings
Acacia dudgeoni	10.71
Burkea africana	1.30
Combretum adenogonium	3.71
Terminalia spp.	1.08
Vitellaria paradoxa	4.21

Tree growth rates

Values for the growth of savanna trees vary widely, and are measured in a variety of ways. Herlocker estimated annual growth of young *Acacia tortilis* as 30 cm (Croze, 1974). Thomson (1975) indicated that *Brachystegia boehmii* regrowth can reach > 2 m high in 5 years under complete fire protection. Pellew (1983) found annual height increment of *Acacia tortilis* plants of < 0.95 m and 1.0-1.95 m in height to be 50.0 cm and 33.0 cm, respectively, while for trees 2.0-4.95 m tall, the mean annual increment was 46.7 cm, all without giraffe browsing. Lewis (1987) measured annual vertical growth in re-sprouted *Colophospermum mopane* trees in Luangwa Valley, Zambia, as 13.4-19.2 cm. From field observations, Dublin *et al*. (1990) found that height classes of *Acacia gerrardii* were roughly equivalent to age such that plants reach 15 cm in approximately 1 year, 1 m in 6 years, 2 m in 11 years and 3 m in 15 years. Thus trees of *Acacia gerrardii* progress through height classes 1, 2 and 3 m in an average period of approximately 5 years each. Although the present model concerns different tree species to *Acacia gerrardii*, a similar height-class:age equivalence was assumed, as this represents the best match. Thus 5 years was used in the model as the average period for tree progression from one height class to the next higher height class. The following assumptions were also made that, during the five-year period: all trees would progress to the next higher height class, except those in the highest height class; and that within 5 years no tree would progress in height beyond the next higher height class.

Initial tree densities

The initial densities of trees (stems/ha) used for the construction of the column vectors of the model are values obtained by Sackey (2006) (Table 3).

The transition matrices

The parameter estimates of tree height reversal, growth, survival (derived from mortality and topkill data in Sackey (2006) and unpublished study by Sackey and Imoro) and seedling production (Table 3) were used to construct the transition matrices for the population models. Two transition matrices were constructed per species, each simulating the tree population dynamics at a

Table 3. Observed stage (height) class distribution of the tree populations used for the respective matrix vectors, expressed as number of stems/ha and relative percentage (in brackets).

Plant species	< 1 m	1 – 2 m	2 – 5 m	> 5 m
Acacia dudgeoni	923 (94.86)	15 (1.54)	15 (3.08)	5 (0.51)
Burkea africana	260 (84.42)	0 (0.00)	10 (3.25)	38 (12.34)
Combretum adenogonium	733 (83.96)	75 (8.59)	40 (4.58)	25 (2.86)
Terminalia spp.	350 (97.77)	8 (2.23)	0 (0.00)	0 (0.00)
Vitellaria paradoxa	2128 (93.17)	53 (2.32)	65 (2.85)	38 (1.66)

Table 4. The matrix cell reference labels for transition matrices **B** (a) and **U** (b) corresponding to the transitions on the life-history graph for the tree species in figure 2.

a

$$\begin{pmatrix} P_1 & R_1 & R_2 & R_3+S \\ G_1 & P_2 & 0 & 0 \\ 0 & G_2 & P_3 & 0 \\ 0 & 0 & G_3 & P_4 \end{pmatrix}$$

b

$$\begin{pmatrix} P_1 & 0 & 0 & S \\ G_1 & P_2 & 0 & 0 \\ 0 & G_2 & P_3 & 0 \\ 0 & 0 & G_3 & P_4 \end{pmatrix}$$

different stage of the fire cycle. The probabilities for the two matrices (**B** and **U**) were calculated using the matrix cell reference labels presented in Table 4. *G* in all cases was estimated as the reciprocal of the duration of the height stages (assumed to be 5 years for all the height stages) in accord with Desmet *et al*. (1996); thus in 1 year, 1/5 or 20% of individual trees in height classes < 1 m, 1-2 m and 2-5 m would progress to the next higher height class. P_1, P_2 and P_3 were calculated as 1 minus the stage-specific mortality and topkill (or height reversal, *R*) and the relevant growth probability, *G*. P_4 was calculated as 1 minus the stage-specific mortality and topkill since it corresponds to the highest height stage. *R* in all cases represents individuals experiencing topkill and subsequently re-sprouting. Matrix **B** (Table 5) simulates dynamics in the year each respective tree population is burned. Burning occurs at the beginning of the one-year period simulated by **B**; so re-sprouting of topkilled individuals would occur during the period. Matrix **U** (Table 6) simulates the dynamics of unburned populations. The time period for the model was 1 year. Therefore, the calculated transition probabilities are expressed as the probability of a transition occurring during that time period. The derived transition matrices were subsequently analysed following the procedure outlined in Enright and Watson (1991) and Desmet *et al*. (1996).

Population projections

The transition matrices **B** and **U** were used to simulate the effects of different fire frequencies on the population dynamics of the five tree species. For instance, to simulate the population dynamics during a 4-year period in which burning occurs only in the fourth year, we use

$\mathbf{N}_4 = \mathbf{B.U.U.U.N}_0$,

where $\mathbf{N}_0$ and $\mathbf{N}_4$ are the population vectors at year 0 and year 4, respectively.

To project the future population growth, the matrix manipulations were programmed using the Microsoft Excel spreadsheet software. With the spreadsheet software, the finite rate of natural increase, λ, never really stabilizes but changes constantly with time at a decimal accuracy beyond that required for a simple population model (Desmet *et al*., 1996). Thus this did not constitute a drawback. Besides, the major object was to examine the behaviour of the transition matrix and the population vector elements over time and to determine the direction of change in the tree populations and how this change might respond to changes in fire frequency and impact. In order to avoid the interpretational problems associated with periodic matrix models as noted by Caswell and Trevisan (1994), the matrix manipulations were programmed with the transition matrices in tables 5 and 6 to simulate the exact burning frequencies instead of using the products of these matrices. For instance, to simulate the population dynamics under biennial fire frequency in which burning occurs in the second year, the transition matrix **U** was multiplied by $\mathbf{N_0}$ (the population vector at year 0). The resulting population vector, $\mathbf{N_1}$, was then multiplied by the transition matrix **B** to obtain $\mathbf{N_2}$. This sequence of matrix manipulations was repeated until the change in λ was < 0.00005.

Table 5. Transition matrix (**B**) and column vectors for the five tree species simulating dynamics in the year each respective tree population is burned. The values in the columns for height classes 2 -5 m and > 5 m, and column vectors are derived from Sackey (2006), while those for height classes < 1 m and 1 – 2 m are from an unpublished study by Sackey and Imoro.

a) *Acacia dudgeoni*

Height class	**< 1 m**	**1-2 m**	**2-5 m**	**> 5 m**
< 1 m	0.4610	0.6300	0.0007	10.7167
1 – 2 m	0.0170	0.1232	0.0000	0.0000
2 – 5 m	0.0000	0.0308	0.7974	0.0000
> 5 m	0.0000	0.0000	0.1994	0.9000

b) *Burkea africana*

Height class	**< 1 m**	**1 – 2 m**	**2 – 5 m**	**> 5 m**
< 1 m	0.3910	0.5970	0.0010	1.3050
1 – 2 m	0.0040	0.0624	0.0000	0.0000
2 – 5 m	0.0000	0.0156	0.7882	0.0000
> 5 m	0.0000	0.0000	0.1970	0.9415

c) *Combretum adenogonium*

Height class	**< 1 m**	**1 – 2 m**	**2 – 5 m**	**> 5 m**
< 1 m	0.3398	0.6730	0.0032	3.7114
1 – 2 m	0.0072	0.1064	0.0000	0.0000
2 – 5 m	0.0000	0.0266	0.7945	0.0000
> 5 m	0.0000	0.0000	0.1982	0.9884

d) *Vitellaria paradoxa*

Height class	**< 1 m**	**1 – 2 m**	**2 – 5 m**	**> 5 m**
< 1 m	0.3786	0.5710	0.0047	4.2136
1 – 2 m	0.0104	0.2208	0.0000	0.0000
2 – 5 m	0.0000	0.0552	0.7941	0.0000
> 5 m	0.0000	0.0000	0.1985	0.9812

e) *Terminalia* spp.

Height class	**< 1 m**	**1 – 2 m**	**2 – 5 m**	**> 5 m**
< 1 m	0.4122	0.6620	0.0288	1.1020
1 – 2 m	0.0148	0.0083	0.0000	0.0000
2 – 5 m	0.0000	0.0332	0.7692	0.0000
> 5 m	0.0000	0.0000	0.1923	0.9667

Table 6. Transition matrix (**U**) for the five tree species simulating dynamics in an unburned year for each respective tree population.

a) *Acacia dudgeoni*

Height class	< 1 m	1 – 2 m	2 – 5 m	> 5 m
< 1 m	0.8000	0.0000	0.0000	10.7100
1 – 2 m	0.2000	0.8000	0.0000	0.0000
2 – 5 m	0.0000	0.2000	0.8000	0.0000
> 5 m	0.0000	0.0000	0.2000	1.0000

b) *Burkea africana*

Height class	< 1 m	1 – 2 m	2 – 5 m	> 5 m
< 1 m	0.8000	0.0000	0.0000	1.3000
1 – 2 m	0.2000	0.8000	0.0000	0.0000
2 – 5 m	0.0000	0.2000	0.8000	0.0000
> 5 m	0.0000	0.0000	0.2000	1.0000

c) *Combretum adenogonium*

Height class	< 1 m	1 – 2 m	2 – 5 m	> 5 m
< 1 m	0.8000	0.0000	0.0000	3.7100
1 – 2 m	0.2000	0.8000	0.0000	0.0000
2 – 5 m	0.0000	0.2000	0.8000	0.0000
> 5 m	0.0000	0.0000	0.2000	1.0000

d) *Terminalia* spp.

Height class	< 1 m	1 – 2 m	2 – 5 m	> 5 m
< 1 m	0.8000	0.0000	0.0000	1.0800
1 – 2 m	0.2000	0.8000	0.0000	0.0000
2 – 5 m	0.0000	0.2000	0.8000	0.0000
> 5 m	0.0000	0.0000	0.2000	1.0000

e) *Vitellaria paradoxa*

Height class	< 1 m	1 – 2 m	2 – 5 m	> 5 m
< 1 m	0.8000	0.0000	0.0000	4.2100
1 – 2 m	0.2000	0.8000	0.0000	0.0000
2 – 5 m	0.0000	0.2000	0.8000	0.0000
> 5 m	0.0000	0.0000	0.2000	1.0000

RESULTS

The intrinsic (r) and finite (λ) rates of increase, as well as the stable stage distribution (**w**) for the matrices in tables 5 and 6 are presented in tables 7 and 8. Generally, the results show that fire has an unambiguous effect on the population dynamics of all the study species.

Effect of fire frequency on population growth rate (λ)

The growth rate of all the species increased with decreasing fire frequency or increasing fire return interval. Qualitatively, the model results are similar for all the species under annual, triennial and quadrennial burning frequencies. The growth rate (λ) of all the species is < 1.00 under an annual burning event; thus all the species are predicted to decline, while $\lambda > 1.00$ is found under triennial and quadrennial fire frequencies and the tree populations are predicted to increase. Despite these similarities in trend, there are important quantitative differences in the rates of population growth among the species. *Acacia dudgeoni* had the lowest growth rate under annual fire (0.924) and is expected to experience the steepest decline, while under triennial and quadrennial burning frequencies, it had the highest growth rates (1.694 and 2.433, respectively) and is predicted to experience the fastest increase in numbers. Generally, *Burkea africana* and *Terminalia* spp. are predicted to have the slowest increase in numbers under triennial and quadrennial fire frequencies.

The model outcome is, however, mixed for the species under biennial fire frequency. *Burkea africana* and *Terminalia* spp. are predicted to decline, while *Acacia dudgeoni, Combretum adenogonium* and *Vitellaria paradoxa* are expected to increase marginally. In summary, the model results indicate that the minimum fire return interval that will permit the persistence of *Burkea africana* and *Terminalia* spp. is 3 years, while that for *Acacia dudgeoni*, *Combretum adenogonium* and *Vitellaria paradoxa* is 2 years.

Effect of fire frequency on the stable stage (height) distribution (w)

The model results show a paucity of individuals (< 2.0%) in height classes 1-2 m and 2-5 m under annual burning for all the study species. The stable height distributions of *Acacia dudgeoni*, *Combretum adenogonium* and *Vitellaria paradoxa* are quite similar for all the burning frequencies, and have the typical inverted-J shape, while those of *Burkea africana* and *Terminalia* spp. have a pronounced U-shape under annual burning, becoming less of a pronounced U-shape with increasing fire return interval. This is partly due to the very low mortality and topkill rates of mature trees. The predicted height distributions of all the species were significantly different (Chi-square tests, $P < 0.001$) from the observed height distributions (Table 3) under all the four burning frequencies. Therefore, the predictions are that the current height distribution is not stable, whatever the burning regime in the future.

DISCUSSION

The model results predict that annual burning of the savanna near Grupe camp will lead to a decline in the woody plant density as predicted by Sackey (2006). All five study tree species are predicted to decline under annual burning. Although different in design and less sophisticated than the systems models of Norton-Griffiths (1979) and Pellew (1983), these model predictions broadly agree with those of these authors. The model of Norton-Griffiths (1979) predicted a rapid decline of the density of mature trees over 3m tall under 50% burning. Similarly, Pellew (1983) predicted a rapid reduction in the

total population of *Acacia tortilis* towards an eventual extinction under annual fire frequency. From matrix model projections, Hoffmann (1999) also predicted declines in the density of five woody plants under annual and biennial burning in the Brazilian cerrado.

The model results show that the minimum fire-free seasons required for the persistence of woody plants vary from one species to another, in agreement with the model predictions of Hoffmann (1999). In this regard, two species, *Burkea africana* and *Terminalia* spp. are the most critical, requiring a minimum fire-return interval of > 2 years, while 2 years minimum burning interval is predicted for the maintenance of *Acacia dudgeoni*, *Combretum adenogonium* and *Vitellaria paradoxa* populations. These differences in critical fire frequencies probably represent variations in fire susceptibility among the species and could be explored through further studies to formulate burning policy for the Park.

The discrepancies between the observed and predicted height distributions for all the species under all the simulated fire frequency regimes suggest that the tree populations are not in balance with the measured rates of growth, survival or reproduction or may well indicate that the life-history parameters of the tree species (tree survival, growth and seedling production) and, by inference, the environmental factors influencing them (e.g. rainfall, fire intensity and frequency) have not been constant as implied in the models, but have varied over time. The discrepancies could possibly indicate inaccuracies in the transition matrix elements arising from the fact that the estimated rates for tree survival derived from data presented in Sackey (2006) were not an accurate reflection of reality. Transition matrices derived from detailed, long-term population life-history data may be required to resolve this interpretational uncertainty.

Deterministic transition matrix models are concerned with revealing demographic information about the population under present conditions, rather than portraying the likely future appearance of the population under study (Enright and Watson, 1991). Thus, what can be concluded from the model results is that the savanna near Grupe camp will decline towards an open, grassy vegetation under annual or biennial burning, given that the measured rates for growth, survival and reproduction in the woody plants will remain constant through time. This conclusion raises one important question about the future of the woody vegetation of the area: will it be possible for the woody plants to persist under annual burning if the rates of growth, survival and reproduction vary over time? The most plausible answer to this question is yes. Within a relatively small vegetation unit, burning can be expected to be thorough. However, in large vegetation units there is bound to be increased variability in site conditions, and burning is more likely than not to be patchy and random. Under such a site-specific random fire regime, there could be occasional fire-free intervals of long enough duration to permit occasional tree recruitment to ensure the maintenance of the woody plant populations even under frequent fires. As the model predictions suggest, fire-free intervals of up to 4 years may be enough to ensure the persistence of the woody plant populations. Such a circumstance has been demonstrated for *Miconia albicans* in the Brazilian cerrado by Hoffmann (1999).

The model results pose an important question about the future of the vegetation near Grupe camp *vis-à-vis* the annual burning policy of the Park management, as well as suggesting several important lines of further research. The model construction relied on some data that were collected at only one time instance, as well as several important assumptions. A larger series of matrices constructed with detailed long-term population life-history data that incorporate fire as a stochastic event would be an improvement. Also, the data incorporated in the model did not permit the examination of other sources of environmental variability, which may have possibly accounted for the discrepancies found between the observed and predicted stage class distributions. It would, therefore, be helpful to characterize the tree population response to other factors (e.g. rainfall) in addition to fire. Lastly, the model analyses did not address the important issue of density-dependent and competitive effects (population-regulation mechanisms) upon the life-history parameters of the tree populations, which may well be important.

Management implications of the results

In the Guinea savanna vegetation near Grupe camp with negligible numbers of large mammalian herbivores to reduce grass fuel, abundant regeneration of woody plants and poor recruitment of trees into large individuals, fire control remains the main viable measure to prevent the inevitable extermination of fire-sensitive woody species such as *Sterculia setigera* and *Parkia biglobosa* and vegetation transformation towards an open grassland, with a few scattered large trees. Although fire and elephant depredation are both regarded as natural ecological factors which have played significant parts in the realization of savanna plant communities, and are thus indispensable to their maintenance and survival, such extreme vegetation transformation is certainly at variance with the Park's objective of ensuring the conservation of wild genetic materials.

It is not certain what the burning frequency and intensity of the vegetation were before the designation of the area as a Game Reserve in 1958 and later a National Park in 1971, as no fire history exists for the entire area. Historically, the area which is now the National Park was fairly heavily populated by the Bole Division of the West Gonja tribe before 1870 (Hossain and Hall, 1996).

Table 7. Intrinsic rate of increase (*r*), finite rate of increase (λ) and the stable stage distribution (**w**) for the five trees species under different fire frequencies.

a) Annual fire frequency.

Plant species	*r*	λ	Stable stage distribution (%)			
			< 1 m	1-2 m	2-5 m	> 5 m
Acacia dudgeoni	-0.030	0.924	93.60	1.99	0.48	3.93
Burkea africana	-0.060	0.942	70.18	0.32	0.03	29.47
Combretum adenogonium	-0.010	0.990	84.54	0.69	0.09	14.68
Terminalia spp.	-0.032	0.968	66.11	1.12	0.17	32.71
Vitellaria paradoxa	-0.013	0.987	86.21	1.17	0.34	12.28

b) Biennial fire frequency

Plant species	*r*	λ	Stable stage distribution (%)			
			< 1 m	1-2 m	2-5 m	> 5 m
Acacia dudgeoni	0.160	1.173	90.37	3.80	2.35	3.47
Burkea africana	-0.034	0.967	75.49	1.41	1.42	21.68
Combretum adenogonium	0.067	1.069	84.59	2.61	2.12	10.67
Terminalia spp.	-0.004	0.996	72.46	1.38	1.92	24.24
Vitellaria paradoxa	0.134	1.144	82.06	4.88	3.73	9.34

c) Triennial fire frequency

Plant species	*r*	λ	Stable stage distribution (%)			
			< 1 m	1-2 m	2-5 m	> 5 m
Acacia dudgeoni	0.527	1.694	87.63	4.23	4.29	3.85
Burkea africana	0.107	1.113	73.47	2.00	5.40	19.13
Combretum adenogonium	0.298	1.347	81.39	3.46	5.26	9.88
Terminalia spp.	0.113	1.120	72.45	1.03	5.46	21.14
Vitellaria paradoxa	0.386	1.471	78.43	6.36	6.37	8.85

d) Quadrennial fire frequency

Plant species	*r*	λ	Stable stage distribution (%)			
			< 1 m	1-2 m	2-5 m	> 5 m
Acacia dudgeoni	0.889	2.433	85.96	4.36	5.53	4.15
Burkea africana	0.280	1.322	71.22	2.25	8.13	18.40
Combretum adenogonium	0.554	1.740	79.09	3.80	7.31	9.80
Terminalia spp.	0.271	1.312	70.38	1.31	8.23	20.09
Vitellaria paradoxa	0.650	1.915	76.21	6.97	8.00	8.81

Table 8. The population growth rate of the five tree species under the different burning frequencies.

Plant species	Population growth rate (λ)			
	Annual burn	Biennial burn	Triennial burn	Quadrennial burn
Acacia dudgeoni	0.924	1.173	1.694	2.433
Burkea africana	0.942	0.967	1.113	1.322
Combretum adenogonium	0.990	1.069	1.347	1.740
Terminalia spp.	0.968	0.996	1.120	1.312
Vitellaria paradoxa	0.987	1.144	1.471	1.915

According to Norton-Griffiths (1979), in the African savannas, other potent forces of disruption to vegetation succession besides elephants and fire are generated following the creation of new national parks, and for Mole, the sudden removal of human impacts (cattle grazing and harvesting of grass as thatch for roofing of houses) may have constituted a major disruptive force. Additionally, the skewed distribution of large mammalian herbivores towards the south-eastern section of the Park, where they are better protected from harassment by poachers, has meant very low grass off-take, and therefore, large amount of grass fuel to support annual intense fires in the vegetation to the southwest near Grupe camp and other areas. It is, therefore, plausible that fire intensities and extent have generally increased since the creation of the Park.

The most important question regarding burning in Mole concerns the frequency. There is every indication that fire frequency and intensity in the savanna near Grupe camp are high and detrimental and, therefore, require management action to reduce them if the Park's objectives are to be met. Complete protection of the entire savanna near Grupe camp, as well as other areas for which the findings of this study may be relevant over an extended period, is a counsel of perfection that will most certainly be rendered virtually unattainable by administrative and practical difficulties. In addition, an inappropriate fire regime may itself constitute a disruptive force to vegetation succession.

As the matrix population projection results suggest, a minmum fire-free interval of 3 years may be sufficient to ensure the maintenance of the main woody species. However, given the fact that other woody species (e.g. *Parkia biglobosa* and *Sterculia setigera*) are less fire-tolerant than the five study species, a minimum fire return interval of > 3 years may be required to permit the persistence of the majority of the woody species. It would, therefore, seem feasible to attempt complete protection in relatively small blocks on a rotational system that would achieve a burning frequency of 3-5 years, depending on the conditions of the vegetation and other factors such as rainfall. This will allow the abundant coppice re-sprouts adequate time to attain a size that will make them less sensitive to fire impacts, thereby increasing tree recruitment potential. Additionally, seedling input will increase through increased seed production and seedling survival rate. In this regard, the existing fire-break at the south-western boundary of the Park should be properly maintained and extended further northwards to prevent uncontrolled anthropogenic fires from outside the park boundary escaping into the Park. Additional fire-breaks should be created and properly maintained around the demarcated vegetation blocks. Also, regular monitoring of the area should be undertaken during the dry season so as to deter poachers who constitute the major cause of wildfire that is started within the Park and also to deal with any fires from accidental causes (e.g. spotting[1]) or fires from natural causes such as lightning.

CONCLUSION

In Mole National Park, the policy is to burn the vegetation annually early in the dry season. The long-term effect of this annual burning policy of the Park's management is likely to be a vegetation transformation from a savanna woodland to a grassland with only a few woody elements. This prediction is supported by the matrix model projections, and is consistent with the results of several studies (e.g. Trapnell, 1959; Charter and Keay, 1960; Ramsay and Rose-Innes, 1963; Hopkins, 1965; Brookman-Amissah *et al*., 1980; Hoffmann, 1999). The model results also suggest that the minimum fire-free interval required for tree population maintenance varies from species to species, and demonstrate the potential of matrix population models as a tool for determining appropriate burning frequencies for different vegetation units in conservation areas located within the savanna ecosystem. The findings indicate a minimum fire-free interval of at least two years for the maintenance of all the five tree species.

ACKNOWLEDGEMENT

The authors are deeply indebted to the government of Ghana for funding the study. We are grateful to the Executive Director of the Wildlife Division of Ghana for permission to undertake the field data collection work in Mole National Park. Our sincere thanks are also due the staff of the Park, especially Mr. D. K. Ewur for his hospitality and Mr. A Majeed for his invaluable assistance in the field.

REFERENCES

Ben-Shahar, R. 1998. Changes in structure of savanna woodlands in northern Botswana following the impacts of elephants and fire. Plant Ecology. 136:189-194.

Brookman-Amissah, J., Hall, JB., Swaine, MD. and Attakorah, JY. 1980. A Re-assessment of a fire protection experiment in North-Eastern Ghana savanna. Journal of Applied Ecology. 17:85-99.

Caswell, H. 1982. Stable population structure and reproductive value for populations with complex life cycles. Ecology. 63:1223-1231.

Caswell, H. and Trevisan, MC. 1994. Sensitivity analysis

[1] The initiation of a new fire ahead of a main fire by an airborne firebrand or ember (Luke and McArthur, 1978).

of periodic matrix models. Ecology. 75(5):1299-1303.

Charter, JR. and Keay, RWJ. 1960. Assessment of the Olokomeji fire-control experiment (Investigation 254) 28 years after institution. Nigeria Forestry Information Bulletin. 3:1-32.

Crouse, DT., Crowder, LB. and Caswell, H. 1987. A stage-based population model for loggerhead sea turtles and implications for conservation. Ecology. 68:1412-1423.

Croze, H. 1974. The Seronera bull problem II: The trees. East African Wildlife Journal. 12:29-47.

Desmet, PG., Shackleton, CM. and Robinson, ER. 1996. The population dynamics and life-history attributes of a *Pterocarpus angolensis* DC. Population in the Northern Province, South Africa. South African Journal of Botany. 62(3):160-166.

Dublin, HT., Sinclair, ARE. and McGlade, J. 1990. Elephants and fire as causes of multiple stable states in the Serengeti-Mara woodlands. Journal of Animal Ecology. 59:1147-1164.

Enright, NJ. and Watson, AD. 1991. A matrix model analysis for the tropic tree, *Araucaria cunninghamii*. Australian Journal of Ecology. 16(4):507-520.

Frost, PGH. and Robertson, F. 1987. The ecological effects of fire in savannas. In: Deterninants of Tropical Savannas. Ed. Walker, BH. IRL Press, Oxford. 93-140.

Hall, JB. and Jeník, J. 1968. Contribution towards the classification of savanna in Ghana. Bull. Inst. Fond. Afr. Noire. 30, ser. A. 1:84-99.

Hartshorn, GS. 1975. A matrix model of tree population dynamics. In: Tropical ecological systems, Eds. Golley, FB. and Medina, E. Springer-Verlag. New York. 41-51.

Hoffmann, WA. 1999. Fire and population dynamics of woody plants in a neotropical savanna: matrix model projections. Ecology. 80(4):1354-1369.

Hopkins, B. 1965. Observations on savanna burning in the Olokomeji Forest Reserve, Nigeria. Journal of Applied Ecology. 2:367-381.

Hossain, M. and Hall, JB. 1996. Tress of Mole National Park, Damongo, Ghana (2nd ed.). Accra: Ghana Institute of Journalism Press.

Lefkovitch, LP. 1965. The study of population growth in organisms grouped in stages. Biometrics. 21:1-18.

Lewis, DM. 1987. Fruiting patterns, seed germination, and distribution of *Sclerocarya caffra* in an elephant-inhabited woodland. Biotropica. 19(1):50-56.

Luke, RH. and McArthur, AG. 1978. Bush fires in Australia. Canberra: Australian Government Publishing Service.

Norton-Griffiths, M. 1979. The influence of grazing, browsing, and fire on the vegetation dynamics of the Serengeti. In: Serengeti: Dynamics of an ecosystem. Eds. Sinclair, ARE. and Norton-Griffiths, M., University of Chicago Press, Chicago. 310-352.

Pellew, RAP. 1983. Modelling and the systems approach to management problems: The *Acacia*/elephant problem in the Serengeti. In: Management of large mammals in African conservation areas. Owen-Smith, RNPretoria. Haum Educational Publishers. 93-114.

Ramsay, JM. and Rose-Innes, R. 1963. Some quantitative observations on the effects of fire on the Guinea Savanna vegetation of Northern Ghana over a period of eleven years. African Soils. 8:41-85.

Rose-Innes, R. 1972. Fire in West African vegetation. Proceedings of the Tall Timbers Fire Ecology Conference. 11:147-173.

Sackey, I. 2006. Aspects of the composition and structure of the woody savanna vegetation of Mole National Park, Ghana, with special reference to fire and elephant impacts. Ph.D. thesis, University of Bradford, UK. (Unpublished).

Sackey, I. and Hale, WHG. 2008. The effects of perennial fires on the woody vegetation of Mole National Park, Ghana. Journal of Science and Technology. 28 (2):36-47.

Silva, JF., Raventos, J., Caswel, H. and Trevisan, MC. 1991. Population responses to fire in a propical savanna grass: a matrix model approach. Journal of Ecology. 79:345-356.

Swaine, MD., Hawthorne, WD. and Orgle, TK. 1992. The effects of fire exclusion on savanna vegetation at Kpong, Ghana. Biotropica. 24(2a):166-172.

Thomson, PJ. 1975. The role of elephants and other agents in the decline of a *Brachystegia boehmii* woodland. Journal of South African Wildlife Management Association. 5(1):11-18.

Trapnell, CG. 1959. Ecological results of woodland burning experiments in Northern Rhodesia. Journal of Ecology. 47:129-168.

Trollope, WSW. 1983. Control of bush encroachment with fire in the arid savannas of southern Africa. Ph.D. thesis, University of Natal, Pietermaritzburg.

Received: Sept 30, 2011; Accepted: Dec 19, 2011

SENRA Academic Publishers, Burnaby, British Columbia
Vol. 6, No. 1, pp. 1759-1783, Feb 2012
Online ISSN: 1920-3853; Print ISSN: 1715-9997

Canadian Journal of pure&applied sciences

EFFECTS OF ENVIRONMENTAL POLLUTION ON AQUATIC VERTEBRATES AND INVENTORIES OF HALEJI AND KEENJHAR LAKES: RAMSAR SITES

M Zaheer Khan, *Darakhshan Abbas, Syed Ali Ghalib, Rehana Yasmeen, Saima Siddiqui,
Nazia Mehmood, Afsheen Zehra, Abeda Begum, Tanveer Jabeen, Ghazala Yasmeen and Tahira A Latif
Department of Zoology, Faculty of Science, University of Karachi, Karachi-75270

ABSTRACT

In the present study, the effects of environmental pollution on aquatic vertebrates of two Ramsar Sites viz. Haleji and Keenjhar Lakes were noted and inventories of the vertebrate fauna were prepared during 2006-2009. In the water samples taken from Haleji Lake, the pesticides of organophosphate (OP) and organochlorine (OC) groups were estimated above the Maximum Acceptable Concentrations (MAC). These concentrations were much higher in muscles and fat contents than other tissues of birds. All water samples from Keenjhar Lake found contained pesticides below the MAC level. The analysis revealed that KB Feeder Canal is the major source of pollution to Keenjhar Lake. The depletion of Dissolved Oxygen indicated organic pollution harmful for aquatic biodiversity. A total of 22 species of mammals, 228 species of birds, 32 species of reptiles, 2 species of amphibia, 37 species of fishes and 33 species of plants were recorded from Haleji Lake, while, 25 species of mammals, 121 species of birds, 29 species of reptiles, 2 species of amphibia, 54 species of fishes and 258 floral species were recorded from the Keenjhar Lake. The biodiversity of Haleji Lake is on decline due to many environmental and anthropological factors. In Keenjhar Lake, the number of water birds visiting the lake during migratory season has fallen considerably mainly due to hunting, disturbance and habitat degradation. There are also problems of increasing pollution and resulting eutrophication.

Keywords: Wetlands of Sindh, Ramsar Sites, aquatic vertebrates, inventories.

INTRODUCTION

Natural wetlands of Pakistan are disappearing due to increased urbanization, expansion of agriculture, irrigation systems and drainage systems.

The biodiversity of Sindh is unique due to presence of various ecosystems and diverse range of landscapes including deserts, wetlands, riverine and mangrove forests, agriculture, and coastal areas. Sindh is located on the Central Asian Flyway which provides many ideal habitats for several migratory species of birds.

Thatta District is very important due to its wetlands, wildlife protected areas and cultural heritage sites. The two study sites i.e. Haleji and Keenjhar Lakes are located in this district (Fig. 1).

Haleji Lake

It is located at 067° 46'E and 24° 47'N with 60m elevation from sea level. The lake is spread in an area 6.58km^2 (1,704ha) with level of water about 1-1.5m and maximum depth about 5-6m. The area is silty, muddy and sandy. The Lake is situated at a distance of 21km from Thatta and 88km from Karachi. It is a perennial freshwater lake with associated marshes and adjacent brackish seepage lagoons, set in stony desert of limestone and sandstone bedrocks. This Lake was a saline lagoon and in late 1930s it was converted into reservoir to provide an additional supply to Karachi. It is a homeland to a number of important fauna especially birds. The area is also important for Marsh Harrier, Pallas's Fishing Eagle, Monitor Lizards and Fishes.

Haleji Lake with its surrounding lagoons provides an important wintering and staging site for a number of waterbirds, including Coots and Ducks, and it is also a breeding site for many birds like Egrets and Herons, Cotton Teal (upto 55), Spotbill Duck (upto 60), Purple Moorhen (upto 1,470) and Pheasant-tailed Jacana (upto 850). Marshes of the area host as roosting sites to some thousand Night Herons.

The Sindh Wildlife Department maintains a Captive Breeding Centre at the lake in which Hog Deer (*Axis porcinus*), Marsh Crocodile (*Crocodylus palustris*), Smooth-coated Otter (*Lutrogale perspicillata*), Mallard (*Anas platyrhynchos*) and Pea Fowl (*Pavo cristatus*) are kept.

Keenjhar Lake

Keenjhar Lake is located at 68° 03'E and 24° 56'N. It is one of the largest lakes of Pakistan with an area 13,468ha and supplies water to the villages around the lake, and to Karachi city, Keti Bunder and Thatta. It is a perennial freshwater lake fed by River Indus. The lake is located at

*Corresponding author email: darakhshan.moon@gmail.com

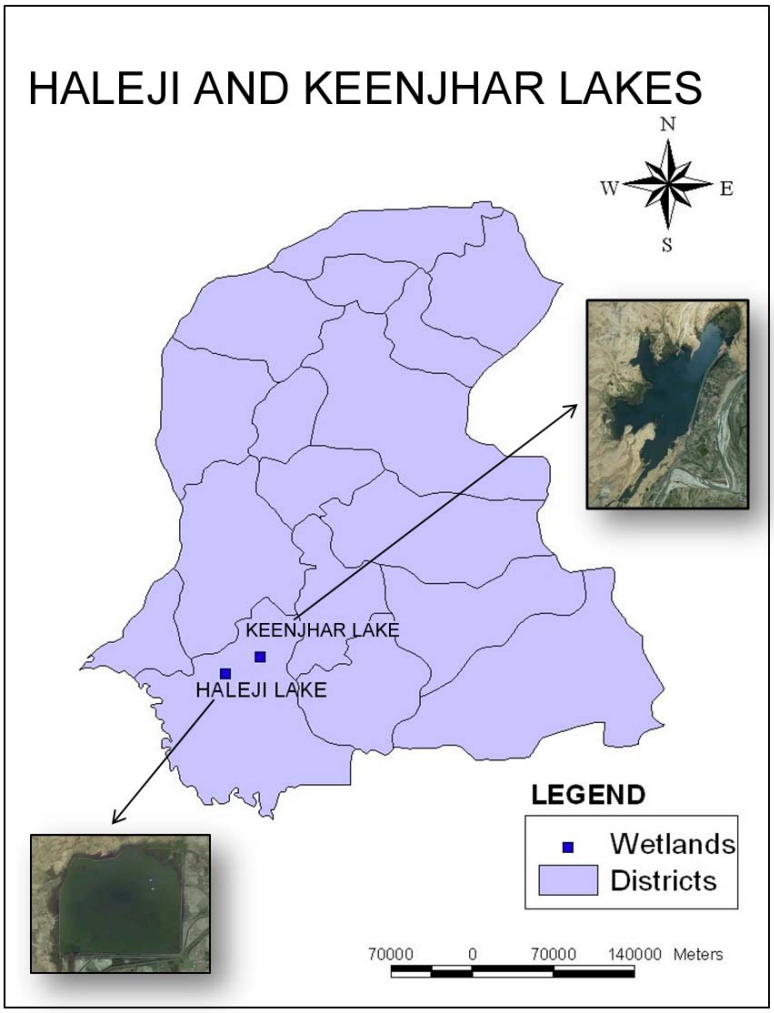

Fig. 1. Map of Sindh province, showing location of Haleji and Keenjhar Lakes.

about 19km North and North-East of Thatta town at a distance of 113km from Karachi city. The lake is associated with adjacent brackish seepage lagoons and marshes which are in a stony desert. It was made in 1930s by the joining of Keenjhar and Kalri Lakes, because of the construction of Chiliya Bangla dam and bunds of 12 km along the east side of the lake. Many small seasonal streams also feed the lake. KB Feeder canal is the main source of water supply to the lake and enters the lake from northwestern corner of lake area. The lake has only one outlet through Jam branch canal towards northern and western parts.

The Lake provides a number of natural resources in which fishing is considerably important because most of the 50 villages nearby are either partially or fully dependent on the lak. Thus, around 35-40,000 people are dependent on the lake.

The area has a great importance as roosting, wintering and breeding site for a number of resident and migratory birds. Night Heron (*Nycticorax nycticorax*), Cotton Teal (*Nettapus coromondelianus*), Pheasant-tailed Jacana (*Hydrophasianus chirurgus*) and Purple Moorhen (*Porphyrio porphyrio*) are some of the important breeding birds of this lake although Cotton Teal has disappeared in the recent years. It is also an important area for the game birds such as Grey Partridge (*Francolinus pondicerianus*) and Chestnut-bellied Sandgrouse (*Pterocles exustus*). Fishing Cat (*Prionailurus viverrinus*), Smooth-coated Otter (*Lutrogale perspicillata*), Cotton Teal (*Nettapus coromandelianus*), Pallas's Fishing Eagle (*Haliaeetus leucoryphus*), Indian Monitor Lizard (*Varanus bengalensis*) and Spiny-tailed Lizard (*Saara hardwickii*) are the key species of the area.

A small patch of Mangrove trees of *Avicinia marina* also exists near the lake area and used by locals as fodder for the camels. Hilaya Forest is also located near the eastern bank of the lake which is under severe logging pressure by the nearby communities.

The published work relating to the biodiversity of these two wetlands and/ or its biological and environmental studies includes the following: Ali and Ripley (1987), Ahmad and Khan (1974), Ashraf and Jaffar (1990), Ashraf *et al*. (1991, 1992), Baqai and Rehana (1973), Baqai and Siddiqui (1973), Baqai *et al*. (1974a,b), Condor (1977), Durranee and Khan (2008), Ghalib *et al*. (1981), Ghalib and Bhaagat (2004), Ghalib *et al*. (2004, 2006), Ghalib and Nawaz (2008), Ghalib *et al*. (2009), Grimmett *et al*. (1998, 2008), Ghani (1975), IFAP (2007, 2009), IUCN (2004), Jaffar *et al*. (1988), Jafri *et al*. (1999), Javed and Rehman (2004), Jalbani (2009), Jehangir *et al*. (2000), Karim (1985), Kazmi *et al*. (2006), Khan (2004, 2005), Khan and Ghalib (2006), Khan and Haleem (1986), Khan *et al*. (2010, 2012), Khanum and Ahmad (1990-1991), Korai *at al*. (2008a,b), Lashari *et al*. (2001, 2009), Mahar *et al*. (2010), Mirza (2001, 2007), Nazneen (1994, 1980), Nazneen and Begum (1992), Qureshi (1965), Rais *et al*. (2009), Rais and Abbas (2010), Rahman and Javed (2004), Roberts *et al*. (1986), Roberts (1991, 1992, 1997, 2005a,b), Sahato *et al*. (2004), Saqib *et al*. (1990-91a,b, 2003), Saqib *et al*. (2005), Scott (1989), Scott and Poole (1989), Sheikh and Molur (2005), Siddiqui *et al*. (1973, 1990), Siddiqui and Saqib (1993) and Siddiqui (1998).

There are several factors that can adversely affect and change biodiversity within aquatic ecosystems. Aquatic biodiversity may decrease due to pollution, fragmentation, habitat destruction, or the introduction of an invasive species. In many countries, anthropogenic activities have lead to aquatic organisms being at a higher risk for extinction compared to terrestrial mammals, water birds and amphibians (Ali *et al*., 2011). The objective of the present study was to investigate the effects of environmental pollution on aquatic vertebrates and preparation of the inventories of the two Ramsar Sites, Haleji and Keenjhar Lakes.

MATERIALS AND METHODS

Study Areas

After baseline study, some important areas were selected for the study as shown in tables 1 and 2.

Methodology of Physico-chemical Samples Collection and Analysis

During the study from 2006- 2009, conductivity meter was used for the estimation of conductivity, Total Dissolved Solids, Turbidity, Salinity, and pH was recorded by pH meter, Alkalinity, Carbon dioxide and Phosphates were examined by the process of Acid Base Titration (Titrimetric methods), Total Hardness, Calcium, Magnesium and Chloride were analyzed by using EDTA (Complexometric Titration), Basic Oxygen Demand was examined by Incubation Method-Redox Titration, while Sulphate was analyzed by Gravimetric method, Nitrate was analyzed by Brucine Colorimetric Method and Cadmium, Chromium, Lead and Nickel were analyzed by atomic absorption Spectro-photometric Method.

Table 1. Main wildlife habitats in Haleji Lake area.

S. No.	Name of study area	Co-ordinates
1.	Main Lake	24 47. 243 N 067 45. 421 E
2.	Near Information Centre	24 47 12.2 N 67 47 24.0 E
3.	Near Rest Houses	24 49.161 N 67 46 .171 E 24 47. 446 N 67 44 .940 E
4.	Seepage Lagoon/Villages	24 49 19.3 N 67 45 36.7 E
5.	Near Regulator	24 49 19.3 N 67 47 58.0 E

Table 2. Main wildlife habitats in Keenjhar Lake area.

S. No.	Name of study area	Co-ordinates
1.	Reservoir area	24 54 .40 N 68 04 .21 E
2.	Daulatpur	24 55 .36 N 68 01 .55 E
3.	Moldi	24 58 .06 N 68 01. 38
4.	Sonehri	25 01 .067 N 68 07 .877 E
5.	Jhimpir	25 02 .163 N 68 05 .740 E
6.	Garhi Mai orFossil Valley	24 54 .486 N 68 01 .348 E
7.	Chilia	24 50 190 N 68 00 081 E
8.	Adam Bhambhro Village	24 51 .102 N 67 59. 761 E
9.	Chull Area	25 03 55.6 N 68 07 45.6 E
10.	Garho Pir /Garho Shah	24 55. 942 N 68 02. 640 E
11.	Main Lake Area	24 54 990 N 68 04 387 E 24 58 .378 N 68 05 .566 E 24 58 7465 N 68 05 .578 E 24 54 .657 N 68 06 .501 E 25 06 .628 N 68 07 .636 E
12.	Chakro	24 01 69.6 N 68 02 06.0 E
13.	Jhol Lake	24 50 988 N

		67 5885.6 E
14.	Amir Peer (Drainage inlet into the lake)	25 00 24.6 N 68 05 24.5 E
15.	K.B. Feeder Canal	25 02 21.7 N 68 07 55.2 E

Methodology for Faunal Surveys

Survey of Mammals

For large and medium size mammals, several direct and indirect methods were used such as roadside counts, counts of tracks, footprints, burrows, pellet counts, point surveys and line transects. One effective way to survey small mammals is active searching, particularly during the daytime. This method is equally applicable to both nocturnal and diurnal species, particularly in potential and suitable microhabitats along the canal banks, open plains, bushy areas and agriculture fields. Active searching is very effective for inventory of *Gerbillus*, *Meriones*, *Hystrix*, and *Hemiechinus spp.*

For small mammals, active searching, traps and trapping procedure were used. Specifically, Sherman traps were used to collect the live specimens of rodents.

Survey of Birds

Each major habitat type in the study area was first identified and surveys were made to record the species of birds found in each discrete habitat such as lakes, canals, ponds, marshes, forest, agriculture fields, vicinity of human habitation and fallow lands. The number of birds observed in each habitat type was also recorded with particular emphasis on the key species and to relate the data to other components of the study area such as vegetation, water and soil etc.

Line transects method was used as the most common field method. It is based on recording birds continually along a predefined route within a predefined survey unit. This method is suitable for extensive, open and uniform habitats and for large and conspicuous species.

Survey of Reptiles and Amphibians

Various methods were employed for observation of reptiles and amphibians.

A: Direct Counting:

In direct counting method, one-hour plot searching, use of pitfall traps, spot lighting or night observations, turning of stones, rock and rotten trees and study of basking behavior were used for searching and observing reptiles and amphibians.

B: Indirect Counting

Indirect counting method was also used for counting and observing reptiles and amphibians including presence of signs like faecal pellets, tracks, den or tunnels (egg laying excavation), evidences from the impression of finger or foot prints, or tail assisted in determing the existence, range and rough population of reptilian fauna.

Fish Collection Methodology

The methods used for obtaining the representative sample of fish species are the gill netting and cast netting.

Gill Netting

Three nets each measuring 15m length with mesh size 2.5x2.5cm and 1.5x1.5cm were used for gill netting. The gill nets were used in the morning.

Cast Netting

Cast nets with known circumference were casted in a stretch of 200m. Five cast nets were used on a line at different stations along the bank of the reservoir. Fish species were collected and identified and released after identification.

RESULTS

In the present study, the environmental impacts of factors such as pollution have been assessed. In addition, inventories of mammals, birds, reptiles, amphibians, fish and plants of the two lakes have been prepared.

Haleji Lake

Physico-chemical Parameters

Several physico-chemical parameters were analyzed to determine water quality of both lakes. Temperature, Conductivity, Total Dissolved Solids, pH, Turbidity, Alkalinity, Total Hardness, Salinity, Basic Oxygen Demand, Carbon dioxide, Magnesium, Sulphates, Chloride, Calcium, Nitrate, Phosphates, Cadmium, Chromium, Lead and Nickel were selected for the analysis of water quality, and parameters were analyzed seasonally.

Aquatic biodiversity is sensitive to changes in water temperature. Temperature is an important water quality parameter and is relatively easy to measure, during the studies, water temperature in pre-monsoon observed from 27 to 33^0C, while in post monsoon it varied from 24 - 30^0 C. The air temperature in pre- monsoon recorded from 26 - 36^0C, while in post monsoon it varied from 27 - 31^0C. Conductivity varied from 390 - 1820mg/l, TDS varied from 190 - 1520mg/l. The pH of water can provide information about several chemical and biological processes and provides indirect correlations to a number of different impairments, here pH ranged from 6.2 - 8.2, turbidity ranged from 2.0 - 8.0NTU, alkalinity ranged from 39 - 132mg/l, total hardness recorded from 81-153mg/l, salinity from 0.5 - 2.02mg/l, Basic Oxygen Demand from 4.2mg/l - 6.78mg/l, Carbon dioxide from 1 - 2mg/l, Calcium from 43 - 82mg/l, the range of

Magnesium was recorded from 39 - 72mg/l, Chloride ranged from 39.6 - 122mg/l, range of Nitrates was 0.13 - 1.09mg/L, range of Phosphates from 0.012 - 0.63mg/l, range of Cadmium varied from 0.00 - 0.021mg/l, Chromium from 0.00 to 0.07mg/l, Lead from 0.00 to 0.01mg/l, and Nickel recorded from 0.2 - 0.6mg/l (Table 3).

Bioecological Studies

Based on field surveys during the study, 22 mammalian species, 228 species of birds, 32 reptilian species, 2 species of amphibians and 37 species of fishes were recorded (Tables 4-8).

Status of Various Species

Mammals

Table 3. Water Quality Analysis of Heleji Lake during 2006-2009.

Parameters	Haleji Lake							
	Average Pre-monsoon				Average Post-monsoon			
	2006	2007	2008	2009	2006	2007	2008	2009
Colour	A	A	A	A	A	A	A	A
Odour	O	O	O	O	O	O	O	O
Water Temperature (^oC)	31.33	27.67	29.00	31.67	15.67	16.67	16.33	15.00
Air Temperature (^oC)	33.67	28.67	32.00	34.33	18.67	19.67	19.67	18.33
Conductivity (µS/cm)	960.00	846.67	913.33	910.00	960.00	960.00	1066.67	1006.67
TDS (mg/l)	456.33	408.33	438.33	422.00	896.67	820.00	885.00	713.33
pH	7.33	7.42	7.44	7.57	7.51	7.41	7.48	7.74
Turbidity (NTU)	2.92	2.53	2.58	2.33	7.71	7.34	6.94	7.15
Alkalinity	123.33	118.00	120.33	114.00	40.00	40.67	40.33	42.33
Total Hardness (mg/l)	146.33	142.33	147.00	142.67	114.67	98.00	128.67	101.33
Salinity (mg/l)	1.82	1.77	1.46	1.79	0.66	0.64	0.65	0.57
BOD (mg/l)	5.38	5.24	4.70	5.38	6.05	6.16	6.11	6.01
Carbon dioxide (mg/l)	1.33	1.67	1.67	1.33	1.33	2.00	1.67	1.00
Calcium (mg/l)	76.67	70.67	75.00	79.67	48.00	44.33	43.67	43.67
Magnesium (mg/l)	55.33	50.33	57.67	57.33	70.67	64.33	42.00	62.67
Sulphates (mg/l)	20.00	20.00	18.33	18.67	119.00	132.67	62.67	116.33
Chloride (mg/l)	41.97	44.43	46.00	47.87	114.67	120.00	123.67	103.67
Nitrates (mg/l)	0.66	0.72	0.65	0.79	0.50	0.51	36.07	0.52
Phosphates (mg/l)	0.05	0.05	0.05	0.05	0.02	0.01	0.55	0.02
Cadmium (mg/l)	0.00	0.00	0.00	0.02	0.01	0.01	0.55	0.02
Chromium (mg/l)	0.02	0.04	0.01	0.02	0.05	0.05	0.02	0.02
Lead (mg/l)	0.01	0.01	0.00	0.00	0.00	0.01	0.05	0.01
Nickel (mg/l)	0.23	0.01	0.10	0.28	0.03	0.09	0.01	0.33

Table 4. List of Mammals of Haleji and Keenjhar Lakes.

S. No.	Order/Family	Scientific name	Common name	**Haleji**	**Keenjhar**
Order	Insectivora				
Family	Ericinaceidae				
1.		*Paraechinus micropus*	Indian Hedgehog	+	--
2.		*Hemiechinus collaris*	Long-eared Desert Hedgehog	+	+
Family	Soricidae				
3.		*Suncus murinus*	House Shrew	+	--
Order	Rodentia				
Family	Hystricidae				
4.		*Hystrix cristatus*	Indian Crested Porcupine	+	+
Family	Sciuridae				
5.		*Funambulus pennanti*	Palm Squirrel	+	+

Continued…

The commn species of mammals found in the area were Palm Squirrel (*Funambulus pennanti*), House Mouse

Table 4 continued…

S. No.	Order/Family	Scientific name	Common name	**Haleji**	**Keenjhar**
Family	Muridae				
6.		*Rattus rattus*	Roof Rat	+	+
7.		*Mus musculus*	House Mouse	+	+
8.		*Mus booduga*	Little Indian Field Mouse	+	--
9.		*Mus saxicola*	Grey Spiny Mouse		+
10.		*Nesokia indica*	Short-tailed Mole Rat	+	+
11.		*Meriones hurrianae*	Indian Desert Jird	+	+
12.		*Tatera indica*	Indian Gerbil	+	+
13.		*Gerbillus nanus*	Balochistan Gerbil	+	+
14.		*Bandicota bengalensis*	Indian Mole Rat	--	+
Order	Chiroptera				
Family	Megadernatidae				
15.		*Hipposideros fulvus*	Leaf-nosed Bat	--	+
Family	Vespertilionidae				
16.		*PipistrellusKuhlii*	Kuhl's Bat	+	+
Family	Pteropidae				
17.		*Rhinopoma microphyllum*	Large Mouse-tailed Bat	--	+
Order	Carnivora				
Family	Canidae				
18.		*Canis aureas*	Asiatic Jackal	+	+
19.		*Vulpes bengalensis*	Bengal Fox	+	+
20.		*Vulpes vulpes*	Desert Fox	--	+
Family	Mustellidae			--	
21.		*Lutrogale perspicillata*	Smooth-coated Otter		+
Family	Herpestidae				
22.		*Herpestes edwardsi*	Grey Mongoose	+	+
23.		*Herpestes javanicus*	Small Indian Mongoose	+	+
24.					
Family	Felidae				
25.		*Felis chaus*	Jungle Cat	+	+
26.		*Felis sylvestris*	Indian Desert Cat	+	--
27.		*Prionailurus viverrina*	Fishing Cat	+	+
Family	Viverridae				
28.		*Viverricula indica*	Small Indian Civet	+	--
Order	Artiodactyla				
Family	Suidae				
29.		*Sus scrofa*	Indian Wild Boar	--	+
Order	Pholidata				
Family	Manidae				
30.		*Manis crassicaudata*	Indian Pangolin	--	+
Order	Lagomorpha				
Family	Leporidae				
31.		*Lepus nigricollis*	Desert Hare	+	+

Table 5. List of Birds of Haleji and Keenjhar Lakes.

S. No.	Order/Family	Scientific name	Common name	**Haleji**	**Keenjhar**
Order	Podicipediformes				
Family	Podicipedidae				
1.		*Tachybaptus ruficollis*	Little Grebe	+	+
2.		*Podiceps cristatus*	Great Crested Grebe	+	--

Continued…

Table 5 continued…

S. No.	Order/Family	Scientific name	Common name	**Haleji**	**Keenjhar**
Order	Pelecaniformes				
Family	Phalacrocoracidae				
3.		*Phalacrocorax carbo*	Great Cormorant	+	--
4.		*Phalacrocorax fuscicollis*	Indian Shag	+	--
5.		*Phalacorcorax niger*	Little Cormorant	+	+
6.		*Anhinga melanogaster*	Snake Bird	+	--
Family	Pelecanidae				
7.		*Pelecanus onocrotalus*	White Pelican	+	--
8.		*Pelecanus crispus*	Delmatian Pelican	+	--
Order	Ciconiiformes				
Family	Ardeidae				
9.		*Ixobrychus sinensis*	Yellow Bittern	+	--
10.		*Ixobrychus cinnamomeus*	Chestnut Bittern	+	--
11.		*Dupetor flavicollis*	Black Bittern	+	--
12.		*Nycticorax nycticorax*	Night Heron	+	+
13.		*Ardeola grayii*	Pond Heron	+	+
14.		*Bubulcus ibis*	Cattle Egret	+	+
15.		*Egretta gularis*	Western Reef Heron	+	--
16.		*Egretta garzetta*	Little Egret	+	+
17.		*Egretta intermedia*	Intermediate Egret	+	+
18.		*Ardea alba*	Great White Egret	+	+
19.		*Ardea cinerea*	Grey Heron	+	--
20.		*Ardea purpurea*	Purple Heron	+	+
Family	Ciconiidae				
21.		*Anastomus oscitans*	Openbill Stork	+	--
22.		*Ciconia ciconia*	White Stork	+	--
Family	Threskiornithidae				
23.		*Plegadis falcinellus*	Glossy Ibis	+	--
24.		*Threskiornis melanocephalus*	White Ibis	+	--
25.		*Platalea leucorodia*	Spoonbill	+	--
Family	Phoenicopteridae				
26.		*Phoenicopterus roseus*	Greater Flamingo	+	--
Order	Accipitriformes				
Family	Accipitridae				
27.		*Elanus caeruleus*	Black-winged Kite	+	+
28.		*Milvus migrans*	Black Kite	+	+
29.		*Haliastur indus*	Brahminy Kite	+	+
30.		*Haliaeetus albicilla*	White-tailed Sea Eagle	+	
31.		*Haliaeetus leucoryphus*	Pallas's Fishing Eagle	+	+
32.		*Gyps bengalensis*	White-backed Vulture	+	+
33.		*Gyps fulvus*	Griffon Vulture	--	+
34.		*Aegypius monachus*	Cinereous Vulture	--	
35.		*Circaetus gallicus*	Short-toed Eagle	+	+
36.		*Circus aeruginosus*	Marsh Harrier	+	+
37.		*Circus macrourus*	Pallid Harrier	+	--
38.		*Accipiter badius*	Shikra	+	--
39.		*Butastur teesa*	White-eyed Buzzard	+	--
40.		*Buteo buteo*	Desert Buzzard	+	--
41.		*Buteo rufinus*	Long-legged Buzzard	+	--

Continued…

Table 5 continued…

S. No.	Order/Family	Scientific name	Common name	**Haleji**	**Keenjhar**
42.		*Aquila clanga*	Greater Spotted Eagle	+	+
43.		*Aquila nipalensis*	Steppe Eagle	+	--
44.		*Aquila rapax*	Tawny Eagle	+	--
45.		*Aquila heliaca*	Imperial Eagle	+	--
46.		*Hieraaetus pennatus*	Booted Eagle	+	--
47.		*Hieraaetus fasciatus*	Bonelli's Eagle	+	--
Family	Pandionidae				
48.		*Pandion haliaetus*	Osprey	+	+
Order	Falconiformes				
Family	Falconidae				
49.		*Falco tinnunculus*	Kestrel	+	+
50.		*Falco chiquera*	Red-headed Merlin	+	+
Order	Anseriformes				
Family	Anatidae				
51.		*Dendrocygna javanica*	Lesser Whistling Teal	+	--
52.		*Dendrocygna bicolor*	Greater Whistling Teal	+	--
53.		*Cygnus columbianus*	Bewick's Swan	+	--
54.		*Anser erythropus*	Lesser White-fronted Goose	+	--
55.		*Tadorna ferruginea*	Ruddy Shelduck	+	--
56.		*Tadorna tadorna*	Common Shelduck	+	--
57.		*Anas acuta*	Pintail	+	+
58.		*Anas penelope*	Wigeon	+	--
59.		*Anas crecca*	Common Teal	+	+
60.		*Anas strepera*	Gadwall	+	+
61.		*Anas platyrhynchos*	Mallard	+	--
62.		*Anas querquedula*	Garganey	+	--
63.		*Anas poecilorhyncha*	Spotbill Duck	+	+
64.		*Anas clypeata*	Shovelller	+	+
65.		*Aythya ferina*	Common Pochard	+	+
66.		*Aythya nyroca*	White-eyed Pochard	+	--
67.		*Aythya fuligula*	Tufted Duck	+	+
68.		*Aythya marila*	Scaup	+	--
69.		*Netta rufina*	Red-crested Pochard	+	--
70.		*Nattapus coromandelianus*	Pygmy Cotton Teal	+	+
71.		*Marmaronetta angustirostris*	Marbled Teal	+	--
Order	Galliformes				
Family	Phasianidae				
72.		*Francolinus francolinus*	Black Partridge	+	--
73.		*Francolinus pondicerianus*	Grey Partridge	+	+
74.		*Coturnix coturnix*	Common Quail	+	--
Order	Gruiformes				
Family	Rallidae				
75.		*Porzana porzana*	Spotted Crake	+	--
76.		*Amaurornis phoenicurus*	White-breasted Waterhen	+	+
77.		*Gallinula chloropus*	Indian Moorhen	+	+
78.		*Porphyrio porphyrio*	Purple Moorhen	+	--
79.		*Gallicrex cinerea*	Watercock	+	--
80.		*Rallus aquaticus*	Water Rail	+	--
81.		*Fulica atra*	Coot	+	+
82.		*Porzana porzana*	Spotted Crake	+	--

Continued…

Table 5 continued…

S. No.	Order/Family	Scientific name	Common name	**Haleji**	**Keenjhar**
Family	Gruidae				
83.		*Grus grus*	Common Crane	+	--
84.		*Grus virgo*	Demoiselle Crane	+	--
Order	Charadriiformes				
Family	Jacanidae				
85.		*Hydrophasianus chirurgus*	Pheasant-tailed Jacana	+	+
86.		*Metopidius indicus*	Bronze-winged Jacana	+	--
Family	Recurvirostridae				
87.		*Himantopus himantopus*	Black-winged Stilt	+	+
88.		*Recurvirostra avosetta*	Avocet	+	--
Family	Burhinidae				
89.		*Glareola pratincola*	Collared Pratincole	+	--
90.		*Glareola lactea*	Small Indian Pratincole	+	--
Family	Charadriidae				
91.		*Charadrius leucurus*	White-tailed Lapwing	+	+
92.		*Vanellus vanellus*	Green Plover	+	--
93.		*Vanellus indicus*	Red-wattled Lapwing	+	+
94.		*Vanellus malabaricus*	Yellow-wattled Lapwing	+	--
95.		*Pluvialis squatarola*	Black-bellied Plover	+	--
96.		*Pluvialis dominica*	Eastern Golden Plover	+	--
97.		*Charadrius dubius*	Little Ringed Plover	+	+
98.		*Charadrius alexandrinus*	Kentish Plover	+	+
Family	Scolopacidae				
99.		*Calidris minuta*	Little Stint	+	+
100.		*Calidris temminckii*	Temminck's Stint	+	+
101.		*Calidris alpina*	Dunlin	+	--
102.		*Philomachus pugnax*	Ruff	+	--
103.		*Gallinago gallinago*	Common Snipe	+	+
104.		*Limosa limosa*	Black-tailed Godwit	+	--
105.		*Numenius arquata*	Curlew	+	--
106.		*Numenius phaeopus*	Whimbrel	+	--
107.		*Tringa erythropus*	Spotted Redshank	+	--
108.		*Tringa totanus*	Redshank	+	--
109.		*Tringa stagnatilis*	Marsh Sandpiper	+	+
110.		*Tringa nebularia*	Greenshank	+	+
111.		*Tringa ochropus*	Green Sandpiper	+	+
112.		*Tringa glareola*	Wood Sandpiper	+	+
113.		*Tringa hypoleucos*	Common Sandpiper	+	+
Family	Laridae				
114.		*Larus argentatus*	Herring Gull	+	+
115.		*Larus heuglini*	Heuglin's Gull	+	--
116.		*Larus ichthyaetus*	Great Black-headed Gull	+	+
117.		*Larus brunnicephalus*	Brown-headed Gull	+	--
118.		*Larus ridibundus*	Black-headed Gull	+	+
119.		*Larus genei*	Slender-billed Gull	+	--
120.		*Larus canus*	Common Gull	+	--
Family	Sternidae				
121.		*Chlidonias hybridus*	Whiskered Tern	+	+
122.		*Chlidonias leucoptera*	White-winged Black Tern	+	--
123.		*Gelochelidon nilotica*	Gull-billed Tern	+	+

Continued…

Table 5 continued…

S. No.	Order/Family	Scientific name	Common name	**Haleji**	**Keenjhar**
124.		*Hydropogne caspia*	Caspian Tern	+	--
125.		*Sterna aurentia*	River Tern	+	+
126.		*Sterna albifrons*	Little Tern	+	+
127.		*Sterna acuticauda*	Black-bellied Tern	--	+
128.		*Sterna bergii*	Large Crested Tern	+	--
Family	Rhynchopidae				
129.		*Rhychops albicollis*	Indian Skimmer	+	--
Order	Columbiformes				
Family	Pteroclididae				
130.		*Pterocles exustus*	Chestnut-bellied Sandgrouse	+	+
Family	Columbidae				
131.		*Columba livia*	Blue Rock Pigeon	+	+
132.		*Columba eversmanni*	Eastern Rock Pigeon	+	--
133.		*Treron phoenicoptera*	Yellow-legged Green Pigeon	+	--
134.		*Streptopelia decaocto*	Collared Turtle Dove	+	+
135.		*Streptopelia tranquebarica*	Red Turtle Dove	+	--
136.		*Streptopelia senegalensis*	Little Brown Dove	+	+
Order	Psittaciformes				
Family	Psittacidae				
137.		*Psittacula krameri*	Rose-Ringed Parakeet	+	+
Order	Cuculiformes				
Family	Cuculidae				
138.		*Clamator jacobinus*	Pied-crested Cuckoo	+	--
139.		*Eudynamus scolopacea*	Koel	+	+
140.		*Centropus sinensis*	Greater Coucal or Crow Pheasant	+	+
Order	Strigiformes				
Family	Strigidae				
141.		*Otus bakkamoena*	Collared Scops Owl	+	--
142.		*Bubo bubo*	Eagle Owl	+	--
143.		*Athene brama*	Spotted Owlet	+	--
Order	Caprimulgiformes				
Family	Caprimulgidae				
144.		*Caprimulgus asiaticus*	Indian Little Nightjar	+	--
145.		*Caprimulgus europaeus*	European Nightjar	+	--
146.		*Caprimulgus mahrattensis*	Syke's Nightjar	--	+
Order	Apodiformes				
Family	Apodidae				
147.		*Apus affinis*	House Swift	+	+
Order	Coraciiformes				
Family	Alcedinidae				
148.		*Ceryle rudis*	Lesser Pied Kingfisher	+	+
149.		*Alcedo atthis*	Common Kingfisher	+	+
150.		*Halcyon smyrnensis*	White-breasted Kingfisher	+	+
Family	Meropidae				
151.		*Merops persicus*	Blue-cheeked Bee-eater	+	--
152.		*Merops orientalis*	Green Bee-eater	+	+
Family	Coraciidae				
153.		*Coracias garrulus*	European Roller	+	--

Continued…

Table 5 continued…

S. No.	Order/Family	Scientific name	Common name	**Haleji**	**Keenjhar**
154.		*Coracias bengalensis*	Indian Roller	+	+
Family	Upupidae				
155.		*Upupa epops*	Hoopoe	+	+
Order	Piciformes				
Family	Picidae				
156.		*Jynx torquilla*	Wryneck	+	--
157.		*Dinopium bengalensis*	Lesser Golden-backed Woodpecker	+	+
158.		*Dendrocopos mahrattensis*	Yellow-fronted Pied Woodpecker	+	--
Order	Passeriformes				
Family	Alaudidae				
159.		*Mirafa erythroptera*	Indian/Red-Winged Bush Lark	+	--
160.		*Eremopterix grisea*	Ashy-crowned Finch Lark	+	+
161.		*Eremopterix nigriceps*	Black-crowned Finch Lark	--	+
162.		*Ammomanes deserti*	Desert Finch Lark	+	+
163.		*Calandrella cinerea*	Yarkan Short-toed Lark	+	--
164.		*Galerida cristata*	Crested Lark	+	+
165.		*Alauda gulgula*	Oriental Sky Lark	--	+
Family	Hirundinidae				
166.		*Riparia paludicola*	Plain Martin	+	+
167.		*Hirundo rustica*	Barn Swallow	+	+
168.		*Hirundo smithii*	Wire-tailed Swallow	+	+
169.		*Hirundo daurica*	Red-rumped Swallow	+	--
Family	Motacillidae				
170.		*Anthus rufulus*	Paddyfield Pipit	+	+
171.		*Anthus campestris*	Tawny Pipit	+	+
172.		*Anthus trivialis*	Tree Pipit	+	--
173.		*Motacilla flava*	Yellow Wagtail	+	+
174.		*Motacilla citreola*	Yellow-headed Wagtail	+	--
175.		*Motacilla alba*	Pied Wagtail	+	+
176.		*Motacilla maderaspatensis*	White-browed Pied Wagtail	--	+
Family	Campephagidae				
177.		*Tephrodornis pondicerrianus*	Common Woodshrike	+	--
178.		*Pericrocotus cinnamomeus*	Wandering Minivet	+	--
Family	Pycnonotidae				
179.		*Pycnonotus leucogenys*	White-cheeked Bulbul	+	+
180.		*Pycnonotus cafer*	Red-vented Bulbul	+	+
Family	Turdidae				
181.		*Cercotrichas galactotes*	Rufous Chat/Rufous-tailed Scrub Robin	+	--
182.		*Luscinia svecica*	Bluethroat	+	+=
183.		*Phoenicurus ochruros*	Black Redstart	+	+
184.		*Saxicola caprata*	Pied Bush Chat	+	--

Continued…

Table 5 continued…

S. No.	Order/Family	Scientific name	Common name	**Haleji**	**Keenjhar**
185.		*Oenanthe alboniger*	Hume's Wheatear	--	+
186.		*Oenanthe deserti*	Desert Wheatear	+	+
187.		*Oenanthe picata*	Pied Chat	+	+
188.		*Saxicoloides fulicata*	Indian Robin	+	+
Family	Sylviidae				
189.		*Sylvia nana*	Desert Warbler	+	--
190.		*Sylvia hortensis*	Orphean Warbler	+	--
191.		*Sylvia curruca*	Lesser Whitethroat	+	+
192.		*Sylvia communis*	Common Whitethroat	+	--
193.		*Cettia cetti*	Cetti's Warbler	+	+
194.		*Prinia buchanani*	Rufous-fronted Long-tailed Warbler	+	--
195.		*Prinia gracilis*	Streaked Wren Warbler	+	--
196.		*Prinia inornata*	Plain Prinia	--	+
197.		*Prinia flaviventris*	Yellow Bellied Long-tailed Warbler	+	+
198.		*Prinia burnesii*	Long-tailed Grass Warbler	+	--
199.		*Orthotomus sutorius*	Tailor Bird	+	+
200.		*Acrocephalus stentoreus*	Clamorous Great Reed Warbler	+	+
201.		*Acrocephalus dumetorum*	Blyth's Reed Warbler	+	--
202.		*Acrocephalus agricola*	Paddy-field Warbler	+	+
203.		*Hippolais caligata*	Syke's Tree Warbler	+	--
204.		*Phylloscopus nitidus*	Bright Green Leaf Warbler	+	--
205.		*Phylloscopus neglectus*	Plain Leaf Warbler	+	+
206.		*Phylloscopus collybita*	Brown Leaf Warblet	+	--
Family	Rhipiduridae				
207.		*Rhipidura rhipidura*	White-browed Fantail Flycatcher	--	+
Family	Muscicapidae				
208.		*Muscicapa striata*	Spotted Flycatcher	+	--
209.		*Ficedula parva*	Red-throated Flycatcher	+	--
210.		*Hypothymus azurea*	Black-naped Flycatcher	+	--
Family	Timaliidae				
211.		*Turdoides caudatus*	Common Babbler	+	+
212.		*Turdoides earlei*	Striated Babbler	+	+
213.		*Turdoides striatus*	Jungle Babbler	+	+
Family	Nectariniidae				
214.		*Nectarinia asiatica*	Purple Sunbird	+	+
Family	Dicruridae				
215.		*Dicrurus macrocercus*	Black Drongo/King Crow	+	+
Family	Laniidae				
216.		*Lanius merodionalis*	Southern Grey Shrike	+	+
217.		*Lanius isabellinus*	Isabelline Shrike	+	+
218.		*Lanius schach*	Rufous-backed Shrike	+	
219.		*Lanius vittatus*	Bay-backed Shrike	+	+
Family	Corvidae				
220.		*Dendrocitta vagabunda*	Tree Pie	+	+

Continued…

Table 5 continued…

S. No.	Order/Family	Scientific name	Common name	**Haleji**	**Keenjhar**
221.		*Corvas corax*	Common Raven	+	--
222.		*Corvus splendens*	House Crow	+	+
Family	Sturnidae				
223.		*Sturnus vulgaris*	Common Starling	+	+
224.		*Sturnus roseus*	Rosy Pastor	+	--
225.		*Acridotheres tristis*	Indian Myna	+	+
226.		*Acridotheres ginginianus*	Bank Myna	+	+
Family	Passeridae				
227.		*Passer domesticus*	House Sparrow	+	+
228.		*Passer hispaniolensis*	Spanish Sparrow	+	--
229.		*Passer pyrrhonotus*	Sindh Jungle Sparrow	+	--
230.		*Petronia xanthocollis*	Yellow-throated Sparrow	+	+
Family	Ploceidae				
231.		*Ploceus philippinus*	Baya/Weaver Bird	+	--
232.		*Ploceus manyar*	Streaked Weaver	+	+
Family	Estrilidae				
233.		*Lonchura malabarica*	White-throated Munia/Indian Silver Bill	+	+
Family	Fringillidae				
234.		*Fringilla montifringilla*	Brambling	+	--
235.		*Bucanetes githagineus*	Trumpeter Finch	+	--
Family	Emberizidae				
236.		*Emberiza buchanani*	Grey-necked Bunting	+	--
237.		*Emberiza melanocephala*	Black-headed Bunting	+	--
238.		*Emberiza striolata*	Striolated Bunting/House Bunting	+	+

Table 6. List of Reptiles of Haleji and Keenjhar Lakes.

S. No.	Order/Family	Scientific name	Common name	**Haleji**	**Keenjhar**
Order	Chelonia				
Family	Trionychidae				
1.		*Lissemys punctata*	Indian Flap-shell Turtle	+	+
Family	Emydidae				
2.		*Geoclemys hamiltonii*	Spotted Pond Turtle	+	--
Order	Squamata				
Family	Elapidae				
3.		*Bungarus caeruleus*	Indian Krait	+	+
4.		*Naja naja*	Indian Cobra	+	+
		Naja oxiana	Oxus Cobra/Brown Cobra	--	+
Family	Colubridae				
5.		*Coluber fasciolatus*	Banded Racer	--	+
6.		*Lycodon striatus*	Spotted Wolf Snake	+	+
7.		*Lytorhynchus paradoxus*	Sindh Awl –headed Snake	+	--
8.		*Platyceps ventromaculatus*	Glossy-bellied Racer	+	+
9.		*Platyceps rhodorachis*	Streaked Kukri Snake	--	+
10.		*Oligodon taeniolatus*	Cliff Racer	--	+
11.		*Psammophis condanarus*	Indian Sand Snake	+	+

Continued…

Table 6 continued…

S. No.	Order/Family	Scientific name	Common name	**Haleji**	**Keenjhar**
12.		*Psammophis leithii*	Pakistan Ribbon Snake	+	--
13.		*Psammophis schokari*	Afro-Asian Sand Snake	+	--
14.		*Ptyas mucosus*	Dhaman	+	+
15.		*Spalerosophis diadema*	Royal Snake	+	--
16.		*Xenochrophis piscator*	Checkered-keel Back	+	--
Family	Boidae				
17.		*Exyx johnii*	Common Sand Boa	+	--
18.		*Eryx conicus*	Russel's Sand Boa	+	+
Family	Viperidae				
19.		*Echis carinatus*	Saw-scaled Viper	+	+
20.		*Daboia russelii*	Russel's Viper	+	+
Family	Lacertidae				
21.		*Acanthodactylus cantoris*	Indian Fringe-toed Lizard	+	+
22.		*Ophisops jerdonii*	Punjab Snake-eyed Lacerta	--	+
Family	Scincidae				
23.		*Ophiomorus tridactylus*	Three-toed Sand Swimmer	+	--
Family	Varanidae				
24.		*Varanus griseus*	Desert Monitor Lizard	+	--
25.		*Varanus bengalensis*	Indian Monitor lizard	+	+
Family	Uromastycidae				
26.		*Saara hardwickii*	Indian Spiny-tailed Lizard	+	+
Family	Agamidae				
27.		*Trapelus megalonyx*	Afghan Ground Agama	+	+
28.		*Trapelus agilis*	Brilliant Agama	+	+
29.		*Calotes versicolor*	Indian Garden Lizard	+	+
Family	Eublepharidae				
30.		*Eublepharis macularius*	Fat-tailed Gecko	--	+
Family	Gekkonidae				
31.		*Cyrtopodian kachhensis*	Warty Rock Gecko	+	+
32.		*Cyrtopodian scaber*	Keeled Rock Gecko	+	+
33.		*Crossobamon orientalis*	Sindh Sand Gecko	+	--
34.		*Hemidactylus flavivirdis*	Yellow-bellied House Gecko	+	+
35.		*Hemidactylus brookii*	Spotted Indian House Gecko	+	+
36.		*Hemidactylus leschenaultia*	Bark Gecko	+	+
Order	Crocodilia				
Family	Crocodylidae				
37.		*Crocodylus palustris*	Marsh Crocodile	+	--

Table 7. List of Amphibians of Haleji and Keenjhar Lakes.

S. No.	Order/Family	Scientific name	Common name	**Haleji**	**Keenjhar**
Order	Anura				
Family	Ranidae				
1.		*Euphlyctis cyanophylictis*	Skittering Frog	+	+
Family	Bufonidae				
2.		*Duttaphrynus stomaticus*	Indus or Marbled Toad	+	+

Continued…

Table 8. List of Fishes of Haleji and Keenjhar Lakes.

S. No.	Order/Family	Scientific name	**Haleji**	**Keenjhar**
Order	Clupieformes			
Family	Clupiedae			
1.		*Gadusia chapra*	+	+
2.	Osteoglossiformes	*Notopterus chitala*	+	+
3.	Notopteridae	*Notopterus notopterus*	+	+
Order				
Family				
4.		*Chela cachius*	+	+
5.		*Salmostoma bacaila*	--	+
6.		*Securicula gora*	--	+
7.		*Amblypharyngodon mola*	--	+
8.		*Aspidoparia morar*	--	+
9.		*Barilius vagra*	--	+
10.		*Esomus danricus*	--	+
11.		*Rasbora daniconius*	+	+
12.		*Barbodes sarana*	+	+
13.		*Catla catla*	+	+
14.		*Cirrhinus mrigala*	+	+
15.		*Cirrhinus reba*	--	+
16.		*Labeo calbasu*	+	+
17.		*Labeo dero*	--	+
18.		*Labeo dyocheilus*	--	+
19.		*Labeo gonius*	+	+
20.		*Labeo rohita*	+	+
21.		*Osteobrama cotio*	--	+
22.		*Puntius chola*	--	+
23.		*Puntius fimbriatus*	+	
24.		*Puntius sophore*	+	+
25.		*Puntius ticto*	+	+
26.		*Cyprinus carpio*	--	+
27.		*Ctenpharyngodon idella*	--	+
28.		*Aristchthys nobilis*	--	+
29.		*Hypophthalmichthys molitrix*	--	+
Order	Siluriformes			
Family	Bugridae			
30.		*Aorichthys aor*	+	--
31.		*Mystus bleekeri*	--	+
32.		*Mystus cavasius*	+	+
33.		*Mystus gulio*	+	--
34.		*Mystus vittatus*	+	+
35.		*Rita rita*	+	+
Family	Sisoridae			
36.		*Bagarius bagarius*	--	+
37.		*Gagata cenia*	--	+
38.		*Nangra nangra*	--	+
Family	Siluridae			
39.		*Ompok bimaculatus*	+	+
40.		*Wallago attu*	+	+

Continued…

Table 8 continued…

S. No.	Order/Family	Scientific name	**Haleji**	**Keenjhar**
Family	Heteropneustidae			
41.		*Heteropneutes fossilis*	+	+
Family	Schilbeidae			
42.		*Ailia coila*	--	+
43.		*Clpisoma garua*	--	+
44.		*Clpisoma naziri*	--	+
45.		*Eutropiichthys vacha*	+	+
Order	Beloniformes			
Family	Belonidae			
46.		*Xenentodon cancila*	+	+
Order	Channiformes			
Family	Channidae			
47.		*Channa marulia*	+	+
48.		*Channa punctata*	+	+
49.		*Channa striata*	+	--
Order	Perciformes			
Family	Chandidae			
50.		*Chanda nama*	+	+
51.		*Parambassis baculis*	--	+
52.		*Parambassis ranga*	+	+
Family	Badidae			
53.		*Badius badis*	+	--
Family	Mugilidae			
54.		*Sicamugil cascasia*	+	+
Family	Gobidae			
55.		*Glossogobium giuris*	+	--
Family	Belontidae			
56.		*Colisa fasciata*	+	+
57.		*Colisa lalia*	--	+
Family	Cichlidae			
58.		*Oreochromis mossambicus*	+	+
Order	Synbranchiformes			
Family	Mastacembelidae			
59.		*Mastacembelus armatus*	+	+

Legend: + present -- absent

(*Mus musculus*), Indian Gerbil (*Tatera indica*). Indian Hare (*Lepus nigricollis*), Smooth-coated Otter (*Lutrogale perspicillata*) and Wild Boar (*Sus scrofa*) previously reported from the area were not found during our study.

A total of six species recorded as they key species of mammals in Haleji Lake (Table 9).

The threatened species of mammals of the area include Fishing Cat (E) and Smooth-coated Indian Otter (V).

Table 9. Key Species of Mammals of Haleji Lake.

S. No.	Common name	Scientific name
1.	Indian Fox	*Vulpes bengalensis*
2.	Fishing Cat	*Prionailurus viverrinus*
3.	Desert Hare	*Lepus nigricollis*
4.	Small Indian Civet	*Viverricula indica*
5.	Jungle Cat	*Felis chaus*
6.	Smooth-coated Otter	*Lutrogale perspicillata*

Birds

The common birds of the area are Black-headed Gull (*Larus ridibundus*), Little Cormorant (*Phalacorcorax niger*), Purple Moorhen (*Porphyrio porphyrio*), Indian Moorhen (*Gallinula chloropus*), Long-legged Buzzard (*Buteo rufinus*), Coot (*Fulica atra*), Little Grebe/Dabchick (*Tachybaptus ruficollis*), Tufted Duck (*Aythya ferina*), Pied Wagtail (*Motacilla alba*), Yellow Wagtail (*Motacilla flava*), Black Drongo (*Dicrurus macrocercus*), Pied Bush Chat (*Saxicola caprata*), Sand Martin (*Riparia paludicola*) and Wire-tailed Swallow (*Hirundo smithi*).

A total of 13 species of birds have been recorded to be the key species of the area (Table 10).

Table 10. Key Species of Birds of Haleji Lake.

S. No.	Common name	Scientific name
1.	Purple Moorhen	*Porphyrio porphyrio*
2.	Dalmatian Pelican	*Pelecanus crispus*
3.	White Pelican	*Pelecanus onocrotalus*
4.	Pheasant-tailed Jacana	*Hydrophasianus chirurgus*
5.	Cotton Teal	*Nettapus coromandelianus*
6.	Pallas's Fishing Eagle	*Haliaeetus leucorhyphus*
7.	Marsh Harrier	*Circus aeruginosus*
8.	Common Coot	*Fulica atra*
9.	Grey Partridge	*Francolinus pondicerianus*
10.	Night Heron	*Nycticorax nycticorax*
11.	Marbled Teal	*Marmaronetta angustirostris*
12.	Greater Flamingo	*Phoenicopterus roseus*
13.	Moorhen	*Gallinula chloropus*

The threatened birds of the area are White-backed Vulture, *Gyps bengalensis* (CE), Imperial Eagle, *Aquila heliaca* (V), Lesser White-fronted Goose, *Anser erythropus* (V), Pallas's Fishing Eagle, *Haliaeetus leucoryphus* (V), Marbled Teal, *Marmaronetta angustirostris* (V), Dalmatian Pelican, *Pelecanus crispus* (V) and Egyptian Vulture, *Neophron percnopterus* (E) and Darter *Anhinga melanogaster* (NT).

Reptiles

Among reptiles, Indian Garden Lizard (*Calotes versicolor*), Indian Fringe-toed Lizard (*Acanthodactylus cantoris*), Glossy Bellied Racer (*Platyceps ventromaculatus*) and Yellow-bellied House Gecko (*Hemidactylus flaviviridis*) are common.

The key species of the area include; Indian Monitor (*Varanus bengalensis*), Desert Monitor (*Varanus griseus*), and Spiny-tailed Lizard (*Saara hardwickii*), while Marsh Crocodile (*Crocodylus palustris*) is a threatened species of the area.

Amphibians

Skittering Frog (*Euphlyctis cyanophlyctis*) and Indus Toad (*Duttaphrynus stomaticus*) are commonly found.

Fishes

A total of 49 species of fishes have been recorded from the lake. Out of these, 10 species have very high commercial value such as Mori (*Cirrhinus mrigala*), Thaila (*Gibelion catla*), Rohu (*Labeo rohita*), Common Carp (*Cyprinus carpio*), Singhari (*Sperata sarwari*), Fauji Khagga (*Bagarius bagarius*), Malli (*Wallago attu*), Thalli (*Clupisoma garua*), Thalli (*Clupisoma naziri*) and Soul (*Channa marulias*) (Rafiq, 2009). At the present time, the numbers of these food fishes have drastically declined in the lake and now only Tilapia (*Oreochromis mossambicus*) is found in abundance.

Flora

A total of 33 species were recorded. *Hydrilla verticillata*, *Phragmites karka* and *Typha angustata* were found common aquatic floral species in the Haleji Lake.

Keenjhar Lake

Physico-chemical Parameters

During the study period the water temperature of Keenjhar Lake in pre-monsoon varied from 28 - 33^{0}C, while in post monsoon it varied from 16 - 20^{0}C. The air temperature in pre-monsoon varied from 31- 36^0 C while in post monsoon it varied from 18- 24^{0}C. Conductivity of the Keenjhar Lake varied from 453 - 742µS/cm, TDS varied from 243 to 492mg/L, pH value ranged from 6.81 to 8.31, turbidity ranged from 1.37 - 12.6NTU, alkalinity range from 28 - 107mg/l, Total Hardness varied from 58 to 144mg/l, Salinity varied from 0.21 to 1.9mg/l, Value of Basic Oxygen Demand varied from 1.12 - 9.9mg/l, Carbon dioxide ranges from 1 to 2mg/l. Range of Calcium varied from 28 to 87mg/l, range of Magnesium varied from 38 - 106mg/l, range of Sulphates varied from 18 to 156mg/l, Chloride ranged from 35.2 to 98mg/l, range of Nitrate in Keenjhar Lake was 0.04 - 0.37mg/l, range of Phosphate determined during the study varied from 0.006 to 0.28mg/l, range of Cadmium varied from 0.00mg/l to 1.32mg/l, the range of Chromium in Keenjhar Lake varied from 0.00mg/l to 1.01mg/l, value of Lead varied from 0.00 - 0.013mg/l and Nickel varied from 0.01 - 0.80mg/l (Table 11).

Biological Studies

A total of 25 species of mammals, 121 species of birds, 29 species of reptiles, 2 species of amphibians, 54 species of fishes and 258 species of plants were recorded.

Table 11. Water Quality Analysis of Keenjhar Lake during 2006-2009.

Parameters	Keenjhar Lake							
	Average Pre-monsoon				Average Post-monsoon			
	2006	2007	2008	2009	2006	2007	2008	2009
Colour	A	A	A	A	A	A	A	A
Odour	O	O	O	O	O	O	O	O
Water Temperature (^oC)	30.40	29.60	29.60	31.40	16.60	19.60	17.00	18.40
Air Temperature (^oC)	33.40	33.00	32.60	34.40	19.20	22.40	19.80	21.00
Conductivity (µS/cm)	516.80	508.20	509.80	518.40	579.40	615.80	571.40	584.20
TDS (mg/l)	256.20	260.20	253.40	263.00	387.00	389.00	373.60	392.80
pH	7.76	7.77	7.74	7.82	7.94	7.93	7.95	8.00
Turbidity (NTU)	2.59	2.45	2.35	2.68	7.11	6.92	6.63	21.72
Alkalinity	98.22	96.66	93.94	97.80	33.60	33.40	32.20	35.60
Total Hardness (mg/l)	132.20	130.40	127.00	133.60	98.00	97.20	94.20	101.80
Salinity (mg/l)	0.62	0.59	0.61	1.58	0.33	0.26	0.56	1.14
BOD (mg/l)	8.32	8.06	7.80	8.53	1.74	1.74	1.52	1.98
Carbon dioxide (mg/l)	1.60	1.40	1.20	1.40	1.40	1.40	1.60	1.60
Calcium (mg/l)	77.60	74.60	69.80	78.80	34.20	34.80	31.60	38.20
Magnesium (mg/l)	57.60	58.20	54.40	62.20	72.80	76.60	70.80	81.20
Sulphates (mg/l)	18.80	18.80	18.20	19.00	137.20	138.40	132.80	143.60
Chloride (mg/l)	52.38	51.46	49.22	53.44	80.20	82.00	78.20	85.80
Nitrates (mg/l)	0.26	0.22	0.21	0.21	0.15	0.07	0.08	0.10
Phosphates (mg/l)	0.02	0.02	0.02	0.02	0.06	0.03	0.07	0.02
Cadmium (mg/l)	0.00	0.22	0.20	0.05	0.49	0.78	0.15	0.27
Chromium (mg/l)	0.01	0.19	0.04	0.03	0.43	0.51	0.19	0.20
Lead (mg/l)	0.00	0.05	0.01	0.05	0.00	0.00	0.04	0.01
Nickel (mg/l)	0.16	0.55	0.35	0.32	0.45	0.51	0.31	0.29

Status of Various Species

Mammals

The common species of the mammals found in the area include Palm Squirrel *(Funambulus pennanti*), Indian Gerbil (*Tatera indica*), Indian Desert Jird (*Meriones hurrianae*), House Mouse (*Mus musculus*), House Rat (*Rattus rattus*), Asiatic Jackal (*Canis aureus*) and Indian Porcupine (*Hystrix indica*).

The key species of the area include Fishing Cat (*Prionailurus viverrina*), Smooth-coated Otter (*Lutrogale perspicillata*), Bengal Fox (*Vulpes bengalensis*), and Indian Pangolin (*Manis crassicaudata*).

The threatened species are the Fishing Cat, *Prionailurus viverrina* (E) and the Smooth-coated Otter, *Lutrogale perspicillata* (V).

Birds

A total of 121 species were recorded comprising of waterbirds, birds of prey, passerines and game birds. The common birds of the area are Shoveller (*Anas clypeata*), Tufted Duck (*Aythya fuligula*), Grey Partridge (*Francolinus pondicerianus*), Striated Babbler (*Turdoides earlei*), Great Grey Shrike *(Lanius excubator*), Ashy-crowned Finch Lark (*Eremopterix griseus*), Indian Robin *(Saxicoloides fulicata)*, White-cheeked Bulbul *(Pycnonotus leucogenys*), Red-vented Bulbul *(Pycnonotus cafer)*, Tailor Bird *(Orthotomus suturius)*, Bluethroat *(Luscinia svecica)*, Lesser white-throat *(Sylvia curruca)*, Bay-backed Shrike *(Lanius vittatus)*, Pied Bush Chat *(Saxicola caprata)* and Crested Lark *(Galerida cristata)*, while 12 species have been recorded to be the key species of birds (Table 12).

Table 12. Key Species of Birds of Keenjhar Lake.

S. No.	Common name	Scientific name
1.	Cotton Teal	*Nettapus coromandelianus*
2.	Night Heron	*Nycticorax nycticorax*
3.	Purple Moorhen	*Porphyrio porphyrio*
4.	Pheasant-tailed Jacana	*Hydrophasianus chirurgus*
5.	Marsh Harrier	*Circus aeruginosus*
6.	Greater Flamingo	*Phoenicopterus rosues*
7.	White Pelican	*Pelecanus roseus*
8.	Dalmatian Pelican	*Pelecanus crispus*
9.	Grey Partridge	*Francolinus pondicerianus*
10.	Pallas's Fishing Eagle	*Haliaeetus leucorhyphus*
11.	Black-bellied Tern	*Sterna acuticauda*
12.	Ferruginous Duck	*Aythya nyroca*

The threatened and other rare birds recorded are: Ferruginous Duck (NT), Black-bellied Tern (NT), Dalmatian Pelican (V), White Ibis (*Threskiornis melanocephalus*), White Stork (*Ciconia ciconia*) and Cotton Teal (*Nettapus cormandelianus*).

Reptiles
A total of 29 species of reptiles were recorded. The key species include Indian Monitor (*Varanus bengalensis*), Spiny-tailed lizard (*Saara hardwickii*), Indian Flap Shell turtle (*Lissemys punctata*), and Fat-tailed Gecko (*Eublepharis macularius*).

Amphibians
Only 2 species were recorded viz. Skittering Frog (*Euphlyctis cyanophlyctis*) and Marbled Toad (*Duttaphrynus stomaticus*).

Fishes
A total of 54 fish species were recorded. *Catla catla*, *Gadusia chapra*, *Heteropneustis fossilis*, *Labeo rohita*, *Tenuelosa ilisha*, *Notopterus notopterus*, *Wallago attu* and *Xenentodon cancila* are the important fishes of Keenjhar Lake.

Flora
Typha angustata was found as common where as *Tamarix spp.* was found abundant. *Eichhornia crassipes* and *Salvinia molesta* are the common invasive species.

Threatened Species of both lakes
Based on our data 17 species including mammals, birds and reptiles have been recorded as Threatened species from Haleji and Keenjhar Lake areas (Table 13).

Table 13. Threatened Species recorded from Haleji and Keenjhar Lake areas.

S. No.	**Threatened Species**
Mammals	
1.	Smooth-coated Otter (V) (Fig. 2)
2.	Fishing Cat (E) (Fig. 3)
Birds	
1.	Darter (NT) (Fig. 4)
2.	Ferrunginous Duck (NT) (Fig. 5)
3.	Blackbellied Tern (NT) (Fig. 6)
4.	Lesser Whitefronted Goose (V) (Fig. 7)
5.	Marbled Teal (V) (Fig. 8)
6.	Whitebacked Vulture (CE) (Fig. 9)
7.	Imperial Eagle (V) (Fig. 10)
8.	Pallas's Fishing Eagle (V) (Fig. 11)
9.	Dalmatian Pelican (V) (Fig. 12)
10.	Egyptian Vulture (E) (Fig. 13)
Reptiles	
1.	Marsh Crocodile (V)
2.	Indian Softshell Turtle (V)
3.	Crowned River Turtle (V)
4.	Peacock Shell Turtle (V)
5.	Narrow-headed Softshell (E)

DISCUSSION

There are several factors that can adversely affect and change biodiversity within aquatic ecosystems. Aquatic biodiversity may decrease due to pollution, fragmentation, habitat destruction, or the introduction of an invasive species. In many countries, anthropogenic activities have lead to aquatic organisms being at a higher risk for extinction compared to terrestrial mammal water birds and amphibians (Ali *et al*., 2011). Many biochemical and physiological changes in aquatic organisms are caused by pesticides which influence the activities of several enzymes (Khan and Law, 2005).

In the water samples of Haleji Lake, the pesticides of OP and OC groups were estimated above the maximum acceptable concentrations. Earlier, Siddiqui (1998) has also recorded much higher concentration of Dimethoate (OP) and DDT and Dieldrin (Cyclodiene) (OC) and Cypermethrin from Haleji Lake. The concentration was much higher in muscles and fat contents than other tissues of the birds. While water samples of Keenjhar Lake showed pesticides below the maximum acceptable concentration.

The analysis revealed that the KB Feeder Canal is the major source of pollution to these lakes. Turbidity, BOD and COD along with other toxic pollutants such as Cd and Pb were found to be closer to upper limits. These pollutants as well as Ni are already present in the water of the Indus due to discharge of municipal and industrial effluents in it mainly from Kotri Industrial Area. The depletion of dissolved oxygen is the indicator of organic pollution harmful for fishes and other aquatic biodiversity.

Lead and phenol levels have been found to increase after monsoon. This may be due to release of lead and phenol containing substances through the rain flow. The rain water, however, causes dilution, aeration and more biological activity as the BOD and COD load is reduced and solubility level of air in water is increased.

Environmental Problems in Haleji Lake
Haleji Lake used to supply water to Karachi before 2006. Water used to be supplied to Haleji Lake from Keenjhar Lake and then it was supplied to Karachi. After the construction of a direct supply line to Karachi from Keenjhar, the water of the lake has become stagnant which has resulted in the deterioration of water quality.

The ongoing RBOD scheme construction work has caused much degradation in the area. The RBOD is hardly 50-100 feet away from the lake and its water level is 20-30 feet below the level of the wetland area. The lake may be affected by the seepage of its water to the drain.

Fig. 2. Smooth-coated Otter.

Fig. 3. Fishing Cat (Courtesy by true wildlife.blogspot.com).

Fig. 4. Darter.

Fig. 5. Ferrunginous Duck.

Fig. 6. Blackbellied Tern.

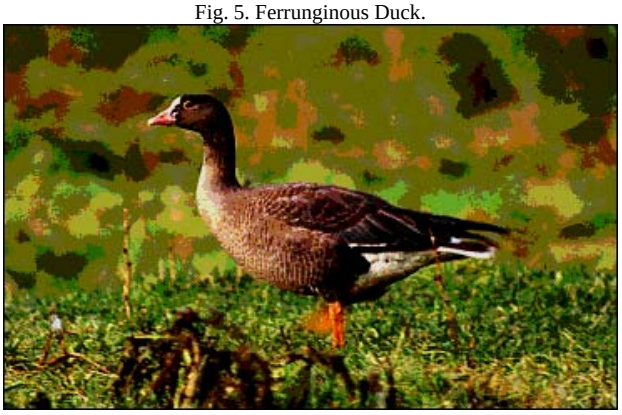

Fig. 7. Lesser Whitefronted Goose.

Most of the marginal area of the lake is overgrown with aquatic vegetation such as Typha, Phragmites and Lotus along with Mesquite elsewhere. So the open water area is shrinking which is the habitat for many waterbirds.

A Few years ago, the Apple Snail (*Pomacea canaliculata*) was introduced into the Haleji Lake. The Snail has since infested the lake and is now the most common species found within. Its negative impacts on the ecology of the lake need to be investigated. Intensive fish angling has been going on in and around the lake area. It has been causing disturbance to the wildlife dependant on the lake.

Environmental Problems in Keenjhar Lake

Keenjhar Lake had been receiving water from the main Indus River through Kalri-Baghar Feeder (KB Feeder)

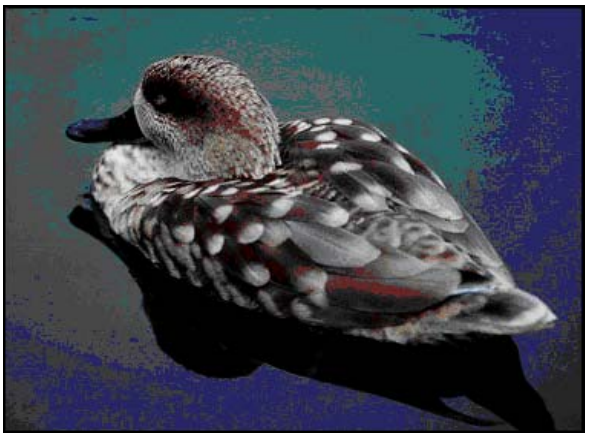

Fig. 8. Marbled Teal (Courtesy by sundancevillas.co.uk).

Fig. 9. Whitebacked Vulture (Courtesy by thefalconrycentre.co.uk).

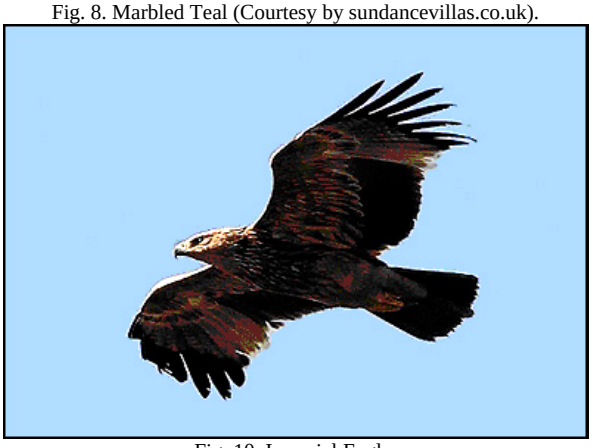

Fig. 10. Imperial Eagle.

Fig. 11. Pallas's Fishing Eagle (Courtesy by indianaturewatch.net).

Fig. 12. Dalmatian Pelican.

Fig. 13. Egyptian Vulture.

canal. Currently the lake's freshwater ecosystem is under threat due to increased industrial and domestic effluent discharge through the Kalri-Baghar Feeder (KB Feeder) canal which carries contaminants from Kotri urban and Industrial area. There are a number of industries in Kotri which dump their effluents into the KB Feeder and these chemicals combined with the sewage discharged by the town end up in Keenjhar Lake (WWFP, 2010).

In the Keenjar Lake, main factor affecting water quality is industrial discharge from Kotri and Nooriabad industries, while eutrophication is also a major problem in the lake. The lake water is being enriched with nutrients causing excessive plant growth. Runoff from agriculture fields containing chemical fertilizers triggers pollution. More than 15,000 people visit this lake every week in the season and the garbage produced is also a source of

Table 14. Annual waterbird Census at Haleji and Keenjhar Lake.

Year	2000	2001	2002	2003	2004	2010	2011
Haleji Lake	69,194	44,931	40,062	15,367	2,570	3,000	2,370
Keenjhar Lake	30,270	38,958	30,470	15,886	3770	7,174	2,252

pollution. Tourists also pollute water by washing their vehicles in the lake.

Tilapia species has been introduced into the lake which is a frequent breeder and a carnivorous fish. It has become widespread in the lake and has somewhat suppressed the native species such as Rohu, Thaila and Murakhi which breed in confined waters.

Moreover, the plant species such as *Eichhornia crassipes* (Water Hyacinth), *Salvania molesta* (Water Fern) *Pistia stratiotus* (Water Lettuce) have occupied most of the open area.

Mats of Water Hyacinth, Water Lettuce and Water Fern impede access to use of waterways for recreational and commercial purposes. These also reduce habitats of waterbirds, moreover, fishes are also facing threats because of these mats which is a negative sign for economy.

Introduction of non-native species of plants and animals may damage the food web, which can in turn destabilize the whole ecosystem resulting in the disappearance of some species or a population buildup of an undesired species.

Due to many environmental and anthropological factors, annual waterbird census from 2000 showed decline in bird population in both lakes (Table 14). Our data shows that Heleji Lake has a rich vertebrate biodiversity as compared to Keenjhar Lake (Table 15), but due to environmental and other anthropogenic factors, this wetland is threatened.

Table 15. Biodiversity recorded from Haleji and Keenjhar Lake.

S. No.	Animal Groups	**Haleji Lake** (number of species)	**Keenjhar Lake** (number of species)
1.	**Mammals**	27	25
2.	**Birds**	225	111
3.	**Reptiles**	32	29
4.	**Amphibians**	02	02
5.	**Fishes**	42	55

CONCLUSION

The results of the present study defined an alarming situation due to pollution in the two wetlands. Detailed studies are required for pollution control. The environmental effects of unlined RBOD system passing through these two lakes area need to be monitored. The overall population of migratory waterbirds has been decreasing over the two wetlands due to large scale disturbance, hunting and trapping in Keenjhar area, while due to hunting and habitat degradation and poor water quality in Haleji Lake. Ecotourism may be developed at Keenjhar Lake by managing the wetland through Public Private Partnership Programme. Wetland conservation may be promoted through policy development, training, capacity building and awareness programs. The data is sufficient enough to chalkout and implement a monitoring program to provide protection to the threatened species and their habitats. Being the first study of its kind, it will serve as a baseline data for the future workers on the biodiversity and environment of the area.

ACKNOWLEDGEMENTS

Thanks are due to WWF-Pakistan Karachi office for extending help and facilities for wildlife surveys at Haleji and Keenjhar Lakes. The authors are also grateful to Mr. Hussain Bux Bhaagat, Conservator Wildlife, Sindh Wildlife Department and Syed Fazal Shah, Incharge, Haleji Wildlife Sanctuary for providing information regarding the wildlife of the area during the visit to the lake. Thanks to Miss. Sumaiya Ahmed, Department of Geography, University of Karachi for preparation of map.

REFERENCES

Ahmad, MF. and Khan, SA. 1974. A Checklist of Freshwater Fishes of Sindh Province, Pakistan. Biologia. 20(2):119-131.

Ali, S. and Ripley, SS. 1987. Compact Handbook of the Birds of India and Pakistan. Oxford University Press, Dehli. pp737.

Ali, SFM., Ben HHS., Alehaideb, Z., Khan, MZ., Louie, A., Fageh, N. and Law, F. 2011. A Review on the Effects of Some Selected Pyrethroids and Related Agrochemicals on Aquatic Biodiversity. Canadian Journal of Pure and applied Sciences. 5(2):1455-1464.

Ashraf, M. and Jaffar, M. 1990. Contents of Selected macronutrients in various local Freshwater Fish. Pakistan Jour. Sc. Ind. Res. 33:278-280.

Ashraf, M., Jaleel, T. and Jaffar, M. 1991. Contents of Trace metals in Fish, Sediment and Water from three Freshwater Reservoirs on the Indus River. Pakistan Fish. Res. 12:355-364.

Ashraf, M., Jaffar, M. and Jaleel, T. 1992. Annual variation of Selected Trace metals in Freshwater Lake Fish, *Labeo rohita*, as an Environmental Pollution. Toxicol. Env. Chem. 35:1-7.

Baqai, IU. and Rehana, I. 1973. Seasonal Fluctuation of Freshwater Copepods of Kinjher Lake, Sindh and its correlation with Physcio-chemical factors. J. Zool. 5 (2): 165-168.

Baqai, IU. and Siddiqui, PA. 1973. Problems of Freshwater fisheries in Sindh with special reference to Pollution and Eutrophication. Jadeed Sci. 14 (in Urdu).

Baqai, IU., M. Iqbal. and VA. Zuberi. 1974[a]. Limnological Studies of Kalri Lake. Agriculture Pakistan. 25 (2):119-135.

Baqai, IU., Siddiqui, PA. and Iqbal, M. 1974[b]. Limnological Studies of Haleji Lake. Agriculture Pakistan. 25 (4):321-344.

Conder, PJ. 1977. Lake Haleji Wildlife Sanctuary Management Plan. (unpublished Report).

Durranee, J. and Khan, MZ. 2008. Birds of Keenjhar. Indus for All Programe. WWF Pakistan, Karachi. pp12.

Ghalib, SA., Rehman, H., Iffat, F. and Hasnain, SA. 1981. A Checklist of Reptiles of Pakistan. Rec. Zool. Sur. Pakistan. 8:37-59.

Ghalib, SA. and Bhaagat, HB. 2004. The Wetlands of Indus Delta Eco-region. In: Proceedings of Consultative Workshop on Indus Delta Eco-region (IDER). Eds. Ahmed, E., Omer, S. and Rasool, F. WWF-Pakistan. 117-142.

Ghalib, SA., Hasnain, SA. and Khan, AR. 2004. Current Status of the Mammals of Sindh. J. Nat. Hist. Wildl. 3(1): 1-6.

Ghalib, SA., Khan, MZ. and Abbas, D. 2006. An Overview of the Asian Waterbird Census in Pakistan. J. Nat. Hist. Wildl. 5 (1):181-189.

Ghalib, SA. and Nawaz, R. 2008. A Quick Identification Guide to the Birds of Indus Eco-region. WWF-Pakistan, Karachi. pp10.

Ghalib, SA., Rais, M., Abbas, D., Tabassum, F., Begum, A. and Jabeen, T. 2009. An Overview of the Status of Shorebirds and Internationally Important Sites in Pakistan. Pakistan. J. Zool. 41(3):165-172.

Grimmett, R., Inskipp, C. and Inskipp, T. 1998. Birds of the Indian sub-continent. Oxford University Press, Delhi. pp890.

Grimmett, R., Roberts, T. and Inskipp, T. 2008. Birds of Pakistan. Christopher Helm, London. pp256.

Ghani, SA. 1975. Sind Game Guide. Sind Wildlife Management Board, Karachi. pp38.

IFAP (Indus for All Programe). 2007. Preliminary Environmental Baseline Study Report. Indus for All Programme Sites: Keti Bunder, Keenjhar, Chotiari Reservoir and Pai Forest, Sindh, Pakistan. (unpublished Report).

IFAP (Indus for All Programe). 2009. Detaileld Ecological Assessment of Fauna including Limnological Studies of Fauna at Keenjhar Lake, 2007-2008. WWF-Pakistan, Karachi. pp170. (unpublished).

IUCN, 2004. Sindh State of Environment and Development. Sindh Programe Office. 18:423.

Jaffar, M., Ashraf, M. and Rasool, A. 1988. Heavy metal contents in some Selected local Freshwater Fish and relevant waters. Pakistan Jour. Sci. Ind. Res. 31:189-193.

Jafri. SIH., Narejo, NT., Baloch, WA. and Saheto, GA. 1999. Studies on Land-locked Population of Palla, *Tenualosa ilisha* from Keenjhar Lake (Sindh), Pakistan. Pakistan J. Zool. 31:347-350.

Javed, HI. and Rehman, H. 2004. Status of Marsh Crocodile in Sindh. Rec. Zool. Surv. Pakistan. 15:22-30.

Jalbani, Z. 2009. Natural Habitat can be Restored. Natura. WWF-Pakistan. 33 (4):18-21.

Jehangir, TM., Khuhawar, SM., Leghari, SM., Baloch,, WA. and Leghari, A. 2000. Some Studies on Water Quality and Biological life at Kinjhar and Haleji Lakes of District Thatta, Sindh, Pakistan. Pakistan Journal of Biological Sciences. 3(11):65-72.

Karim, SI. 1985. A Note on the Birds of Prey of Haleji Lake and its Surrounding Areas. Rec. Zool. Surv. Pakistan. 10:75-80.

Kazmi, SJH., Qureshi, S., Siddiqui, MU. and Arsalan, MH. 2006. Depleting Wetlands of lower Sindh, Pakistan: A Spatio-Temporal Study through Satellite Remote Sensing Proceeding of the International Conference on advances in Space Technologies. (ICAST 2-3 Sept. 2006: Islamabad). 1-5.

Khan, KM. and Haleem, I. 1986. Haleji Lake. Sindh Wildlife Management Board, Karachi. pp26.

Khan, MZ. 2004. Protected Areas with Reference to Pakistan. J. Nat. Hist. Wildl. 3(1):7-12.

Khan, MZ. 2005. Wetlands of Sindh with reference to Ramsar Sites. J. Nat. His. Wildl. 4(2):141-145.

Khan, MZ. and Law, FCP. 2005. Adverse Effects of Pesticides and related Chemicals on Enzyme and Hormone Systems of Fish, Amphibians and Reptiles. Proc. Pakistan Acad. Sci. 42(4):315-323.

Khan, MZ. and Ghalib, SA. 2006. Birds Population and Threats to Some Selected Important Wetlands in Pakistan. J. Nat. Hist. Wildl. 5(2):209-215.

Khan, WA., Qasim, M., Ahmad, E., Chaudhry, AA., Bhaagat, HB. and Akhtar, M. 2010. Status of Smooth-Coated Otter (*Lutrogale perspicillata*) in Pakistan. Pakistan J. Zool. 42(6):817-824.

Khan, MZ., Ghalib, SA., Siddiqui, S., Yasmeen, G., Siddiqui, TF., Abbas, D., Farooq, R. and Zehra, A. 2012. Current Status and Distribution of Reptiles of Sindh. Journal of Basic and Applied Sciences. (in press).

Khanum, Z. and Ahmed, M. 1990-91. A note on the birds of Haleji Area (Sindh-Pakistan). Zoolgica Pakistan. 2(1): 33-37.

Korai, AL. Sahato, GA. and Lashari, KH. 2008[a]. Fish Diversity in Relation to Physic-chemical Properties of Keenjhar Lake (District Thatta), Sindh, Pakistan. Research Journal of Fisheries and Hydrobiology. 3(1):1-10.

Korai, AL. Sahato, GA., Lashari, KH. and Arbani, SN. 2008[b]. Biodivesity in Relation to Physic-chemical Properties of Keenjhar Lake (District Thatta), Sindh, Pakistan. Turkish Journal of Fisheries and Aquatic sciences. 8:259-268.

Lashari, KH. Sahato, GA. and Arbani. SN. 2001. Ecological Studies of Zooplankton in Keenjhar Lake, Sindh, Pakistan. Hamdard Medicus. 44(1):78-81.

Lashari, KH., Korai, AL., Sahato, GA. and Kazi, TG. 2009. Limnological Studies of Keenjhar Lake (District Thatta), Sindh, Pakistan. Pak. J. Anal. Environ. Chem. 10(1 and 2):39-47.

Mahar, MA., Larick, ZA., Narejo, NT. and Jafri, SIH. 2010. Limnological Study of Fishponds and Kalri Baghar Lower Canal at Chilya Fish Hatchery Thatta, Sindh, Pakistan. Pakistan J. Zool. 42(4):419-430.

Mirza, ZB. 2001. A Pocket Guide to Kirthar National Park and its adjoining protected areas. PKP Premier-Kufpec Pakistan. pp178.

Mirza, ZB. 2007. A Filed Guide to the Birds of Pakistan. Bookland, Lahore. pp366.

Nazneen, S. 1974. Seasonal Distribution of Phytoplankton in Kinjhar (Kalri) Lake. Pak. J. Bot. 6:69-82.

Nazneen, S. 1980. Influence of Hydrological Factors on the Seasonal Abundance of Phytoplanktos in Keenjhar Lake, Pakistan. Inst. Rev. Ger. Hydrobiol. 65:269-285.

Nazneen, S. and Begum, F. 1992. Seasonal Distribution of Molluscs of Kinjhar Lake. Pakistan. J. Zool. 24(2): 175-177.

Qureshi, MR. 1965. Common Freshwater Fishes of Pakistan. Agriculture Research Council, Govt. of Pakistan, Karachi. pp61.

Rafiq, M. 2009. Fish Fauna of Haleji Lake, Sindh, Pakistan. Rec. Zool. Surv. Pak. 19:61-65.

Rais, M., Khan, MZ., Ghalib, SA., Abbas, D., Khan, WA and Islam, S. 2009. Recent Record of Smooth-coated Otter (*Lutrogale perspicillata*) from Sindh, Pakistan. Pakistan. J. Zool. 41(5):413-414.

Rais, M., and Abbas, D. 2010. Withering Wet Treasures of the Indus Ecoregion-Haleji Lake. Tigerpaper. 37(1): 12-15.

Rehman, H. and Javed, HI. 2004. Revised Checklist of Amphibians of Pakistan. Rec. Zool. Surv. Pakistan. 15: 31-33.

Roberts, TJ., Passburg, R. and Van Zalinge, NP. 1986. A Checklist of Birds of Karachi and Lower Sind, Pakistan. World Wide Fund for Nature Pakistan.

Roberts, TJ. 1991-1992. The Birds of Pakistan (2 volumes). Oxford University Press, Karachi.

Roberts, TJ., 1997. The Mammals of Pakistan (Revised Edition), Oxford University Press Karachi, Pakistan. pp525.

Roberts, TJ. 2005[a]. Field Guide to the Large and Medium Sized Mammals of Pakistan. Oxford University Press Karachi. pp260.

Roberts, TJ. 2005[b]. Field Guide to the Small Mammals of Pakistan. Oxford University Press Karachi. pp280.

Sahato, GA., Lashari, KH. and Sahato, SB. 2004. Ecological Survey of Phytoplankton (*Oscillatoriaceae*) of Keenjhar Lake (District Thatta), Sindh, Pakistan. Hamdard Medicus. 47 (4):100-104.

Saqib, TA., Siddiqui, PA. and Qureshi, WM. 1990-91[a]. Study on the Productivity of Bottom Fauna in Kinjher Lake (Sindh-Pakistan) as Index of Eutrophy. Zoologica Pakistan. 2(1):43-49.

Saqib, TA., Siddiqui, PA. and Qureshi, WM. 1990-91[b]. Study on the Productivity of Bottom Fauna in Haleji Lake (Sindh), Pakistan. Zoologica Pakistan. 2(1):51-58.

Saqib, TA., Naqvi, SNH. and Siddiqui, PA. 2003. Determination of Lipid Content in Different Organs of Three Species of *Labeo* Found in Haleji Lake, Sindh. J. Nat. Hist. Wildl. 2(2):37-39.

Saqib, T., Naqvi, SNH., Siddiqui, PA. and Azmi, MA. 2005. Detection of Pesticides in Muscles, Liver and Fat in three Species of *Labeo* found in Kalri and Haleji Lakes. Env. Biol. 26:433-448.

Scott, DA.(Eds.), 1989. A Directory of Asian Wetlands, Pakistan Section. IUCN, Gland, Switzerland. 295-365.

Scott, DA. and Poole, CM. 1989. A Status Overview of Asian Wetlands. Asian Wetland Bureau, Kuala Lumpur, Malaysia. pp42.

Sheikh, KM. and Molur, S. 2005. Status and Red List of Pakistan's Mammals. IUCN Pakistan. pp344.

Siddiqui, PA., IU. Baqai and Iqbal, M. 1973. Check List of Fishes of Kinjher (Kalri) Lake with Notes on Environmental Conditions and Fishes Potential. Agri. Pak. 24(2):201-220.

Siddiqui, PA., Muzammil, SS., Saqib. TA. and Saeed, N. 1990. Ecological Distribution and Habitat Blending in Forest Birds occurring in Sindh. Karachi Univ. J. Sc. 18:99-105.

Siddiqui, PA. and Saqib, TA. 1993. Phosphates, Nitrates and Productivity in Haleji Lake. Zoologica Pakistan. 3:3-8.

Siddiqui, PA. 1998. Bioecology of Wetlands of Lower Sindh with reference to Avifauna and Organophosphate Pollution. Ph.D thesis, Department of Zoology, University of Karachi. (unpublished).

WWF Pakistan. 2010. Consultative Workshop on Keenjhar Lake. WWF Pakistan. pp13.

Received: Oct 6, 2011; Revised: Nov 22, 2011;

Accepted: Dec 5, 2011

SENRA Academic Publishers, Burnaby, British Columbia
Vol. 6, No. 1, pp. 1785-1795, Feb 2012
Online ISSN: 1920-3853; Print ISSN: 1715-9997

Canadian Journal of pure&applied sciences

THE EFFECTS OF HOT OIL TREATMENT PROCESS ON THE CHEMICAL, COLOUR AND STRENGTH PROPERTIES ON 15-YEAR-OLD CULTIVATED *ACACIA* HYBRID

*Razak Wahab[1], Izyan Khalid[1], Nurul Ain' Mohd[1]. Kamal, Mahmud Sudin[2], Othman Sulaiman[3] and Aminuddin Mohamed[2]
[1]Faculty of Agro Industry and Natural Resources, Universiti Malaysia Kelantan, 16100 Pengkalan Chepa, Kelantan, Malaysia
[2]School International Tropical Forestry, Universiti Malaysia Sabah, 88999, Kota Kinabalu, Sabah, Malaysia
[3]School Industrial Technology, Universiti Sains Malaysia, 11800 Penang, Malaysia

ABSTRACT

The effects of hot oil treatment on the chemical, colour and strength properties of 15-year-old cultivated *Acacia* hybrid were investigated. Logs of *A.* hybrid were harvested and cut at the bottom, middle and top sections. The wood sections were treated in the hot oil treatment process using palm oil at temperatures of 180, 200 and 220°C for durations of 30, 60 and 90 min. The hot oil treatment process causes some modification in the wood features especially in the chemical constituents, colour appearances and strength properties of *A.* hybrid. Parameters such as temperatures and treatment time were closely monitored as they influence the chemical, colour and strength changes in the treated wood. The degradation in holocellulose, cellulose, and hemicellulose contents was recognized when acacia woods were exposed to oil thermally modified process. Holocellulose and celulose degraded with the increasing of treatment temperature and duration of heating exposure, while lignin showed the increment in content through this treatment. The colour changes in the sap and heartwood were measured using a Minolta Chroma-meter CR-310 and the results are presented in the CIE L*a*b* colour co-ordinates system. The results show that the colour of the treated sapwood can be improve to match the colour of the natural *A.* hybrid heartwood. The strength properties of the oil heat treated *A.* hybrid wood decreases in values of both MOR and MOE throughout the treatment process. The decreases in values were influenced by temperature and duration of the treatment.

Keywords: Cultivated *Acacia* hybrid**,** hot oil treatment process, chemical changes, colour changes, strength reductions.

INTRODUCTION

Declining of timbers from the natural forests has pressured the wood-based industry to shift to forest plantation for consistent supply of wood. The sensitivity of the consumers in Europe and North America about logging activities of naturally grown species from tropical rainforest has further aggregate the problem. Plantation forestry rotations which are shorter than of natural stands provide attractive investments for government and private sectors to fulfill the needs of the timber industries and, at the same time, conserve the natural forest from continuously being depleted by logging activities. *Acacia* which can easily adapted itself to the local soil condition, having high growth rate and possess high wood quality make them most suitable for used as a plantation species.

The hot oil thermal process seems to be a suitable modification because of its competitive advantage as an environment friendly process, since it does not require the uses of chemicals preservative (Razak *et al*., 2011, 2005). Most of current woods treatment techniques uses preservative which are harmful and has negative effect to the environment. Corome Copper Arsenic (CCA) treated wood which has heavy metals and can discharge toxin to the environment has totally been banned by many developed countries (Berard *et al*., 2006). The advances in environmental awareness and the implementation of policies which support the use of renewable resources and environment-friendly chemicals have resulted in high interest in the uses of non-biocides. Effort has been put forward in developing new chemical wood preservatives with no or little impact to the environment (Hyvonen *et al*., 2006).

The present study investigated on the changes that occurred in the main chemical components of an oil heat treated cultivated *A.* hybrid, their effects on the colour appearances and strength of the wood. Chemical constituents, colour changes and strength properties are parameters that influenced durability, appearances and stability of the wood. The results of this study will be beneficial in improving the technologies in treating acacia wood for the industry.

*Corresponding author email: razak@umk.edu.my

MATERIALS AND METHODS

Materials

A. hybrid wood was cut from the 15-year-old *A.* hybrid trees obtained from the Sabah Forest Development Authority in Kinarut, Kota Kinabalu, Sabah, Malaysia. The trees were selected based on their long straight bole with minimum branches, good physical appearances and diameter ranging from between 250 to 300 mm. The logs were cut and segregated into different height, namely, bottom, middle and top sections, corresponding to 50, 30 and 20% of the merchantable height respectively. Blocks of 600 mm long were cut from the middle of each section. The wood blocks were then transported to Universiti Malaysia Sabah (UMS) for further processing and subsequent testing. The study was conducted in UMS from Jan. 2009 to Oct 2010.

Sample preparation

The wood blocks were air dried at room temperature for about a month to reduce the moisture to equivalent moisture content (15%) and to remove stresses in them. After drying, the wood blocks were planed into sizes of 300 mm × 100 mm x 25 mm (length × width × thickness) for the oil heat treatment process. These samples were mixture of sapwood and heartwood. They were then oil heat treated using palm oil as the heating medium. Untreated wood were used as control for comparison purposes.

Hot oil thermal modification process

A. Hybrid samples were hot oil treated in a stainless steel tank connected to a locally designed heat treatment machine. Palm oil was used as the heating medium. The temperatures of the oil and the wood samples were control through a control panel located on the out-side of the tank. An electric generator was used to generate heat. The wood samples moisture were stabilized to 12% in a conditional chamber set at 65% relative humidity and temperature 25 °C before they were put into the tank. Eighty woods were prepared prior to the treatment. The weights of the woods were recorded before and after treatment to determine weight loss caused by the treatment. The tank was filled with the oil until it reached three quarters full. The treatment temperature and duration were set at 180°C, 200°C and 220°C for 30, 60 and 90 min. respectively. The wood samples were initially placed into hot oil at 80°C and the real treatment time started only when the oil bath reached the targeted temperature. The temperatures were recorded every 10 min respectively. At the end of each treatment period, the wood samples were taken out from the tank and wiped clean with cloth to avoid oil seeping into the wood tissues. The wood samples were later cooled and conditioned in a conditioning chamber set at 20 ± 2 ºC and 65 ± 5% relative humidity before reweighing. The wood samples were later cut into various sizes for respective testing for chemical analysis and strength tests. The procedure Razak *et al*. (2005) were followed for the wood treatment and testing.

Chemical Properties

Chemical Analysis

The main chemical components evaluated in the oil heat treated wood were the alcohol-toluene solubility, holocellulose, alpha-cellulose and klason lignin. Separated chemical analysis was done each for the sapwood and heartwood respectively. The amount of chemical constituents presents were calculated based on their ratios. Tests were conducted in accordance with using TAPPI T203 om-99 (1999) and TAPPI T222 om-02 (2002) standards.

Wood Sample Preparation

In the study of the chemical constituents the wood were divided into 2 groups namely the sapwood and heartwood. The woods were chipped before undergoing grinding process. Willey's mill was used in turning the wood into powdery form in order to pass BS 40-mesh sieve and retained on a BS 60-mesh sieved. The grinded samples were then dried for 7 days until their moisture is in equilibrium with the atmosphere before undergoing chemical analysis process. 2g air-dried sawdust was placed in the weighing bottle and weigh to the nearest 0.01 g. The sawdust was later dried in an oven set at 103±2°C for 3 hours with the cover off. The bottle was then taken out and placed in a desiccators for 15min. Moisture content of the sawdust was later determined.

Colour Measurement of Hot Oil Heat Treated Wood

Measurement for colour were taken before and after the wood samples had completed the hot oil treatment process at temperatures 180, 200, 220ºC for treatment time of 30, 60, and 90 minutes respectively. The surfaces on the woods to be measured were marked before undergoing the hot oil heat treatment process. This was to ensure the wood surface measured were consistent throughout the process. Marked point was made using a sharp pencil on the wood surfaces measuring 2 x 2 cm at the cross-sectional surface of each sapwood and heartwood. This section in the wood was the most representative area for revealing the colour difference (Unsal *et al*., 2003). Measurement for the colour appearances were done at the middle of each sapwood and heartwood in the cross sections of the *A.* hybrid at each section height. The samples were sanded slightly for about 3 mm using P100 sandpaper and brushed cleanly to minimize the risk of colour variation values cause by differences in surface structure. Measurements of colour appearances were done in accordance to the CIE L*a*b* (1986) system using a Minolta Chroma Meter CR-10. The colour reader measures the colour difference on the surface of wood specimens between two colours which that before and after treatment. The results were presented following the

CIE L* a* b* colour co-ordinates system base on the D65 light source with the reflection spectrum measured in the 400 – 700 nm regions. The values were used to calculate the colour change as a function of thermal treatment.

Strength Properties (Modulus of Rupture and Modulus of Elasticity in Static Bending)

Evaluation of the modulus of rupture (MOR) and modulus of elasticity (MOE) in Static Bending static bending of the wood was conducted in accordance with ASTM D4761 (1999) standard. A Universal Testing Machine located in Forest Research Center, Sandakan, Sabah, was used for bending testing. The dimensions of wood samples for static bending test were 20 x 20 x 300 mm. The specimen was supported on a span of 280 mm and the force applied at mid-span using a loading head. The rate of loading was 6.6 mm/min. Wood were loaded on the radial surface. The tests were stopped when the wood started to break. The proportional limit and ultimate load and deflection were recorded, and the MOE and MOR were calculated automatically by the computer connected to the machine.

RESULTS AND DISCUSSION

Chemical Properties

Table 1 shows the chemical composition of the treated acacia wood before and after undergoing the hot oil treatment process. Both the control sapwood and heartwood had the highest chemical compositions of holocellulose and cellulose compared to the hot oil heat treated wood at various treatment temperature and time. The results clearly showed that the changes of chemical components compositions occurred when the wood were treated at higher temperature and duration (Razak *et al*., 2011; Izyan *et al*., 2010). At temperature above 180°C, the hot oil treated wood experiences the loss of polysaccharide material (Hill, 2006). The holocellulose contents varied between 63.1% and 70.8% for the hot oil treated sapwood. The cellulose contents between 37.7% and 46.2%, with hemicelluloses contents varied between 23% and 26.1% and lignin between 19.2% and 24.9% at 180-220°C with 30 to 90 minutes treatments. For the heartwood, the holocellulose contents for treated varied between 64% and 71.7%, cellulose between 38.1% and 47.8%, hemicelluloses contents varied between 23.2% and 26.2% with and the lignin between 22.4% and 27.0% at 180 - 220°C with 30 to 90 minutes treatments.

***Holocellulose*:** Slight reduction on the holocellulose contents in the treated sapwood and heartwood occurred with the increment in of treatment temperature and time in comparison to both untreated sapwood and heartwood. The holocellulose contents for sapwood ranged between 63.1 to 70.8 % and for heartwood from 64.0 to 71.7% depending on the temperature and duration applied. Studies by Inari *et al.* (2007) and Boonstra and Tjeerdsma

Table 1. Average values of chemical changes of 15-year-old oil heat-treated *A.* hybrid wood.

Wood type	Temp. (°C)	Treatment duration (min)	Chemical Composition (%)			
			Holocellulose	Cellulose	Hemicellulose	Lignin
Sapwood	Control	Control	71.5 (0.00)	47.1 (0.00)	24.4 (0.00)	20.8 (0.00)
	180	30	70.8 (-1.0)	46.2 (-1.9)	24.6 (0.8)	20.7 (-0.5)
		60	69.7 (-2.5)	45.1 (-4.2)	24.6 (0.8)	22.0 (5.8)
		90	66.6 (-6.9)	43.6 (-7.4	23.0 (-5.7)	22.1 (6.3)
	200	30	68.6 (-4.1)	42.5 (-9.8)	26.1 (7.0)	23.9 (14.9)
		60	65.3 (-8.7)	39.2 (-16.8)	26.0 (6.6)	23.8 (14.4)
		90	64.5 (-9.8)	38.5 (-18.3)	26.0 (6.6)	24.7 (18.8)
	220	30	66.4 (-7.1)	41.6 (-11.7)	24.8 (1.6)	23.7 (13.9)
		60	64.9 (-9.2)	38.9 (-17.4)	26.0 (6.6)	24.3 (16.8)
		90	63.1 (-11.7)	37.7 (-20.0)	25.4 (4.1)	24.0 (15.4)
Heartwood	Control	Control	73.4 (0.00)	48.9 (0.00)	24.5 (0.00)	22.4 (0.00)
	180	30	71.7 (-2.3)	47.8 (-2.3)	23.9 (-2.5)	21.7 (-3.1)
		60	70.6 (-3.8)	46.3 (-5.3)	24.3 (-0.8)	22.9 (2.2)
		90	67.9 (7.5)	44.7 (-8.6)	23.2 (-5.3)	23.0 (2.7)
	200	30	68.8 (-6.3)	42.6 (-12.9)	25.9 (5.7)	24.5 (9.4)
		60	68.3 (-6.9)	42.1 (-14.0)	26.2 (6.9)	24.9 (11.2)
		90	66.5 (-9.4)	40.9 (-16.4)	25.6 (4.5)	25.0 (11.6)
	220	30	67.1 (-8.6)	42.0 (-14.1)	25.7 (4.9)	24.7 (10.3)
		60	65.1 (-11.3)	39.7 (-18.8)	25.4 (3.7)	24.8 (10.7)
		90	64.0 (-12.8)	38.1 (-22.1)	25.9 (5.7)	24.9 (11.2)

( ) = % change from control,

Holocellulose is the total polysaccharide fraction of wood that is composed of cellulose and all of the hemicelluloses and what is obtained when the extractives and lignin are removed from the natural material.

(2005) also reported similar observations. The holocellulose content of beech and pine decreases between 50% and 60% after heat treatment (Inari *et al*., 2007). Boonstra and Tjeerdsma (2005) noted that holocellulose content of heat treated Scots pine decreased between 79.7% and 63.3%. The decreases occurred when the wood were heated at a temperature above 100°C (Hill, 2006). The content decrease is associated with the loss of cellulose and hemicellulose chains during the process.

***Cellulose*:** The cellulose content determined for the hot oil treated sapwood was between 80 - 98% and heartwood between 78-97%. The results showed occurrence of minor degradation in celluloses content when the wood were treated at 180°C for 30 min and continue to decrease with the increase in treatment temperature. From the analysis of molecule size of cellulose in heat treatment by using intrinsic viscosity measurement, it showed that heat treatment results in a considerable reduction in molecule size of cellulose. Different process conditions and treatment time applied during the heat treatment can influence the degradation rate of cellulose content (Boonstra and Tjeerdsma, 2005). The degree of polymerization of cellulose is already decreased in thermally treated spruce at temperatures above 120°C due to cleavage of the glucosidic bonding that is accelerated by the presence of acids that catalyzed the reaction (Fengel and Wegener, 1989). Chain scission of the cellulose occurred with extended heating, producing alkaline soluble oligosaccharides, with a concomitant decrease in the cellulose degree of polymerization (DP) and degree of cyrstallinity (Hill, 2006).

***Hemicellulose*:** Hemicelluloses content for both heat treated sapwood and heartwood showed fluctuation values, but with no specific trend. The hemicelluloses for sapwood experiences changes in content from 24.4% in control to 26.1% in heat treated samples. While in the heartwood the content changes from 24.5% to 26.2%. Both wood experiences an increases in the hemicelluloses contents. A study by on *Grevillea robusta* wood found that the increment in lignin content with treatment time confirming higher susceptibility of hemicelluloses to thermal treatment (Mburu *et al.,* 2008). Rowell *et al.,* (2005), stated that the hemicelluloses change is predominate at temperatures below 200°C. When wood undergo a heat treatment process, most of the heat labile hemicelluloses begins to deteriorate, resulting in the output of methanol, acetic acid and other volatile heterocyclic compounds (Hill, 2006). Acetic acid is produced when the acetylated hydroxyl groups of the hemicellulose chains are split off during the heating (Johansson, 2008). Volatile organic acids formed during to the heating of wood are trapped and promote the degradation rate (Viitaniemi, 2001).

***Lignin*:** The lignin content of sapwood and heartwood in the *A.* hybrid increases with temperature and heat treatment duration.

Table 2. Average values of colour variation in L*, a* and b* of oil heat-treated *A.* hybrid wood.

Wood types	Temp. (ºC)	Treatment duration (min.)	L*			a*			b*		
			B	M	T	B	M	T	B	M	T
	Control	Control	73.6	73.0	71.4	6.9	6.6	7.3	21.2	22.3	21.4
		30	66.7	70.0	65.5	7.4	8.7	8.5	21.9	23.3	23.4
	180	60	65.4	62.7	63.0	8.8	9.9	9.8	25.7	26.3	24.1
		90	65.6	61.9	62.9	9.3	10.9	10.2	27.3	27.5	26.3
		30	63.5	63.5	58.2	9.5	10.0	9.9	26.4	26.1	26.2
Sapwood	200	60	56.9	57.2	56.9	11.4	11.9	10.7	27.5	27.1	26.5
		90	50.7	54.6	51.6	12.2	12.4	12.2	27.9	28.9	28.0
		30	56.5	53.0	53.4	11.7	10.6	10.3	27.6	26.9	26.7
	220	60	48.7	47.9	43.2	12.3	12.7	11.2	27.8	27.6	27.8
		90	41.5	40.6	39.2	13.9	13.5	12.6	28.1	29.3	28.9
	Control	Control	54.1	54.8	53.5	14.2	15.1	13.9	26.8	26.3	25.2
		30	53.6	52.7	52.9	13.4	12.9	12.0	25.0	24.8	24.1
	180	60	51.7	51.6	50.7	11.9	11.1	11.5	23.6	23.2	23.5
		90	50.4	50.2	48.2	11.2	10.8	10.7	23.0	21.5	22.3
		30	51.4	52.1	48.6	11.5	10.3	11.3	23.7	24.1	23.9
Heartwood	200	60	49.1	50.5	46.9	11.0	9.7	10.7	23.4	21.5	21.9
		90	45.9	46.7	43.5	9.9	8.9	10.2	23.1	21.2	20.9
		30	50.7	50.8	46.3	10.0	9.0	10.2	22.6	22.9	21.0
	220	60	46.6	47.4	38.8	8.3	8.3	8.4	21.1	19.8	17.2
		90	40.0	40.9	33.1	6.7	7.1	7.3	20.5	19.0	15.1

Note: Temp. = temperature, L*= lightness, a* = red, b* = yellow, B = Bottom, M = Middle, T = Top

There was an increment of lignin content in the sapwood from 20.8% (untreated wood) to 24.7% (hot oil treated wood), while the lignin content of the heartwood from 22.4% (untreated heartwood) to 25.0% (hot oil treated wood). Similar observations were also made by Brito *et al.* (2008), Mburu *et al.* (2008), Inari *et al*. (2007), Yildiz *et al*. (2006) and Sarni *et al*. (1990) in their respective heat treatment studies. Changes in the lignin constituents indicated some changes occurred in the lignin structure of wood. Sandermann and Augustin (1964) stated that the loss of polysaccharides material during the heating process leads to an increase in the lignin content of wood.

Analysis of Variance on Chemical Composition

Significant different were observed between the temperatures and treatment duration relating to content of lignin (see Table 5). Almost all of the chemical components were significantly affected by temperature, treatment duration and wood types. Significant different were also noted between the treatment temperature, duration and wood type of the treatment in the constituents of holocellulose, cellulose and lignin. It can be concluded that the effects of treatment temperature, duration and wood types were the primary caused in the change in chemical constituents of these chemical

Table 3. Bending strength (MOR, MOE) of sap- and heartwood *A.* hybrid through hot oil-heat treatment process.

Wood Type	Temp. (ºC)	Treatment duration (min)	MOR (N/mm²)			MOE (N/mm²)		
			B	M	T	B	M	T
Sapwood	Control	Control	69.78	67.22	65.08	3864.54	3803.57	3776.72
	180	30	64.05 (8.21)	61.98 (7.80)	63.37 (2.63)	3535.7 (8.51)	3455.43 (9.15)	3492.52 (7.53)
		60	63.43 (9.10)	59.66 (11.25)	52.23 (19.74)	3475.95 (10.06)	3416.45 (10.18)	3265.79 (13.53)
		90	62.31 (10.71)	55.82 (16.96)	47.99 (26.26)	3470.29 (10.20)	3412.22 (10.29)	3207.16 (15.08)
	200	30	55.06 (11.64)	54.85 (18.40)	45.31 (30.28)	3407.97 (11.81)	3328.01 (12.50)	3094.19 (18.07)
		60	60.11 (13.86)	54.70 (18.63)	44.86 (31.07)	3333.09 (13.75)	3228.98 (15.11)	3035.35 (19.63)
		90	55.38 (20.64)	50.41 (25.01)	42.85 (34.16)	3244.75 (16.04)	3172.19 (16.60)	2972.25 (21.30)
	220	30	53.9 (22.76)	49.72 (26.03)	40.57 (37.66)	3216.75 (16.76)	3101.06 (18.47)	2938.18 (22.20)
		60	51.42 (26.31)	46.89 (30.14)	38.15 (41.38)	3133.38 (18.92)	3046.50 (19.90)	2716.33 (28.08)
		90	41.21 (40.94)	40.33 (40.00)	37.03 (43.10)	3001.51 (22.33)	2787.39 (26.72)	2599.31 (31.18)
Heartwood	Control	Control	68.51	70.76	90.43	3975.49	4004.07	4067.94
	180	30	67.42 (1.59)	65.24 (7.80)	66.70 (26.24)	3676.91 (7.51)	3637.29 (9.16)	3721.56 (8.51)
		60	66.77 (2.54)	63.47 (10.30)	54.98 (39.20)	3658.9 (7.96)	3634.52 (9.23)	3437.94 (15.49)
		90	65.59 (4.26)	58.81 (16.89)	51.06 (43.54)	3587.34 (9.76)	3599.88 (10.09)	3376.74 (16.08)
	200	30	63.27 (7.65)	58.75 (16.97)	47.74 (47.21)	3577.19 (10.02)	3547.83 (11.39)	3291.87 (19.08)
		60	58.8 (14.17)	57.74 (18.40)	47.7 (47.25)	3545.84 (10.81)	3503.17 (12.51)	3229.33 (20.62)
		90	58.57 (14.51)	53.63 (24.21)	45.67 (49.50)	3488.98 (12.24)	3435.31 (14.20)	3162.30 (22.26)
	220	30	57.96 (15.40)	52.89 (25.25)	43.62 (51.76)	3422.08 (13.92)	3299.28 (17.60)	3159.49 (22.33)
		60	55.30 (19.28)	50.42 (28.75)	41.02 (54.6()	3369.22 (15.25)	3275.80 (18.19)	2920.83 (28.20)
		90	44.31 (35.32)	44.7 (36.83)	39.81 (55.98)	2997.64 (24.60)	3227.43 (19.40)	2794.95 (31.29)

Note: ( ) = % change from control samples, B = Bottom, M = Middle, T = Top

component. There was no significant difference in the wood type in the treatment relating to the content of hemicelluloses. The wood types did not affect the changed in hemicellulose content in oil thermally modified process. The effect of the temperature and treatment duration causes the decrement in hemicellulose constituents. The changes in the chemical contents of the wood increased with the increased in temperature. The chemical constituents in *A.* hybrid wood were highly affected by the hot oil treatment temperature, duration and wood types in oil thermally modified process.

Colour Changes

Table 2 presents the colour changed values of treated sapwood and heartwood. Based on the colour measurement of both the sapwood and heartwood, the effect on colour through oil heat treatment can be readily observed at different treatment temperature and treatment time, compared to the original color of the specimen.

Lightness (L*) of Wood Colour

The factor that effect the colour changes for both the sapwood and heartwood is the lightness (L*). The variation in L* has as more responsive sign in the colour change to the human eye which accompany the change in chromic characters a* and b* (Keey, 2004). Thulasidas *et al*. (2006) reported that the variability in darkness or lightness is the main cause of wood colour variability.

The changed in lightness (L*) values for both the sapwood and heartwood showed decreases in lightness in the first 30 minutes of every treatment. The changes continued progressively with the increase of treatment temperature and duration. The L* values of heartwood did not changed considerably when compared to L* values of sapwood. This might be due to the brightness in the wood colour itself as the sapwood of acacia has a brighter colour than heartwood. The sapwood becomes slightly darker, while heartwood becomes considerably darker when exposed to vary treatment conditions.

The bottom, middle and top sections of the sapwood treated at 220°C in 30 minutes showed L* values almost similar with L* values of untreated heartwood. This also can be observed obviously from the below figure shown.

Table 4. Correlations between mechanical, colour and chemical properties of 15 year-old cultivated *A.* hybrid.

Wood Properties	MOR	MOE	L*	a*	b*	Holo	Hemi	Cell	Lignin
MOR	1.00	0.60**	0.40**	-0.06 ns	0.02 ns	0.42**	-0.19*	0.42**	-0.36**
MOE		1.00	0.34**	0.05 ns	-0.01 ns	0.35**	-0.24**	0.37**	-0.31**
L*			1.00	-0.37**	0.11 ns	0.51**	-0.33**	0.53**	-0.75**
a*				1.00	0.47**	0.11 ns	-0.02 ns	0.10 ns	0.15*
b*					1.00	-0.07 ns	-0.07 ns	-0.04 ns	-0.01 ns
Holo						1.00	-0.34**	0.96**	-0.69**
Hemi							1.00	-0.59**	0.61**
Cell								1.00	-0.77**
Lignin									1.00

Table 5. ANOVA on chemical compositions of oil heat treated 15 year-old *Acacia* hybrid.

Source of Variance	Dependent Variable	Sum of Squares	Df	Mean Square	F-Ratio
Temperature	Holocellulose	1618.96	3	539.65	564.15**
	Hemicellulose	139.12	3	46.37	85.82**
	Cellulose	2460.23	3	820.08	1018.75**
	Lignin	368.90	3	122.97	461.45**
Duration	Holocellulose	250.82	2	125.41	131.10**
	Hemicellulose	7.43	2	3.72	6.88**
	Cellulose	210.26	2	105.13	130.60**
	Lignin	12.69	2	6.35	23.81**
Wood types (Sap and Heartwood)	Holocellulose	96.80	1	96.80	101.20**
	Hemicellulose	0.01	1	0.01	0.01ns
	Cellulose	95.20	1	95.20	118.27**
	Lignin	52.22	1	52.22	195.94**

The decreased in L* values from 200°C-220°C was larger than at 180°C in sapwood when compared to heartwood. The L* values in heartwood changed slightly when temperature exceed 200°C. The major changed of treatment duration of both wood types occurred between treatments of 60 - 90 minutes. This indicates the changed in L* values gradually decreased with the increased in the treatment temperature and treatment time.

The summary of correlation coefficient of colour variation with other wood properties of treated acacia is given in table 4. There was a correlation between L* and chemical component of acacia wood. The holocellulose and cellulose constituents shows positive correlations with L*. The hemicellulose and lignin on the other hand were negatively correlated with the colour. The conclusion is that the changed in wood colour were influenced by the chemical components of the wood. The differences in the chemical constituents of the sapwood and heartwood extractive and lignin might probably be the main reason for the dissimilar in colour appearances (Sundqvist, 2004). Burti *et al*. (1998) stated that during heat treatment at elevated temperatures, polyphenols compounds found in hybrid walnut heartwood which conferred dark color to heartwood, may migrate in the sapwood region and changed the sapwood colour from light to dark colour.

The decreased in lightness resulted from the high temperature of heat treatment was due to decrement in certain chemical constituents in wood such as hemicelluloses and lignin (Mitsui *et al*., 2001; Bourgios *et al*., 1991). The wood colour changes can be an indicator of chemical modification that took place in wood (Burti *et al*., 1998; Bekhta and Niemz, 2003; Sundqvist *et al*., 2004).

Chroma Colour, a* (Reddish Colour)

The a* and b* are a combination of red (a*) and yellow (b*) in the chroma coordinates, Both of the sapwood and heartwood showed some differences due to changes in a* and b* values. The a* values of the sapwood increased while a* values of heartwood decreased through this treatment. This might be due of the original colour of the wood itself. The original colour of the sapwood is light yellowish red while the colour of heartwood is brownish red. Increased in treatment temperature tends to increase the a* values of sapwood. The a* values reaches a maximum values after treated at 220°C temperature.

Table 6. ANOVA of colour appearances of treated *A.* hybrid

Source of Variance	Dependent Variable	Sum of Squares	Df	Mean Square	F-Ratio
	L*	9538.60	3	3179.53	110.70**
Temperature	a*	9.33	3	3.11	0.42ns
	b*	35.41	3	11.80	1.10ns
	L*	1257.57	2	628.79	21.89**
Duration	a*	1.43	2	0.72	0.10ns
	b*	2.67	2	1.33	0.12ns
	L*	6537.30	1	6537.30	227.60**
Wood Types	a*	94.80	1	94.80	12.82**
(Sap and	b*	294.70	1	294.70	27.55**
Heartwood)	L*	222.61	2	111.31	3.88*
Sampling Height	a*	0.78	2	0.39	0.05ns
	b*	23.77	2	11.89	1.11ns

Table 7. ANOVA on the strength properties of oil heat treated *A.* hybrid

Source of Variance	Dependent Variable	Sum of Squares	Df	Mean Square	F-Ratio
Temperature	MOR	12076.80	3	4025.59	15.99**
	MOE	1.81	3	6.02	12.66**
Duration	MOR	3425.40	2	1712.70	6.80**
	MOE	2.72	2	1.36	2.86ns
Wood Types	MOR	565.80	1	565.80	2.25ns
(Sap and Heartwood)	MOE	2.16	1	2.16	4.55*
Sampling Height	MOR	3098.58	2	1549.29	6.15**
	MOE	2.06	2	1.03	2.17ns

** = significant at $p \leq 0.01$, * = significant at $p \leq 0.05$, ns = not significant, MC= Moisture Content, BD= Basic Density, MOR= Modulus of Rupture, MOE = Modulus of Elasticity, L*= Lightness, a*= Reddish, b*= Yellowish, Holo= Holocellulose, Hemi= Hemicellulose, Cell= Cellulose

The colour of sapwood becomes more reddish than before while the red colour in heartwood becomes lessen. The reddish colour and the increased in saturation substantiated as a decrease in hue and increase in chroma might be the results of the formation in secondary condensation or degradation products of the quinine and quinonemethide types (Hon *et al*., 1991).

There was a correlation between a* and chemical component of acacia wood (see Table 4). Positive correlations were observed between a* and b*, holocellulose, cellulose and lignin. However, the hemicellulose were negatively correlated with a*. However a* did not significant correlated with all chemical component except for lignin.

The heat treated wood colours changed from yellow to brown as the results of the photo-oxidation of lignin and wood extractives, with produced coloured quinines component (Charrier *et al*., 2002; Grelier *et al*., 1997).

Chroma Colour, b* (Yellowish Colour)

The b* values of heartwood shows the negative change from the start of the treatment. The yellowish colour in the heartwood started to decrease once the temperature reached 180°C and it decreases drastically when exposed to 220°C at longer treatment duration.

There was a correlation between b* and a* of *A.* hybrid wood (Table 4). Positive correlations were noted between the a* and b*. Besides a*, b* does not significantly correlated with other wood properties in this study.

Strength Properties (MOR and MOE in Bending Tests)

The result of strength properties of treated *A.* hybrid wood is presented in table 3. It is clearly observed the values of both wood types (sapwood and heartwood) for modulus of rupture (MOR) and modulus of elasticity (MOE) decreased through oil thermally modified. The untreated wood still obtained the highest strength values compared to treated wood. The strength properties of wood usually decrease with increasing temperature and increase with decreasing temperature (Smith *et al*., 2003). For the thermally modified wood, the highest values of MOR and MOE of every portion were starting to decreased when the treatment temperature reaching 180°C. This strength values respectively decreased when treated at 200°C and 220°C. From the results obtained the values of MOR and MOE of untreated and treated wood showed a decrement with increasing sampling height. The variations in MOR and MOE along the tree height can be explained by the decrease in maturity of wood and fibre length from the base to the top of the tree (Rulliarty and America, 1995).

Wood treated at 180 to 200°C in the presence of moisture was noted to result in a large reduction of their resistance to MOR, MOE and compression strength (Giebeler, 1983). The wood strength can be reduced by up to 50% if the treatment temperature reached over 200°C (Bekhta and Niemz, 2003; Sailer *et al*., 2000; Kamden *et al*., 1999). The increased treatment duration which is 30 to 90 minutes also prolong the decreasing effect on strength. This testifies a value of MOR for treated wood is influenced by treatment temperature and duration. The higher the temperature the longer the treatment duration the lower is the strength value. However, MOE did not show significantly difference with treatment duration and this is reinforced by the ANOVA in tables 4 and 7.

The strength properties of the oil heat treated wood are reduced by the oil treatment process. The strength reduction is mainly due to the hemicelluloses degradation (Kocaefe *et al*., 2007). The effects, however varies according to the wood species, anatomical features and the treatment methods (Mburu *et al*., 2008; Kocaefe *et al*., 2007). Studied on the effect of high temperature on spruce wood found that MOE of spruce wood started to decrease once the temperature rose over 100°C (Bekhta and Niemz, 2003). The mechanical properties of the wood started to weaken and become brittle when the treatment temperatures reached over 200°C (Sundqvist, 2004).

Compression failure typically occurs in wood having low density (Nordahlia, 2008; Bodig and Jayne, 1982). The reduction of density in the treated material can caused reduction in some of the strength properties (Rafidah *et al*., 2008; Janssen, 1981). The strength loss increases with the increased in treatment temperature and time. This is why the oil heat treated wood is no recommended for use in the load bearing constructions application (Korkut *et al.*, 2007; Jamsa and Viitaniemi, 2001). However, their dimensional stability and durability increases (Yildiz *et al*., 2006).

Analysis of Variance on the Strength Properties

The analysis of variance for the strength properties are shown in table 7. The analysis was conducted to determine whether there was significance difference between physical properties with treatment temperatures, duration, wood types and sampling height. There were significant difference between moisture content with treatment temperatures, duration and wood types. No significant difference was observed between the moisture content and the wood height (bottom to the top). For basic density, there were significant difference was observed with treatment temperatures, duration, wood types and sampling height.

The analysis of variance indicated that for MOR there are significant differences in treatment temperature, duration of treatment and sampling height. However, there is no significant difference in the wood type. For MOE, only two significant differences were observed, which are

treatment temperature and wood types. There is no significant difference in duration of treatment and sampling height.

Correlation Coefficient between the Chemical, Colour and Strength Properties

The correlation among wood properties of *A.* hybrid wood is presented in table 4. There exist strong correlation between the moisture content and the chemical composition in the cultivated acacia wood. Moisture contents has positive correlation to the holocellulose (r = 0.81) and cellulose (r = 0.82). While hemicellulose (r = -0.40) and lignin (r = -0.76) were negatively correlated with moisture content. According to Smith *et al*. (2003), due to the existence of hydrogen bonding sites in hydroxyl groups present in cellulose, hemicellulose and lignin, wood is a hygroscopic material. From this treatment, dimensional stability is increased due to decrement in moisture. There was positive correlation between moisture content and basic density of acacia wood in this treatment, but the correlation was not significant. A similar result was observed by Nordahlia (2008) in *Azadirachta excelsa* where moisture content and basic density was not correlated.

There was also a correlation between moisture content and strength properties in this study. Positive correlations were observed between moisture content and modulus of rupture (r = 0.50) and modulus of elastic (r = 0.40). Smith *et al.* (2003) noted that wood contains five or six layers of attached water molecules when in the saturated condition. While only one layer of water molecules at moisture of about 6% which is directly attached to cells walls by hydrogen bonding in dried wood. Mechanical properties of wood may degrade when there is a change happen in this layer due to many new hydrogen bonds are generated in the microfibrils with removal water molecules from cell walls, resulting in an increase of crystalline regions. The correlation between the basic density and other wood properties are presented in table 4. There was a correlation between basic density and strength properties (MOR and MOE) and chemical composition of acacia wood. Positive correlations were observed between basic density and modulus of rupture (r = 0.37), modulus of elasticity (r = 0.42), holocellulose (r = 0.24) and cellulose (r = 0.24).

The correlation between the strength properties and other wood properties are presented in table 4. There were a correlation between MOR and MOE, physical properties, colour and chemical composition of treated wood. Positive correlation were obtained between MOR and MOE (r = 0.60), moisture content (r = 0.50), basic density (r =0.37), lightness (L*) (r = 0.40), holocellulose (r = 0.42) and cellulose (r = 0.42). While hemicellulose (r = -0.19) and lignin (r = -0.36) were negatively correlated with MOR. For MOE there were also a correlation between physical properties, colour and chemical composition of treated wood. Positive correlation were obtained between MOE and moisture content (r = 0.40), basic density (r = 0.42), lightness(r = 0.34), holocellulose (r = 0.35) and cellulose (r = 0.37). While hemicellulose (r = -0.24) and lignin (r = -0.31) were negatively correlated with MOE.

CONCLUSIONS

The hot oil thermal modification process caused some features changed in the chemical composition of *A.* hybrid wood. The degradation in holocellulose, cellulose, and hemicellulose contents was recognized when acacia woods were exposed to oil thermally modified process. Holocellulose and celulose degraded with the increasing of treatment temperature and time of heating exposure, while lignin showed the increment in content through this treatment. The sapwood and heartwood of *A.* hybrid colour becomes darker once they are exposed to the high temperature and longer treatment time in the hot oil thermal modification process. The degree of the changes varies between both wood types. The sapwood tends to darken more than the heartwood. The increment in colour of both woods increases with temperature and treatment time. Treatment temperature at 200°C and treatment time of 90 min. and 220°C at 30 min. of the sapwood becomes uniform with the colour of the original untreated heartwood. The hot oil thermal modification process induced extensive darkening and reddening of *A.* hybrid wood. For the strength properties of the oil heat treated *A.* hybrid wood, the values of both MOR and MOE decreased throughout the treatment process. The decreases in values were influenced by treatment temperature and duration. The value of MOR and MOE of the treated wood were influenced by the treatment temperature. The increase in the holocellulose and cellulose contents causes an increase in the strength (MOR and MOE) of the *A.* hybrid wood. On the other hand, the reduction of the hemicellulose and lignin contents causes the drop in strength of the hot oil treated *A.* hybrid.

ACKNOWLEDGEMENT

The research was financed by The Ministry of Science, Technology and Invention, Malaysia, under the Science Fund Project SCF0037-IND-1/2007.

REFERENCES

American Society for Testing and Material. 1999. ASTM D4761-05: Section 4: Construction (vol. 04.10). Wood West Conshohocken, Pennsylvania, USA.

Bekhta, P. and Niemz, P. 2003. Effect of High Temperature on the Change in Color, Dimensional

Stability and Mechanical Properties of Spruce Wood. Journal of Holzforschung. 57:539-546.

Berard, P., Laurent, T. and Dumonceaud, O. 2006. Use of Round Wood of Chestnut Tree Coppices: Crack Risk and Effects of a Hot Oil Bath Treatment. Journal of Holz als Roh-und Werkstoff. 64: 287-293. DOI 10.1007/s00107-005-0086-4.

Bodig, J. and Jayne, BA. 1982. Mechanics of Wood and Wood Composite. Van Nostrand Reinbold Co. New York, USA.

Boonstra, MJ. and Tjeerdsma, B. 2005. Chemical Analysis of Heat Treated Softwoods. European Journal of Wood and Wood Products. 64(3):204-211. DOI: 10.1007/s00107-005-0078-4.

Bourgois, PJ., Janin, G. and Guyonnet, R. 1991. La Mesure de Couleur. Une Methode d'Etude et d' Optimisation des Transformations Chimiques du Bois Thermolyse. Journal of Holzforchung. 45:377-382.

Brito, JO., Silva, FG., Leao, MM. and Almeida, G. 2008. Chemical Composition Changes In Eucalyptus and Pinus Woods Submitted to Heat Treatment. Journal of Bioresource Technology. 99(18):8545-8548. DOI 10.1016/j.biortech.2008.03.069.

Burti, P., Jay-Allemand, C., Charpentier, JP. and Janing, G. 1998. Natural Wood Colouring Process in Juglans Spp. (J.nigra, *J.regia*, and Hybrid *J. nigra* x *J. regia*) Depends on Native Phenolic Compounds Accumulated in the Transition Zone between Sapwood and Heartwood. Journal of Trees. 12:258-264.

Charrier, B., Charrier, F., Janin, G., Kamdem, DP., Irmouli, M. and Goncalez, J. 2002. Study of Industrial Boiling Process on Walnut Colour: Experimental Study Under Industrial Conditions. Journal of Holz als Roh-und Werkstoff. 60:259-264. DOI 10.1007/s00107-005-0082-8.

CIE (Commission Internationale De Eclairage). 1986. Publication 15.2. Colorimetry, Second Edition Central Bureau of the CIE. Viena, Austria.

Fengel, D. and Wegener, G. 1989. Wood Chemistry, Ultrastructure, Reactions.Walter de Gruyter and Co. Berlin, New York, USA.

Giebeler, E. 1983. Dimensional Stabilization of Wood by Moisture-heat-pressure. Journal of Holz als Roh-und Werkstoff. 41:87-94.

Grelier, S., Castellan, A., Desrousseaux, S., Nour, A., Ode, A. and Podgorski, L. 1997. Attempt to Protect Wood Colour Against UV/Visible Light by Using Antioxidants Bearing Isocyanate Groups and Grafted to the Material with Microwave. Journal of Holzforschung. 51: 511-518.

Hill, C. 2006. Wood Modification: Chemical, Thermal and Other Processes. John Wiley & Sons, Ltd. England.

Hon, DNS. and Minemura, N. 1991. Color and Discoloration. In Wood and Cellulosic Chemistry. Eds. Hon, DNS. and Shirashi, N. Marcel Dekker Inc, New York, USA. 395-454.

Hyvonen, A., Piltonen, P. and Niinimaki, J. 2006. Tall Oil/Water- Emulsions as Water Repellents for Scots Pine Sapwood. Journal of Holz als Roh-und Werkstoff. 64:68-73. DOI 10.1007/s00107-005-0040-5.

Inari, GN., Petrissans, M. and Gerardin, P. 2007. Chemical Reactivity of Heat-treated Wood. Journal of Wood Science and Technology. 41:157-168.

Izyan, K., Razak, W., Mahmud, S., Othman, S., Affendy, H., Hanim, RA. and Andy, RM. 2010. Chemical Changes in 15 year-old Cultivated *Acacia* hybrid Oil-Heat Treated at 180, 200 and 220°C. International Journal of Chemistry. 2 (1):97-107.

Johansson, D. 2008. Heat Treatment of Solid Wood; Effects on Absorption, Strenght and Colour. Ph.D thesis, Lulea University of Technology. ISSN: 1402-1544.

Jamsa, S. and Viitaniemi, P. 2001. Heat Treatment of Wood Better Durability without Chemicals. Review on Heat Treatments of Wood. Cost Action E22. Proceedings of the Special Seminar, Antibes, France. 17-22.

Janssen, JA. 1981. Bamboo in Building Structures. Ph.D thesis, University of Technology, Holland.

Kamden, DP., Pizzi, A., Guyonnet, R. and Jermannaud, A. 1999. Durability of Heat-treated Wood. IRG WP: International Research Group on Wood Preservation 30. Rosenheim, Germany.

Kocaefe, D., Chaudry, B., Ponscak, S., Bouazara, M. and Pichette, A. 2007. Thermogravimetric Study of High Temperature Treatment of Aspen: Effect of Treatment Parameters on Weight Loss and Mechanical Properties. Journal of Material Science. 42:854-866.

Korkut, S., Kok, MS., Korkut, DS. and Gurleyen, T. 2008. The Effects of Heat Treatment on Technological Properties in Red-Bud Maple (*Acer trautvetteri* Medw.). Journal of Bioresource Technology. 99 (6):1538-1543. DOI 10.1016/ j.biortech. 2007. 04.021.

Keey, RB. 2004. Colour development on drying. Proceedings of the 14th International Drying Symposium (IDS 2004), Sao Paulo, Brazil. 33-47.

Mburu, F., Dumarcay, S., Bocquet, JF., Petrissans, M. and Gerardin, P. 2008. Effect of Chemical Modifications Caused by Heat Treatment on Mechanical Properties of *Grevillea robusta* Wood. Journal of Polymer Degradation and Stability. 93:401-405. DOI: 10.1016/j.polymdegradstab.2007.11.017.

Mitsui, K., Takada, H., Sugiyama, M. and Hasegawa, R. 2001. Changes in the Properties of Light-Irradiated Wood

with Heat Treatment. Part 1. Effect of Treatment Conditions on the Change in Color. Journal of Holzforschung. 55:601-605.

Nordahlia, AS. 2008. Wood Quality of 10-Year-Old Sentang (*Azadirachta excelsa*) Grown from Seedlings and Rooted Cuttings. Master thesis, University Putra Malaysia.

Rafidah, S., Razak, W. and Zaidon, S. 2008. Effect of Oil thermally modified on Chemical Constituents of Semantan Bamboo (*Gigantochloa scortechinii Gamble*). Journal of Sustainable Development. 1(2):91-98. Canadian Center of Science and Education.

Razak, W. Izyan, K., Othman, S., Aminuddin, M., Tamer, AT. and Rafidah, S. 2011. The chemical and strength properties of hot oil thermal modification on 15 year-old cultivated *Acacia* hybrid. Journal of Applied Sciences Research 7(4):517-525.

Razak, W., Aminuddin, M., Hashim, WS. and Othman, S. 2005. Effect of heat treatment using palm oil on properties and durability of Semantan bamboo. Journal of Bamboo and Rattan 4 (3):211-220.

Rowell, RM., Pettersen, R., Han, JS., Rowell, JS. and Tshabalala, MA. 2005. Cell Wall Chemistry. In: Handbook of Wood Chemistry and Wood Composites, Ed. Rowell R.M. Madison: CRC Press. 37-72.

Rulliarty, S. and America, WA. 1995. Natural Variation in Wood Quality Indicators of Indonesian Big Leaf Mahogany (Swietenia macrophylla. King). XX IUFRO World Congress Proceedings, Tampere.

Sailer, M., Rapp, AO., Leithoff, H. and Peek. RD. 2000. Improved Resistance of Scots Pine by Application of an Oil thermally modified. European Journal of Wood and Wood Products. 58(1-2):15-22. DOI: 10.1007/s001070050379.

Sandermann, W. and Augustin, H. 1964. Chemical Investigations on the Thermal Decomposition of Wood. Part III: Chemical Investigation on the Course of Decomposition. Journal of Holz als Roh-und Werkstoff. 22(10):377-386.

Sarni, F., Moutounet, M., Puech, JL. and Rabier, P. 1990. Effect of Heat Treatment on Oak Wood Extractable Compounds. Journal of Holzforschung. 44(6):461-466.

Smith, I., Landis, E. and Gong, M. 2003. Structure and Properties of Wood. In Fracture and Fatigue in Wood. Chichester: John Wiley & Sons Ltd. 7-34.

Sundqvist, B. 2004. Colour Changes and Acid Formation in Wood during Heating. Ph.D thesis, Lulea University of Technology.

TechnicaL Association of the Pulpa and Paper Industry. 1999. TAPPI Standard T203 om-99. Atlanta, USA.

TechnicaL Association of the Pulpa and Paper Industry. 2002. TAPPI Standard T222 om-02. Atlanta, USA.

Thulasidas, PK., Bhat, KM. and Okuyama, T. 2006. Heartwood colour variation in home garden teak (*Tectona grandis*) from wet and dry localities of Kerala India. Journal of Tropical Forest Science. 18:51-54.

Unsal, O., Korkut, S. and Atik, C. 2003. The effect of heat treatment on some properties and colour in Eucalyptus (*Eucalyptus camaldulensis* DEHN.) wood. Journal of Maderas. Ciencia Technologia. 5(2):145-152.

Viitaniemi, P. 2001. The Thermal Modification of Wood with Heat Treatment. VTT Building and Transport. Espoo, Findland. 1-21.

Yildiz, S., Gezer, ED. and Yildiz, UC. 2006. Mechanical and Chemical Behaviour of Spruce Wood Modified by Heat. Journal of Building and Environment. 41:1762-1766.

Received: July 20, 2011; Revised: Oct 22, 2011; Accepted: Oct 24, 2011

SENRA Academic Publishers, Burnaby, British Columbia
Vol. 6, No. 1, pp. 1797-1802, Feb 2012
Online ISSN: 1920-3853; Print ISSN: 1715-9997

Canadian Journal of pure&applied sciences

ROLE OF PHYTOLACCA AMERICANA AND PHYTOLACCA BERRY IN LIPID PROFILE ALLERATION IN HYPERCHOLESTROLEMIA INDUCED RABBITS *ORYCTOLAGUS CUNICULUS*

*Ruqaiya Hasan, Kalim R Khan and Sadia Kiran
Department of Physiology, University of Karachi, Karachi-75270, Pakistan

ABSTRACT

Present study is concerned to find out the induced effects of two herbal weight reducing drugs Phytolaccca Americana (PA) and Phytolacca Berry (PB) in hypercholestrolemia on lipid profile of Rabbits (*Oryctolagus cuniculus*). Pokeweed was the single constituent of PB, the other additional ingredients of PA are bladder wrack, garlic and grape fruit. Both herbal drugs were administered orally to the respective test animals in the doses of 33.3mg PA/day and 1.15mg PB/day, for 27 days and blood samples drawn on day 0,3,9,14,21 and 27 were used to measure mean plasma cholesterol, triglycerides (TG), low density lipoprotein (LDL-C) and high density lipoprotein (HDL-C) concentrations. After one week of administration of drugs although both drugs reduced the cholesterol and TG concentrations to lower levels but PB effectively decreased them below their normal concentrations when given approximately for four weeks. Similarly, both drugs lowered plasma LDL-C concentration after two weeks of treatment again PB reduced concentration below normal. However plasma HDL-C levels declined to normal levels following the one week of treatment, started to elevate along the passage of treatment and decreased to normal in the later part of experiment. These findings suggested that pokeweed comparatively, more effectively maintained the lipid profile at normal concentrations probably inhibiting the HMG-CoA reductase activity and affecting the lipoprotein metabolism. In case of PA interactions of ingredients may interfered the enzymes of lipoprotein metabolism thus constant elevated levels of LDL- C and TG were observed.

Keywords: Poke weed, phytolacca berry, phytolacca Americana, herbal drugs, lipid profile.

INTRODUCTION

Obesity is a chronic disease and should be treated with reasonable expectations (Scheen and Lefébvre, 1999) because of its related complications, an immediate safe and effective treatment is required (Sidhaye and Cheskin, 2006). Unfortunately, medication-induced weight loss is often associated with rebound weight gain after the cessation of drug use, side effects from the medications, and the potential for drug abuse. In the present study, two herbal weight reducing drugs Phytolacca Americana (PA) with a single constituent of Poke weed and Phytolacca Berry (PB) in addition to Poke weed, containing Bladder wrack, garlic and grape fruit, are used to assess the efficacy in the management of weight reduction through their effects on lipid profile in common rabbits.

The extract of various parts of poke weed plant are used in homeopathic medicines for the treatment of many diseases specially the obesity (Ravikiran *et al*., 2011). Weight loss in response to poke weed was noticed in molting hens (Willis *et al*., 2008) and in mice (Lazarus *et al*., 1998). Bladder wrack has three major active components; iodine and two types of dietary fibers, alginic acid and fucoidan (Chevrel, 1980). Iodine is used to treat obesity through its thyroid gland stimulating effect (Björvell and Rössner, 1986; Teas *et al*., 2007) while animal and in vitro studies had proposed the LDL- C lowering effects of both alginic acid and fucoidan (Vázquez *et al*., 1996). Garlic was known to be effective in decreasing plasma lipids and a number of studies have shown that garlic significantly decreased the total cholesterol and LDL – C in human (Milner, 1996 ; Steiner *et al*.,1996; Stevinson *et al*., 2000) and moderately raised HDL-C (Ashraf *et al*., 2005, 2011). Experimental studies by Gorinstein *et al*. (2006) have shown the plasma lipid and cholesterol lowering effects of garlic in rats.

Grapefruits are a good food to include in a sensible weight-loss diet. Grapefruit seed extracts with high concentrations of vitamin C and E claimed to have antimicrobial and antioxidant properties (Armando, 1998; von Woedtke *et al*., 1999; Dembinski *et al*., 2004). Experimental studies in rats have shown that naringenin, a flavonoid present in grapefruit might reduce the risk of coronary heart disease and other chronic diseases through its hypocholesterolemic effects (Daher *et al*., 2005; Cho *et al*., 2011). Reduction of serum cholesterol levels were also observed in laying hens with supplemented flavonoids (Lien *et al*., 2008).

*Corresponding author email: ruqaiya55@gmail.com

MATERIALS AND METHODS

Animals
Rabbits (*Oryctolagous cuniculus*) used in the experiment were one to one and half years old; 12 in number with their average weight 1160 to 1510gm were obtained from local supplier. They were kept in barred cages, placed in well ventilated environment. Four *O. cuniculus* were kept as control (Lab standard) and the remaining eight in equally divided two groups were used as test animals.

Induction of hypercholesterolemia
All rabbits were made hypercholesterolemic by feeding a modified diet of 5g of butter fat per kg of daily diet (Moghadasian *et al*., 1999) for 15 days and blood samples were collected at day 0 and 15.

Drug Therapy
The herbal weight reducing drugs used for experimental purpose include PA and PB, purchased from local chemist shop in tablet form. A dose of PA calculated for daily oral administration was 33.3mg. While an oral daily dose of PB calculated was 1.15mg.

Blood Sampling
Blood samples were obtained with the help of 3cc disposable syringes from the marginal vein of ear. Sampling was done from day 0,3,9,14,21 and 27. In order to obtain plasma; heparinized blood samples were centrifuged at 3600rpm for 5minutes and the supernatants were stored at 4^0C to be read on spectrophotometer (Model No. NV 201, China).

Biochemical and Statistical Analysis
Blood lipid profile i.e. cholesterol, TG, LDL–C and HDL-C were measured by using commercial biochemical kits (Randox, Cat. No. CH200, TR1696, CH203, CH1350). The absorbance of samples was read on spectrophotometer. The data was statistically analyzed by t-test and two-way ANOVA.

RESULTS

A consideration of table1 indicates that control and test rabbits fed on the diet with additional 5g butter fat per kg of diet for 15 days resulted in a significant rise ($P<0.05$) in mean plasma concentrations of cholesterol, TG, LDL-C and HDL-C.

Control
Control rabbits after 15 days when reverted to their normal diet showed a reduction in mean plasma concentration of cholesterol and HDL-C from day 3 and reached to normal levels. However mean plasma TG and LDL-C remained significantly higher ($P<0.05$) than normal concentrations (Figs. 1-4).

Cholesterol
Test 1 (T1) rabbits with initial mean plasma cholesterol level of 227.44±49.40 mg%, when administered with a dose of 33.3 mg/day of PA for 27 days showed an immediate fall in mean cholesterol concentration on day 3 then a rise on day 9, followed by a gradual significant ($P<0.05$) reduction of 138.17±8.87 mg% on day 27 (Fig. 1).

Test 2 (T2) rabbits with mean plasma cholesterol concentration of 185.2± 26.39 mg% on day 0, administered a dose of 1.15 mg/day of PB for 27 days showed a fall and rise of mean cholesterol concentration in similar pattern on day 3 and day 9 respectively. However, the reduction in cholesterol concentration continues to fall non-significantly below normal level i.e. 36.958±10.77mg% on day 27 (Fig. 1).

TG
T1 animals with increased mean plasma TG concentration of 354.63±36.47mg% following the treatment showed a reduction and elevation of TG level on day 3 and day 9 respectively. Afterward the mean triglyceride

Table 1. Effect of Butter Fat (5g/kg diet) on Mean Plasma lipid profile (mg%) of rabbits *Oryctolagus cuniculus*.

	Cholesterol			Triglyceride		
Days	C	T1	T2	C	T1	T2
0	67.65±7.52	70.97±6.70	68.24±3.21	149.99±6.82	157.97±4.89	149.67±7.34
15	202.01±14.43	227.441±49.40	185.26±26.39	326.13±14.44	354.63±36.47	443.98±69.94

LDL			HDL		
C	T1	T2	C	T1	T2
72.08± 8.557	52.16 ± 6.03	59.76 ± 6.68	101.20 ±1.59	118.29 ± 31.19	102.41 ±22.08
326.67 ±6.08	402.82±137.12	275.32±47.19	242.86 ±14.88	256.56 ± 10.69	246.01 ±4.92

Each figures is the Mean ± SD of four values
C = Control, T1 = Phytolacca Americana (33.3 mg/day), T2 = Phytolacca Berry (1.15 mg/day)

concentration continued to reduce up to day 27, but remained significantly higher than normal concentration. Animals treated with PB also followed the similar pattern of changes in mean plasma TG concentration from day 3 to day 9, but the reduction of TG concentration from day 9 on-wards was significantly below the normal levels (Fig. 2).

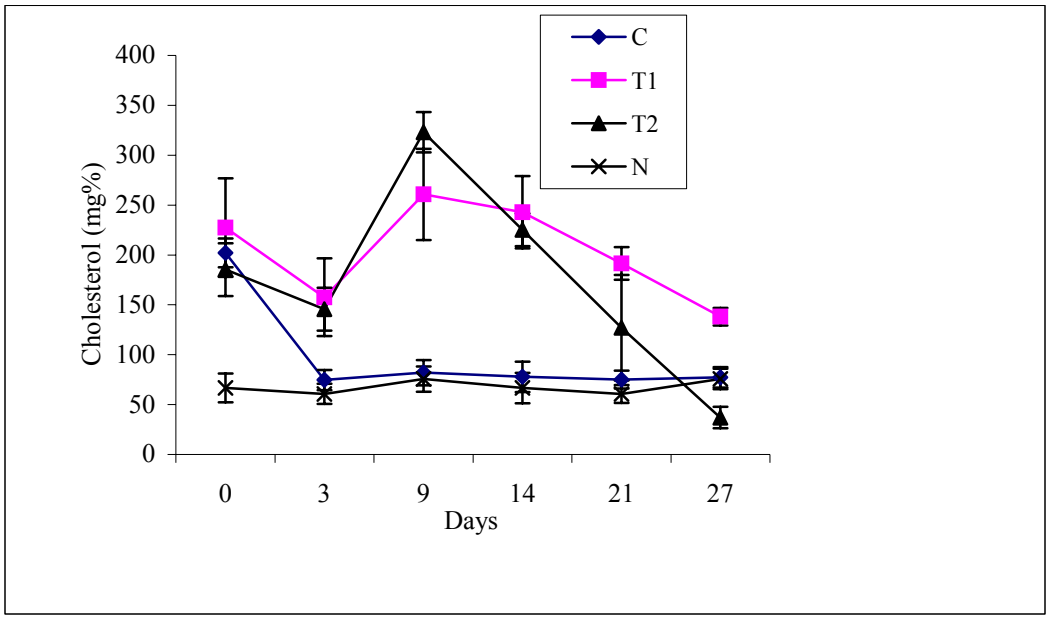

Fig. 1. Comparison of mean plasma cholesterol concentration in control and test rabbits *Oryctolagus cuniculus* following the administration of weight reducing drugs.
Each figures is the Mean ± SD of four values.
C = Control, T1 = Phytolacca Americana (33.3 mg/day), T2 = Phytolacca Berry (1.15 mg/day), N= Normal

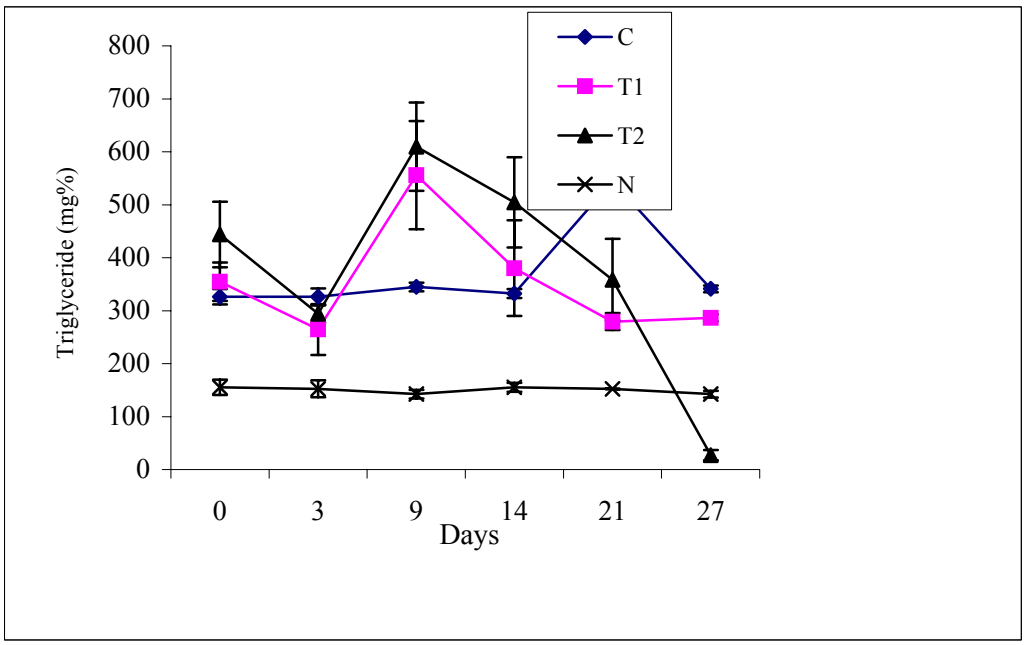

Fig. 2. Comparison of mean plasma TG concentration in control and test rabbits *Oryctolagus cuniculus* following the administration of weight reducing drugs.
Each figures is the Mean ± SD of four values
C = Control, T1 = Phytolacca Americana (33.3 mg/day), T2 = Phytolacca Berry (1.15 mg/day), N= Normal

LDL-C

Figure 3 shows the animals of T1 group have a reduction in mean plasma LDL-C concentration on day 3 followed by a rise and fall on day 9 and day 14 respectively along the treatment. However the mean LDL-C concentration remained higher i.e. 243.80± 21.93 mg% on day 27 and did not reach to normal value.

T2 animals following the treatment with PB have a maximum mean LDL-C concentration of 473.30±94.53 mg% on day 9 and reduced to normal level on day 27 (Fig. 3).

HDL-C

T1 rabbits when treated with PA for 9 days showed a reduction in mean plasma HDL-C concentration of 115.87±9.89 mg%. Further administration of drug increased the mean HDL-C level followed by a reduction to near normal concentration (Fig. 4).

In T2 rabbits, administration of drug also resulted in a fall of mean HDL-C concentration on day 9, which gradually elevated up to day 21 and returned to approximately normal levels.

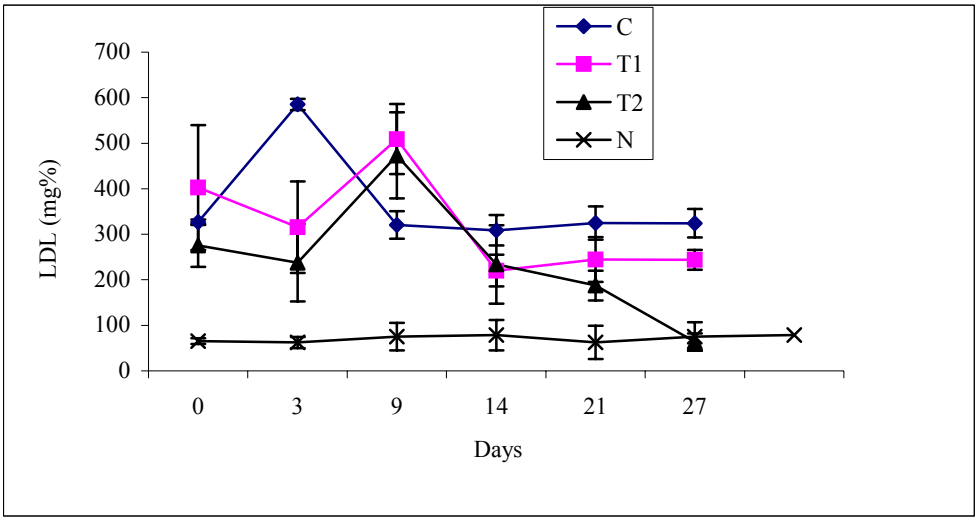

Fig. 3. Comparison of mean plasma LDL-C concentration in control and test rabbits *Oryctolagus cuniculus* following the administration of weight reducing drugs.
Each figures is the Mean ± SD of four values
C = Control, T1 = Phytolacca Americana (33.3 mg/day), T2 = Phytolacca Berry (1.15 mg/day), N= Normal

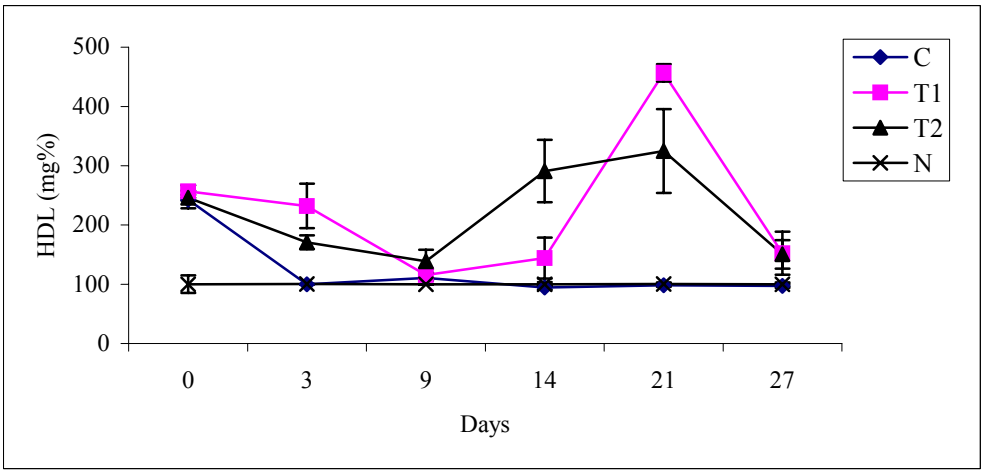

Fig. 4. Comparison of mean plasma HDL-C concentration in control and test rabbits *Oryctolagus cuniculus* following the administration of weight reducing drugs.
Each figures is the Mean ± SD of four values
C = Control, T1 = Phytolacca Americana (33.3 mg/day), T2 = Phytolacca Berry (1.15 mg/day), N= Normal

DISCUSSION

The mechanism of reduction of body fat and ultimate reduction in body weight by herbal drugs is achieved either by suppression of appetite and decreasing the intestinal absorption (Fanghanel *et al*., 2000; Smith and Goulder, 2001) or stimulating the satiety centers with increased metabolic rates (Girola *et al*., 1996; Allison *et al*., 2001). The ingredients of both drugs i.e. PA and PB used in this study are laxative (Väzquez *et al*., 1996), thus limiting the intestinal absorption and increasing the loss of fluid.

A diet with added butter fat given to rabbits cause a significant rise in lipid profile concentrations, although removal of fat from the diet in control animals show the reversal plasma mean concentrations of cholesterol and HDL-C to normal level while TG and LDL-C remained elevated.

The experimental animals of T1 and T2 administrated with PA and PB for 27 days respectively show the lipid profile of both treatments returning to normal values. Comparatively PB more effectively decreases the mean cholesterol, TG and LDL-C concentrations to very low values.

One of the major constituents of PA is bladder wrack and the alginic acid present in it is a good source of iodine that affects the thyroid function and lipid metabolism (Katamine *et al*., 1985; Zhao *et al*., 2011) while other constituent, fucoidan, which is a type of polysaccharide, significantly lowers blood cholesterol, TG, LDL-C with an increase in HDL-C in hypercholesterolemic mice (Li *et al*., 2008; Huang *et al*., 2010) as well as hyperlipidemic patients without any adverse effects on liver and kidney (Wang and Bi, 1994).

The garlic present in PA is known to reduce total cholesterol moderately without a significant reduction and elevation in LDL-C and HDL-C respectively (Reinhart *et al*., 2009) actually produces this effect by interfering the cholesterol metabolism through the inhibition of HMG-CoA reductase activity.

Grape fruit present in PA can reduce the LDL-C and TG levels (Cerda, 1987; Carper, 1988; Daher *et al*., 2005). One of the grapefruit flavonoids, naringenin is found to affect lipoprotein metabolism resulting in hypolipidemia (Anthony *et al*., 1997) and the other constituent nootkatone, greatly increases the energy metabolism in skeletal muscle and liver cells, as a result diet induced reduction in body weight is achieved through the increased activity of enzyme adenosine monophosphate kinase (Murase *et al*., 2010).

Finally, it may be concluded that herbal drugs might not be free of side effects specially when used in combination form, as the chances of adverse interactions of herbal ingredients increase. Also studies on human beings are insufficient thus herbal drugs should be used under the supervision of health care professionals.

ACKNOWLEDGEMENT

We thank the Dean, Faculty of Science, University of Karachi for the research grant awarded for this study.

REFERENCES

Allison, DB., Fontaine, KR., Heshka, S., Mentore, JL. and Heymsfeild, SB. 2001. Alternative treatment for weight loss: A critical review. Food. Sci. Nutr. 41(1):1-28.

Anthony, MS., Clarkson, TB., Bullock, BC. and Wagner, JD.1997. Soy protein versus soy phytoestrogens in the prevention of diet-induced coronary artery atherosclerosis of male cynomolgus monkeys. Arterioscler. Thromb. Vasc. Biol. 17:2524-2531.

Armando, C., Maythe, S. and Beatriz,NP. 1998. Antioxidant activity of grapefruit seed extract on vegetable oils. J. Sc. Food Agri. 77:463-467.

Ashraf, R., Aamir, K., Shaikh, AR. and Ahmed, T. 2005. Effects of garlic on dyslipidemia in patients with type-2 diabetes mellitus. J. Ayub Med. Coll. 17(3): 60-64.

Ashraf, R., Khan, RA. and Ashraf, I. 2011. Garlic (*Allium sativum*) supplementation with standard antidiabetic agent provides better diabetic control in type-2 diabetic patients. Pak. J. Pharm. Sci. 24(4):565-570.

Björvell, H. and Rössner, S. 1986. Long term effects of commonly available weight reducing programmes in Sweden. Int. J. Obes. 11:67-71.

Carper, J. 1988. Grapefruit In: The Food Pharmacy. Bantam Books, New York, USA. 213-215.

Cerda, J. 1987. The role of grapefruit pectin in health and disease. Trans. Am. Clin. Climatol. Assoc. 99:203-213.

Chevrel, B. 1980. A comparative crossover study on the treatment of heartburn and epigastric pain: Liquid Gaviscon and a magnesium-aluminum antacid gel. J. Int. Med. Res. 8:300-303.

Cho, KW., Kim, YO., Andrade, JE., Burgess, JR. and Kim, YC. 2011. Dietary naringenin increases hepatic peroxisome proliferators – activated receptor α protein expression and decreases plasma triglyceride and adiposity in rats. Eur. J Nutr. 50 (2):81-88.

Daher, CF., Abou- Khalil, J. and Baroody, GM. 2005. Effect of acute and chronic grapefruit, orange and pineapple juice intake on blood lipid profile in normolipidemic rat. Med. Sci. Monit. 11(12):465-472.

Dembinski, A., Warzecha, Z., Konturek, SJ., Ceranowicz, P., Dembinski, M., Pawlik, WW., Kusnierz-Cabala, B. and Naskalski, JW. 2004. Extract of

Grapefruit-Seed Reduces Acute Pancreatitis Induced by Ischemia/Reperfusion in Rats; Possible Implication of Tissue Antioxidants. J. Physiol. Pharmacol. 55(4):811-821.

Franghanel, G., Cortinas, L., Sanchez, RL. and Berber, A. 2000. A clinical trial of the use of subutramine for the treatment of patint suffering essential obesity. Int. J.Obes. Relat. Metab. Disord. 24(2):144-150.

Girola, M., DeBernardi, M. and Contos, S. 1996. Dose effect in lipid lowering activity of new dietry integrator (Chitosan, Garcinia cambogia extract and Chrome).Toxicol. Ther. 17:25-40.

Gorinstein, S., Leontowicz, H., Leontowicz, M., Drzewiecki, J., Najman, K., Katrich, E., Barasch, D., Yamamoto, K. and Trakhtenberg, S. 2006. Raw and boiled garlic enhances plasma antioxidant activity and improves plasma lipid metabolism in cholesterol-fed rats. Life Sci. 655-663.

Huang, L., Wen, K., Gao, X. and Liu, Y. 2010. Hypolipidemic effect of fucoidan from Laminaria japonica in hyperlipidemic rats. Pharm. Biol. 48(4):422 - 426.

Katamine, S., Hoshino, N., Totsuka, K. and Suzuki, M. 1985. Effects of the long – term (17 – 19 months) feeding of high – iodine eggs on lipid metabolism and thyroid function in rats. J. Nutr. Sci. Vitaminol. 31 (3):339-353.

Lazarus, DD., Trimble, LA. and Moldawer, LL. 1998. The metabolic effects of pokeweed mitogen in mice. Metab. 47 (1):75-82.

Li, B., Lu, F., Wei, X. and Zhao, R. 2008. Fucoidan: Structure and bioactivity. Molecules. 13(8):1671-1695.

Lien, TF., Yeh, HS. and Su, WT. 2008. Effect of adding extracted hespertin, naringenin and pectin on egg cholesterol, serum traits and antioxidant in laying hens. Arch. Anim. Nutr. 62(1):33-43.

Milner, JA. 1996. Garlic: Its anticarcinogenic and antitumorigenic properties. Nutr. Rev. 54:82-86.

Moghadasian, MH., Manus, BM., Godin, DV., Rodrigues, B. and Frohlich, JJ. 1999. Proatherogenic and antiatherogenic effect of probucol and physterols in apolipoprotein E deficient mice, possible mechanism of action. Circulation. 99:1733-1739.

Murase, T., Misawa, K., Haramizu, S., Minegishi, Y. and Hase, T. 2010. Nootkatone, a characteristic constituent of grapefruit, stmulates energy metabolism and prevents diet – induced obesity by activating AMPK. Am. J Physiol. Endocrinol. Metab. 299:266-275.

Ravikiran, G., Raju, AB. and Venugopal, Y. 2011. Phytolacca Americana: A Review. Int. J. Res. Pharma.Biomed. Sci. 2(3):942-946.

Reinhart, KM., Talati, R., White, CM. and Coleman, CI. 2009. The Impact of garlic on lipid parameters: A systematic rewiew and meta – analysis.Nutr. Res Rev. 22 (1): 39-48.

Scheen, AJ. and Lefébvre, PJ. 1999. Pharmacological treatment of obesity: present status. Int. J. Obes. Relt. Metab. Disord. 23(1):47-53.

Sidhaye, A. and Cheskin, LJ. 2006. Pharmacologic Treatment of Obesity. In: Health and Treatment Strategies in Obesity. Ed. Vaidya, V. Adv. Psychosom. Med. Basel, Karger, Switzerland. 27:42-52.

Smith, IJ. and Goulder, MA. 2001. Randomized placebo controlled trail of long term treatment with sibutramine in mild to moderate obesity. J. Fan. Pract. 50(6):505-512.

Steiner, M., Khan, AH., Holbert, D. and Lin, RI. 1996. A double-blind crossover study in moderately hypercholesterolemic men that compared the effect of aged garlic extract and placebo administration on blood lipids. Am. J. Clin. Nutr. 64:866-870.

Stevinson, C., Pittler, MH. and Ernst, E. 2000. Garlic for treating Hypercholesterolemia. Ann. Intern. Med. 133:420-428.

Teas, J., Braverman, LE., Kurzer, MS., Pino, S., Hurley, TG. and Hebert, JR. 2007. Seaweed and soy: companion foods in Asian cuisine and their effects on thyroid function in American women. J. Med. Food. 10(1):90-100.

Vázquez-Freire, MJ., Lamela, M. and Calleja, JM. 1996. Hypolipidaemic activity of a polysaccharide extract from Fucus vesiculosus L. Phytother. Res. 10:647-650.

von Woedtke, T., Schlüter, B., Pflegel, P., Lindequist, U. and Jülich, WD. 1999. Aspects of the antimicrobial efficacy of grapefruit seed extract and its relation to preservative substances contained. Pharmazie. 54:452-456.

Wang, SZ. and Bi, AF. 1994. Clinical observation of fucoidan on patients with hyperlipidemia. Med. J.Qilu. 173-174.

Willis, WL., Goktepe, I., Isekhuemhen, OS., Reed, M., King, K. and Murray, C. 2008. The effect of mushroom and pokeweed extract on salmonella, egg production and weight loss in molting hens. Poult. Sci. 87(12):2451-2457.

Zhao, SJ., Ye, Y., Tian, EJ. and Chen, ZP. 2011. The impact of dietary iodine intake on lipid metabolism in mice. Biol. Trace Elem. Res. 142(3):581-588.

Received: Oct 20, 2011; Accepted: Dec 19, 2011

SENRA Academic Publishers, Burnaby, British Columbia
Vol. 6, No. 1, pp. 1803-1807, Feb 2012
Online ISSN: 1920-3853; Print ISSN: 1715-9997

Canadian Journal of pure&applied sciences

Short Communication

SOXHLET EXTRACTION, PHYSICOCHEMICAL ANALYSIS AND COLD PROCESS SAPONIFICATION OF NIGERIAN *JATROPHA CURCAS* L. SEED OIL

*Warra, AA[1], Wawata, IG[2], Umar, RA[3] and Gunu, SY[1]
[1]Department of Biochemistry, Kebbi State University of Science & Technology, PMB 1144, Aliero, Nigeria
[2]Department of Pure & Applied Chemistry, Kebbi State University of Science & Tech., PMB 1144, Aliero, Nigeria
[3]Department of Biochemistry, Usmanu Danfodiyo University, PMB 2346, Sokoto, Nigeria

ABSTRACT

In search of oils that can replace edible oils used for soap making, *Jatropha curcas* L. seed oil was exploited. The lipid was extracted using n- hexane and analyzed for chemical properties. The parameters analyzed were Acid value, (1.20 ± 0.065mgKOH/g) Iodine value, (73.46 ± 5.00g I_2/100g) and saponification value (122.49 ± 2.59mgKOH/g). The percentage oil yield was 48. The lipid was used to prepare soap. The pH of the soap was 9.11, comparably within the higher pH range of 9-11 set by the National Agency for Food and Drug Administration and Control (NAFDAC), mostly due to incomplete alkali hydrolysis resulting from the saponification process. The foam height of the soap was 5.4 cm and was higher than that of all other soap solutions analyzed. The soap forms a clear solution and was slightly soluble in distilled water.

Keywords: Jatropha oil, extraction, saponification, physicochemical analysis.

INTRODUCTION

Jatropha curcas (Linnaeus) is a multipurpose bush/small tree belonging to the family of *Euphorbiaceae*. It is a native of tropical America, but now thrives in many parts of the tropics and sub tropics in Africa and Asia. Although most of the *Jatropha* species are native to the new world, approximately 66 species are native to the Old World (Heller, 1996). It is a tropical plant that that can be grown in low to high rainfall areas (Openshaw, 2000). It is considered as a potential source of non-edible fuel producing plant along with its different medicinal properties (Verma and Gaur, 2009). In Nigeria it is known as "binidazugu/cinidazugu" and 'lapa lapa" in Hausa and Yoruba languages respectively (Blench, 2007; Blench, 2003). *J. curcas* is being explored for its oil yield potential throughout the world (Ginwal *et al.*, 2004). Various methods for recovering this oil from the seeds have been investigated. Shah *et al.,* (2005) reported the use of combination of ultrasonication and aqueous enzymatic oil extraction method. Extracting oil from Jatropha seeds can be done either with a manual press, such as the ram press, or with a mechanical press, such as the oil expeller. With mechanic expellers (like sundhara press) up to 75-80% of the oil can be extracted. With hand press like the Bielenberg ram press only 60-65% of the oil can be extracted (5kg of seeds give about 1litre of oil (Henning, 2003). Extraction with organic solvents and water has been the main approaches. For research purposes, Sayyar *et al.* (2009) in their research on optimization and kinetics in the extraction of oil from *Jatropha* found Hexane to be the best solvent for the process as compared to petroleum ether. High oil content of *Jatropha Curcas* indicated that the oil is suitable as non-edible vegetable oil feedstock in oleochemical industries (biodiesel, fatty acids, soap, fatty nitrogenous derivatives, surfactants and detergents (Akbar *et al.*, 2009).

Due to its toxicity consequent upon presence of curcin and phorbol esters (King *et al.*, 2009) *J. curcas* oil is not edible and is traditionally used for manufacturing soap and medicinal applications (Jongschaap *et al.*, 2007). Goel *et al.* (2007) suggests that the detoxification or complete removal of phorbol esters is essential before its use in industrial or medicinal applications. The major toxin phorbol ester is not vulnerable to heat, but can be hydrolyzed to less toxic substances extractable by either water or ethanol (Usman *et al.*, 2009). The use of Jatropha in soap industry, (alternative Karitee Butter) and cosmetics is regarded as one of its non-energy use (Rijssenbeek, 2007).

Chemical structure

Jatropha seed oil chemically consists of triacylglycerol with linear fatty acid chain (unbranched) with/without double bonds.

*Corresponding author email: aliyuwarra@yahoo.com

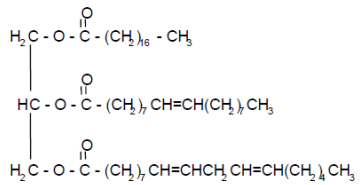

This work is aimed at preparation of soap from soxhlet extracted Nigerian *Jatropha curcas* L. seed oil.

MATERIALS AND METHODS

Seed material

Indigenous *J. Curcas* L. seeds were obtained from *Jatropha Curcas* plant in a test plot in Warra town Ngaski local government area of Kebbi State, Nigeria. The plant was identified and authenticated by a Botanist at the Biological Sciences Department, Bayero University, Kano (BUK) Nigeria. Confirmation of taxonomic identity of the plant was achieved by comparison with voucher specimen (voucher No. 110) kept at the Herbarium of the Department of Biological Sciences. The seeds were selected and damaged ones were discarded. The seeds were cleaned, de-shelled and well dried and ground using laboratory plastic pestle and Mortar prior to extraction.

Oil extraction

The extraction of 5.0g of the grounded seed kernels was conducted in a soxhlet extractor using n-hexane (boiling point of 40–60ºC) for 6hours. The lipid was obtained after the solvent was removed under reduced temperature and pressure and refluxing at 70ºC to remove excess solvent used in the oil. Extracted seed oil was stored in freezer at −2ºC for subsequent physicochemical analyses.

Oil Yield

The oil, which was recovered by complete distilling of most of the solvent on a heating mantle was then transferred to measuring cylinder. The measuring cylinder is then placed over water bath for complete evaporation of solvent for about 2-3hours in accordance with the method reported by Pant *et al.* (2006) and volume of the oil was recorded and expressed as oil content (%) as follows:

$$\text{Oil content (\%)} = \frac{\text{Oil weight}}{\text{Sample weight}} \times 100$$

Chemical Analysis

The chemical analysis of the oils was carried out using the methods reported by Bassir (1978), AOAC (1998), and Akpan *et al.* (2006) with modifications.

Saponification value: About 2g of the oil sample was added to a flask with 30cm^3 of ethanolic KOH and was then attached to a condenser for 30minutes to ensure the sample was fully dissolved. After sample has cooled, 1cm^3 of phenolphthalein was added and titrated with 0.5M HCl until a pink endpoint was reached.

Saponification value was calculated from the equation

$$SV = \frac{(S-B) \times M \times 56.1}{\text{Sample weight (g)}}$$

Where S = sample titre value
B = blank titre value
M = molarity of the Hcl
56.1 = molecular weight of KOH

Iodine value: 0.4g of the sample was weighed into a conical flask and 20cm^3 of carbon tetra chloride were added to dissolve the oil. Then 25cm^3 of Dam's reagent were added to the flask using a safety pipette in fume chamber. Stopper was then inserted and the content of the flask was vigorously swirled. The flask was then placed in the dark for 2hours 30minutes. At the end of this period, 20cm^3 of 10% aqueous potassium iodide and 125cm^3 of water were added using a measuring cylinder. The content was titrated with 0.1M sodium-thiosulphate solution until the yellow colour almost disappeared.

Few drops of 1% starch indicator were added and the titration continued by adding thiosulphate drop wise until blue coloration disappeared after vigorous shaking. The same procedure was used for blank test and other samples (Akpan *et al.*, 2006).

The iodine value (I.V) was obtained from the expression

$$I.V = \frac{12.69C\ (V_1-V_2)}{M}$$

Where C = Concentration of sodium
V_1 = Volume of sodium thiosulphate used for blank
V_2 = Volume of sodium thiosulphate used for determination
M = Mass of the sample.

Acid value: 100cm^3 of neutral ethyl alcohol were heated with 10 g of oil or fat sample in a 250 cm^3 beaker until the mixture began to boil. The heat was removed and was titrated with N/10 KOH solution, using two drops of phenolphthalein as indicator with consistent shaking for which a permanent pink colour was obtained at the end point.

The Acid value was calculated using the expression; A.V = 0.56 x No. of ml. N/10 KOH used.

Saponification Procedure

For each soap formulation 70cm^3 of 170g/dm^3 alkali solution were poured directly into the beaker containing the fat and oils in the ratio 1:1(v/v). The fats/oil was warmed gently and was poured into the beaker followed

by the alkali solution to form an intimate mix and then stirred frequently for 10-15minutes using stirring rod. The saponification mixture was then poured into moulds. After pouring, the soap was allowed to harden by air-drying for 24hours to obtain the soap bars.

pH Determination

The pH was determined using a pH meter (827 pH lab Model). 10g of the soap shavings were weighed and dissolved in distilled water in a 100ml volumetric flask. This was made up to prepare 10% soap solution in line with literature report (Dalen and Mamza, 2009). The electrode of the pH meter was inserted into the solution and the pH reading was recorded. The steps were repeated using soaps produced from each fat or oil.

Foam ability Tests

We used the method reported by Isah (2006) for synthetic detergent. About 2.0g each of soap (shavings) was added to a 500cm^3 measuring cylinder containing 100cm^3 of distilled water. The mixture was shaken vigorously so as to generate foams. After shaking for about 2minutes, the cylinder was allowed to stand for about 10minutes. The height of the foam in the solution was measured and recorded. The steps were repeated using soaps produced from each fat or oil.

RESULTS

The results obtained are presented in tables 1 to 4.

Table 1. Physicochemical characteristics of *J. curcas L* seed oil.

Parameter	Observation
Saponification value mgKOH/g	122.49 ± 2.591
Iodine value gI_2/100g	73.46 ± 5.00
Acid value mgKOH/g	1.20 ± 0.065
Oil yield (%)	48
Physical state at room temperature	Liquid

The values are mean and standard deviation of triplicates determination.

Table 2. Physical and chemical characteristics of the prepared *Jatropha* soap.

Parameter	Observation
pH	10.11
Foam height (cm)	5.4
Color of soap solution	Clear solution
Solubility in water	Highly Soluble

The values are mean of triplicates determinations.

Table 3. pH of the various soap samples compared with *J. curcas* seed oil soap.

Soap sample	pH value
Castor oil based soap	9.70
Castor glycerine soap	9.60
Cotton oil soap	9.38
Jatropha oil based soap	10.11
Neem oil	9.90
Sesame oil soap	9.88
She nut fat soap	10.33

The values are mean of triplicates determinations.

Table 4. Foam ability as a function of foam height of the various soap samples compared with *J. curcas* seed oil soap.

Soap sample	Foam height (cm)
Castor oil based soap	1.6
Castor glycerine soap	1.4
Cotton oil soap	4.5
Jatropha oilbased soap	5.4
Neem oil	2.0
Sesame oil soap	4.8
Shea nut fat soap	4.2

The values are mean of triplicates determinations.

DISCUSSION

The physicochemical analysis (Table 1), determined for the soxhlet extracted indigenous Jatropha seed oil includes; Saponification value of 122.49 ± 2.591 mgKOH/g the value obtained was lower than that of *Dennettia tripatala* fruit oil(Pepper fruit)159.33±1-20 suitable for soap making (Nwinuka, and Nwiloh, 2009) but higher than that of beeswax (93 mgKOH/g), which are commonly used in soap making (Mabrouk, 2005). This indicates that the oil could be used in soap making since its saponification value falls within the range of these oils. Higher saponification justifies the usage of fat or oil for soap production.

Iodine value of 50.50 ± 8.023 I_2/100g (less than 100) was obtained, which shows that the oil belongs to the class of Non-drying oils, which are useful in the manufacture of soaps (Kochhar, 1998). An Acid value of 14.77 ± 0.065mgKOH/g was obtained which is lower than that of olive oil 17mgKOH/g (Davine and Williams, 1961) higher than the 10.49 3mgKOH/g reported by Oyedele (2002), which signifies a maximum purity and made it suitable for soap production. For the prepared soap the pH was 9.11 (Table 3) comparably within the higher pH range of 9-11 but favourably higher than the pH range of 3-5, which are considered as high and low levels respectively by the National Agency for Food and Drug

Administration and Control (NAFDAC), (Umar, 2002) mostly due to incomplete alkali hydrolysis resulting from the saponification process. This can be overcome by the addition of excess fat or oil or any other superfatting agent to reduce the harshness of the soap. Superfatting soaps with 1-2% neutral oils or glycerine also resulted in the better quality of soaps that were free of cracks (Kuntom *et al*., 1999).The foam height of the soap was 5.4cm (Table 4) higher than that of all other soap solutions analysed. The soap forms a clear solution and was and slightly soluble in distilled water. Although foam generation has little to do with cleansing ability (Mainkar and Jolly, 2000), it is of interesting importance to the consumer and is therefore considered as a parameter in evaluating soaps and detergents. Mainkar and Jolly (2000) mentioned commonly used test protocols for foam test. The pour foam test developed by Ross and Miles (1941), which for long has been accepted method for measuring foaming performance. Hart and Degeorge (1980) preferred to measure the lather drain times, whereas Sorkin *et al*. (1966) called for rotating a shampoo solution in a glass stoppered cylinder. Neu (1960) used kitchen blender to produce foam and found that the foam characteristics were similar to those observed in practice.

CONCLUSION

From the results obtained after the chemical analysis of the oil, it can be concluded that the selected oil is utilizable for soap making. The properties exhibited by the soap solution indicated its suitability for commercial production. Hence even if the current boom for Jatropha production is based mainly on the incentive of producing biofuel, other possible range of products can be derived from Jatropha seed oil such as soap as demonstrated by this present research, which appears to be the first reported work in Nigeria.

ACKNOWLEDGEMENTS

The Authors wish to acknowledge all of the different scientists, technologists and lab assistants in the Chemistry laboratory, Department of pure and Applied Chemistry, Kebbi State University of Science and Technology, Aliero, Nigeria for their maximum support and cooperation.

REFERENCES

Akbar, E.,Yaakob, Z., Kamarudin, SK., Ismail, M. and Salimon J. 2009. Characteristics and Composition of *Jatropha curcas* Oil seed from Malaysia and its Potential as Biodiesel Feedstock. Eur J Sci Res. 29:396-40.

Akpan, UG., Jimoh, A. and Mohammed, AD. 2006. Extraction and characterization and Modification of Castor seed. Leonardo J. Sci. 8:43-52.

AOAC. 1998. Official Methods of Analysis of the Association of Official Analytical Chemists, 16th Edition, Gaithersburg, USA.

Bassir, O. 1978. Handbook of practical biochemistry. Ibadan University Press, Ibadan, Nigeria

Blench, R. 2007. Hausa names for plants and trees. http://www.rogerblench.info/RBOP.htm Printout December 11, 2007. Accessed at http://www.rogerblench.info/Ethnoscience% 20data/Hausa%20plant%20names.pdf 11/5/2009

Blench, R. 2003. Hausa names for plants and trees. Available at http://www.org/odi/staff/r.

Dalen, MB. and Mamza, PA. 2009. Some Physico-Chemical Properties of Prepared Metallic Soap-Driers of Aluminium, Copper and Zinc. Sci. World J. 4:7- 9.

Ginwal, HS., Rawat, PS. and Srivastava, R. L. 2004.Seed Source Variation in Growth Performance and Oil Yield of *Jatropha curcas* L in Central India. Silvae Genetica. 53:4-7.

Goel, G., Makkar, HPS., Francis, G. and Becker, K. 2007. Phorbol Esters: Structure, Biological Activity, and Toxicity in Animals. Int J Toxicol. 26:279 -288.

Hart, JR. and DeGeorge, MT. 1980. The Lathering potential of surfactants - a simplified approach to measurement. J. Soc. Cosmet. Chem. 31:223-236.

Heller, J. 1996. Physic nut. *Jatropha curcas* L. Promoting the conservation and use of underutilized and neglected crops. 1. Institute of Plant Genetics and Crop Plant Research, Gatersleben/ International Plant Genetic Resources Institute, Rome. p7.

Henning, RK. 2003.The Jatropha Booklet: A guide to Jatropha Promotion in Africa. Bagani GbR. Weissensberg, Germany. pp5-33. Accessed at http://www.jatropha.de/documents/jcl_ _booklet_Africa.pdf.

Isah, AG. 2006. Production of Detergent from Castor oil. Leonardo J. Pract. Tech. 9:153-160.

Jongschaap, REE., Corre, WJ., Bindraban, PS. and Brandenburg, WA. 2007. Claims and Facts on *Jatropha curcas* L: Global *Jatropha curcas* evaluation, breeding and propagation Programme. Plant Research International, B.V. Wageningen, The Netherlands. 1-3.

King, AJ., He, W., Cuevas, JA., Freudenberger, RD. and Graham, IA. 2009. Potential of *Jatropha curcas* as a source of renewable oil and animal feed. J. Exp Bot. 1-9.

Kochhar, SL. 1998. Economic Botany in the tropics (2nd ed.). Macmillan India Ltd, Delhi, India.

Kuntom, A., Ahmad, I., Kifli, H. and Mat Shariff, Z. 1999. Effects of Superfatting Agents on Cracking Phenomena in Toilet Soap. J. Surf Detergts. 2:325-329.

Mabrouk, ST. 2005. Making useable quality, opaque or tranparent soaps. J. Chem. Edu. 82:1534-1537.

Mainkar, AR. and Jolly, CI. 2000. Evaluation of Commercial Herbal Shampoos. Int. J. Cosmet. Sci, 22: 385-391.

Neu, GE.1960. Techniques of foam measurement. J. Soc. Cosmet. Chem.11:390-414.

Nwinuka, NM. and Nwiloh, BI. 2009. Physico-chemical Properties and Fatty Acid Composition of *Dennettia tripetala* Fruit Oil (Pepper Fruit). Nigerian Journal of Biochemistry and Mol. Biol. 24:42-46.

Oyedele, AO. 2002. The skin tolerance of shea fat employed as excipient in topical preparations. Nigerian J. Nat. Prod. Med. 66:26-29.

Openshaw, K. 2000. A review of *Jatropha curcas*: an oil plant of unfulfilled promise. Biomass and bioenergy. 19:1-15.

Pant, KS., Koshla,V., Kumar, D. and Gairola, G. 2006. Seed oil content variation in *Jatropha curcas* L in different altitudinal ranges and site conditions in H.P. India. Lyonia. 11**:**31-34.

Rijssenbeek,W. 2007. Jatropha Global Position.Workshop EU Brussels. RR Energy for FACT Foundation. pp37.

Ross, J and Miles, GD.1941. An apparatus for comparison of foaming properties of soaps and Detergents. Oil soap. 18:99-102.

Sayyar, S., Zainal Abidin, Z., Yunus, R. and Muhammad, A. 2009. Extraction of oil from Jatropha seeds-Optimization and Kinetics. Am. J. Appl. Sci. 6:1390-1395.

Shah, S. Sharma, A. and Gupta, MN. 2005. Extraction of oil from *Jatropha curcas* L seed kernels by combination of ultrasonication and aqueous enzymatic oil extraction. Bioresource Tech. 96:121-123.

Sorkin, M., Shapiro, B. and Kass, GS.1966. The Practical evaluation of Shampoos. J Soc Cosmet Chem.17:539-557.

Usman, LA., Ameen, OM., Lawal, A. and Awolola, GV. 2009. Effect of alkaline hydrolysis on the quantity of extractable protein fractions (prolamin, albumin, globulin and glutelin) in *Jatropha curcas* seed cake. African. J. Biotech. 8:6374-6378.

Verma, KC. and Gaur, AK. 2009. *Jatropha curcas* L. Substitute for Conventional Energy. World J. Agric. Sci. 5:552-556.

Received: March 4, 2011; Revised: March 14, 2011;
Accepted: May 9, 2011

SENRA Academic Publishers, Burnaby, British Columbia
Vol. 6, No. 1, pp. 1809-1813, Feb 2012
Online ISSN: 1920-3853; Print ISSN: 1715-9997

Canadian Journal of pure&applied sciences

Short Communication

GAS CHROMATOGRAPHY/ MASS SPECTROSCOPY FOR PHYTOCHEMICAL SCREENING OF *TECOMA STANS*

*Amad M Al-Azzawi[1] and Alyaa G Al-Juboori[2]
[1]Ras Al Khaimah College of Pharmaceutical Sciences
Ras Al Khaimah Medical and Health Sciences University, Ras Al Khaimah
[2]Department of General Education, Ras Al Khaimah Medical and Health Sciences University, Ras Al Khaimah, UAE

ABSTRACT

Tecoma stans (*Bignoniaceae*) is a Central and South American tree, and popularly used for the control of diabetes. The alkaoidal fraction isolated from the dried leaves of *Tecoma stans* collected from the gardens of Al-Jadria, Iraq were investigated for its phytochemical constituents through the Gas chromatography/ mass spectroscopy with preparative thin layer of chromatography. The analysis of the alkaloidal fraction confirmed the presence of previously reported alkaloids and two new indolic alkaoids.

Keywords: *Tecoma stans*, gas chromatography/ mass spectroscopy, indolic alkaloids.

INTRODUCTION

Plant *Tecoma stans* commonly growing in Latin America and is used traditionally in Mexico for the control of diabetes. The presence of alkaloids in *T. stans* was first reported in 1899 (Boorsma and Meded, 1899) and the first alkaloid was isolated by Hanrnouda and Motawi (1959). The structure of tecomine was determined Jones *et al*. (1963) and a number of pyrindane alkaloids of obvious monoterpene relationship have been isolated from the plant Dickinson and Jones (1969). Hammouda *et al.* (1971) and Youssef and Nawal (1971) indicated that the degradation of the alkaloid is dependent on the pH of its solution and that antioxidants are beneficial in delaying its deterioration. In 1983, the indolic alkaloids were isolated from the leaves of *T. stans* and a new indole oxygenase from the leaves of *T. stans* was isolated and purified (Kunapuli and Vaidyanathan, 1983; Satya and Vaidyanathan, 1984).

In 1988 GCMass of the crude base fraction indicated the presence of several related alkaloids as very minor constituents (Harris *et al*., 1988). In 1993 phytochemical investigation of an ethanolic extract from fruits of *Tecoma stans* led to the isolation of two monoterpenic alkaloids, 7-hydroxyskytanthine and 4-hydroxytecomanine (Arlete and Joana, 1993). The objective of this study was to investigate the phytochemical constituents of *Tecoma stans* using Gas chromatography–mass spectrometry (GC-MS).

*Corresponding author email: amadazzawi@yahoo.com

MATERIALS AND METHODS

Collection of plant material

The leaves of *Tecoma stans* (*Bignoniaceae*) grown in Iraq were collected from the area of University of Baghdad (Al-Jadria) in August and November 2004. The specimen was authenticated by Dr. Ali Al- Mousawi, Department of Biology, College of Science, University of Baghdad. The leaves were dried at room temperature in the shade and pulverized by mechanical mills.

Extraction procedure

The 50g dried leaves were extracted by a Soxhlet apparatus using diethyl ether/ammonia (15%) (80:20) as a solvent for four hours. The filtrate was in turn extracted with 4N HCl at room temperature. The aqueous phase was extracted three times with hexane, then ethyl acetate and finally with diethyl ether. The acidic aqueous phase was then treated with ammonia (30%) until pH 12 which was accompanied with a change in the color to a dark greenish brown, and introduced to a separatory funnel, where it was extracted with dichloromethane three times (1:3v/v). The organic layer was then dried with anhydrous sodium sulphate and the solvent was removed under reduced pressure at 40^{o}C, giving dark brown greenish crude alkaloidic fraction (4g) (Madhavi *et al*., 1998). A column with a length of (75cm×20mm) was packed with (50g) of silica gel (kieselgel 60) suspended in dichloromethane (100mL). The crude alkaloidic fraction was fractioned using as mobile phase dichloromethane/ methanol (from 0 to 40% v/v). Fractions were collected and each fraction was evaporated from the solvent (Peter, 2002).-All fractions were sent for GC-Mass, Fractions 5 and 12 they were further purified by preparative TLC.

Preparative Thin layer chromatograph

The analysis was performed on precoated 20×20cm (2mm thickness) TLC Kieselgel GF254 plates (Merck, Germany) and then activated by heating at 110°C for an hour before use. The fraction which contained more than one compound was dissolved in minimum quantity of dichloromethane and applied on a number of preparative TLC plates using -Dichloromethane: methanol: ammonia (89.5:10: 0.5 v/v)solvent system, major bands were observed under UV light (254nm), this was assured by spraying side of the plate with dragendroff spraying reagent to indicate the position of the bands. The major bands were scrapped off, eluted with dichloromethane then filtered; the filtrate was evaporated to dryness under vacuum (Peter, 2002).

Gas chromatography/mass spectroscopy

Shimadzu 2010 QB gas chromatography with a MSD detector equipped with HP-5 fused silica capillary Column (30m×0.25mm×25µm film thickness) is used for this purpose. The samples were injected via an all- glass injector working with split mode, with the Heleium as the carrier gas with a flow rate of 1ml/min (Hegazi and Abd El Hady, 2002). Temperature program: Injected temp 200°C, Ion source 200°C, Interphase 200°C. Column temperature was raised to 45°C (3min hold at 45°C, 4°C/min), then gradually increased to 150°C (3min hold at 150°C, 4°C/min) then raised to 250°C and a 15min hold (Antoanela *et al*., 2002).

1DNMR spectrum

^{1}H NMR data were acquired at room temperature on a Bruker AMX 300 spectrometer operating at ^{1}H (300MHZ) using ($CDCl_3$) as a solvent chemical shifts are shown in δ(ppm) value with TMS (tetramethylsilane) as an internal standard coupling constant (*J*) are given in hertz.

RESULTS AND DISCUSSION

Gas chromatography–mass spectrometry (GC-MS)

1- Fraction 5 showed major peaks, as shown in (Fig. S1).

The analysis for each peak in the chromatograms according to Library WILEY229.LIB suggested:

1- Formula $C_{10}H_{11}NO$, mol.wt. 161, retention time 36.958, mass peak 80, base peak 161. As shown in the mass spectrum (Fig. S2), this gave us an idea the presence of Boschniakine.
2- A new indolic compound: 2,3-dihydro-4, 4- dimethyl indol-4-ol-2-one, mol.wt. 177, retention time 43.292,

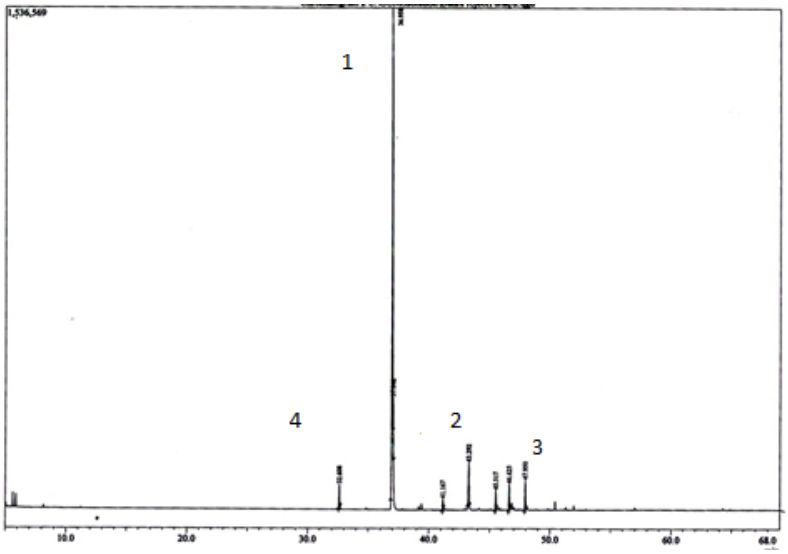

Fig. S1. Gas chromatography/ mass spectroscopy for fraction 5 showing major peak and two other new indolic compounds.

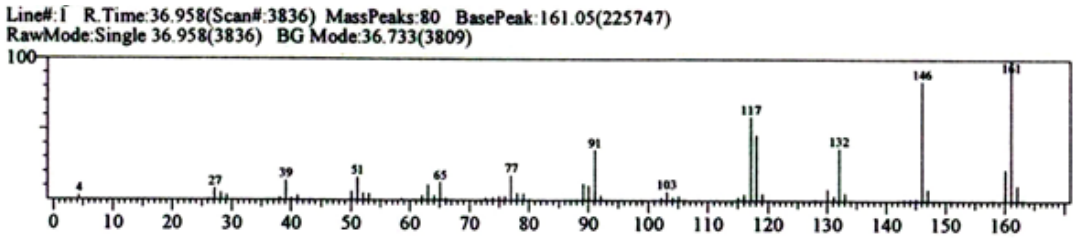

Fig. S2. Mass spectrum of Boschniakine.

mass peak 44, base peak162. Formula $C_{10}H_{11}NO_2$. As shown in the mass spectrum (Fig. S3).

3- A new indolic compound: Indole-2,3-dione, 1-methyl, 3- oxime, mol.wt 176, retention time 47.95, mass peak 35, base peak 176, fromula $C_9H_8N_2O_2$. As shown in the mass spectrum (Fig. S4).

4- Precursor for the Boschniakine, benzoic acid amide, mol.wt.121. Retention time 32.608, mass peak 18, base peak 105. Formula C_7H_7NO. As shown in the mass spectrum (Fig. S5).

2- Fraction 12 showed major peaks, as shown in (Fig. S6).

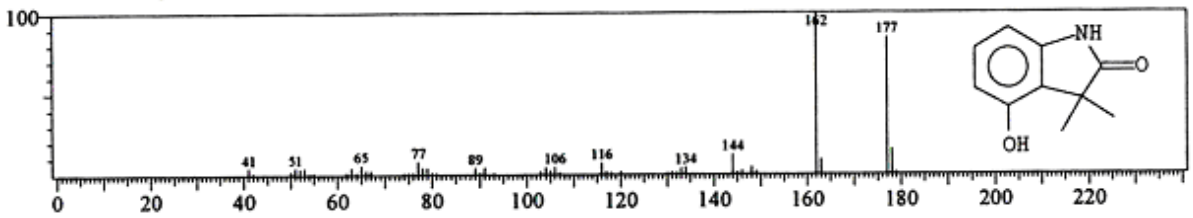

Fig. S3. Mass spectrum of a new indolic compound.

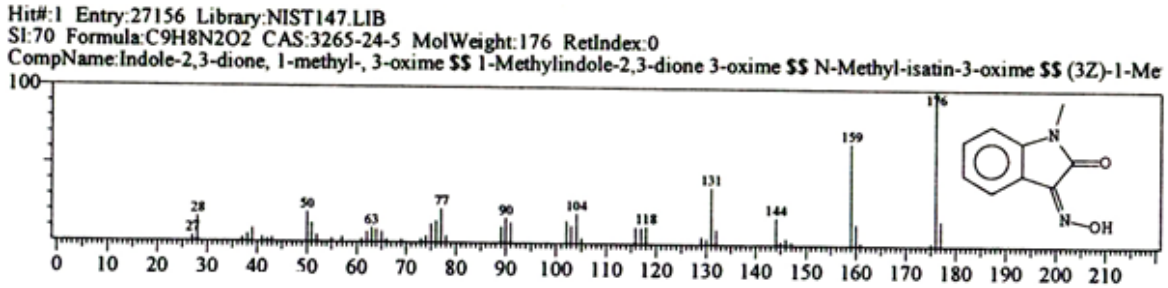

Fig. S4. Mass spectrum of a new indolic compound.

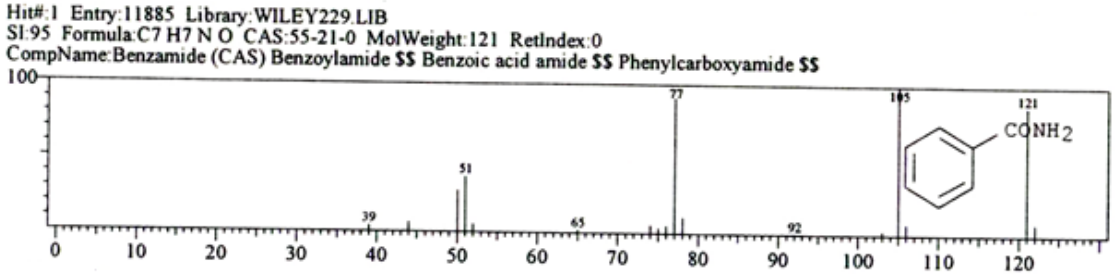

Fig. S5. Mass spectrum for a precursor for the Boschniakine.

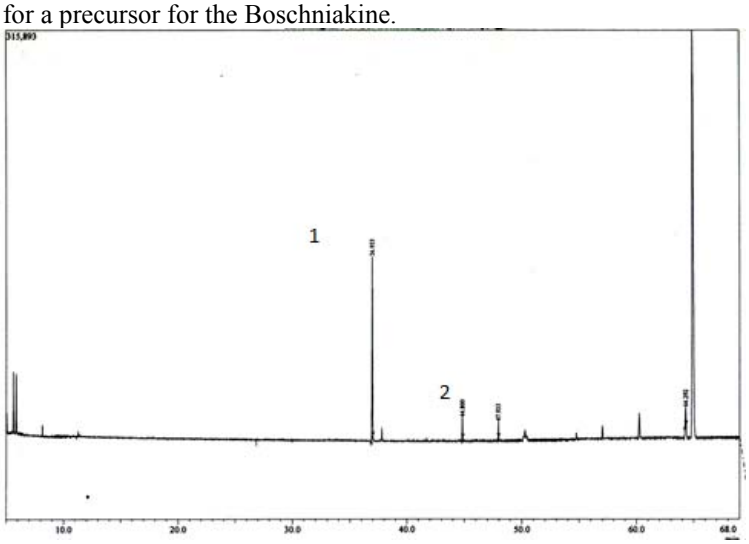

Fig. S6. Gas chromatography/ mass spectroscopy for fraction 12 showing major peak and minor peak.

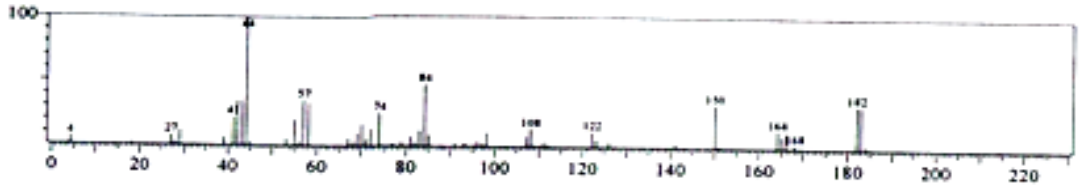

Fig. S7a.

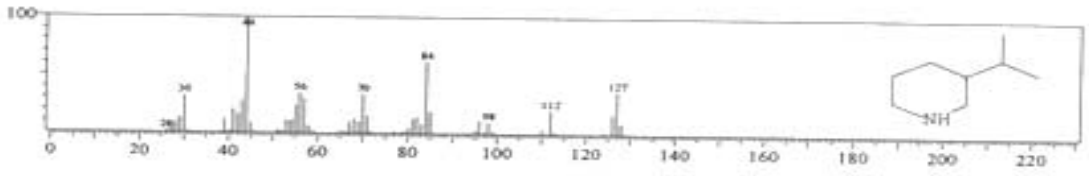

Fig. S7b.

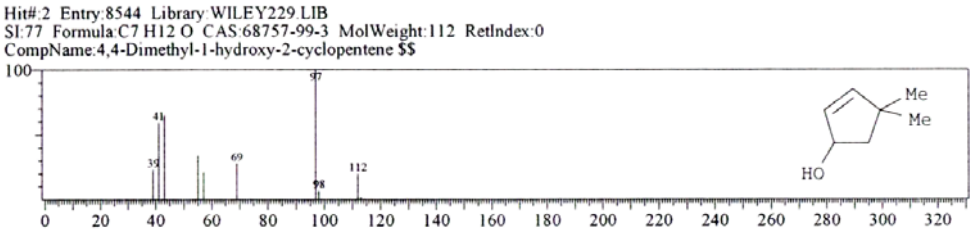

Fig. S8. A precursor of the indolic alkaloids.

The analysis for each peak in the chromatograms according to Library WILEY229.LIB suggested:

1- A compound with a molecular weight of 182 as shown in (Fig. S7a) or a precursor for the tecomine compound as shown in (Fig. S7b).
2- A precursor of the indolic alkaloids:4, 4, dimethyl-1-Hydroxy-2-cyclo pentene. Mol.wt. 112, mass peak 11, base peak 97, retention time 44.8. Formula $C_7H_{12}O$. As shown in the mass spectrum (Fig. S8).

Spectroscopic

1- Boschniakine chemical structure as shown in (Fig. S9), an oil of a formula $C_{10}H_{11}NO$ mol.wt. 161 with pungent odor yields 0.1g. UV λmax 250 and 263 nm (ethanol). IR (KBr) cm^{-1}: 3028, 2960, 2856, 1739 and 758. ^{1}H-NMR (CDCl3) (300 MHz): 1.12 (3H , d, J 6.7) , 1.5-1.8 (1H , m) , 2.9-3.4 (3H , m) , 8.5 (1H , s) , 10.2 (1H, s) (Costantino *et al*., 2003).
2- Beta-Hydroxyskitanthine, chemical structure as shown in (Figure S10), an oil of a formula $C_{11}H_{20}NO$ mol.wt. 182; yields 0.1g. UV λmax 220nm (ethanol). IR (KBr) cm^{-1}: 3396, 2923, 2854. ^{1}H-NMR (CDCl3) (300 MHz): 0.85 (3H , d, J 6.9) , 0.95 (3H , d, J 7.0), 1.3-1.35 (1H , m) , 1.7 (2H , m) , 2.1 (3H, s), 3.3-3.6 (1H ,ddd, J 10.3, 4.2, 2.1) (Costantino *et al*., 2003).

GC-MS is a valuable tool to screen alkaloids, present investigation of the Iraqi *T. stans* revealed four alkaloids by GC-MS. The combination of two techniques such as GC-MS and preparative TLC has led to a rapid chemical screening of already two known alkaloids (Boschniakine, Beta- Hydroxyskitanthine) and two unknown indolic alkaloids. This method is simpler, fast and inexpensive method to search for secondary metabolites from natural sources in order to be further investigated for biological activity.

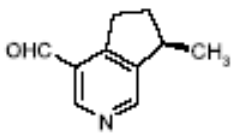

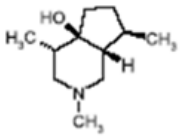

Fig. S9. Boschniakine.Fig. S10. Beta-Hydroxyskitanthine.

CONCLUSION

To the best of our knowledge, this is the first report of the Iraqi *tecoma stans* confirming the presence of known alkaloids and using GC-Mass for screening of new indolic alkaloids.

ACKNOWLEDGEMENT

I would like to thank the Jordan University College of Science, Department of Chemistry and College of Medicine, Department of Microbiology for their help with this work.

REFERENCES

Antoanela, I., Ivajla, D., Iva, T., Atanas, K. and Ivanka, K. 2002. GC- MS Analysis and Anti- Microbial Activity of Acidic Fractions Obtained from Paeonia pergrina and Paeonia tenuifoia Roots. Z. Naturforsch. 57:624-628.

Arlete, PL. and Joana, DF. 1993. Monoterpene alkaloids from *Tecoma stans*. Phytochemistry. 3:876-878.

Boorsma, GE., Meded, Lands' Plantent (1897);18:39. See Wehmer C, Die Pflanzenstoffe 2, 1136, Edwards JW, Edwards Brothers, Inc. Ann Arbor, Michigan (1950).

Costantino, L., Raimondi, L., Pirisino, R., Brunetti, T., Pessotto, P., Giannessi, F., Paulino-Lins A., Barlocco, D., Antolini, L. and Samia A El-Abady. 2003. Isolation and pharmacological activities of the *Tecoma stans* alkaloids. Farmaco Il. 9:781-785.

Dickinson, EM. and Jones, G. 1969. Pyrindane alkaloids from *Tecoma stans*. Tetrahedron. 25:1523-1529.

Hammouda, Y. and Motawi, MM. 1959. Principal alkaloid isolated from Tecoma stans (L.) H.B.K. (*Bignonia stans* L.), *Bignoniaceae* Egypt Pharm Bull. 41, 73.

Harris, GH., Fixman, EC., Stermitz, FR. and Castedo, L. 1988. (-)-delta-N-normethylskytanthine from Tecoma arequipensis. J. Nat. Prod. 51:543-8.

Hegazi, AG. and Abd El Hady, FK. 2002. Egyption propolis Antioxidant, Antimicrobial Activities and chemical Composition of propolis Reclaimed Lands, Z. Naturforsch. 57c:395-402.

Jones, GH., Fales, M. and Wildman, WC. 1963. The Structure of Tecomanine. Tetrahedron Lett. 6:397-400.

Kunapuli, SP. and Vaidyanathan, CS. 1983. Purification and Characterization of a New Indole Oxygenase from the Leaves of *Tecoma stans* L. Plant Physiol. 71:19-23.

Madhavi, DL, Ser, MA., Smith, L. and Singletary, K. 1998. Isolation of bioactivity constituents from Vaccinium myrtillus (bilberry) fruits and cell cultures. Plant Sci. 131:95-103.

Peter, JH. 2002. Chromatography of the chromosome and flavinoide alkaloids. Journal of Chromotoghraphy. 75-84.

Satya, PK. and Vaidyanathan, CS. 1984. Indolic compounds in the leaves of *Tecoma stans*. Phytochemistry. 8:1826-1827.

Youssef, H. and Nawal, K. 1971. Stability of tecomine, the major antidiabetic factor of *tecoma stans* (Juss.) *F. bignoniaceae.* Journal of Pharmaceutical Sciences. 60:1142-1145.

Received: Nov 6, 2011; Accepted: Dec 9, 2011

SENRA Academic Publishers, Burnaby, British Columbia
Vol. 6, No. 1, pp. 1815-1819, Feb 2012
Online ISSN: 1920-3853; Print ISSN: 1715-9997

Canadian Journal of pure&applied sciences

Short Communication

CHARACTERIZATION OF WOOL OF THALLI SHEEP BY GAS CHROMATOGRAPHY – MASS SPECTROMETER (GC-MS)

*Z Hussain[1] and F Sehar[2]
[1]Institute of Chemistry, University of the Punjab, Lahore 54590
[2]Department of Chemistry, Lahore College for Women University, Lahore, Pakistan

ABSTRACT

Organic compounds present in wool wax have several applications. They can be used either direct or as raw materials to synthesize many important products. In the present study, these compounds were extracted from sheep wool with n-hexane, benzene and chloroform using a Soxhlet apparatus. The extracts were characterized using gas chromatograph coupled to a mass spectrometer. Chloroform and n-hexane infusions were found to contain 3-butyn-1-ol, cyclopropene, 2-methyl octane, 2-methyldecane, p-xylene, benzonitrile and ethyl benzene while extract of benzene own 2, 4-dimethyl hexane, 1, 2-dimethyl cyclohexane, 1-ethyl 3-methyl cyclopentane, octane, 2-methyl octane, n-propyl cyclopentane, ethyl cyclohexane, 1, 3-dimethyl benzene, o-xylene, nonane, 1-pentanol, 1, 2, 3-trimethyl benzene, decane, 5-ethyl-2-methyl heptane, 1, 6-diol-2, 7-octadiene, 5-(2-methylpropyl)-nonane, pentyl cyclohexane, 1, 7, 7-trimethyl-2-vinyl-bicyclo-hept-2-ene and 2, 3, 5, 8-tetramethyl decane.

Keywords: Sheep wool, extraction; benzene, chloroform, n-hexane, soxhlet.

INTRODUCTION

Sheep wool is known as a strong fiber. It can bend on itself 20,000 times without breaking, which is high compared with other fibers such as cotton (3,200), silk (1,800) and rayon (75) (Nostran, 2006). Wool, which usually contains up to 20 amino acids, has a complex chemical structure, which accounts for its unique character as a fiber (Ludecke and Invanvszky, 1958). Efficiency in handling body moisture in both hot and cold conditions results from the porous structure of wool creating millions of miniature air pockets which help to regulate temperature and humidity. Sheep wool is covered in a protective layer of lanolin, a waxy substance with a faint characteristic odor which is a mixture of animal fats. Lanolin is formed by the oleaginous glands of sheep and is vital for greasing the wool and preserving the skin (Eychenne *et al*., 2001). Lanolin is removed in a pretreatment process and is widely used in the pharmaceutical and cosmetic industries in the production of moisturizers and body lotions.

A numbers of organic compounds are present in lanolin which can be used either directly or as a starting material for many important products. Wool is often considered as a potential internal source of volatile organic compounds (Lisovac and Shooter, 2003). Factors such as diet, sheep breed, living conditions, pregnancy, lactation, color and texture affect emission of volatiles from sheep wool. In addition, different types of bacterial and fungal flora use wool as their source of nutrition (Burrell, 1990; Gochel *et al*., 1990). Although, fleece wool may have some antibacterial properties (Meyer *et al*., 2001). The Maillard reaction between amino acids and reducing sugars, or amino acids and lipid deterioration products are two important reactions in the formation of volatile organic compounds of wool (Farmer, 1996).

The amount of wool grown per sheep is a function of the geographical area, the wool follicle density and volume of fiber per follicle (Adelson *et al*., 2004). Sheep wool is composed of fibrous and hard α-keratins (Marshall *et al*., 1991) and is metabolically dead after leaving the epidermis (Raab *et al*., 2002). Wool consists of three basic components; the cuticle, the cortex and medulla. The internal cortical cells have long polyhedral spindle-shaped structures (Jones, 2001). The natural coloring in the fibers is provided by the pigment melanin (Feughelman, 2001).

The present study describes the extraction of various organic compounds from wool fibers of Thalli sheep (a local breed) and the evaluation of the performance of n-hexane, chloroform and benzene as solvent for the extraction of these compounds using a Soxhlet apparatus. The resulting extracts were characterized by using a gas chromatograph coupled with the mass spectrometer.

*Corresponding author email: drzh1972@hotmail.com

MATERIALS AND METHODS

Wool sampling

Wool samples from six months old male Thalli sheep were collected from the local market Lahore, Pakistan. The samples were thoroughly washed with water to remove contaminating dust, grass and other exogenous materials. The samples were dried in an oven at 50°C and cut into small strands with a sharp knife.

Extraction with Soxhlet extractor

A Soxhlet extractor with cellulose thimble was used for the solvent extraction. The sheep wool (8.25g) was placed in the thimble and 500mL of pure solvent put into the round bottomed flask. The three components of the extractor were put together with flask in an isomantle fitted with a regulator and cold water (20°C) running continuously in the condenser. The temperature was adjusted so that the solvent boiled. The sample was extracted for 10hours. When extraction was complete the extract was washed from the flask with the respective solvent. The solvent was removed by simple distillation.

Characterization

The components extracted from the sheep wool were characterized using gas chromatograph coupled with the mass spectrometer figures 1-3. A Shimadzu (QP-2010 GC-MS, Japan) equipped with column (HP DB5 Agilent, length: 30m, internal diameter: 0.25mm, film thickness: 0.25mm), was used. The flow rate of the helium carrier gas was adjusted to 1mL/min. The GC-MS operating conditions were: injection temperature, 280°C; detector temperature, 200°C; initial oven temperature, 30°C; electron impact, 70 eV; mass range, 4-1020m/z and ion source temperature, 200°C.

RESULTS AND DISCUSSION

Volatile organic compounds, most of which were aliphatic hydrocarbons (saturated and unsaturated), aromatic hydrocarbons, amines and alcohols, were detected and identified in sheep wool using GC-MS equipped with library NIST 127/47. The retention time, molecular formula and weights of various compounds acquired by extraction with n-hexane, chloroform and benzene are shown in tables 1-3 respectively.

The n-hexane extract contains 3-butynyl-1-ol, 2-methyloctane, cycloprene, and 2-methyldecane. The chloroform extract contains 1, 3-cyclopent-di-ene, ethyl benzene, 3-butynyl-1-ol, p-xylene, 1-benzyloxy -5-diethylamino-2, 4-dinitro benzene and 4-benzyloxy benzyliden amino benzonitrile. It appears that benzene is the most suitable solvent because of the number of compounds extracted, but the choice of solvent is also governed by the compound required. The benzene extract contains 2, 4-dimethyl hexane, 1, 2-dimethyl cyclohexane, 1-ethyl 3-methyl cyclopentane, octane, 2-methyl octane, n-propyl cyclopentane, ethyl cyclohexane, 1, 3-dimethyl benzene, o-xylene, nonane, 1-pentanol, 1, 2, 3-trimethyl benzene, decane, 5-ethyl-2-methyl heptane, 1, 6-diol-2, 7-octadiene, 5-(2-methylpropyl)-nonane, pentyl cyclohexane, 1, 7, 7-trimethyl-2-vinyl-bicyclo-hept-2-ene and 2, 3, 5, 8-tetramethyl decane.

Table 1. Different constituents extracted by n-hexane.

Name	Mol. Formula	Mol. Weight	Retention Time (min)
3-Butynyl-1-ol	C_4H_6O	70	10.850
2-Methyl octane	C_9H_{20}	128	10.850
Cycloprene	C_3H_4	40	12.908
2-Methyl decane	$C_{11}H_{24}$	156	14.375

It is not suggested that each type of wool will contain the specific volatile organic compounds found here. The composition of the extracts depends on factors such as sheep breed, age, diet and habitat. Additionally, detection of compounds depends on the sensitivity of the current analytical technology. Gas chromatography-mass spectrometry (GC-MS) is a combination method which is used to identify different volatile substances in a sample. The use of a mass spectrometer as the detector in gas chromatography was developed during the 1950s (Gohlke and McLafferty, 1959). Only compounds with vapor pressures exceeding about 10^{-10} torr can be analyzed by (GC-MS). Many compounds with lower pressures can be analyzed by this method, but they must first chemically derivatized to a form with required vapour pressure. Deciding positional substitution on aromatic rings is often difficult. Certain isomeric compounds cannot be

Table 2. Different constituents extracted by chloroform.

Name	Mol. Formula	Mol. Weight	Retention Time(min)
1, 3-Cyclopent-di-ene	C_8H_{10}	106	4.400
Ethyl benzene	C_8H_{10}	106	4.400
3-Butynyl-1-ol	C_4H_6O	70	4.867
p-Xylene	C_8H_{10}	106	4.233
1-Benzyloxy -5-diethylamino-2, 4-dinitro benzene	$C_{17}H_{19}N_3O_5$	345	4.233
4-Benzyloxy benzyliden amino benzonitrile	$C_{21}H_{16}N_{20}$	312	4.233

Table 3. Different constituents extracted by benzene.

Name	Mol. Formula	Mol. Weight	Retention Time (min)
2, 4-Dimethyl hexane	C_8H_{18}	114	3.208
1, 2-Dimethyl cyclohexane	C_8H_{16}	112	3.292
1, 4-Dimethyl cyclohexane	C_8H_{16}	112	3.831
1-Ethyl 3-methyl cyclopentane	C_8H_{16}	112	3.158
Octane	C_8H_{18}	114	3.208
2-Methyl octane	C_9H_{20}	128	3.625
n-Propyl cyclopentane	C_8H_{16}	112	3.733
Ethyl cyclohexane	C_8H_{16}	112	3.808
1, 3-Dimethyl benzene	C_8H_{10}	106	4.408
o-Xylene	C_8H_{10}	106	4.875
Nonane	C_9H_{20}	128	4.967
1-Pentanol	$C_9H_{20}O$	144	5.775
1, 2, 3-Trimethyl benzene	C_9H_{12}	120	7.467
Decane	$C_{10}H_{22}$	142	8.275
5-Ethyl-2-methyl heptanes	$C_{10}H_{22}$	142	8.275
1, 6-Diol-2, 7-octadiene	$C_{10}H_{18}O_2$	170	11.417
5-(2-Methylpropyl)-nonane	$C_{13}H_{28}$	184	11.750
Pentyl cyclohexane	$C_{11}H_{22}$	154	12.117
1, 7, 7-Trimethyl-2-vinyl-bicyclo-hept-2-ene	$C_{12}H_{18}$	162	12.908
2, 3, 5, 8-Tetramethyl decane	$C_{12}H_{30}$	198	13.092

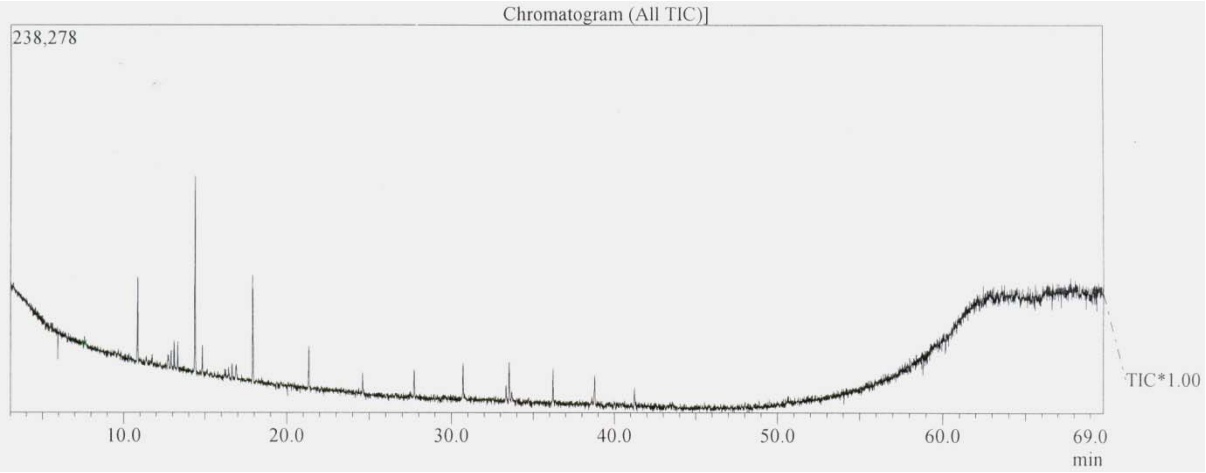

Fig.1. Extraction of sheep wool with n-hexane.

distinguished by mass spectrometry, but can often be separated chromatographically (Hites, 1997). No sulphur compound was detected in the present study, even though such substances are responsible for the smell of raw sheep wool.

CONCLUSION

In the present study, different organic compounds have been extracted from sheep wool. These compounds were characterized by GC-MS. The study assessed the performance of benzene, n-hexane and chloroform as solvent. Benzene extracted more compounds compared to the other solvents.

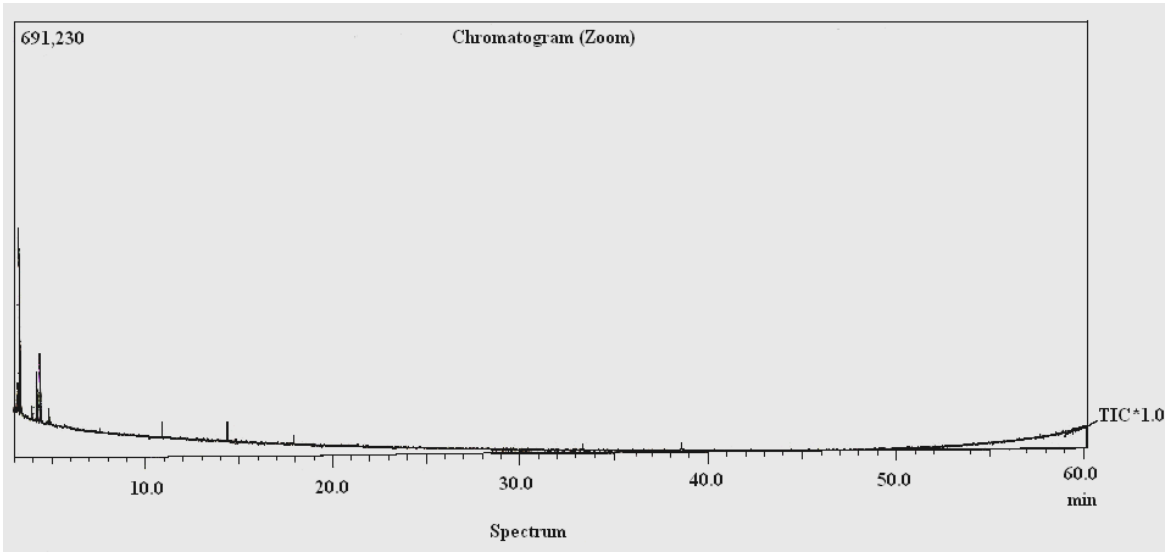

Fig. 2. Extraction of sheep wool with chloroform.

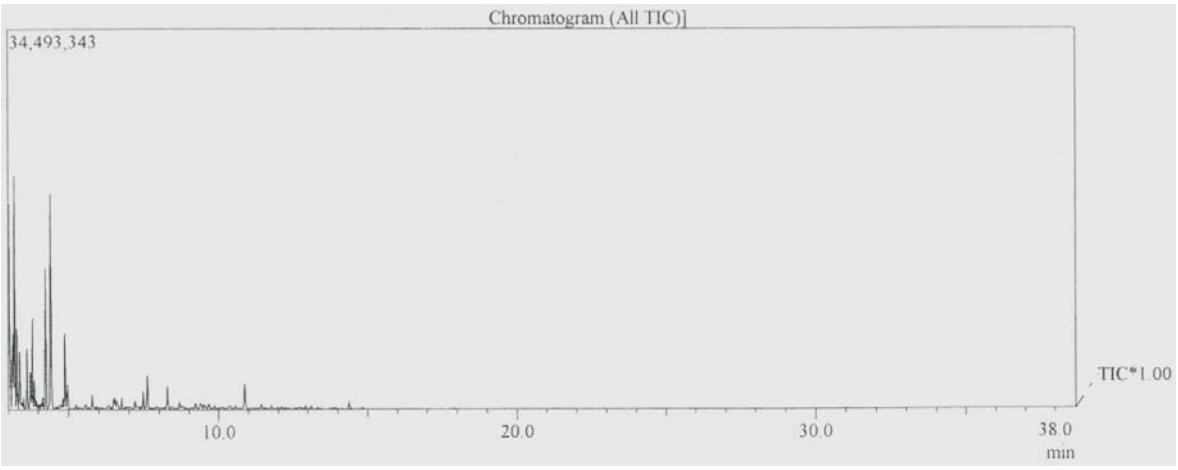

Fig. 3. Extraction of sheep wool with benzene.

ACKNOWLEDGEMENTS

The authors wish to thank Dr. Douglas Dick (C.E.R., Brunel University, London, UK), Umer Shafique, Manzar Islam and Babar Tariq (University of the Punjab, Lahore) for their technical assistance and guidance.

REFERENCES

Adelson, DL. Cam, GR., Desilva, U. and Franklin, I. 2004. Gene Expression in Sheep Skin and Wool (Hair). Genomics. 83:95-105.

Burrell, DH. 1990. Advances in Veterinary Dermatology. Bailtiare Tindall, London.

Eychenne, V., Sáiz, S., Trabelsi, F. and Recasens, F. 2001. Near-critical solvent extraction of wool with modified carbon dioxide - experimental results. J. Supercrit Fluid. 21:23-31.

Farmer, LJ. 1996. Interactions between lipids and the Maillard reaction. Flavor–food interactions. ACS Symp Ser. 633:48-58.

Feughelman, M. 2001. Natural Protein Fibers. J. Appl. Polym Sci. 83:489-507.

Gochel, M., Belly, M. and Knott, J. 1990. Biodegradation of wool during storage, Proceedings of the Eighth International Wool Textile Research Conference on Biodegradation of Wool During Storage, Wool Research Organization of New Zealand, New Zealand. pp139.

Gohlke, RS. and McLafferty, FW. 1959. Mass Spectrometric Analysis. Spectral Data File Utilizing Machine Filing and Manual Searching. Anal Chem. 31:1160-1163.

Hites, RA. 1997. Handbook of instrumental techniques for analytical chemistry. Ed. Settle, FA. Prentice Hall PTR, University of Michigan, USA.

Jones, LN. 2001. Hair structure anatomy and comparative anatomy. Clin Dermatol. 19:95-103.

Lisovac, AM. and Shooter, D. 2003. Volatiles from sheep wool and the modification of wool odour. Small Ruminant Res. 49:115-124.

Ludecke, C., Invanvszky, L. and Taschenbuch. 1958. Fur die Wachsindustrie (4th ed.), Wissen Chaftl Verlagsgesellschaft, Stuttgart. 33-36

Marshall, RC., Orwin, D. and Gillespie, JM. 1991. Structure and biochemistry of mammalian hard keratin. Electron Microsc Rev. 4:47-83.

Meyer, W., Neurand, K. and Tanyolac, A. 2001. General anti-microbial properties of the integument in fleece producing sheep and goats. Small Ruminant Res. 41:181-190.

Nostran, V. 2006. Wool management mixing wool returns, Mid state wool growers cooperative association. Website: http://www.midstateswoolgrowers.com/management.htm

Raab, A., Hansen, HR., Zhuang, L. and Feldmann, J. 2002. Arsenic accumulation and speciation analysis in wool from sheep exposed to arsenosugars. Talanta. 58:67-76.

Whitfield, FB. 1992. Volatiles from interactions of Maillard reactions and lipids. CRC Crit Rev Food Sci Nutr. 31:1-58.

August 16, 2011; Accepted: Nov 28, 2011

SENRA Academic Publishers, Burnaby, British Columbia
Vol. 6, No. 1, pp. 1821-1825, Feb 2012
Online ISSN: 1920-3853; Print ISSN: 1715-9997

Canadian Journal of pure&applied sciences

Short Communication

THE TOXIC AND NON-APHRODISIAC POTENTIALS OF OILS FROM *JATROPHA CURCAS* SEEDS ON MICE

*Valentine Chi Mbatchou and Frank Osei
Department of Applied Chemistry and Biochemistry
University for Development Studies, PO Box 24, Navrongo, Ghana

ABSTRACT

Jatropha curcas is a multipurpose, drought resistant, perennial plant belonging to the Euphorbiceae family which is gaining lots of importance for the production of biodiesel from its oil. This study revealed the other potentials of the oil. Qualitative analysis was carried out on oil extract from the seed of *J. curcas* which revealed the presence of phytochemicals. The oil extract was also tested for aphrodisiac potentials and toxicity on mice. Results indicated the presence of saponins, terpenoids, cardiac glycosides, flavonoids and steroids which have been reported to have pharmacological attributes. The oil extract did not exhibit aphrodisiac potentials on the male mice at different doses administered (0.5, 1.0 and 1.5 ml). Mortalities were recorded for the oil extract tested on both the male and female mice. Hence, the studies indicated that the oil extract from the seed of *J. curcas* does not possess aphrodisiac potentials but contained toxins which can be removed to make the oil edible.

Keywords: n-hexane, extraction, seed-oil, *Jatropha curcas*, toxic phytochemicals, non-aphrodiasiac potentials and mice.

INTRODUCTION

Jatropha curcas is a species of flowering plant in the spurge family, Euphorbiceae that is native to the American tropics especially Mexico and Central America. It is cultivated in tropical and sub-tropical regions around the world. The plant can grow in wastelands and almost on every terrain even on gravelly, sandy and saline soil. The plant grows best on well-drained soil with a preferable pH of 6 to 9 with good aeration but it is well adapted to marginal soil with low nutritional content. It grows well with more than 600mm rainfall per year and it can withstand long periods of drought. The plant sheds leaves during prolonged drought. The preferred temperature for the cultivation of *J. curcas* is the average of 20°C to 28°C. However, it withstands a very light frost which causes it to lose all its leaves and may produce a sharp decline in seed yield.

The plant grows to a height of about 6m (20ft). The color of the leaves ranges from green to pale-green with both the male and female flowers being produced in the same inflorescence having an average of twenty male flowers to each female flower. The fresh fruits also have green color with a yellow color indicating maturity (en.wikipedia. org/wiki/*Jatropha curcas*).

Jatropha curcas is a non-edible oil crop mostly used to produce biodiesel. In addition to this the tranesterifcation process of *J. curcas* ends up with by-products that can be used to make great deal of products such as high quality paper, energy pellets, soap, cosmetics, tooth paste, embalming fluid, pipe joint cement, cough medicine, and as a moisturizing agent in tobacco. Moreover, *Jatropha* seed cake which is a waste by-product of the biodiesel transesterification can be used as organic manure.

The seeds of *J. curcas* contain viscous oil, which can be used for the manufacture of candles and soap, in cosmetics industry, as a diesel/paraffin wax or extender. This latter use has important implication for meeting the demand of rural energy services and also exploring practical substitutes of fossil fuels to counter greenhouse gas accumulation in the atmosphere. These characteristics along with its versatility make it of vital importance to developing countries (Foidl and Kashyap, 1999).

Various parts of the plant are of medicinal value. Its stem-bark contains tannin, the flowers attract bees and thus the plant has a honey production potential. Its wood and fruit can be used for numerous purposes including fuel (Kumar and Sharma, 2008).

Jatropha curcas seed-oil can be used as fuel in diesel engines directly and by blending it with methanol (Gubitz *et al*., 1999). The seed oil of *Jatropha* plant was used as a fuel substitute during the World War II. Engines tested with *Jatropha curcas* seed-oil in Thailand, demonstrated satisfactory engine performance (Takeda, 1982).The feasibility of the production of fatty acid ethyl esters from *Jatropha* plant seed-oil has been studied (Eisa, 1997). In addition to being a source of oil, *Jatropha* also provides a meal that serves as a highly nutritious and economic protein supplement in animal feed, if the toxins are

*Corresponding author email: mcvalentinechi@gmail.com

removed (Berker and Makkar, 1998). Although there is an increased international recognition of the plant, all attention has been drifted to the use of its oil to produce biodiesel due to the increasing demand for energy across the globe. As a result all other potentials of the plant have been relegated to the background.

Most works carried out on the plant presented in journals, articles, books, and other forms of media mostly talk about the production of oil from its seeds which can be used to produce appreciable quantities of biodiesel with little or no consideration to other benefits that could be derived from the plant. The objectives of this research project are to test for the presence of phytochemicals and non aphrodisiac potentials in the oil of *J. curcas* seeds. The work is also aimed at testing for toxicity of the oil on mice and creating awareness of these potentials of the plant.

MATERIALS AND METHODS

The materials used for this research included seeds of *J. curcas* from which oils were extracted, and mice. The seeds were obtained from Tokuroano in the Krachi East district of the Volta region in Ghana. The mice were procured from Kwame Nkrumah University of Science and Technology (KNUST), Ghana.

Justification of seeds

The seed being of *Jatropha curcas* was authenticated by Dr. Isaac Sackey, a botanist at the Applied Biology Department of the Faculty of Applied Sciences, University for Development Studies (UDS), Ghana.

Methods

Sample collection and preparation

Seeds together with its outer coats were randomly collected from *Jatropha curcas* plants. The outer coats were then removed, while the inner coats containing the seeds were dried for about a week. The inner coats were also removed to obtain the actual seeds which were dried for one week to remove moisture, and later ground to fine powder.

Extraction of oil

Soxhlet extractor was used in the extraction of oil from the powdered seeds of *J. curcas* using petroleum ether (40-60°C). Ten grams of the seeds was extracted with 90 ml of petroleum ether for a period of 3 hrs. The solvent was then evaporated in vacuo and the residual oil was dried in an oven at 40°C to a constant weight. The recovered oil was stored in a vial and kept at room temperature.

Tests for phytochemicals

Alkaloids: To 2 ml of the oil, 10 ml of methanol was added and then filtered. 1% HCl was added to the filtrate and steamed. To 1 ml of the steamed filtrate, 6 drops of Mayer's reagent were added which gave a creamish/brown/red/orange precipitate that indicated the presence of alkaloids.

Saponins: To 0.5 ml of the oil, 5 ml of distilled water was added. Frothing persistence indicated the presence of saponins.

Terpenoids: To 5 ml of the oil in a test tube, 2 ml of chloroform was added. 3 ml of conc. H_2SO_4 was then carefully added to form a layer. An interface with a reddish brown coloration indicated the presence of terpenoids.

Cardiac glycosides (Keller killiani test): To 2 ml of the oil, 1 ml of glacial acetic acid which contained Iron (III) Chloride and conc. H_2SO_4 was added. The formation of a green or blue precipitate indicated the presence of cardiac glycosides.

Steroids: To 2 ml of the oil in a test tube, 2 ml of chloroform was added. This was followed by pouring equal amount of concentrated H_2SO_4 by sides into the test tube. The upper layer turned red, and the sulphuric acid layer appeared yellow with green fluorescence. This indicated the presence of steroids.

Flavonoids: To 2 ml of the oil, few drops of conc. H_2SO_4 were added. This was followed by the addition of magnesium ribbon into the mixture. A pink or tomato red color indicated the presence of flavonoids or glycosides.

Tannins: To 2 ml of the oil, 2 ml of $FeCl_3$ solution was added. A blue and black precipitate indicated the presence of tannins and phenols respectively.

Anthraquinones: To 5 ml of the oil, 3 drops of diluted conc. H_2SO_4 were added. The mixture was further extracted with benzene, and 1 ml dilute ammonia was added to it. A rose pink coloration indicated the presence of anthraquinones.

Amino acids: Aqueous mixture of the oil was treated with drops of ninhydrin (n-butanol). The appearance of a purple color indicated the presence of amino acids.

Coumarins: A test tube was filled with 2 ml of the oil. The test tube was covered with a piece of filter paper moistened with dilute NaOH solution, and placed in a hot water bath. After several minutes, the paper was removed and exposed to UV light for few minutes. Coumarins gave a yellow fluorescence under UV.

Test for toxicity

To determine toxicity of the oil extracts, doses of 0, 0.5, 1.0 and 1.5 ml were given to 4 groups of 3 mice each. The mice were then observed continuously for 1 hr for any

gross behavioral changes and deaths, if any, for the next 6 hrs and at 24 hrs after dosing. The changes in behavior, if any were observed and recorded (Suresh *et al*., 2000).

RESULTS AND DISCUSSION

The results obtained (Table 1) showed the presence of saponins, flavonoids, cardiac glycosides, steroids and terpenoids in the oil extracts from the seeds of *Jatropha curcas* extracted by soxhlet extractor using n-hexane as solvent.

Table 1. Qualitative analysis results for phytochemicals in oil extracts from the seeds of *Jatropha curcas.*

Phytochemicals	Observation
Saponins	+
Tannins	−
Flavonoids	+++
Cardiac glycosides	+++
Steroids	+++
Terpenoids	+++
Alkaloids	−
Coumarins	−
Anthraquinones	−
Amino acids	−

Key: +++ = strongly present; + = weakly present; − = absent.

A number of herbal extracts contain different phytochemicals that display lots of biological activity with valuable therapeutic index. The protective effects fruits and vegetables have are largely attributed to the composition of their phytochemicals which are non-nutritive plant compounds. Different phytochemicals have been identified possessing wide range of activities capable of protection against chronic diseases. For instance saponins, terpenoids, flavonoids, tannins and steroids have anti-inflammatory effects (Liu, 2003; Manach *et al*., 1996; Latha *et al*., 1998; Akindele and Adeyemi, 2007; Ilkay *et al*., 2007). A report by Rupasinghe *et al*. (2003) indicated that saponins have antidiabetic properties. Also, Luo *et al*. (1999) have reported that terpenoids are capable of decreasing blood sugar levels in animals. Steroids and saponins are responsible for activities of the central nervous system (Argal and Parthak, 2006). Cardiac glycosides are therapeutically used for the treatment of cardiac failure. This effect is caused by the ability to increase cardiac output by increasing intracellular calcium, increasing calcium-induced calcium release and thus contraction (en.wikipedia.org/wiki/Cardiac glycosides).Therefore, the oil extracts from the seeds f *Jatropha curcas* can be said to have medicinal properties such as anti-inflammatory and anti-diabetic activities. It can also enhance the activities of the central nervous system and decrease blood sugar levels. The presence of cardiac glycosides also makes the oil a potential for the prevention of heart failure.

The phytochemicals in the oil extracts showed no aphrodisiac properties. Administration of the oil in doses of 0.5 ml, 1.0 ml and 1.5 ml to the mice in groups of two males for each dose did not display any mounting and mating behavior in the animals. The mounting behavior relatively diminished as the doses increased. In the case of 0.5 ml dose, the male made advances towards the female but no mounting was observed. No such advances were observed for doses at 1.0 and 1.5 ml.

With the oil extracts not displaying any aphrodisiac property, toxicity test was carried out. The oil extracts were again given to the animals in dosages of 0.5, 1.0 and 1.5 ml. There were three mice for each dosage in two different feeding conditions. In the first case, the mice were fed immediately after the dosage, and in the second case 2 hours after the dosage (Tables 2a and 2b).

Gross changes in behavior were observed in the dosages as there were increased respiration, loss of body weight and decline in feeding (food and water). The general behavior of the mice also changed as they become less active, and finally there were mortalities in all cases.

For the first condition where the mice were fed immediately after dosage, the mortality rate increased from 0.5 to 1.0 ml. The time at which deaths occurred at the dose of 1.5 ml was more than at 0.5 and 1.0 ml. This anomaly could be attributed to the prevalence of strong immune systems of the mice at that dosage. Also, no mortality was recorded for one of the mice at the dose of 0.5 ml in the first condition even though there were changes in the other behaviors. This therefore indicated that the toxicity of the oil extracts mostly depended on the dosage (Tables 2a and 2b).

For the second condition where the mice were fed 2 hours after dosage, the mortality rate increased as the dosage increased. Comparing this condition with the first, mortality rate for the second condition was greater at doses of 0.5, 1.0, and 1.5 ml.

The experiment conducted revealed that the phytochemicals present in the oils from the seeds of *Jatropha curcas* lack aphrodisiac potentials as it resulted in sharp decline in the sexual behavior of the mice with increasing dosage. Rather, it could be said that the phytochemicals present in the oil extracts possessed potent pharmacological properties.

The oil extracts upon administration induced changes in the general behavior of the mice which included loss of body weights, poor feeding ability, respiration increase and mortality. These results do not counter the fact that the oil possesses pharmacological activities and other

Table 2a. Toxicity test results for oil extracts from the seeds of *Jatropha curcas* on mice.

Condition	Dosage(ml)	Time elapsed before mortality and after dosage (Hrs min)	Average Duration Before mortality(min)	Weight after Death(g)	Percentage Mortality (%)
Fed immediately after dosages	0.5	42 06	3,127 ± 849.94	23.92	66.67
		62 08		29.80	
		-		-	
	1.0	54 37	2, 447 ± 803.5	22.03	100
		39 51		22.97	
		27 53		21.17	
	1.5	30 50	4, 202 ± 4, 373.3	30.49	100
		154 08		13.16	
		25 08		27.53	
Fed 2 hours after dosages	0.5	83 50	5, 225 ± 1, 949.8	17.90	100
		121 05		15.86	
		56 20		25.87	
	1.0	26 32	1,954.7 ± 462.1	16.80	100
		29 57		26.70	
		41 15		19.50	
	1.5	28 32	1, 847.7 ± 243.7	18.20	100
		35 29		22.20	
		28 22		23.64	

Table 2b. Toxicity test results for oil extracts from the seeds of *Jatropha curcas.*

Condition	Dosage (ml)	Number of mice used	Number of deaths recorded	Percentage Mortality (%)
Fed immediately after dosages	0.5	3	2	66.67
	1.0	3	3	100
	1.5	3	3	100
Fed 2 hours after dosages.	0.5	3	3	100
	1.0	3	3	100
	1.5	3	3	100

beneficial qualities, because it could be treated to remove its toxins, and administered in different modes.

CONCLUSION

This study revealed that the oil extracts from the seeds of *Jatropha curcas* do not possess aphrodisiac potentials. Besides, the oils contained toxins which resulted to the death of mice with the death rate depending mostly on the dosages administered. Also, the phytochemicals present in the oil extracts from the seeds of this plant indicated that the seeds possessed potent pharmacological compounds.

RECOMMENDATION

Further studies should be carried out on the seed-oil of *Jatropha curcas* to ascertain the cause of it being toxic to mice and to eliminate its toxins. This could create room for its aphrodisiac potentials to be examined once again, and could also pave way for the oil to be edible. With the oil possessing phytochemicals which have pharmacological properties, more studies are required to determine the main active components to enhance its full exploitation.

REFERENCES

Akindele, AJ. and Adeyemi, OO. 2007. Anti-inflammatory activity of the aqueous leaf extract of *Byroscarpus coccineus*. Fitoterapia. 78:25-28.

Argal, A. and Pathak AK. 2006. CNS activity of *Calotropis gigantea* roots. J. Ethnopharmacoogyl. 106: 142-145.

Berker, K. and Makkar, HPS. 1998. Toxic effects of Phorbol esters in carp (*Cyprinus carpio* L.). Vet. Human Toxicol. 40:82-86.

Eisa, MN. 1997. Production of ethyl esters as diesel fuel substitutesin the developing countries. In: Biofuels and Industrial Products from *Jatropha curcas* L. DBV Graz. Eds. Gubitz, GM., Mittelbach, M. and Trabi, M. 110-112.

en.Wikipedia.org/wiki/Cardiac glycosides.
en.wikipedia.org/wiki/*Jatropha curcas*
Foidl, N. and Kashyap, A. 1999. Exploring the potential of *Jatropha curcas* in Rural Development and Environmental Protection. Rockefeller Foundation, New York, USA.
Gubitz, GM., Mittelbech, M. and Trabi, M. 1999. Exploitation of tropical oil seed plant *Jatropha curcas* L. Bioresour. Technol. 67:73-82.
Ilkay, O., Esra, K., Bilge, S. and Erdem, Y. 2007. Appraisal of anti-inflammatory potential of the club moss, *Lycopodium clavatum* L. J. Ethnopharmacol. 109:146-150.
Kumar, A. and Shamar, S. 2008. An evaluation of multipurpose oil seed crop for industrial uses (*Jatropha curcas* L): review, Ind. Crops Prod.
Latha, RM., Geetha, T. and Varalaskshmi, B. 1998. Effects of *Vermonia cinerea* less flower extract in adjuvant-induced arthritis. General Pharmacol. 31:601-606.
Liu, RH. 2003. Health benefits of fruit and vegetables are from additive and synergic combinations of phyto-chemicals. Am. J. Clin. Nutr. 78:517S-520S.
Luo, J., Cheung, J. and Yevich, E. 1999. Novel terpenoid-type quinones isolated from *Pycnanthu angolensis* of potential utility in the treatment of type-2 diabetes. J. Pharmacol. Exptl. Therapy. 2008:529-534.
Manach, C., Regerat, F. and Texier, O. 1996. Bio-availability, metabolism, and physiological impact of 4-oxo-flavonoids. Nutr. Res. 16:517-544.
Suresh, PKA., Subramoniam, A. and Pushpangadan, P. 2000. Aphrodisiac activity of *Vanda tessellata* (Roxb.) Hook. Ex Don extract in male mice. Indian J. Pharmacol. 32:300-304.
Takeda, Y. 1982. Development study on *Jatropha curcas* (Sabu Dum) oil as a substitute for Diesel Engine Oil in Thailand. Interim report of the Ministry of Agriculture, Thailand.

Received: Sept 21, 2011; Accepted: Jan 17, 2012

SENRA Academic Publishers, Burnaby, British Columbia
Vol. 6, No. 1, pp. 1827-1835, Feb 2012
Online ISSN: 1920-3853; Print ISSN: 1715-9997

Canadian Journal of pure&applied sciences

LINEAR AND NON LINEAR OPTICAL PROPERTIES OF ELECTRON DONOR AND ACCEPTOR PYRIDINE MOIETY: A STUDY BY AB INITIO AND DFT METHODS

Sana Zafar, Zahid H Khan and *Mohd Shahid Khan
Laser Spectroscopy Laboratory, Department of Physics, Jamia Millia Islamia, New Delhi, India

ABSTRACT

The Donor-Acceptor type conjugated molecular structures containing pyridine as a bridge have been explored for Non linear optical properties. The ab- initio Hartee Fock calculations and Density Functional Theory with B3LYP method have been carried out employing 6-31G basis set. The dipole moments (μ), polarizability (α), first hyperpolarizability (β), and HOMO-LUMO energy gap are calculated using the same level of theory. The dependence of the hyperpolarizability of different molecular structure on the nature of donor and acceptor on the pyridine is discussed on the basis of molecular orbital picture. Of all the molecular systems studied, the molecular system containing nitro as an acceptor and dimethylaniline as a donor is found to have largest value of hyperpolarizability; 49.92 X 10^{-30} esu and 164.61x10^{-30} esu with ab-initio/HF and DFT/B3LYP respectively. The large value of β for the Donor-Acceptor pyridine derivative suggests the potential applications of these molecular systems in the development of non linear materials.

Keywords: DFT, non linear optics, polarizability, first hyperpolarizability, frontier molecular orbital's, Ab initio.

INTRODUCTION

Organic compounds with delocalized π-electrons showing large values of non linear optical parameters are gaining interest among researcher because of their potential applications in field of optoelectronics such as optical communication, optical computing, optical switching and image processing (Chemla and Zyss, 1987; Prasad and Williams, 1990; Zyss, 1994; Venkatram *et al*., 2005). Organic molecules are good candidates for nonlinear devices as they are chemically flexible, and they show large and fast non linear optical response (Gunter, 2000) as a result of which, their optical and electronic properties can be tuned. Variety of organic and organometallic molecular systems has been studied for predicting nonlinearity (Kanis *et al*., 1994). Organic compounds with electron donating group on one side of the molecule and electron accepting group on other side have been studied by experimental and theoretical scientists for NLO properties (Poornesh *et al*., 2009). Designs of these organic NLO active materials are based on the approach of charge transfer (CT) due to π- electron cloud movement from donor (D) to acceptor (A) groups on either side of these π-conjugated systems which in turn affects the value of hyperpolarizability (Prasad and William, 1990). It has been known from the recent studies that molecular systems, based on electron donor (D) and electron acceptor (A) units connected through pi electron moieties show many interesting non linear optical characteristics and have higher value of second order NLO properties (Cheng *et al*., 1991; Thanthiriwatte *et al*., 2002; Liyanage *et al*., 2003; Tillekaratne *et al*., 2003). The types of pi-bridges studied so far for developing efficient NLO materials and molecules include D-A acetylenes (Atalay *et al*., 2008), azo complexes (Moylan *et al*., 1993) aromatic ring (Cheng *et al*., 1991) and heteroaromatic rings (Rao *et al*., 1994). A good deal of work has been done for investigating nonlinear optical behavior of conjugated polymers consisting of six-member and five-member aromatic units such as benzene, pyridine, Thiophene and pyrrole etc (Rao *et al*., 1994; Jen *et al*., 1993). Their derivatives are also considered to be promising candidates for electronic and nonlinear optical technology. Pyridine, pyridine-oxide (POM1, POM2) and nitro pyridine oxide (Berthier *et al*., 1992; Hammoutenea *et al*., 1993; Soscun *et al*., 2002) have large optical nonlinearities, which were associated with intramolecular charge transfer between the NO donor and the aromatic (pyridine) ring and the NO_2 acceptor. So far many studies have also been carried out to investigate the nonlinear behavior of two π-conjugated rings attached with a single bond such as biphenyls (Rumi *et al*., 1999) and phenylpyridine (Alyar *et al*., 2006). However, pyridine moiety can further be investigated as a bridge for the search of better NLO material and for understanding the mechanism at the atomic level.

Theoretical calculations are quite useful both in understanding the relationship between the molecular structures and nonlinear optical properties as well as they also provide guidelines to experimentalists for the design and synthesis of new organic NLO materials. A large

*Corresponding author email: mskhan@jmi.ac.in

number of semi-empirical and ab initio calculations have been reported on molecular hyperpolarizability (β), which is one of the key parameter in investigating second order NLO materials (Soscun *et al*., 2002; Li *et al*., 2006; Champagne *et al*., 2009). The aim of the present work is to design and predict NLO properties of molecular systems with better NLO behavior. The idea is to study the charge transfer effect from donor to acceptor through pyridine moiety. For calculating non linear behavior for the designed molecular systems, ab-initio and DFT calculations have been carried out with 6-31G basis set. Though there is a effect of basis set of the calculation used on the estimated value of β, but the effect is not very profound and the β value has been reported to be slightly increased on taking up higher basis sets like 631G (d), 6-31G (d) (Atalay *et al*., 2008), and this is the reason for not carry out the computation of β values with higher basis set at this stage.

Computational Methodology

All calculations of polarizability and first static hyperpolarizability of pyridine derivatives were performed using Gaussian 03W (Frisch *et al*., 2003). Geometries of all molecules were optimized with 6-31G basis set by employing ab initio Hartee Fock and Becke three-parameter mixing of exchange and Lee–Yang–Parr correlation functional (B3LYP) method. All NLO calculations were performed at same level of theory, which provides reliable results for β (Atalay *et al*., 2008).

The values of mean polarizability (α) of molecular systems, reported in the present work can be calculated by the following equations:

$$\alpha = 1/3(\alpha_{XX}+\alpha_{YY}+\alpha_{ZZ}) \quad (1)$$

The total hyperpolarizability is defined as

$$\beta_{tot}= (\beta_x^2+ \beta_y^2+ \beta_z^2)^{1/2} \quad (2)$$

The magnitude of β_{tot} is calculated from the computed components β using following equation:

$$\beta_{tot} = [(\beta_{xxx}+\beta_{xyy}+\beta_{xzz})^2+(\beta_{yyy}+\beta_{yzz}+\beta_{yxx})^2+ (\beta_{zzz}+\beta_{zxx}+\beta_{zyy})^2]^{1/2} \quad (3)$$

Since the values of β components of GAUSSIAN 03W output are reported in atomic units, thus, the calculated values have been converted into electrostatic units.

RESULTS AND DISCUSSION

The molecular structures of the donor-acceptor pyridine based seven molecular systems viz N,N-dimethyl-5-nitropyridin-2-amine (DMNP), N,N-diethyl-5-nitropyridin-2-amine (DENP), 5-nitro-2-phenylpyridine (NPP), N,N-dimethyl-5-(1,3,4-oxadiazol-2-yl)pyridin-2-amine (DMOP), N,N-diethyl-5-(1,3,4-oxadiazol-2-yl) pyridin-2-amine (DEOP), 5-(1,3,4-oxadiazol-2-yl)-2-phenylpyridine (OPP) and N,N-dimethyl-4-(5-nitropyridin-2-yl) aniline (DMNPA) are shown in Table 1. Ab initio and DFT Calculations for optimized geometry show that all the molecular structures have C1 point group symmetry. The ground state dipole moments (μ), polarizability (α), hyperpolarizability (β) and Homo-Lumo energy gap of all molecular structures computed using ab initio Hartee Fock method and DFT/B3LYP method with 6-31G basis set are presented in table 2. The fact that the magnitude of polarizability depends on the strength of donor and acceptor unit substituted across conjugated bridge (Atalay *et al*., 2008), led us to investigate pyridine as a conjugated bridge and the effect of the substitution of donors and acceptors on its nonlinear behavior. To begin with, we started the study by adding nitro group as an acceptor with different donors viz dimethylamine ($N(Me)_2$), diethylamine ($N(Et)_2$) and phenyl on the pyridine. The choice of nitro as an acceptor has been obvious due to the large values of β for molecules containing nitro as an acceptor (Latajka *et al*., 2007).

For DMNP the value of β obtained using ab initio/HF method is ~$12x10^{-30}$ esu. In order to improve the electronic conjugation between donor and acceptor group the conjugated length is increased in the next molecular structure (DENP), which has diethylamine as donor. The value of β for DENP as computed by using HF method is found to increase ~$13.58x10^{-30}$ esu. The value of β for 5-nitro-2-phenylpyridine (NPP) computed with ab initio/RHF and that with DFT/B3LYP are found to be $13.58x10^{-30}$ esu $42.95x10^{-30}$ esu and respectively. The substitution of the nitro group as an acceptor has resulted in large enhancement of β value, as compared with computed values of β as 1.90 $x10^{-30}$, $0.74x10^{-30}$, $1.21x10^{-30}$ esu respectively for 2-,3-,4- phenylpyridines using HF method as reported by Alyar et al (Latajka *et al*., 2007). They also reported the β values of $3.94x10^{-30}$, $1.72x10^{-30}$ and $2.62x10^{-30}$ esu respectively for the same molecules using DFT/B3LYP method (Rumi *et al*., 1999). By employing DFT/B3LYP method on DMNP and DENP, the value of β is found to be $24.56x10^{-30}$ esu for DMNP which is slightly larger than that of DENP (~$23.62x10^{-30}$ esu). The value of α and β obtained with HF method is observed to follow the increasing order as DMNP<DENP<NPP and with DFT/B3LYP the value of hyperpolarizability for these molecular structures is found to be in the order of DENP<DMNP<NPP. Phenyl is found to be conjugating well with pyridine to give larger value of polarizability and hyperpolarizability as predicted by two theoretical methods. The next three molecular structures viz DMOP, DEOP, OPP in the series are studied to examine the behavior of pyridine with some other acceptor keeping the donor at the same position. For this we have chosen 1, 3, 4- oxadiazole as an acceptor. The magnitude of hyperpolarizability for DEOP using HF/6-31G method is found to be more than that of DMOP as expected but it is found to decrease as the donor is

changed to phenyl in OPP. Whereas the polarizability (α) is found to increase in the same manner when the nitro group is used as an acceptor on the pyridine. The values of hyperpolarizability as estimated using HF/6-31G method for the molecules with oxadiazole acceptor is found to increase as OPP<DMOP<DEOP. By employing DFT/B3LYP method the trend has been found to be, DMOP<DEOP<OPP. A close examination of table 2 tells that nitro as an acceptor across pyridine is continuing to give good value of hyperpolarizability as compared to 1,3,4- oxadiazole as estimated using HF as well as DFT method. The last molecular structure reported in the present study is DMNPA designed with strong acceptor NO_2 and a strong donor dimethylaniline (Atalay *et al*., 2008). The good electronic communication through pyridine from donor to acceptor in this molecule (DMNPA) is inferred from the enhanced value of hyperpolarizability. Using the HF method, the calculated value of β for the DMNPA is found to be $49.92x10^{-30}$ esu and larger value of β (~ $164.61x10^{-30}$ esu) is obtained with DFT/B3LYP method. The values of hyperpolarizability estimated for the molecular systems in present work are quite high as compared with that of para nitro aniline (PNA) (Yang *et al*., 2006; Isborn *et al*., 2007). The enhancement in β value for the pyridine based D-A systems is significant as compared to the β value of $0.168x10^{-30}$ esu, $0.305x10^{-30}$ esu and $2.3x10^{-30}$, $1.65x10^{-30}$ esu for pyridine and pyridine N-oxide respectively as computed with HF and B3LYP methods respectively (Soscun *et al*., 2002). The magnitude of hyperpolarizability as predicted in the present work is two order higher than the magnitude reported in the literature.

In order to evaluate the effect of polarizability, which is associated with the electronic distribution of charges, intermolecular charge transfer is analyzed. The Mulliken Population Analysis (MPA) using HF/6-31G and B3LYP/6-31G methods have been carried out to understand the charge transfer (CT) in the molecular systems, as shown in Table 3. The molecular systems were regarded as three fragments NO_2 or 1,3,4-oxadiazole groups an acceptor, pyridine (PY) and substituents (R). The charge distribution over atoms for the seven molecular structures obtained using the ab-initio/HF and DFT/B3LYP with 6-31G basis set optimizations, evidences the charge transfer from donors (($N(Me)_2$, $N(Et)_2$, phenyl, dimethylaniline) to acceptors (NO_2 and 1,3,4-oxadiazole) are displayed in figures 1 and 2. The donor and acceptor moieties affect the electron withdrawing or releasing ability of pyridine and thus influencing CT in molecular systems. The acceptor property of nitro and oxadiazole group is analyzed by the delocalization of negative charge over the fragments. The dipole moment is an important factor as it is mainly used to study the intermolecular charge transfer. The introduction of $N(Me)_2$ and $N(Et)_2$ in DMNP and DENP leads to the displacement of electronic cloud from pyridine, which in turn leads to the increase in dipole moment, as predicted by HF/6-31G and B3LYP/6-31G methods. The similar results have been obtained for DMOP and DEOP with B3LYP/6-31G method. The positive charge on dimethylaniline at pyridine in DMNPA, on expected ground showed the donor behavior as predicted by results of ab initio as well as with DFT calculations. The strong conjugation predicted in DMNPA manifested the high dipole moment and large value of hyperpolarizability of DMNPA, and is attributed to electron releasing and accepting ability of donor and acceptor substituent, thus influencing the charge transfer.

N,N-dimethyl-5-nitropyridin-2-amine (DMNP)

N,N-diethyl-5-nitropyridin-2-amine (DENP)

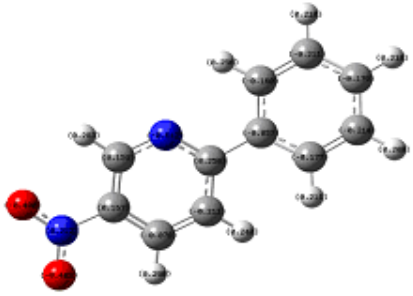

5-nitro-2-phenylpyridine (NPP)

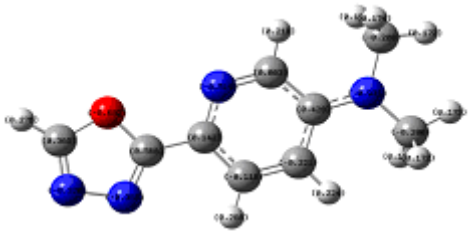

N,N-dimethyl-5-(1,3,4-oxadiazole-2-yl)pyridine-2-amine (DMOP)

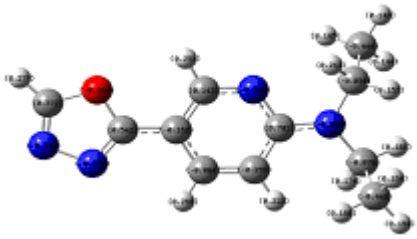

N,N-diethyl-5-(1,3,4-oxadiazole-2-yl)pyridine-2-amine (DEOP)

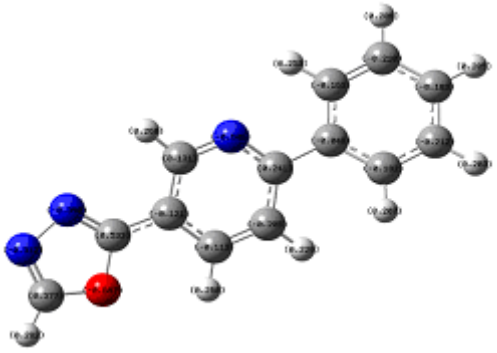

5-(1,3,4-oxadiazole-2-yl)-2-phenylpyridine(OPP)

N,N-dimethyl-4-(5-nitropyridin-2-yl)aniline (DMNPA)

Fig.1. Optimized geometries and Mulliken atomic charges for pyridine based pyridine D-A molecular structures obtained by using HF/6-31G. The red, blue spheres correspond to oxygen and nitrogen atom. The grey and white corresponds to carbon and oxygen.

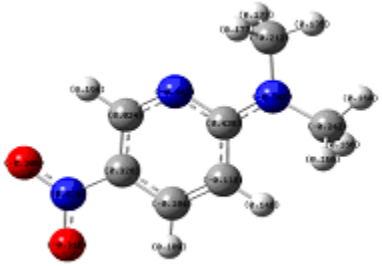

N,N-dimethyl-5-nitropyridin-2-amine (DMNP)

N,N-diethyl-5-nitropyridin-2-amine (DENP)

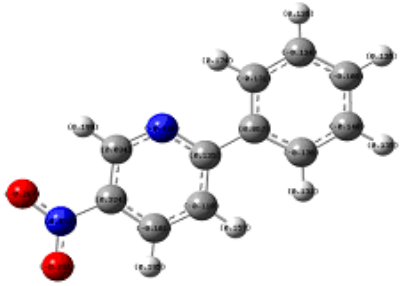

5-nitro-2-phenylpyridine (NPP)

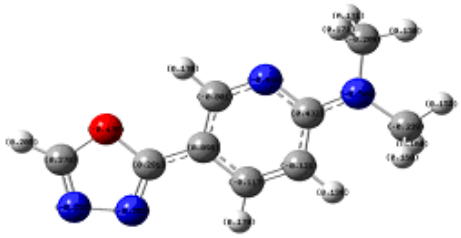

N,N-dimethyl-5-(1,3,4-oxadiazole-2-yl)pyridine-2-amine (DMOP)

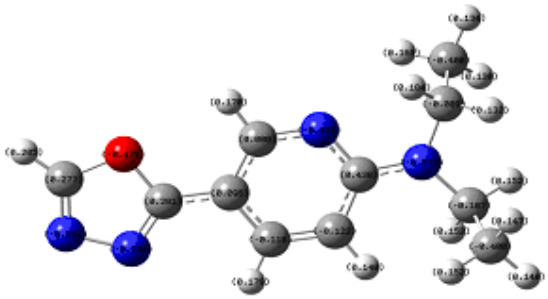

N,N-diethyl-5-(1,3,4-oxadiazole-2-yl)pyridine-2-amine (DEOP)

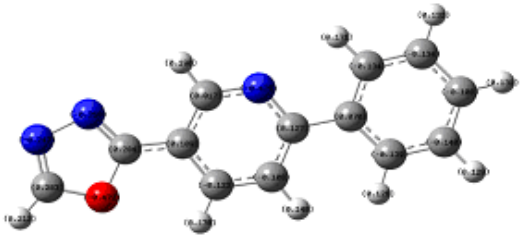

5-(1,3,4-oxadiazole-2-yl)-2-phenylpyridine(OPP)

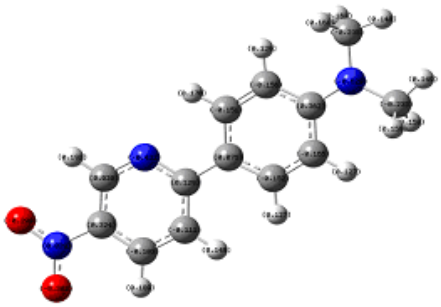

N,N-dimethyl-4-(5-nitropyridin-2-yl)aniline (DMNPA)

Fig. 2. Optimized geometries and Mulliken atomic charges for pyridine based pyridine D-A molecular structures obtained by using B3LYP/6-31G. The red, blue spheres correspond to oxygen and nitrogen atom. The grey and white corresponds to carbon and oxygen.

The NLO properties of these molecular systems can be understood by examining the frontier molecular orbitals, viz HOMO and LUMO energies. The values of HOMO and LUMO energies as predicted by ab initio/HF method and DFT/B3LYP method for all molecular structures are summarized in table 4. The variation of calculated HOMO and LUMO energies and the variation of

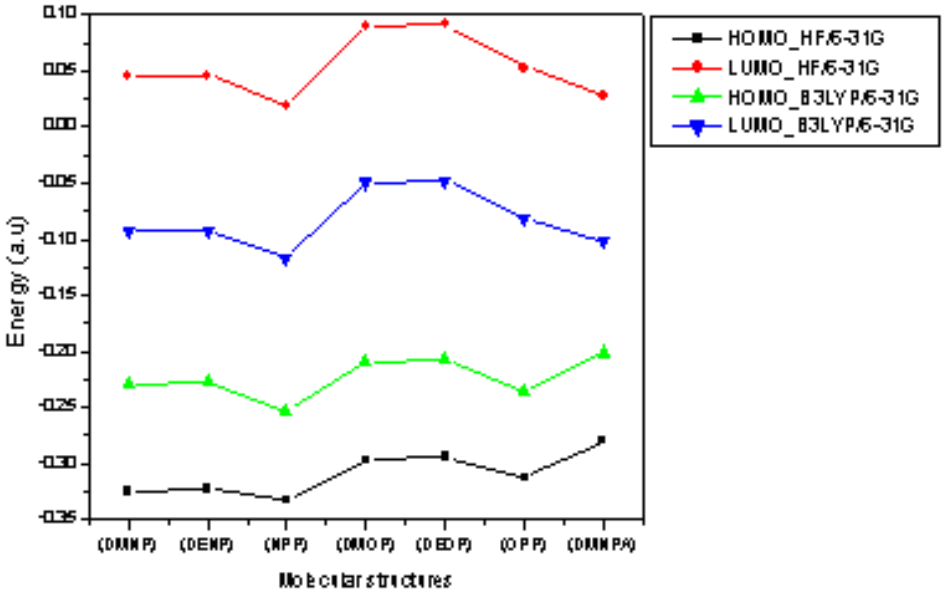

(a)

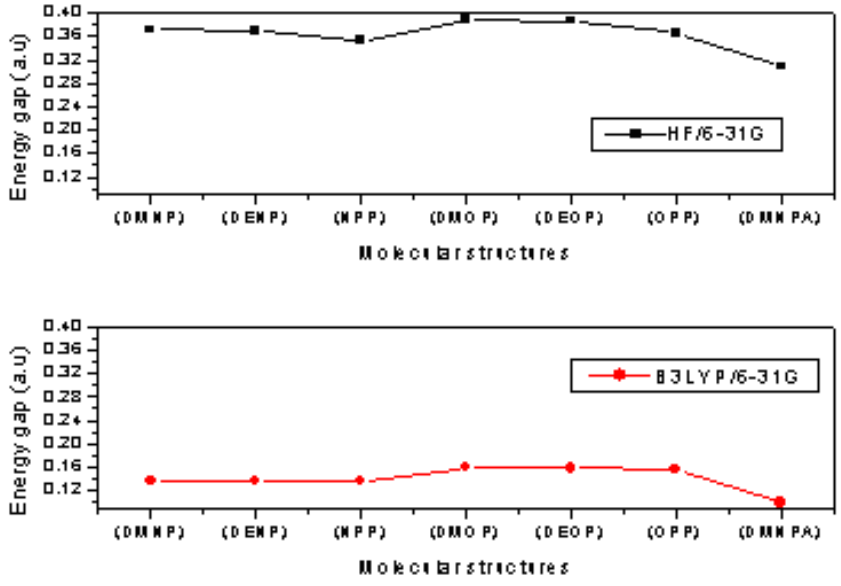

(b)

Fig. 3. Variation of (a) HOMO and LUMO energies and (b) HOMO-LUMO energy difference of the molecular structures using HF/6-31G and B3LYP/6-31G methods.

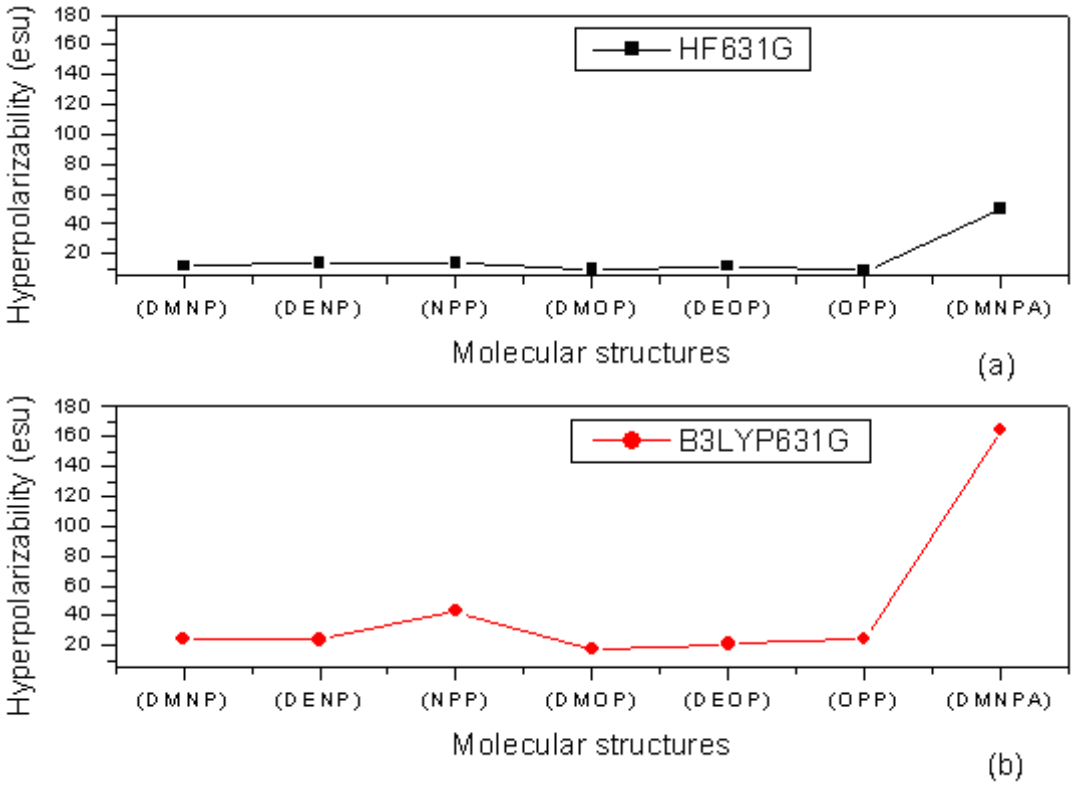

Fig. 4. Variation of theoretical hyperpolarizability of all molecules obtained by using (a) HF/6-31G and (b) B3LYP/6-31G methods.

calculated HOMO- LUMO energy gap are shown in figure 3, whereas the variation of values of hyperpolarizability of all the molecular structures estimated by using HF/631G method is depicted in figure 4. The graphical representation of HOMO and LUMO energies calculated with ab initio/HF method, indicates that HOMO energy for the molecular structures with same acceptors changes slightly except for DMNPA, for which a significant change in HOMO energy on change of donor is observed. The LUMO energies for the molecular

systems DMNP, DENP, DMOP, DEOP are found to increase due to different donors $N(Me)_2$ and $N(Et)_2$. As a result, the energy gap in these systems is larger and a correlation between the higher energy gap and low value of hyperpolarizability is observed. The values of HOMO and LUMO are found to be slightly increased and reduced respectively due to the substitution of phenyl and that led to a reduced energy gap which in turn is manifested as the increased value of hyperpolarizability. Of all the molecular structures, only OPP is not found to obey the inverse relationship between energy gap and the low value of hyperpolarizability (8.83×10^{-30} esu) is estimated despite for its low energy gap, as predicted by HF/6-31G. It can be observed from Fig. 3 that there is a steady change in HOMO and LUMO energies calculated with DFT. The molecular systems containing nitro as an acceptor, having low difference in HOMO-LUMO energies are found to have large value of β as in NPP, DMNP, DENP, while molecular systems OPP, DMOP and DEOP having oxadiazole as an acceptor have large band gap as predicted using HF/6-31G and DFT/B3LYP methods and thus low values of their hyperpolarizability. A large value of hyperpolarizability for DMNPA as obtained with DFT/B3LYP method can be attributed to the decrease in LUMO energy and an increase in HOMO energy thus reducing the energy gap drastically.

CONCLUSIONS

The seven Donor-Acceptor type conjugated molecular structures based on pyridine have been designed and studied theoretically for examining their non-linear optical behavior. Among seven molecular systems studied in this work only N, N-dimethyl-5-nitropyridine (DMNP) has been synthesized by Arumugam Kodi-muthali (Kodimuthali *et al.*, 2010). The NLO properties of this molecule and other molecular structures in the study have not been predicted yet to the best of our knowledge. The ground state dipole moment (μ), polarizability (α) and hyperpolarizability (β) for these seven molecular systems have been investigated by employing ab initio/ HF 6-31G

Table 1. Designed pyridine based donor-acceptor type molecular structures.

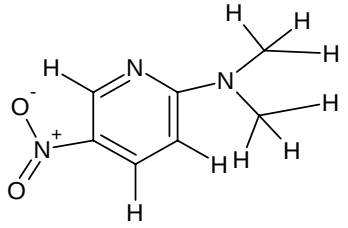

N,*N*-dimethyl-5-nitropyridin-2-amine (DMNP)

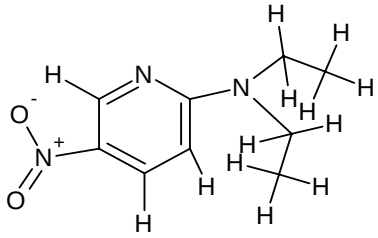

N,*N*-dimethyl-5-nitropyridin-2-amin (DENP)

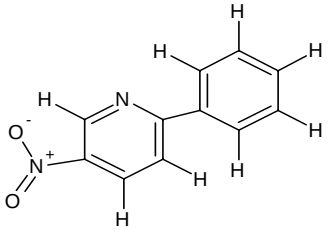

5-nitro-2-phenylpyridine (NPP)

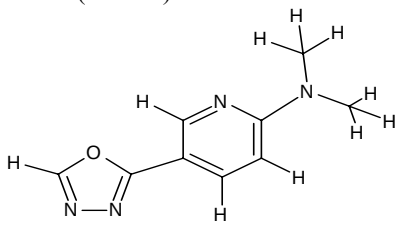

N,*N*-diethyl-5-(1,3,4-oxadiazol-2-yl)pyridin-2-amine (DMOP)

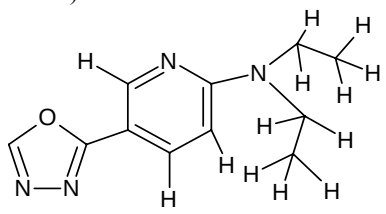

N,*N*-diethyl-5-(1,3,4-oxadiazol-2-yl)pyridin-2-amine (DEOP)

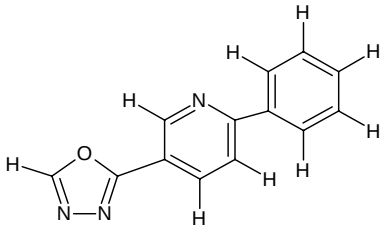

5-(1,3,4-oxadiazol-2-yl)-2-phenylpyridine (OPP)

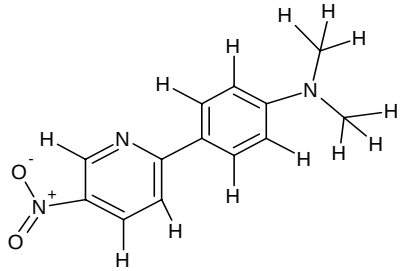

N,*N*-dimethyl-4-(5-nitropyridin-2-yl)aniline (DMNPA)

Table 2. Calculated ground state dipole moment (μ in Debye), polarizability (α in a.u), hyperpolarizability (β x 10^{-30} esu) using ab- initio/ HF and DFT/ B3LYP with 6-31G basis set.

		Ab-initio HF/6-31G			DFT B3LYP/6-31G	
Molecule	μ	α	β	μ	α	β
N,N-dimethyl-5-nitropyridin-2-amine (DMNP)	8.02	96.48	12.00	8.13	111.05	24.56
N,N-diethyl-5-nitropyridin-2-amine (DENP)	7.99	118.15	13.58	8.14	134.80	23.62
5-nitro-2-phenylpyridine (NPP)	6.02	125.74	13.93	5.70	145.52	42.95
N,N-dimethyl-5-(1,3,4-oxadiazol-2-yl)pyridin-2-amine (DMOP)	4.38	115.18	9.94	5.07	132.85	17.83
N,N-diethyl-5-(1,3,4-oxadiazol-2-yl)pyridin-2-amine (DEOP)	4.35	137.38	11.63	5.09	157.31	21.14
5-(1,3,4-oxadiazol-2-yl)-2-phenylpyridine (OPP)	5.11	146.46	8.83	4.83	169.60	24.84
N,N-dimethyl-4-(5-nitropyridin-2-yl)aniline (DMNPA)	9.13	169.40	49.92	10.15	215.94	164.61

and DFT/B3LYP 6-31G methods. The value for hyperpolarizability predicted for DMNPA, 49.92 X 10^{-30} and 164.61 X 10^{-30} esu by HF/6-31G and B3LYP/6-31G methods, respectively, are two orders larger in order as compared to pyridine based structures reported in literature (Atalay *et al*., 2008). An inverse relationship

Table 3. Theoretical Mullikien charge analysis over fragments by HF/6-31G and B3LYP/6-31G -R= dimethylamine, diethylamine[b], Phenyl[c], dimethylaniline[d]

Molecular Structure	HF/6-31G			DFT/6-31G		
	HOMO	LUMO	Energy Gap	HOMO	LUMO	Energy Gap
DMNP	-0.32548	0.04565	0.37113	-0.22954	-0.09271	0.13683
DENP	-0.32292	0.04629	0.36921	-0.22768	-0.09194	0.13574
NPP	-0.33343	0.01861	0.35204	-0.25314	-0.11649	0.13665
DMOP	-0.29730	0.09022	0.38752	-0.20922	-0.04961	0.15961
DEOP	-0.29485	0.09140	0.38625	-0.20714	-0.04861	0.15853
OPP	-0.31294	0.05313	0.36607	-0.23649	-0.08094	0.15555
DMNPA	-0.28016	0.02809	0.30825	-0.20121	-0.10184	0.09937

Table 4. Theoretical predicted HOMO (a.u), LUMO (a.u), HOMO-LUMO energy gap (a.u) by HF/6-31G and B3LYP/6-31G

Molecular structure	Ab initio/ Acceptor	HF		DFT/ Acceptor	B3LYP	
		PY	- R		PY	-R
DMNP	-0.630	0.831	-0.199[a]	-0.591	0.647	-0.054[b]
DENP	-0.633	0.828	-0.197[b]	-0.594	0.644	-0.048[c]
NPP	-0.593	0.496	0.097[c]	-0.541	0.407	0.132[a]
DMOP	-0.184	0.413	-0.227[a]	-0.249	0.333	-0.085 [b]
DEOP	-0.185	0.415	-0.231[b]	-0.252	0.332	-0.081[c]
OPP	-0.157	0.084	0.074[c]	-0.209	0.105	0.104[a]
DMNPA	-0.611	0.485	0.124[d]	-0.572	0.367	0.205[d]

between energy gap and hyperpolarizability is established on the basis of the results of calculations based on both HF/6-31G and DFT/B3LYP/6-31G. The large β values predicted theoretically for the designed molecular systems suggest the potential applications of these systems in nonlinear optical devices.

REFERENCES

Alyar, H., Bahat, M., Kasap, E. and Kantarci, Z. 2006. Torsional barriers and nonlinear optical properties of 2-, 3-, 4-phenylpyridine molecules. Czech. J. Phys. 56:349-358.

Atalay, Y., Avci, D. and Basoglu, A. 2008. Linear and non-linear optical properties of some donor–acceptor oxadiazoles by ab initio Hartree-Fock calculations. Structural Chemistry.19:239-246.

Berthier, G., Defranceschi, M., Lazzeretti, P., Tsoucaris, G. and Zanasi, R. 1992. Dipole moments and polarizabilities of some substituted pyridine-1-oxides for optoelectronics. J. Mol. Struct. (Theochem). 254:205.

Chemla, DS. and Zyss, J. 1987. Nonlinear Optical Properties of Organic Molecules and Crystals, Academic press, Orlando.

Cheng, LT., Tam, W., Stevenson, SH., Meredith, GR., Rikken, G. and Marder, SR. 1991. Experimental investigations of organic molecular nonlinear optical polarizabilities. 1. Methods and results on benzene and stilbene derivatives. J. Phys. Chem. 95:1063-1064.

Champagne, B. and Spassova, M. 2009. Theoretical investigation on the polarizability and second hyperpolarizability of polysilole. Chem. Phy. Lett. 471:111-115.

Frisch, MJ., Trucks, GW., Schlegel, HB., Scuseria, GE., Robb, MA., Cheeseman, JR., Montgomery, JA., Jr., Vreven T., Kudin, KN., Burant, JC., Millam, JM., Iyengar, SS., Tomasi, J., Barone,V., Mennucci, B., Cossi, M., Scalmani, G., Rega, N., Petersson, GA., Nakatsuji, H., Hada, M., Ehara, M., Toyota, K., Fukuda, R., Hasegawa, J., Ishida, M., Nakajima, T., Honda, Y., Kitao, O., Nakai, H., Klene, M., Li ,X., Knox, JE., Hratchian, HP., Cross, JB., Akken, V., Adamo, C., Jaramillo, J., Gomperts, R., Stratmann, RE., Yazyev, O., Austin, AJ., Cammi, R., Pomelli, C., Ochterski, JW., Ayala, PY., Morokuma, K., Voth, GA., Salvador, P., Dannenberg J. J., Zakrzewski, VG., Dapprich, S., Daniels, AD., Strain, MC., Farkas, O., Malick, DK., Rabuck, AD., Raghavachari, K., Foresman, BJ., Ortiz, JV., Cui, Q., Baboul, AG., Clifford, S., Cioslowski, J., Stefanov, BB., Liu, G., Liashenko, A., Piskorz, P., Komaromi, I., Martin, RL., Fox, DJ., Keith, T., Al-Laham, MA., Peng, CY., Nanayakkara, A., Challacombe, M., Gill, PM. W., Johnson, B., Chen, W., Wong, MW., Gonzalez, C. and Pople, JA. 2003. Gaussian 03, Revision E.01, Gaussian, Inc., Pittsburgh PA, USA.

Gunter, P. 2000. Nonlinear Optical Effects and Materials, Springer, Verlag, Berlin.

Hammoutenea, D., Boucekkinea, G., Boucekkinea, A. and Berthier, G. 1993. The semiempirical challenge for the calculation of molecular hyperpolarizabilities. J. Mol. Struct. (Theochem). 287:93-97.

Isborn, CM., Leclercq, A., Vila, FD., Dalton, LR., Bredas, JL., Eichinger, BE. and Robinson, BH. 2007. Comparison of Static First Hyperpolarizabilities Calculated with Various Quantum Mechanical Methods. J. Phys. Chem. A. 111:1319-1327.

Jen, AKY., Rao, VP., Wong, KY. and Drost, KJ. 1993. Functionalized thiophenes: second-order nonlinear optical materials. J. Chem. Soc. Chem. Commun.1:90-92.

Kanis, DR., Ratner, MA. and Marks, TJ. 1994. Design and construction of molecular assemblies with large second-order optical nonlinearities. Quantum chemical aspects. Chem. Rev. 94:195-242.

Kodimuthali, A., Mungara, A., Prasunamba, PL. and Pal, M. 2010. A Simple Synthesis of Aminopyridines: Use of Amides as Amine Source. J. Braz. Chem. Soc. 21:1439-1445.

Liyanage, PS., De Silva, RM. and De Silva, KMN. 2003. Nonlinear optical (NLO) properties of novel organometallic complexes: high accuracy density functional theory (DFT) calculations J. Mol. Struct. (Theochem). 639:195-201.

Li, H., Han, K., Shen, X., Lu, Z., Huang,Z., Zhang, W., Zhang, Z. and Bai, L. 2006. The first hyperpolarizabilities of hemicyanine cationic derivatives studied by finite-field (FF) calculations J. Mol. Struct. (Theochem). 767:113-118.

Latajka, Z., Gajewski, G., Barnes, AJ. and Ratajczak, H. 2007. Hyperpolarizabilities of strongly hydrogen-bonded molecular complexes: PM3 and ab initio studies. J. Mol. Struct. 844:340-342.

Moylan, CR., Twieg, R. J., Lee, VY., Swanson, SA., Betterton, KM. and Miller, RD. 1993. Nonlinear optical chromophores with large hyperpolarizabilities and enhanced thermal stabilities. J. Am. Chem. Soc. 115:12599-12600.

Prasad, PN. and Williams, DJ. 1990. Introduction to Nonlinear Optical Effects in Molecules and Polymers, Wiley, New York, USA.

Poornesh, P., Umesh, G., Hegde, PK., Manjunatha, MG., Manjunatha, KB. and Adhikari, AV. 2009. Studies on third-order nonlinear optical properties and reverse saturable absorption in polythiophene/poly (methylmethacrylate) composites. Appl. Phys. B. 97:117-124.

Rao. VP., Cai, YM. and Jen, AKY. 1994. Ketene dithioacetal as a π-electron donor in second-order nonlinear optical chromophores. J. Chem. Soc., Chem. Commun. 14:1689-1690.

Rumi, M. and Zerbi, G. 1999. Conformational dependence of linear and nonlinear molecular optical properties by ab initio methods: the case of oligo-p-phenylenes. Chem. Phys. 242:123-140.

Soscun, H., Castellano, O., Bermúdez, Y., Toro-Mendoza, C., Marcano, A. and Alvarado, Y. 2002. Linear and nonlinear optical properties of pyridine N-oxide molecule. J. Mol. Struct. (Theochem) 592:19-28.

Thanthiriwatte, KS. and De Silva, KMN. 2002. Non-linear optical properties of novel fluorenyl derivatives—ab initio quantum chemical calculations. J. Mol. Struct. (Theochem) 617:169-175.

Tillekaratne, AD. and De Silva, KMN. 2003. Push–pull porphyrins as non-linear optical materials: ab initio quantum chemical calculations. J. Mol. Struct. (Theochem). 638:169-176.

Venkatram, N., Akundi, MA. and Narayana Rao, D. 2005. Nonlinear absorption, scattering and optical limiting studies of CdS nanoparticles. Optics express. 13:867-872.

Yang, GC., Shi, SQ., Guan, W., Fang, L. and Su, ZM. 2006. Hyperpolarizabilities of para-nitroaniline and bis[4-(dimethylamino)phenyl] squaraine: The effects of functional/basis set based on TDDFT–SOS method. J. Mol. Struct. (Theochem). 773:9-14.

Zyss, J. 1994. Molecular Non Linear Optics, Academic Press, Boston, USA.

Received: July 26, 2011; Revised: Nov 2, 2011; Accepted: Nov 3, 2011

SENRA Academic Publishers, Burnaby, British Columbia
Vol. 6, No. 1, pp. 1837-1845, Feb 2012
Online ISSN: 1920-3853; Print ISSN: 1715-9997

Canadian Journal of pure&applied sciences

THE STATUS OF SOIL AT THE PERMANENT SITE OF THE NNAMDI AZIKIWE UNIVERSITY, AWKA, SOUTHEASTERN NIGERIA

*BI Odoh[1], BCE Egboka[1] and PO Aghamelu[2]
[1] Department of Geological Sciences, Nnamdi Azikiwe University, P.M.B. 5025 Awka
[2] Department of Geology and Exploration Geophysics, Ebonyi State University, P. M. B., 058, Abakaliki, Nigeria

ABSTRACT

This paper presents an investigation on the properties of soils underlying the permanent site of the Nnamdi Azikiwe University, Awka, Nigeria. A total of 450 samples collected from 150 Hand auger drilled holes across the campus were subjected to different geotechnical tests. Geotechnical parameters tested for in the soil samples were mechanical analysis, Atterberg limits, compaction, CBR, bulk density, natural moisture content and shear strength. Results indicated that the soils consisted of predominantly sand-sized grains overburden (either ***SM*** or ***SC***); percentage of fines ranged from 7 to 72%, sand 28 to 93% and gravel 0 to 40 %. Liquid limit values ranged from minimum value of 15 (at depth 0 to 1.5m) to maximum value of 78 (at depth ≥1.6m), while Plasticity index values ranged from non-plastic samples to a maximum value of 41. Plots of samples in the plasticity chart revealed the fines are predominantly clays and silts of low plasticity (***CL - ML***), and less amount of organic silts (***MH*** or ***OH***). Medium to high plasticity resulting from moderate to high clay content of the soil suggests volumetric changes, especially when the site is waterlogged. The bearing capacity and settlement (in particular compressibility) analyses confirmed that most locations within the site have low stability. A number of sampled points have their compression index values above 0.20, suggesting that those points would experience moderate compressibility over engineering time.

Keywords: Awka, soil investigation, geotechnical tests, settlement analysis, structural failure.

INTRODUCTION

The ground is a product of dynamic natural and anthropogenic processes and there exhibits a variety of characteristics and properties which is not homogeneous and isotropic. Geophysical, geotechnical and environmental engineering involve assembling and assimilating limited facts about these characteristics and properties in order to understand or unravel the behavior of the ground and groundwater on a particular site under certain conditions. The efficiency of any building or structural projects on the earth surface, to a large extent, depends on suitability of its foundation material.

In Nigeria, several factors could lead to failure of structural projects. They may include poor construction material, improper designing, quackery on the side of the building personnel involved and expansive foundation soil (Ede, 2010), amongst others. Expansive soils are generally known to cause instability in foundations, in particular and failures of most structural projects, in general. Currently, some existing buildings at the permanent site of the Nnamdi Azikiwe University are exhibiting evidences to suggest imminent failure. The site is located within the Awka Capital Territory of Anambra State, along the Enugu-Onitsha Dual Carriage way near the Amansea Boundary of the Anambra and Enugu States of Nigeria. It is underlain by the Imo Shale. Shale is a problem soil that is notoriously unpredictable, especially the soft non-indurated type, which undergoes volumetric changes when subjected to changes in moisture content as a result of annual rainy and rainy seasons. The volumetric change problem is well pronounced on almost all roads within the University Campus and is also evident in cracks on some buildings at the Science Village of the University. Shale is also an aquiclude and consequently results in waterlogged terrains.

Geology

The Nnamdi Azikiwe University, Awka, site is underlain by the Imo Shale (Fig. 1 and Table 1 summarize the stratigraphy of the Anambra Basin within which the study area lies). The dominant lithology of this formation is shale. Occurrences of siltstone, sandstone and laterite are noted, and they overlie the shale (depth of overburden ranges from 0.0 – 3.5m) in most locations within the University site. The *in-situ* shale (fresh sample) is bluish to dark colored. The siltstone and sandstone are milky to brownish, while the laterite is generally dark brownish to reddish in color (Fig. 2).

Shale is a problem soil that is notoriously unpredictable, especially the soft non-indurated type, which undergoes volumetric changes when subjected to changes in moisture content as a result of annual rainy and rainy seasons. This volumetric change problem is well

*Corresponding author email: bi.odoh@unizik.edu.ng

pronounced on almost all roads within the University Campus and is also evident in cracks on some buildings at the Science Village of the University. The site lies at an elevation of approximately 150ft and is generally undulating in the SE direction.

Hydrogeology

Water table lies within 2 to 3m below the surface of native ground during the investigation; testing was carried out in the peak of dry season (January – February). Ditches in the site also showed water at a similar elevation. The low-lying portions of the site area are generally water-logged, suggesting low permeability of the underlying soil (i.e., aquiclude). Flow direction of the surface water is in the northeast direction.

Physiography and climate

The permanent site of the Nnamdi Azikiwe University falls within the highland region of a low asymmetrical ridge or Cuesta in the northern portion of the Awka-Orlu Uplands (Aghamelu *et al*., 2011b). The Cuesta trends roughly southeast to northwest, in line with the geological formations that underlie it. It is highest in the southeast, about 410 m above mean sea level, and gradually decreases in height to only 33 m in the northwest on the banks of the Anambra River and the Niger River.

The major river that drains the area is the perennial the Anambra River and its tributaries, which usually overflow their banks at the peak of the rains. Stunted trees and pockets of derelict wood land exist where the lithology has undergone high degree of laterization. Elsewhere, typical characteristics of the tropical rain forest are displayed; multitude of evergreen trees, climbing plants, parasitic plants that live on the other plants, and creepers.

Two main seasons exist in the Awka area, the dry season which lasts from November to March and the rainy season which begins in April and ends in October with a short period of reduced rains in August commonly referred to as "August break". Temperature in the dry season ranges from 20 to 38°C, and results in high evapotranspiration, while during the rainy season temperature ranges from 16 to 28°C, with generally lower evapotranspiration. The average monthly rainfall ranges from 31mm in January to 270mm in July, with the dry season experiencing much reduced volume of rainfall unlike the rainy season, which has high volume of rainfall. Average annual rainfall varies from 1,500 to 1,650mm. Aghamelu *et al*. (2011b) pointed out that the climatic conditions prevalent in the Awka area might be responsible for the development of *in situ* lateritic covers in some parts of the area.

The purpose of this research is to provide the results, as well as findings regarding the subsurface soil conditions at the various points sampled by means of geotechnical analysis, and make recommendations where necessary. Hence, the objectives of the site investigation were identification of the various soil and horizons, groundwater levels encountered in test pits and recommendation of suitable foundation types, levels and California Bearing Capacity (CBR) values for pavement design.

MATERIALS AND METHODS

Field Investigation

The master Plan of the University Campus is indicate the construction of some multi-storey buildings, roads, stadium, shopping centre and other civil engineering structures in different locations within the University. Some of these projects are at various stages of development; some already developed, while some are either under construction or proposed. To assess the engineering properties and bearing capacities of the foundation soils within the area marked out for these construction works, in particular and that of the entire Campus in general, soil samples were collected from 150 sampling points spread across, about 2,500sq km, area of the campus.

A 6-in diameter Hand Auger was deployed for the sample collection for all the tests except for the Triaxial shear strength; a 2inch diameter tube, fixed at the end of an Adapter (special device for the purpose), was utilized for the collection of soil samples for the triaxial shear strength tests. Depths vary from 0 to 3.5m; range of depths of drilling was restricted by difficulty in drillability of the underlying shale in some locations and close of water-table to the surface at the other locations. The sampling points were selected by preference (joint decision with the client). The description and exact locations of the points are given in the detailed report of the investigation (Aghamelu and Ezeh, 2010).

The soils were characterized on-site using field classifications in accordance with Visual-Manual procedure (American Society for Testing and Material, ASTM D2488, 1989) and were logged at the time of drilling. These logs were then updated as appropriate using laboratory test results and the Unified Soil Classification System (USCS) using ASTM D2487 (1989).

Laboratory Analyses

Laboratory analyses were performed on the samples collected from 150 Hand Auger drilled boreholes, 131 for classification and foundation bearing capacity analyses and 19 for subgrade analysis. The tests carried out on the soil samples included; mechanical analysis, Atterberg limits, compaction, California Bearing Ratio (CBR), bulk density, natural moisture content and shear strength. These tests followed procedures specified by Lambe

(1951), British Standard Institute, BSI 1377 (1990) and Bailey (1976). Scalping was employed such that materials used for the compaction tests (Modified Standard Proctor) passed the ¾ in. (i.e., 19.05mm) mesh of the BSI test sieves, while the CBR mould was preferred to enable immediate determination of CBR values at varying moisture contents and compaction densities.

The samples for the shear strength tests were compacted at optimum moisture contents to simulate the best possible field moisture compaction condition. The test was essentially an unconsolidated undrained shear strength test; without pore pressure measurement. Each test specimen was subjected to all-round confining pressure, δ_3 and loaded to failure with increased vertical pressure, δ_1. With the of δ_3 and corresponding δ_1, the Mohr circles and envelopes of failure were constructed to determine the angle of shearing resistance, ϕ (recorded in^0) and cohesion, c (recorded in kN/m^2) of the specimens.

Settlement and Bearing capacity analyses

The Settlement and Bearing capacity analyses carried out in this study followed a procedure outlined by Aghamelu *et al*. (2011a). The procedure was utilized because it has been shown to be significantly appropriate to the estimation of behaviour of a shallow foundation similar to the present study.

Table 1. Sedimentary succession of the Anambra Basin.

Age*	Epoch	Geological Unit
54	Eocene	Ameki/Nanka Formations
63	Paleocene Danian	Imo Formation Nsukka Formation Ajali Formation
	Maastrichtian	
75		Mamu Formation
82	Campanian	Nkporo Shale/Enugu Shale

*in million year ago.

Table 2. Summary of the results of geotechnical analyses on studied soils.

Parameter	Range	Average	StD*	No.**
Grain Size Distribution				
Fines (%)	7 – 72	46	114	415
Sand (%)	28 – 93	68	122	415
Gravel (%)	0 – 40	22	108	415
Atterberg limits				
Liquid Limit	15 – 78	56	202	388
Plastic Limit	NP – 49	31	188	388
Plasticity Index	NP – 42	23	-	388
Compaction				
Maximum Dry Density (Mg/m^3)	1.64 – 1.94	1.77	64	150
Optimum Moisture Content (%)	6.8 – 21.4	12.4	96	150
California Bearing Ratio (CBR)				
CBR, after 24 hrs soaking (%)	48 – 72	59	77	150
Shear Strength				
Cohesion (kN/m^2)	0 – 46	28	88	125
Angle of shear resistance (^{o})	12 – 37	22	63	125
Density				
Bulk density (Mg/m^3)	1.33 – 2.20	1.86	106	150
Natural moisture content	12.5 – 22.7	18.4	86	150
Classification				
USCS	SM, SC, CL-ML, MH, OH	-	-	-

*Standard deviation, *Number of samples tested, NP Non plastic (plastic limit test was not possible)

Table 3. Results of the site bearing capacity analysis*.

Bore-Hole No.	Location	Ultimate bearing capacity (kN/m^2)	Safe bearing capacity (kN/m^2)	Compression index
BH 1	Second main gate	375	150	0.16
BH 2	Chapel of Glory	420	168	0.19
BH 3	Bus Stop	539	216	0.14
BH 6	Electric Power Station	925	370	0.14
BH 7	Fire Station	1073	429	0.19
BH 11	Solar Panel	358	143	0.14
BH 13	Tower	352	141	0.18
BH 15	Day Care	480	192	0.15
BH 19	Law Faculty	317	127	0.05
BH 25	Conference Centre	423	169	0.05
BH 26	Guest House	309	124	0.09
BH 28	Central Bank Building	425	170	0.17
BH 29	Amphi Theatre	378	151	0.51
BH 30	Stadium	300	120	0.21
BH 35	SW Boundary	300	120	0.15
BH 37	Sports Complex	409	164	0.23
BH 38	Admin. Block	534	214	0.14
BH 40	Entrepreneur Centre	356	142	0.17
BH 42	Reserved area	391	156	0.11
BH 55	Water Reservoir	574	230	0.23
BH 57	New Law Faculty	354	142	0.09
BH 59	Male Hostel	332	133	0.12
BH 65	Female Hostel	1200	480	0.10
BH 66	Faculty of Agriculture	673	269	0.13
BH 69	Main Library	391	156	0.51
BH 70	Future Expansion	532	213	0.08
BH 84	Proposed Students' Hostel	299	120	0.08
BH 104	Alumni Centre	821	328	0.23
BH 108	Science Village	613	245	0.32
BH 112	Buka	580	232	0.34
BH 120	Faculty of Education	956	382	0.22
BH 124	Post Graduate School	440	176	0.16
BH 125	Department of Mech. Engineering	806	322	0.38
BH 127	Staff Canteen	998	400	0.24
BH 129	Natural Science Laboratory	658	263	1.80
BH 136	Shopping Complex	790	316	0.07

*mean values at depth range of 0 to 1.5m.

RESULTS AND DISCUSSION

Mechanical Analysis and Atterberg limits Analyses

The results of the tests are in table 2. The results showed that the soils consist of predominantly sand sized grains overburden (i.e., **SM** or **SC**, according to Unified Soil Classification System). The maximum occurrence of sand occurs at a drilled hole at Law Faculty of the University (depth range 0 to 1.5m), while the minimum occur at the Bus Station in the campus and at another hole within the Law Faculty (depth range both 1.6 to 2.5 m). Below the depth of 1.0 to 1.5m the soil samples generally recorded a significant reduction in sand sized particles, thus an increase in fines percentage. Field observation suggests that the gravels are associated with lateritic soils most probably derived from the underlying Imo Shale Formation.

Plots of samples in the Plasticity Chart (see Fig. 3) revealed the fines are predominantly clays and silts of low plasticity (**CL - ML**), and less amount of organic silts

Table 4. Comparison of results with Nigerian specification for general filling and embankment material.

Properties of material	Nigerian specifications[a]	Studied soils[b]	Remarks
MDD (Mg/m^3)	> 0.047	1.64 – 1.94	Favourable
OMC (%)	< 18	6.8 – 14.6	Favourable
LL	< 40	15 – 71	Unfavourable
PI	< 20	6 – 42	Unfavourable
% Passing No. 200 (%)	$\leq$ 35	7 – 72	Unfavourable
CBR (24 hrs soaked) BS (%)	> 5	48 – 57	Favourable

[a]Nigerian Federal Ministry of Works (1970).
[b]range

Table 5. An engineering evaluation of some physical properties of the Imo Shale.

Physical properties			Imo Shale[a]	*Remarks*
Laboratory test and *in-situ observations*	Average range of values (Underwood, 1967)			
	Unfavourable	*Favourable*		
Cohesive strength (kN/m^2)	35 – 700	700 – 10,500	15 – 28	Unfavourable
Angle of internal friction (°)	10 – 20	20 – 65	5 – 46	Favourable
Dry density (Mg/m^3)	1.13 – 1.76	1.76 – 2.56	1.66 – 1.94	Favourable
Natural Moisture content (%)	20 – 35	5 – 15	14 – 19	Unfavourable
Predominant clay minerals	Montmorillonite, illite	Kaolinite, chlorite	-	Unfavourable

([a]data from Aghamelu *et al*., 2011b)

(**OM** or **OH**). LL ranges from minimum value of 15 (at points within the Law Faculty and Male Hostel, depth 0 to 1.5m) to maximum value of 78 (at Bus Station, depth ≥ 1.6m), while PI ranges from non-plastic samples (at the Fire Station, Solar Panel Station, Day Care and Administrative block) to maximum value of 41 (at a Multi Purpose Hall near the new Law Faculty, ≥ 2.6m). LL values were utilized for the settlement analysis in this study.

Compaction and California Bearing Ratio tests

The values of maximum dry density (ρ_{dmax}) recorded by the compacted soil samples from the site range from 1.64 Mg/m^3 (at a point along the Law Faculty Road) to 1.94 Mg/m^3 (at a point along the proposed By-pass near the main entrance of the campus), as presented in Table 2. The samples recorded minimum optimum moisture content ($W_{opt.}$) value of 6.8 % (on samples from the proposed By-pass near the main entrance and future expansion area) and maximum value of 21.4% (on sample from a point along the Law Faculty Road). The average soaked California Bearing Ratio (CBR) value of the site subgrade is about 59%; maximum soaked CBR is 48% (on sample from a point along the Law Faculty Road) and maximum 72% (sample from a By-pass near the main entrance).

CBR has been correlated with pavement performance as well as used to establish design curves for pavement thickness (Sowers and Sowers, 1970). The CBR value of a construction material is often used as a benchmark in the assessment of its strength for pavement design according to Mannering and Kilareski (1998) and Wignall *et al*. (1999).

Bulk density and Triaxial shear strength tests

The results of the bulk density (ρ) and shear strength tests are summarized in table 3. The values were recorded on soil samples from a drilled hole at the southwest boundary of the campus and Faculty of Education, respectively. Sampling depths at the two locations were both at 0 to 1.5m. The strength tests results indicate that cohesion (c_u) and angle of shearing resistance (φ_u) of the tested samples ranged from 0 to 46 kN/m^3 and 12 to 37^0, respectively. The lowest c_u value was recorded on soil sample from the Bus Station and the site for the proposed Water Reservoir, while the highest value was recorded on soil sample from the Electric Power Station. The lowest φ_u value was recorded on soil sample from the Solar Panel Station and the highest value on sample from the Faculty of Agriculture. The strength parameters values were utilized in this report for bearing capacity analysis.

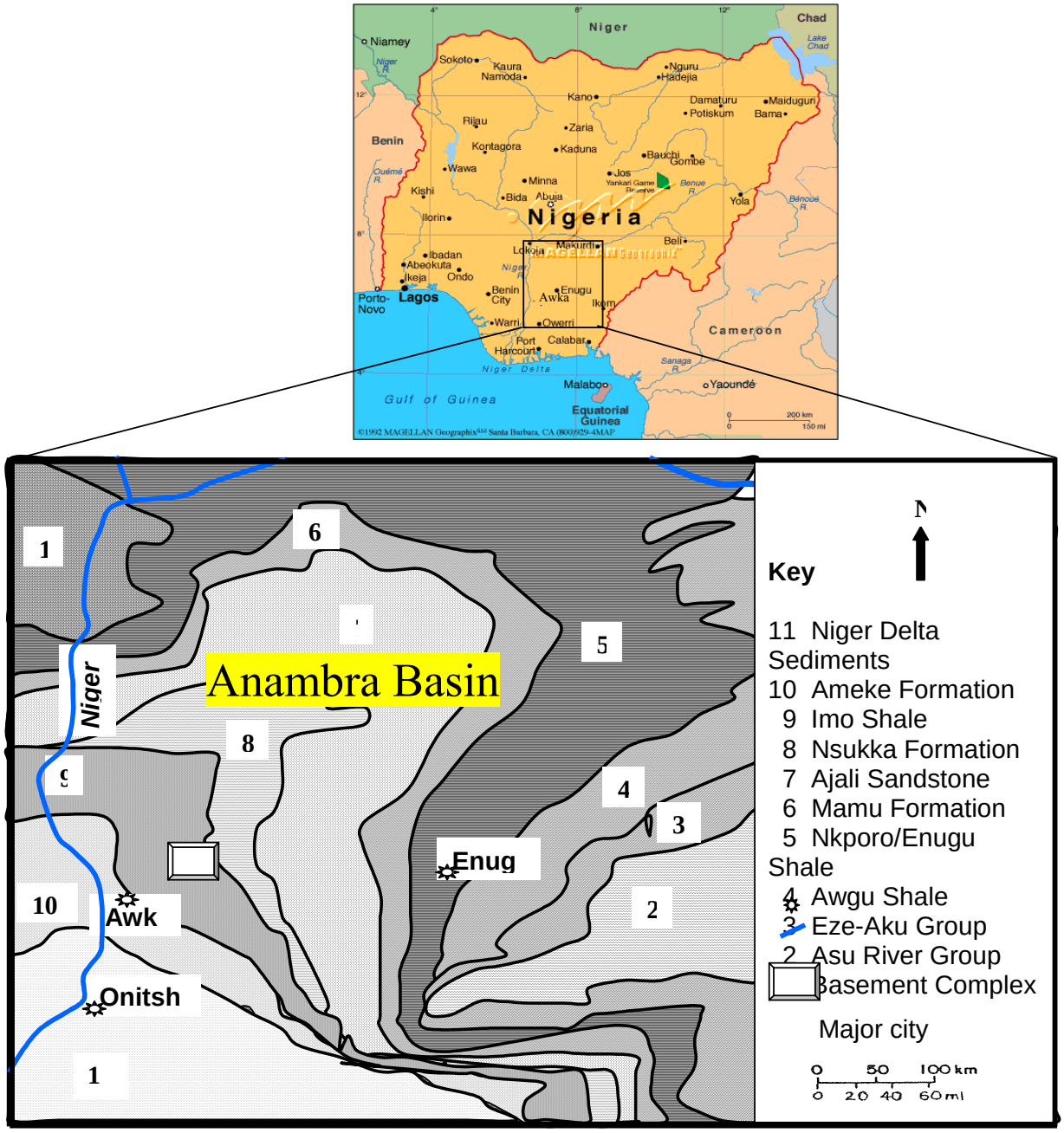

Fig. 1. Geological map of southeastern showing the position of the Anambra Basin and lateral distribution of the Imo Shale (Adapted from Aghamelu *et al*., 2011b).

Settlement and Bearing capacity characteristics

The results are summarized in table 3. Based on the results the site is unsuitable to fairly suitable for most engineering construction. Medium to high plasticity resulting from moderate to high clay content of the soil suggests volumetric changes, especially when waterlogged. The considerably high ρ_{dmax} value and W_{opt} may imply that less moisture would be needed during field compaction on the soil, for use as fills and embankment materials. High soaked CBR values (all significantly about 5%) may be used to rate the subgrade as fair to good; the standard soaked CBR values for filling and embankment material is >5% (Nigerian Federal Ministry of Works and Housing, 1970). It should, however, be noted that the testing depth was limited to 0.8 – 2.0m which is the generally recommended depth for pavement subgrade material assessment. The underlying shale, in addition to other expansive components, is bound to influence the pavement constructed on the site, especially under heavy traffic.

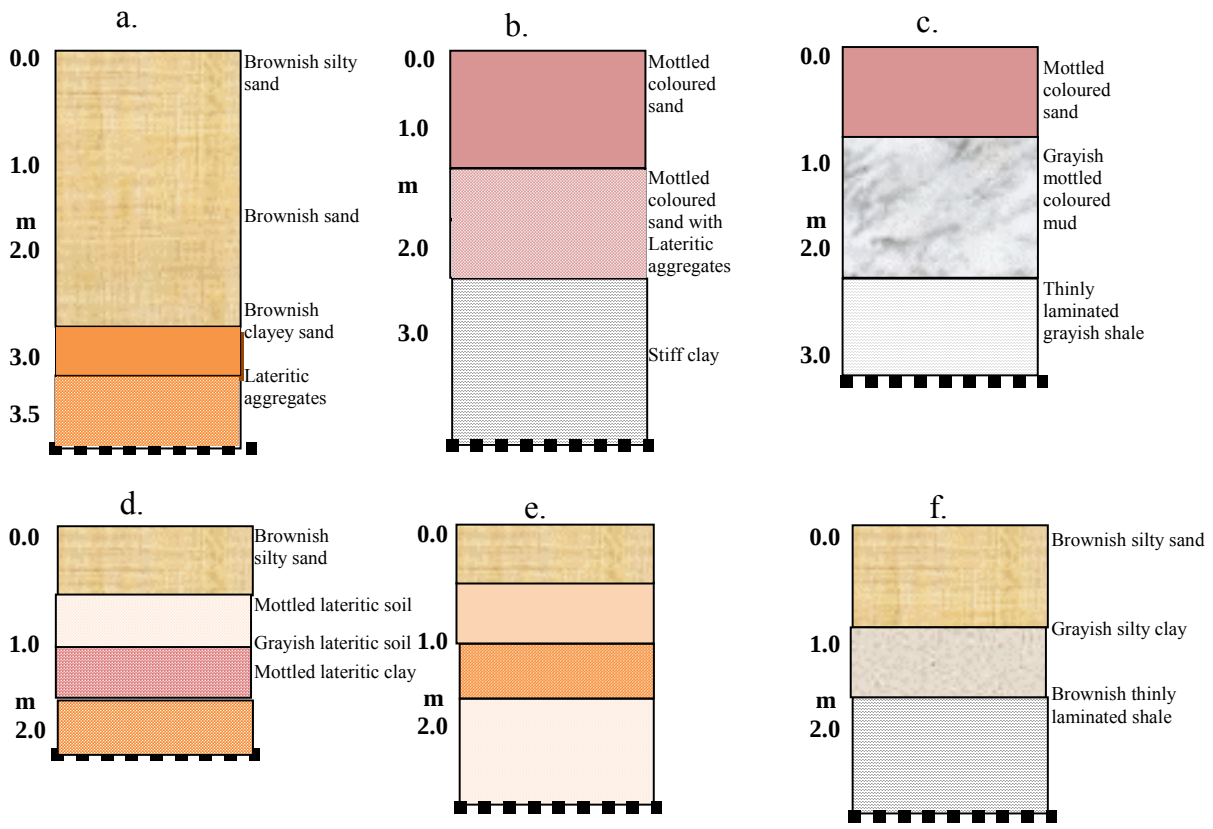

Fig. 2. Soil logs from some of the sampled points [a). Second front gate, b). Chapel of Glory, c). Stadium, d). Fuel Station, e). Science Village and f). Library].

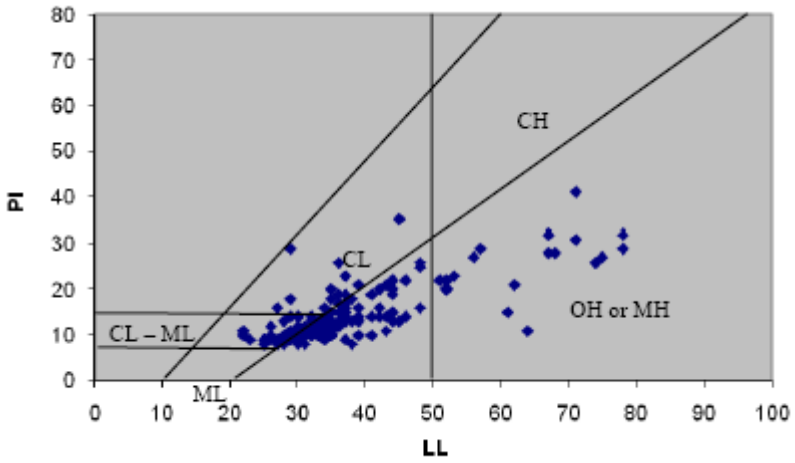

Fig. 3. Plots of the soil samples in the Plasticity Chart.

The wide range of strength parameters (cohesion and angle of shear resistance) shown by the soil samples from the site suggest wide suitability, which may range from moderate to fair bearing capacity as foundation material. However, the bearing capacity and settlement (in particular compressibility) analyses show some locations within the site have low stability; lowest at a point within the Future Expansion reserve, where the ultimate bearing capacity (q_o) is 222 kN/m^2, 291 kN/m^2 and 360 kN/m^2 at the depth ranges of 0 to 0.5m, 1.6 to 2.5m and 2.6 to 3.5m, respectively.

Other locations which recorded low stabilities include Solar Panel Station, Tower in the front of the

Administration block, Law Faculty, proposed Guest House, Stadium, Reserved area, proposed Multipurpose Hall, New Law Faculty, Male Hostel, Faculty of Agriculture, Future expansion reserve, Proposed Students' Hostel and Science Village. Safe bearing capacities of these locations were, as would expect, very low; range from 89 - 1446 kN/m^2. Reasonable stabilities were noted at other locations, especially at the Fire Station. Maximum compression index is 0.51% (at the main library). According to Sowers and Sowers (1970), soils with compression index values that ranged from 0 to 0.19 would have slight or low compressibility, those with compression index values ranging from 0.20 to 0.39 would have moderate or intermediate compressibility, while those with compression index values of 0.40 and above would high compressibility. This suggests that the soil around the main library would experience moderate compressibility and the building projects constructed on it would settle marginally, over an engineering time.

CONCLUSIONS

The field soil geotechnical investigation and soil sample testing program identified the soil underlying the studied site to be primarily shale, with weathered shale, laterite and sandstone to siltstone overburden. The overburden ranges in thickness between 0 and 3.0m. The overburden materials are generally porous and permeable (aquiferous), but infiltration of meteoric (or surface water) is being restricted by the dense, somewhere fissile, underlying shale (most probably the Imo Shale Formation).

The general subsurface stratification, however, was apparent from the subsurface investigation. This was owing to high degree of disturbance associated with the sampling method adopted. Low drillabilty of the underlying shale, which may be misinterpreted to mean high strength as foundation material, and high water table (with respect to mean-sea-level) hampered the sampling depth capacity of the hand auger.

In view of the observed characteristics of the underlying soils on the campus, excavation (i.e., stripping of the soil prior to pavement and building foundation construction) of the expansive top or residual soils should be carried out with conventional earthmoving equipment, especially where they the thin in thickness and also fail to meet a number of requirements for material used as filling and embankment material (see Table 4). The excavated soils can be reused for landscaping purposes at other locations on the campus.

Construction of foundations on different bearing stratums usually increases the risk of differential movements of the foundations. It is therefore recommended that all of the foundations for individual buildings should be founded on the same bearing stratum. The following options are considered appropriate:

- Slab on ground (founded on residual soil or on the unweathered shale bedrock)
- Stiffened raft (founded on residual soil)
- Pad footing (founded on the unweathered shale bedrock)

A stiffened raft option may, however, be the best option as it provides a stiffer foundation solution than a slab on ground but it does not completely eliminate differential movement. Previous study (Aghamelu *et al*., 2011b) has also revealed that the unweathered underlying Imo Shale might be unsuitable as foundation material (see Table 5).

Good drainage should be constructed in other to control runoffs and other surface water bodies, thereby preventing flooding. Slope stability problems may occur where the slope is high. This should be put into consideration while designing the structure in those sloppy areas. Heavy traffic may be restricted where soil investigation indicated materials that would be poor to fair as pavement subgrades.

ACKNOWLEDGEMENTS

The authors acknowledge the Vice-Chancellor of the Nnamdi Azikiwe University, Awka, and Odiche Resources, LTD, Abakaliki, for their permission to publish this work. Dr. P. U. Echiegu of the Department of Geology and Exploration Geophysics, Ebonyi State University, drafted the figures. He is warmly acknowledged. The authors also appreciate the assistance rendered by A. U. Utom of the Department of Geological Sciences, Nnamdi Azikiwe University, Awka, during the data analysis.

REFERENCES

Aghamelu, OP., Odoh, BI. and Ezeh, HN. 2010. A Report on the Soil, Groundwater and Near-surface Geophysical Investigation at the Permanent Site of Nnamdi Azikiwe University, Awka, Anambra State. pp685.

Aghamelu, OP., Odoh, BI. and Ezeh, HN. 2011[a]. Use of Accelerated Procedure to Estimate the Behaviour of Shallow Foundation. International Journal of Basic and Applied Sciences. 11(3):106-116.

Aghamelu, OP., Odoh, BI. and Egboka, BCE. 2011[b]. A Geotechnical investigation on the Structural failures of Building Projects in parts of Awka, Southeastern Nigeria. Indian Journal of Science and Technology. 11. (In press).

American Society for Testing and Materials, ASTM D2487. 1989. Methods of Testing Soils for engineering

purposes. American Society for Testing and Materials. Philadelphia, USA.

American Society for Testing and Materials, ASTM D2488. 1989. Methods of testing soils for engineering purposes. American Society for Testing and Materials. Philadelphia, USA.

British Standard Institution (BSI) 1377. 1990. Methods of testing soils for civil engineering purposes. BS, London.

Bailey, MJ. 1976. Degradation and other parameters related to the use of the shale in compacted embankments. Joint Highway Research Project No. 23, Purdue University and Indiana State Highway Commission. pp209.

Ede, AN. 2010. Building collapse in Nigeria: the trend of casualties in the last decade (2000 -2010). International Journal of Civil & Environmental Engineering. 10(6):32-42.

Lambe, TW. 1951. Soil Testing for Engineers. Wiley, New York, USA. pp165.

Mannering, FL. and Kilareski, NP. 1998. Principles of highway engineering and traffic analysis (2nd ed.), Wiley, New York, USA. pp340.

Nigerian Federal Ministry of Works. 1970. General Specifications (roads and bridge works). Federal Government of Nigeria, Lagos.

Sowers, GB. and Sowers, GE. 1970. Introductory Soil Mechanics and Foundations. Macmillan, New York, USA. pp556.

Wignall, A., Kendrick, PS., Ancill, R. and Capson, M. 1999. Roadwork: Theory and Practice (4th ed.). Butterworth-Heinemann, Oxford. pp309.

Received: Aug 22, 2011; Accepted: Dec 1, 2011

SENRA Academic Publishers, Burnaby, British Columbia
Vol. 6, No. 1, pp. 1847-1853, Feb 2012
Online ISSN: 1920-3853; Print ISSN: 1715-9997

Canadian Journal of pure&applied sciences

PARAMETRIC ANALYSIS OF BEAM RESTING ON ELASTIC FOUNDATION (ANN)

*Mostafa A M Abdeen and S M Bichir
Department of Engineering Mathematics and Physics
Faculty of Engineering, Cairo University, Giza 12211, Egypt

ABSTRACT

Mathematical formulation for Timoshenko beam resting on an elastic foundation is presented. Parametric analysis is presented for three types of boundary conditions. In the current paper, artificial intelligence technique is implemented to simulate and then predict the beam's deflection using one raw of the results from DQM (Differential Quadrature Method) analysis to study the effect of foundation parameter, beam stiffness and applied load on the Timoshenko beam's deflection for the three types of boundary conditions. The ANN (Artificial Neural Network) results presented in the current study showed that the designed ANN models can simulate and predict very accurately the beam's deflection and the effect of different DQM parameters.

Keywords: Timoshenko beam, elastic foundation, analytic formulation, numerical simulation; artificial neural network.

INTRODUCTION

There are many applications for beam on elastic foundation mainly in mechanical and civil engineering e.g. disc brake pad, shafts supported on ball, roller, building and bridges, submerged floating tunnels, buried pipelines, railroad tracks etc. Two simple models have been used to analyze a beam on an elastic foundation. One is the Winkler (1867) foundation model, which is based on a pure bending beam theory. The second is the Pasternak (1954) shear model, which is based on the assumption of pure shearing of the beam (no bending).

Timoshenko (1921, 1956) solved analytically the problems of beams on elastic foundation with several loading and boundary conditions. DQM is a numerical method used for solving many problems in engineering and mathematics (Bert and Malik, 1997).

Artificial intelligence has been widely used to simulate and predict the behavior of the different physical phenomena in most of the engineering fields. Kheireldin (1998) developed ANN model to study the characteristics of sever contractions in open channels. Allam (2005) developed artificial intelligence model to predict the maximum and minimum settlement under building near tunnel construction. Mohamed (2006) developed ANN model to reduce the design time of multi-story steel frames. Abdeen (2008) developed several ANN models to simulate the flow discharges of water surface profile in open channels. Simulation and prediction for the internal properties of different materials, using ANN technique, were very important in many researches as in Abdeen and Hodhod (2010) and Gaafar *et al*. (2011). In the present paper, the parametric analysis of the beam resting on elastic foundation is presented. The ANN technique is used to understand, simulate and predict the beam's deflection for three different end conditions.

Formulation of the Problem

Figure (1) shows the beam model resting on elastic foundation with modulus K_s.

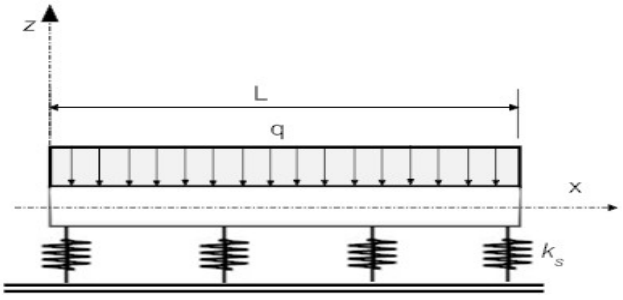

Fig. 1. Proposed Beam Model.

The beam's material is assumed to be homogeneous with elasticity modulus E and shear modulus G. The cross section area and bending stiffness are A and D respectively. The Timoshenko effect constant $C = KGA$
Where: K is the Timoshenko effect.

The equilibrium differential equation for the lateral deflection w can be written as:

$$D\frac{\partial^4(w)}{\partial x^4} - \frac{k_s D}{C}\frac{\partial^2(w)}{\partial x^2} + k_s(w) = q - \frac{D}{C}\frac{\partial^2(q)}{\partial x^2} \qquad (1)$$

Where:
$D = Eh^3/12(1-\nu^2)$

*Corresponding author email: Mostafa_a_m_abdeen@hotmail.com

Equation (1) is the general equilibrium equation of the beam resting on elastic foundation. By using the DQM the governing differential equation (1) will be in the following form:

$$\sum_{j=1}^{N} a_{ij}^{(4)} w_j - \frac{k_s}{C}\sum_{j=1}^{N} a_{ij}^{(2)} w_j + \frac{k_s}{D} w_i = \frac{q_i}{D} - \frac{q_i''}{C} \qquad (2)$$

Where:

N is the number of node points and

a_{ij} is weighting coefficients.

Boundary Conditions

Simply Supported (SS)

Boundary conditions are: $w = 0$ at $x = 0, L$,

$w'' = 0$ at $x = 0, L$

or, in the DQ discrete domain:

$$\begin{cases} w_i = 0 & \text{at } i = 1, N \\ \sum_{j=1}^{N} a_{ij}^{(2)} w_j = 0 & \text{at } i = 1, N \end{cases}$$

Clamped-Clamped (CC)

Boundary conditions are: $w = 0$ at $x = 0, L$,

$w' = 0$ at $x = 0, L$

or, in the DQ discrete domain:

$$\begin{cases} w_i = 0 & \text{at } i = 1, N \\ \sum_{j=1}^{N} a_{ij}^{(1)} w_j = 0 & \text{at } i = 1, N \end{cases}$$

Clamped-Free (CF)

Boundary conditions are: $w = 0$ at $x = 0$

$w' = 0$ at $x = 0$

$w'' = 0$ at $x = L$

$w''' = 0$ at $x = L$

or, in the DQ discrete domain:

$$\begin{cases} w_1 = 0, & \sum_{j=1}^{N} a_{1,j}^{(1)} w_j = 0 \\ \sum_{j=1}^{N} a_{N,j}^{(2)} w_j = 0, & \sum_{j=1}^{N} a_{N,j}^{(3)} w_j = 0 \end{cases}$$

Numerical Models

Artificial Neural Network (ANN) is a numerical model depends on a certain number of neurons in different layers. Every neuron acts very closely to the real neuron of the human brain. Each layer has a different function than the others. The input layer with its neurons gets the information from the external world (given data), while the hidden layers are working as detectors of these data. The output layer is the final layer of the network and it produces the required results. Neuralyst software, Shin (1994) is used to design the ANN models in the present work.

Simulation Cases

To fully investigate the effect of foundation parameter, bending stiffness and applied load on the beam's response (deflection) for the three types of boundary conditions, three numerical boundary condition models, using ANN technique, are designed in this study. The developed simulation models used one solution output obtained from DQM to design the ANN models.

Numerical Models Design

To design ANN models to simulate and predict the beam's deflection, the input and output variables have to be determined. Table 1 shows the three neural network boundary condition models (SS, CC, CF).

Table 1. Key Input and Output Variables for Neural Network Models.

Boundary Condition Model	Input Variables				Output
SS	Beam's Span x (m)	K_s (N/m^3)	D (N.m)	q (Pa)	Deflection w(m)
CC					
CF					

Several ANN models are tested for all numerical models to finally choose the best networks design to simulate, very accurately, the effect of foundation parameter, bending stiffness and applied load on beam's deflection based on minimizing the Root Mean Square Error (RMS-Error).

The training procedure for the developed ANN models, in the current study, uses one raw of the data from the results of the DQM to let the ANN understands the behavior. After sitting finally the NN models, these models are used to predict the beam's deflection for different values of K_s , D and q and others.

Table 2 presents the final design of the developed ANN models for the three boundary conditions. The structure of the three models is chosen to be the same but the difference between them will be in RMS-Error and the number of trials to achieve accepted accuracy represented by maximum percentage relative error.

Table 2. The Designed ANN Models.

Boundary Condition Model	No. of layers	No. of Neurons in each layer			
		Input Layer	First Hidden	Second Hidden	Output Layer
SS	4	4	8	6	1
CC					
CF					

The parameters of the designed ANN models are presented in table 3, where:

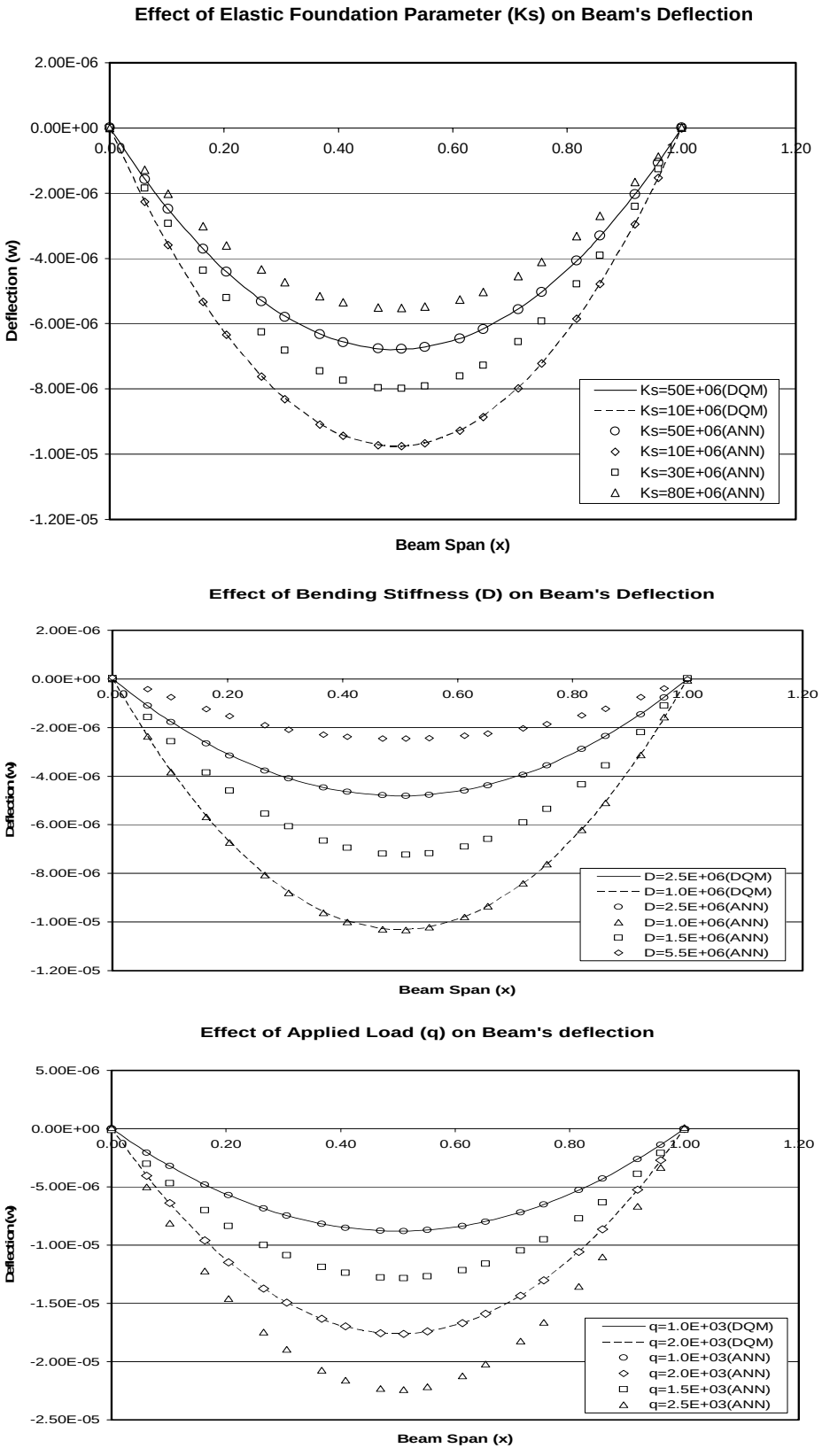

Fig. 2. Simple Supported Edged Beam's Deflection.

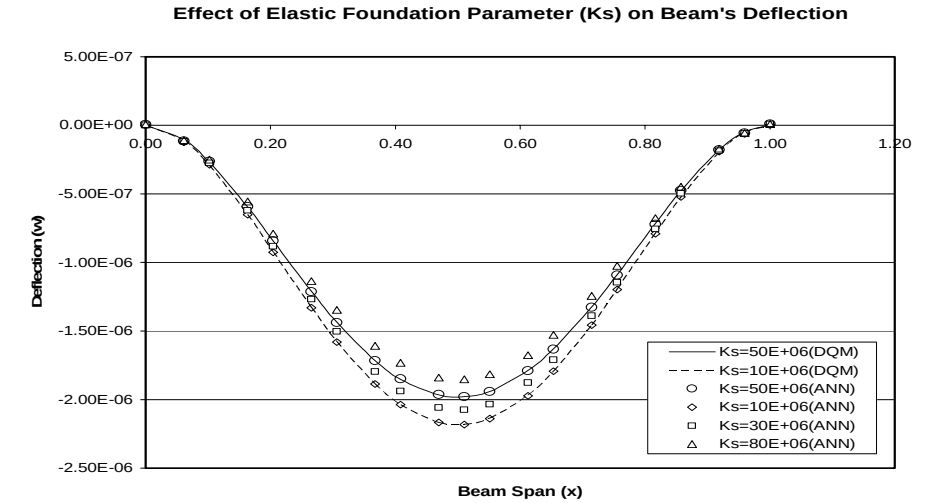

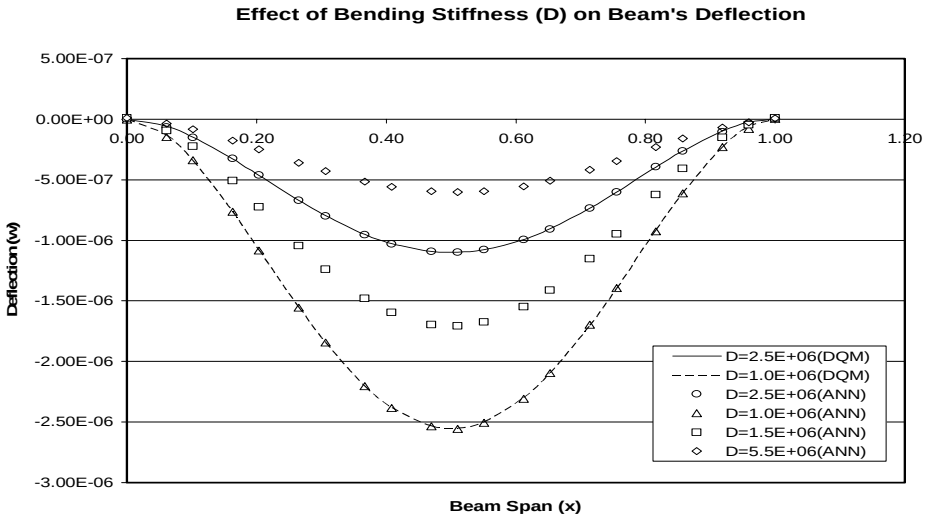

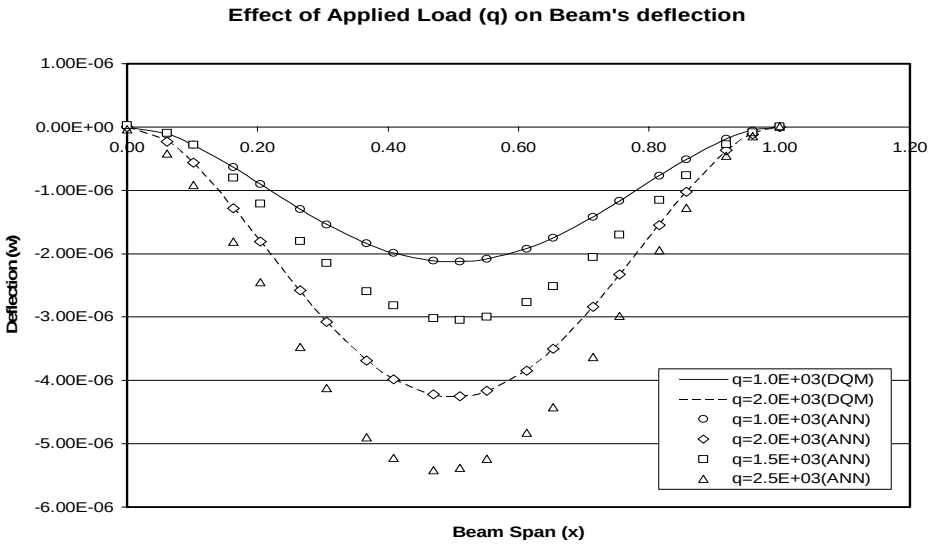

Fig. 3. Clamped-Clamped Edged Beam's Deflection.

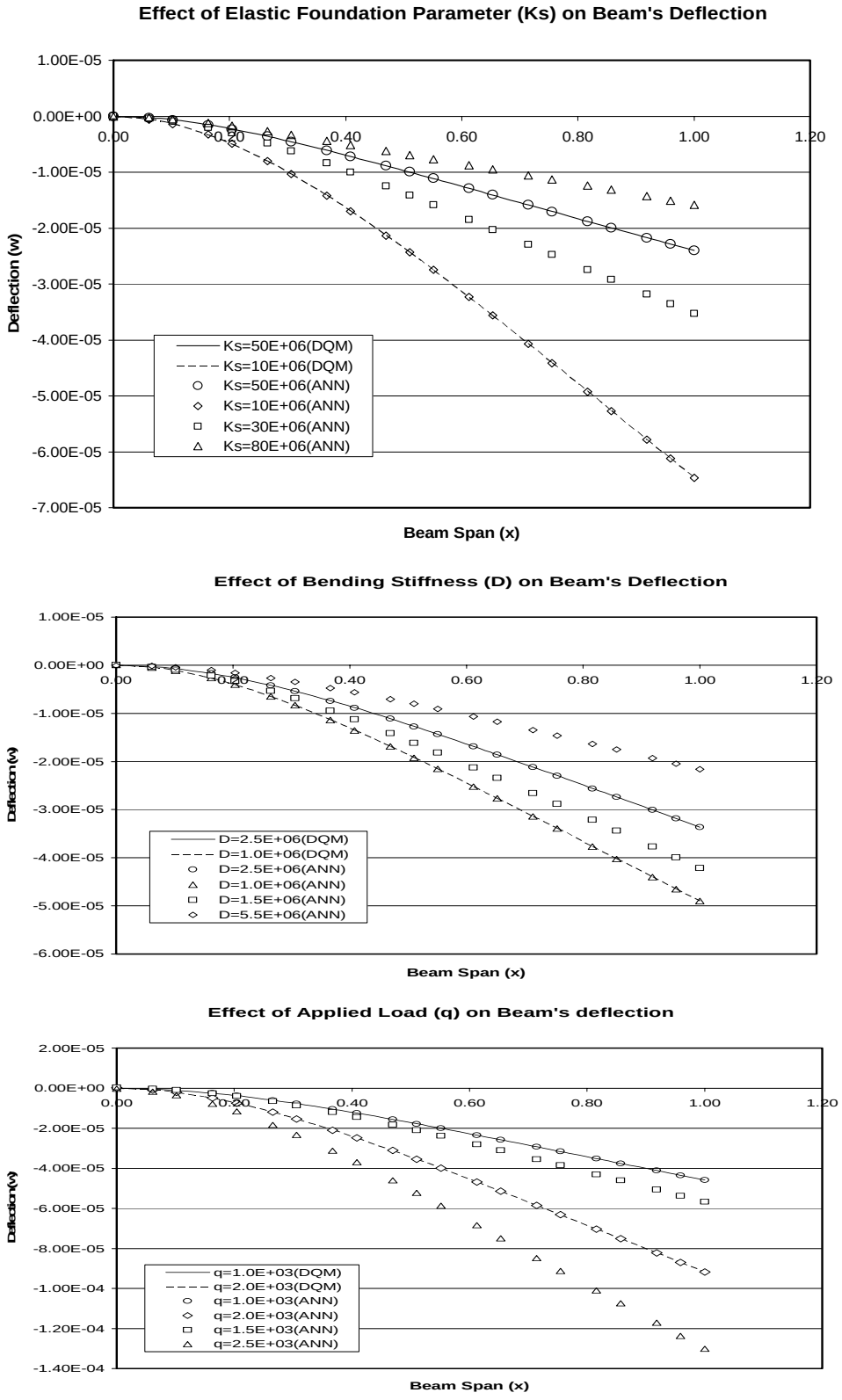

Fig. 4. Clamped-Free Edged Beam's Deflection.

Training Epochs: Number of trails to achieve the present accuracy.

Percentage Relative Error (PRR): Percentage relative error between the numerical results and actual measured value for and is computed according to equation (6) as follows:

PRE = (Absolute Value (ANN_PR - AMV)/AMV)*100

Where :

ANN_PR : Predicted results using the developed ANN model

AMV : Actual Measured Value

MPRE: Maximum percentage relative error during the model results for the training step (%)

Table 3. Parameters used in the Artificial Neural Network Models.

Simulation Parameter	SS	CC	CF
Training Epochs	558516	685412	473258
MPRE	0.65	0.88	0.45
RMS-Error	0.0007	0.0008	0.0004

(SS-Simply Supported, CC- Clamped-Clamped, CF-Clamped-Free)

RESULTS AND DISCUSSION

Numerical results using ANN technique will be presented in this section for the three neural network boundary condition models (SS, CC and CF) to show the simulation and prediction powers of ANN technique studying the effect of elastic foundation parameter, bending stiffness and applied load on beam's deflection. Figures 2-4 shows the ANN results (symbols) and DQ results (line and dash) for the three boundary condition models. It is very clear, from these figures, that the developed neural network models can simulate and predict the beam's deflection for any variation of foundation parameter, bending stiffness and applied load very accurately.

For all of the case studies, the default values used before varying each parameter are:

k_s = 20e6 N/m^3, C = 26.667e6 N/m, D = 1.2e6 N.m, N = 13, q = 1e3 Pa (uniformly distributed load).

From the parametric studies conducted in the present work, it could be noticed that, by increasing the elastic foundation parameter and bending stiffness the deflection decreases, while by increasing the applied load the deflection increases.

CONCLUSION

Based on the output results of the developed ANN models in this study, the following can be concluded:

1. The developed ANN boundary condition models are very smarting in understanding the effect of elastic foundation parameter, bending stiffness and applied load on the beam's deflection.
2. The designed ANN models can successfully capable of direct predicting the response behavior of beam resting on an elastic foundation for different parameters and boundary conditions.
3. Using single set of output results from DQM, The ANN models succeeded to understand the behavior of beam on elastic foundation and became ready to give the beam's response for different parameters without solving such kind of problem again.

REFERENCES

Abdeen, MAM. 2008. Predicting the Impact of Vegetations in Open Channels with Different Distributaries' Operation on Water Surface Profile using Artificial Neural Networks. Journal of Mechanical Science and Technology. KSME Int. J. Korea. 22. 1830-1842.

Abdeen, MAM. and Hodhod, H. 2010. Experimental Investigation and Development of Artificial Neural Network Model for the Properties of Locally Produced Light Weight Aggregate Concrete. Scientific Research Organization, Engineering. 2. (6):408-419.

Allam, BSM. 2005. Artificial Intelligence Based Predictions of Precautionary Measures for Building Adjacent to Tunnel Rout during Tunneling Process. Ph.D. thesis, Faculty of Engineering, Cairo University, Egypt.

Bert, CW. and Malik, M. 1997. Differential Quadrature: A Powerful New Technique for Analysis of Composite Structures. Composite Structures. 39:179-189.

Gaafar, MS., Abdeen, MAM. and Marzouk, SY. 2011. Structure Investigation and Simulation of Acoustic Properties of Some Tellurite Glasses using Artificial Intelligence Technique. Journal of Alloys and Compounds. Elsevier. 509:3566-3575.

Kheireldin, KA. 1998. Neural Network Application for Modeling Hydaulic Characteristics of Sever Contraction. Proceeding of the 3rd Int. Conference, Hydroinformatics, Copenhagen, Denmark. 41-48.

Mohamed, MAM. 2006. Selection of Optimum Lateral Load-Resisting System using Artificial Neural Networks. M. Sc. Thesis, Faculty of Engineering, Cairo University, Egypt.

Pasternak, PL. 1954. On a New Method of Analysis of an Elastic Foundation by means of Two Foundation Constants, Moscow.

Shin, Y. 1994. Neuralyst™ User's Guide. Neural Network Technology for Microsoft Excel. Cheshire Engineering Corporation Publisher.

Timoshenko, SP. 1921. On the Correction for Shear of the Differential Equation for Transverse Vibration of Prismatic Bars. Philosophical Magazine. 41. 744.

Timoshenko, SP. 1956. Strength of Materials. Part II. Third ed. Princeton, NJ: Van Nostrand.

Winkler, E. 1867. On Elasticity and Fixity. Pragus.

Pasternak, PL. 1954. On a New Method of Analysis of an Elastic Foundation by means of Two Foundation Constants, Moscow.

Received: May 20, 2011; Revised and Accepted: Oct 13, 2011

SENRA Academic Publishers, Burnaby, British Columbia
Vol. 6, No. 1, pp. 1855-1862, Feb 2012
Online ISSN: 1920-3853; Print ISSN: 1715-9997

Canadian Journal of pure&applied sciences

EVALUATION OF THE TEMPERATURE EFFECT OF A THERMOSYPHON SOLAR WATER HEATER

*Aasa, SA and Ajayi, O O
Department of Mechanical Engineering, Covenant University
P.M.B 1023 Ota, Ogun state, Nigeria

ABSTRACT

This study investigated the effect of system temperature on the performance of thermosyphon solar water heater. Solar collector was designed and developed with galvanized steel, wood and copper pipes for the experiment. While the copper pipes serves as the tube through which the cold water flows, the wood was employed for the frame and stand, and the galvanized steel for the collector material. Also employed were two hot and cold water tanks of 60 and 110 litre capacities respectively. The period of experiment were taken to be 3 days each for sunshine, sun-off and moderate sunshine days, with the average data employed for the analysis. The results showed that temperature has a domineering effect on the performance of the thermosyphon system. The maximum outlet temperature obtained for sunshine, moderate sunshine and sun-off days were 94.6, 73.5 and 51^{o}C respectively. Also the system efficiency was found to be 61.04%, demonstrating good performance. However, considering the fact that the experiment was carried out in rainy season (between April and September), it was concluded that if it is repeated during the dry periods (October to March), the efficiency of performance will be more as these period is characterized by low cloud cover, high temperature and high radiation intensities. The outcome of the study was compared with published results and it clearly demonstrates that the designed system can suitably be employed for both domestic and industrial uses.

Keywords: Thermosyphon, solar water heater, flat plate collector, system temperatures.

INTRODUCTION

Globally, water heating dominates energy needs of household, and in developing countries it is the most intensive and therefore the most expensive (Beckman and Duffie, 1991). The intensity of energy demand in developing countries has been identified as one of the principal contributors to deforestation (Rasheed, 1995). These energy options are however unsustainable, costly, depleting and contributes to build-up of green house gases in the atmosphere. With the rural communities faced with limited fuel and intermittent electricity supplies, ability to access hot water for hygiene and domestics uses become restricted. More so, in terms of energy consumptions water heating is second only to space heating and air conditioning in most developed nations. Making it very important to find alternative ways by which the process can be achieved without necessarily burdening the environment. Such process must however be affordable to rural communities. The sources of the energy must be easily accessible, naturally applicable, enormously available, non toxic and providing valuable and usable energy (Agbo and Oparaku, 2006).

One potential option is the use of solar water heating technology. This technology is employed in many parts of the world for a wide range of used patterns and climatic conditions. Today engineer and scientist can harness solar energy with common materials and basic technology. Globally, the application of solar water heating began early twentieth century. Thermosyphon solar water heater is the oldest type of water heating system and has been in used since 1920 in Israel and United State of America. With availability of resources, it is pertinent that sustainable alternatives are highly imperative and its prospect is bright (Agbo *et al*., 2005).

Thermosyphon solar water heater is a passive system in which the flow of working fluid occurs by natural circulations. As the working fluid in the collector is heated up, its density changes and becomes less dense, rising up naturally to the header pipe through the riser tubes. This is an advantage as hot water could be made available all year round. The complete design of Thermosyphon solar water heater involves system design, optimization and integration with the existing heating system. Detail design involves accurate information about ambient condition, which is a complex process (Agbo, 2006). Moreover, various studies have been carried out on thermosyphon system's performance. Some of these studies include a proposed modified efficiency for thermosyphon solar heating systems achieved by modifications of CNS 12557 B7276 test standard. It employed a precise, on-line operation to derive the heat

*Corresponding author email: samson.aasa@covenantuniversity.edu.ng

removal efficiency of the system (Chang *et al.*, 2004). Another involved the performance of a closed coupled thermosyphon system which employed a vertical baffle and cross plumbing to divide the water tank into two sections (Morrison, 1986). More on this was the evaluation of the effect of hot water withdrawal rate which was based on gross analysis of simulated hot water temperature (Agbo, 2006). Some other studies involved the performance estimation of a thermosyphon water heater, to assess the level of its prospect under various weather conditions (Agbo and Unachukwu, 2006). Also, a study which dwelt on the performance evaluation of solar operated thermosyphon hot water system was analysed based on its numerical and experimental results (Adegoke and Bolaji, 2000). All of these studies have basically dwelt on estimating the system's performance which was to evaluate the values of density, pressure or temperature. The deductions of effectiveness were then based on the relative values of these parameters. However, none of the studies have been able to determine and explain the actual individual effects of the parameters on the system's performance. It is worthy of note also, that of the three parameters, temperature is the most important and the domineering parameter. The knowledge of the value and effect of temperature on the system can lead to the evaluation of the values of density and pressure and by extension their effects. This study is therefore used to focus on determining the exact effect of system temperature on the performance of a thermosyphon water heater using the average experimental data obtained and also evaluate the magnitude of the pressure and density and their effects using the establish expression derive from this study with further formulation of correlation relationship between temperature, density and pressure of the system.

MATERIALS AND METHODS

In order to carry out the study, the thermosyphon solar water heater was first designed and constructed. The materials employed for the construction were mild steel, galvanized steel and wood. The mild steel was employed for the construction of the outer part of the hot water tank and the support stand of the cold water tank. Also, galvanized steel was used for the construction of the inner part of the hot water tank, cold water tank and the flat plate collector. The inner part of the hot water tank was lagged with fibre glass. The solar collector was supported with the aid of a wooden stand. Figure 1 presents the engineering drawing of the thermosyphon system while figure 2 presents the exploded view of the solar collector.

The system design was carried out based on already established principle for thermosyphon system (Fairbairn and Mario, 1999).

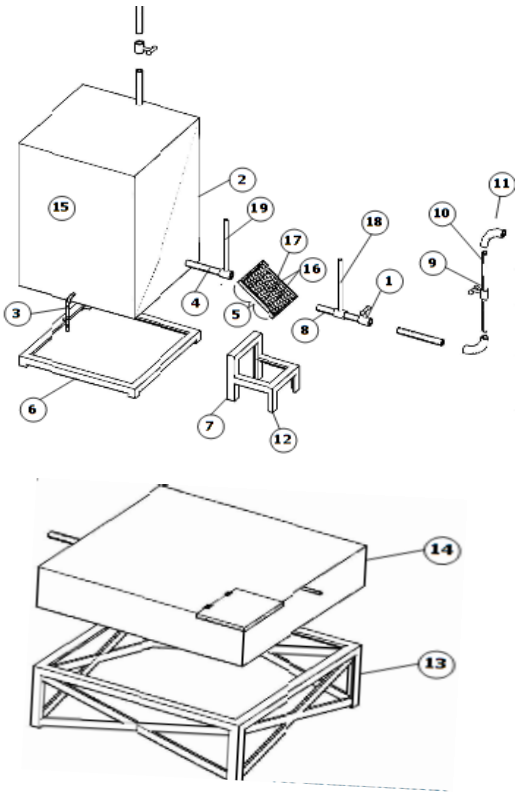

Fig. 1. Thermosyphon Solar Water Heater.

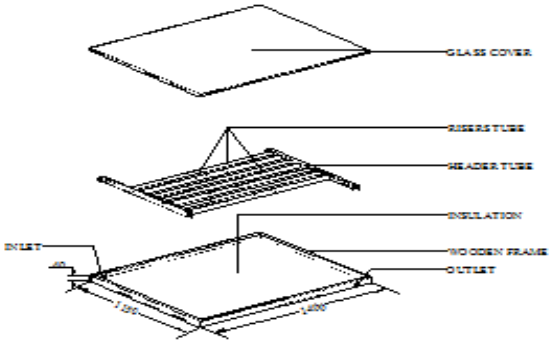

Fig. 2. Collector System.

This involved first and foremost the determination of the thermosyphon head, using Eq. 1 (Agbo and Unachukwu, 2006), in order to determine the exact height of the cold water tank above ground.

$$H_t = [\rho_o gH - \rho_i gdl] / \rho' g \quad (1)$$

Where:
H_t = Thermosyphon head
dl = length of the developing flow
H = height of tank to the collector
ρ_o = density of water at outlet of the collector
g = Acceration due to gravity
ρ_i = Density of water at the inlet of collector
ρ' = average density of the water in the system

The thermosyphon head generated was used to overcome the resistance in the circulations loop.

Heating load

The heating load refers to the quantity of water that will be required per person in a building. For this study however, the heating load was based on monthly water utilization of a family of seven people (N_p) living together in a building over a range of 30 days.

This is evaluated from Eq. 2 (Mani and Rangarajan, 2005).

$$L = N_d N_p V_p \rho C (T_m - T_a) \quad 2$$

where:
L = load required
N_d = number of days
N_p = Number of people
V_p = Volume of water required per person
ρ = density of water at required temperature
c = specific capacity of water
T_m = mean system temperature
T_a = Ambient temperature of water.

Solar collector area (A)

The area of the solar collector was evaluated using Eq. 3 (Sambo and Bello, 1992)

$$A = \frac{L}{\eta \times I} \quad 3$$

where:
η = system's efficiency
I = global solar radiation

However, the thermosyphon system's efficiency (or performance) is determined from (Agbo, 2006).

$$\eta = \frac{A F_R[Io(\alpha\tau)_e - U_L(T_m - T_a)}{A I} \quad 4$$

Where:
A = collector Area
F_R = heat removal factor
I_o= Global Solar radiation
$\alpha\tau$ = Absorbance transmittance product

Moreover, with the knowledge that A, F_R and U_L are constants; Eq. 4 can be directly expressed as:

$$\eta_c \alpha \frac{(T_m - T_i)}{I} \quad 5$$

Thus from Eq. 5 it can be deduced that the performance of the thermosyphon system is directly related to the ratio of the difference in the output and input temperatures to the global solar radiation.

Tube spacing

The spacing in between two consecutive tubes bearing water to be heated is determined using (Agbo and Okeke, 2007).

$$\omega = \frac{A}{n\tau} \quad 5$$

where:
ω = tube spaing
n = number of tubes
τ = length of the collector tube

Overall heat loss from the system

The design of the system was carried out such that, its overall heat loss was very minimal. Moreover, heat losses through the system usually occur from three faces – top (side facing the sun), edge (sides of the collector) and the bottom (end view of the collector). The overall loss is related by Eq. 6 (Agbo and Unachukwu, 2006).

$$U_L = U_T + U_b + U_s \quad 6$$

where:

U_L= Overall loss coefficient,

U_T = Top loss coefficient

U_e = edge loss coefficient, U_b= Bottom loss coefficient

and $U_T = \left[\frac{N_G}{\frac{c\{(Tm - Ti)\}}{Tm(N_G + f)}} + \frac{1}{h_W}\right]^{-1} + \frac{\sigma(T_m - T_i)(T_m^2 - T_i^2)}{\varepsilon_p + 0.0059(N_G h_W)^{-1} + \frac{2N_G + f - 1 + 0.133\varepsilon_p}{\varepsilon_g} - N_G}$ 7

Where: c,e,f, are constant expressed as:

f = $(1 + 0.0898h_wC_p)(1 + 0.007866N_G)$

c = $520(1 - 0.000051\beta^2)$ for $0^o \le \beta \le 70^o$, for $70^o \le \beta \le 90^o$ use 70^o

e = $0.43\left(1 - \frac{100}{T_m}\right)$

N_G = Number of glass cover

h_W = Water heat transfer coefficient

σ = Stefan Boltzman constant

ε_p = Plate emittance

ε_g = Glass emittance

It should be noted that for a natural circulation, the edge loss coefficient is negligible which made overall coefficient U_L to be

$$U_L = U_T + U_b \quad 8$$

Also, using the relation in [8] the density of the system can be easily determined and by extension the pressure of the system is determined. The equations are expressed below in Eqs.9 and 10. However, no model evaluates the pressure of a thermosyphon system from its temperature.

$$\rho(T) = -0.00000405T^2 - 0.00003906T + 1.0002556 \quad 9$$

Where;

ρ = density

T = Temperature (^{o}C)

and pressure is expressed as

$P = (\rho_{in} - \rho_{out})gH_{z}$

Where;

P = Pressure 10

After complete design, construction and installation of the studied Thermosyphon system, the experiment was conducted by taking the inlet and outlet water temperature at an interval of one hour. There was no appreciable temperature difference for about an hour, because the radiation is yet to be effectively absorbed by the system. The experiment was conducted for 3 sun-off, 3 sunny and 3 moderate sunshine days. On sun-off days when the cloud overshadowed the days, the radiation took time before its effect was felt. In all the periods of the experiment it was observed that the system temperatures increased until a maximum temperature was reached, and this occurred between the same ranges of time. The behaviour and general system performance for the days of the experiment are presented using figures 1 to 5.

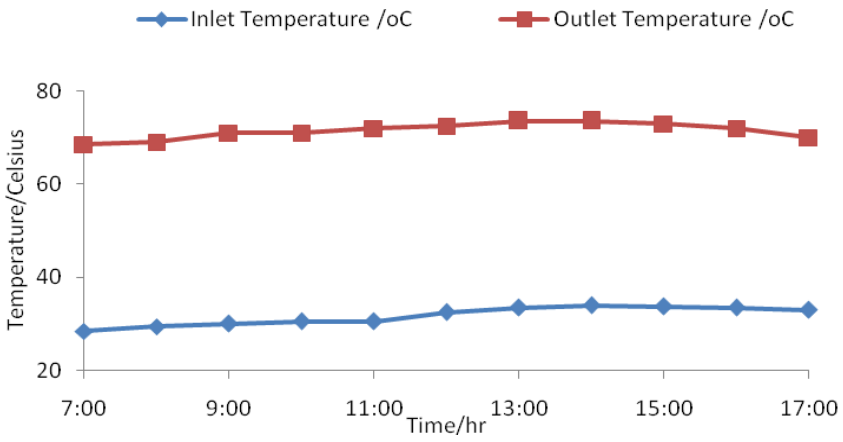

Fig. 3. Plot of Temperature against Time during Moderate Sunshine Day.

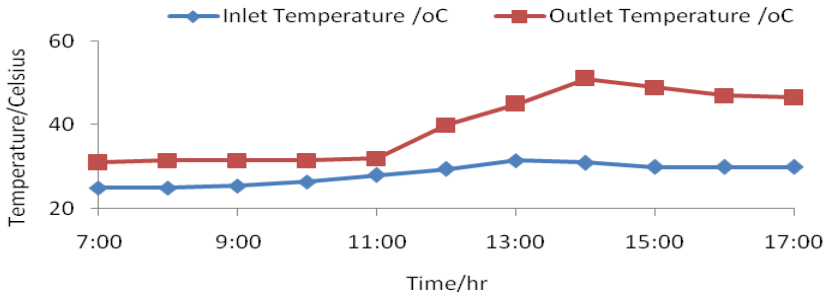

Fig. 4. Plot of Temperature against Time during sun off Day.

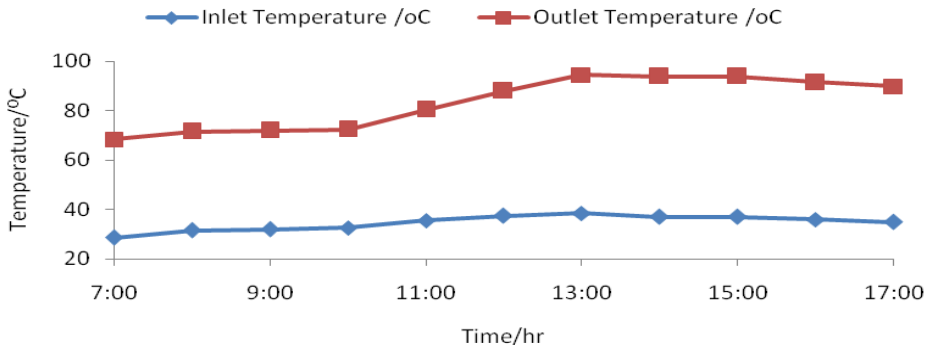

Fig. 5. Plot of Temperature and Time during Sun up day.

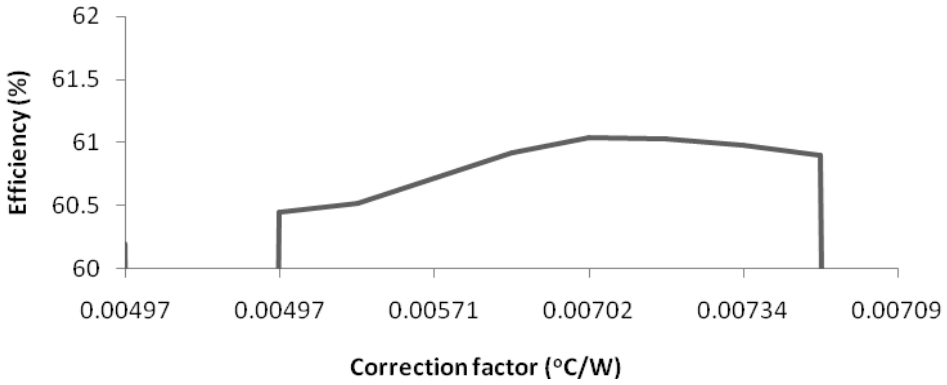

Fig. 6. Performance of Solar Collector.

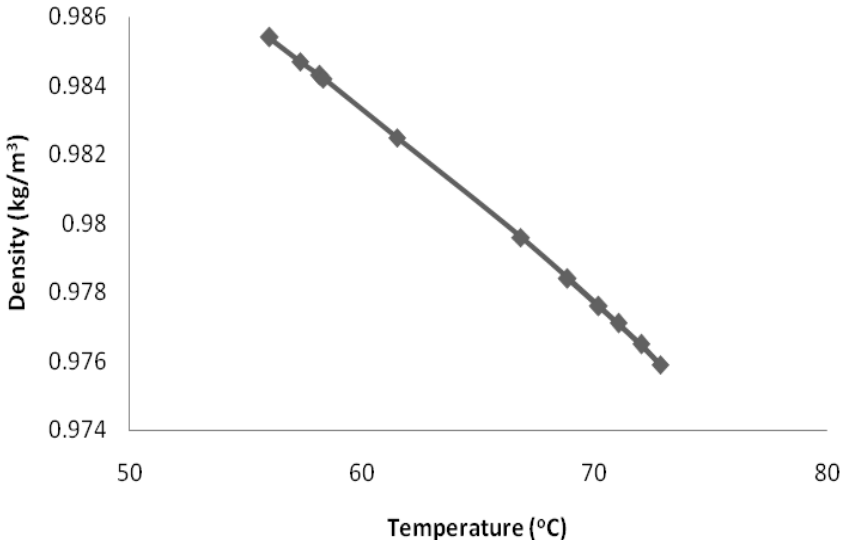

Fig.7. Plot of Density-Temperature Variations.

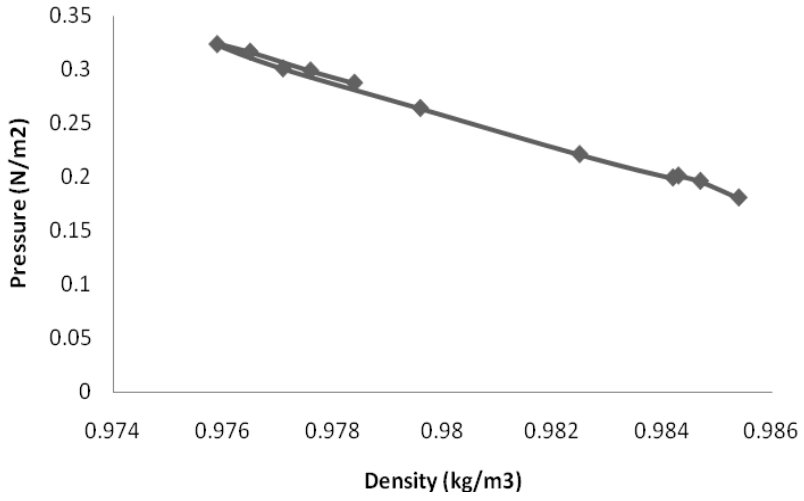

Fig. 8. Plot of Pressure-density Variation.

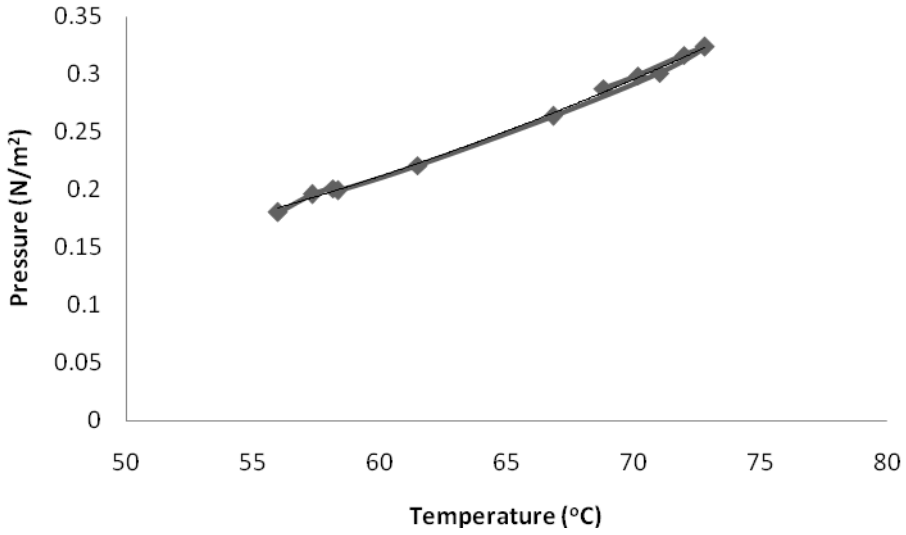

Fig. 9. Plot showing the relationship between pressure and temperature of the thermosyphon system.

RESULTS AND DISCUSSION

Figure 3 shows that the average hourly variations of the system temperature for moderate sunshine days gave a maximum system temperature of 73.50°C. This according to (Fairbairn and Mario, 1999) is effective for most domestic and probably industrial needs where low pressure is required. Figure 4 however, indicates that average maximum system temperature was reached between 1.00 pm to 3.00 pm for sun off days. The maximum average value for the period gave 51°C. This value is within the range reported to be effective for use as bathing, washing and sometimes for steaming purposes according to (Fairbairn and Mario, 1999).

Figure 5 on the other hand, indicates the operations of the system for sunny days. This gave the highest system performance because of high radiation intensity and its rate of absorptions, judged by the high temperature readings throughout the experiment period. Comparing the system performance between the sunny, sun-off and moderate sunshine days, it could be seen that maximum temperatures occurred during the same period, between 1.00 pm and 3.00 pm. However, due to low radiation for sun off days, the rates of absorption were low. This consequently affected the system's water temperature. While in the sunny days, the rates of absorption were high and consequently the water temperatures were high (up to 94.6°C). The performance for moderate sunshine days were found to lie between those of the sun-off and sunny days. These results show that the performance of a Thermosyphon Solar Water Heater is affected by the system temperature. Worthy of note is the fact that, when the maximum water temperature of 94.5°C for sunny days was achieved, the inlet temperature was 38.5°C. The difference in temperature of 56°C is the impact of the system on the inlet water. Moreover, (Fairbairn and Mario, 1999) reported that, a system which can add temperatures between 50°C-60°C is adjudged to be effective. Based on this, the thermosyphon water heating system of this study was found to be effective.

In order to determine the efficiency of the developed thermosyphon system, Eqs.4 and 5 were employed and the result gave in figure 6. Here figure 6 shows that the highest efficiency of 61.04 % was obtained and this demonstrates good performance. More important to this study is the period of the experiment, which was in June (a month within the rainy season in Nigeria). During this period, there is always low radiation intensity, high cloud cover leading to more scattering of global solar radiation. The efficiency is expected to be higher in the dry season (October to March) when temperature is always high and very low cloud cover.

Furthermore, it was discovered that the efficiency increased with time up to 3:00 pm after which it dropped to lowest 60.81%. The decrease in performance was caused by the effect of its loss factor, $[U_L(Tm-Ti)]$, which occurred as outlet temperature reduces. However this may be improved upon by better material selection. The effects of system temperature and ambient parameters showed clearly the direct variation with hourly efficiency. This was also confirmed by (Agbo *et al*., 2005).

Moreover, the knowledge of the values of the system temperature can aid in the knowledge of the other system parameters of density and pressure and by extension their relative effects. Figures 5 to 7 give the relative values of the system's parameters. However, figures 5-6 reveal

inverse relationship between density and temperature as well as between pressure and density. Figures 7 shows that while the temperature increased from 56 to 72.8°C, the density varied marginally from 0.99 to 0.98 kg/m^3. Thus showing that, temperature changes have a marginal effect on the density variation of water in the thermosyphon system. Further to this, Fig. 8 shows the variation between pressure of the system and density of the water. This reveals that a minimal increase of density from 0.98 to 0.99 kg/m^3 led to a decrease of 0.14 Pa (from 0.32 to 0.18 Pa). This invariably showed that while temperature greatly affects the pressure of the system, the density is marginally affected.

Therefore, finding the relationship between pressure and temperature buildup in the thermosyphon system (Fig. 9). Figure 9 clearly demonstrates a quadratic relationship between the parameters. Thus, a regression analysis of pressure of the thermosyphon system against its temperature buildup gave Eq. 11. The standard error is small enough to make the model as fitted acceptable.

$$P(T) = 0.0001T^2 - 0.006T + 0.1738$$

(R^2-value = 0.998, e = 0.003) 11

where:
R^2 = coefficient of determination
e = standard error

Eq. 11 thus is a model explanation of the inter-relationship between pressure and temperature in a thermosyphon system. The R^2 statistics reveal that the model as fitted explains 99.8% of variability in pressure, at 95% confidence level, as it depends on the system's temperature.

Correlating the three parameters to determine the exact cumulative effect of temperature and pressure on density gave Eq. 12.

$$\rho = 1.0118 - 0.0004T - 0.0177P$$

(R^2 = 99.97%, e = 7.53 x 10^{-5}) 12

Therefore, Eqs 11 and 12 can be employed to determine the parameters of the thermosyphon system without necessarily the need of a repeated experiment.

CONCLUSION

The study has been used to evaluate the relative effect of temperature on a thermosyphon solar water heater. It established that a thermosyphon system performs adequately with optimum efficiency and temperature of 61.04% and 94.5°C respectively. Also comparing results with the previous studies, a more accurate and higher temperature was achieved. This is because the data were evaluated based on the average values of the various days considered instead of on a one day experimental period. The temperature of 51°C was obtained during peak period of sun-off day. This simply shows that usable hot water could be made available all year round and that a higher system temperature has been achieved compared with the previous experiments. This study has therefore been used to determine the exact effect of system temperature on the performance of a thermosyphon water heater. The study was also able to evaluate the relative effects of pressure and density as they depend on the system's temperature. Further to this, the study developed new models that correlate temperature and pressure and also temperature, pressure and density.

Table1. List of component parts according to the labelling of figure 1.

Key	Name	Qty	Materials
1	By pass valves	3	Brass
2	Hot water tank	1	Galvanise steel
3	Hot water pipe	1	Galvanise steel
4	Collector assembly	1	Glass, wood, collctor
5	Support stands	1	Mild steel
6	Inlet pipe	1	Galvanised steel
7	Non returned valves	1	Brass
8	Pipe line	1	Galvanise steel
9	Elbow joint	4	Galvanise steel
10	Collector support	1	Wood
11	Cold water tank	1	Galvanise steel
12	Riser pipe	7	copper
13	Tank supports	1	Mild steel
14	Cold water tank	1	Galvanise steel
15	Header pipe	2	copper
16	Dull black paint		
17	Collector	1	Galvanise steel

REFERENCES

Adegoke, CO. and Bolaji, BO. 2000. Performance evaluation of solar operated thermosyphon solar hot water system. Int. J. Engineering and Engineering Technology. 2:35-40.

Agbo, SN. 2006. Effect of hot water withdrawal rate on a mean system temperature of a thermosyphon solar water heater, The Pacific Journal of Sci. and Technology. 7:33-42.

Agbo, SN. and Okeke, CE. 2007. Correlation between collector performance and the tube spacing for various absorber plate materials in a natural circulation solar water heater. Trends in Applied Science Research. 2(3):251-254.

Agbo, SN. and Oparaku, OU. 2006. Positive and future prospect of solar water heating in Nigeria. The Pacific Journal of Sci. and Technology. 7(2):191-198.

Agbo, SN. and Unachukwu, GO. 2006. Performance evaluation and optimization of ncerd thermosyphon solar water heater. Proc. World renewable Energy Congress Aug. 19-25, Florence, Italy.

Agbo, SN., Unachukwu, GO., Enibe, SO. and Okeke, CE. 2005. Solar energy heating for residential university student. Nigeria Journal of Solar Energy. 15:85-89.

Beckman and Duffie. 1991. Solar Engineering of Thermal Process, (2nd ed.), John Wiley and Son, New York, USA.

Chang, JM., Leu, JS., Shen, MC. and Hang, BJ. 2004. A proposed modified efficiency for thermosyphon solar water heater system. Solar Energy. 76:693-701.

Fairbairn, P. and Mario, R. 1999. Solar water heater, a SOPAC Technical Reports. (unpublished).

Morrison, GL. 1986. Solar domestic water heater design sensitivity study, Report No 1986/FMT/2 (unpublished).

Mani, A. and Rangarajan, S. 2005. Solar radiation over India. Solar Energy. 15:131-126.

Rasheed, KB. 1995. Participatory forestry as a strategy for reforestation in Bangladesh. Geo Journal. 37:39-44.

Sambo, AS. and Bello, MB. 1992. Simulation Studies on Pipe Spacing for a Collector and Tank for Solar Water Heaters. Nig. J. of Solar Energy. 9(3):215-223.

Received: Sept 16, 2011; Accepted: Dec 27, 2011

SENRA Academic Publishers, Burnaby, British Columbia
Vol. 6, No. 1, pp. 1863-1867, Feb 2012
Online ISSN: 1920-3853; Print ISSN: 1715-9997

Canadian Journal of pure&applied sciences

COMPLEXING AGENT EFFECT ON THE PROPERTIES OF IRON SULPHIDE THIN FILMS

Anuar Kassim[1], Ho SoonMin[1], Loh YeanYee[1], *Tan WeeTee[1] and Saravanan Nagalingam[2]
[1]Department of Chemistry, Faculty of Science, Universiti Putra Malaysia, 43400 Serdang, Selangor
[2]Department of Bioscience and Chemistry, Faculty of Engineering and Science
Universiti Tunku Abdul Rahman, 53300 Kuala Lumpur, Malaysia

ABSTRACT

Thin films of iron sulphide were prepared by chemical bath deposition technique in aqueous solutions. The influence of complexing agent for the formation of thin films was determined. The structure, morphology and optical properties of thin films of iron sulphide grown on microscope glass slide were investigated by X-ray diffraction, scanning electron microscopy and UV-Vis spectrophotometer. The films deposited using 0.1 M of sodium tartrate indicated the highest number of FeS peaks and covered substrate surface completely based on X-ray diffraction data and scanning electron microscopy results, respectively. However, when the concentration of sodium tartrate was increased to 0.2 M and above, the number of FeS peaks decreased and the films showed incomplete coverage of material over the surface of the substrate with inhomogeneous grain size.

Keywords: Chemical bath deposition, complexing agent, thin films, iron sulphide.

INTRODUCTION

The iron sulphide thin films have attracted considerable attention in recent years, because of abundant and posses semiconducting properties. Numerous deposition techniques including chemical vapor transport (Willeke *et al.,* 1992) metal-organic chemical vapour deposition (Thomas *et al.,* 1997), sputtering (Birkholz *et al.,* 1992) molecular beam deposition (Bronold *et al.,* 1997) flash evaporation (Ferrer *et al.,* 1990) electrodeposition (Nakamura and Yamamoto, 2001) and chemical bath deposition (Anuar *et al.,* 2009) have been employed for the growth of iron sulphide thin films. Among these deposition techniques, the chemical bath deposition is a very common deposition method (Sonawane *et al.,* 2004; Goudarzi *et al.,* 2008; Hankare *et al.,* 2008; Moualkia *et al.,* 2009; Asenjo *et al.,* 2010; Ekuma *et al.,* 2010; Gopakumar *et al.,* 2010; Anuar *et al.,* 2011) with respect to economic considerations.

In this investigation, deposition of iron sulphide thin films on microscope glass slides using chemical bath deposition method is presented. To our knowledge, a study on the properties of the chemical bath deposited iron sulphide thin films in the presence of sodium tartrate as a complexing agent has not been reported so far. Here, we report the influence of sodium tartrate on the structure, morphology and optical properties of thin films using X-ray diffraction, scanning electron microscopy and UV-Visible spectrophotometer, respectively.

*Corresponding author email: soonminho@yahoo.com

MATERIALS AND METHODS

All the chemicals used for the deposition were analytical grade reagents and all the solutions were prepared in deionised water (Alpha-Q Millipore). The iron sulphide thin films were prepared from an acidic bath using aqueous solutions of iron nitrate, sodium thiosulfate and sodium tartrate. The microscope glass slide was used as the substrate for the chemical bath deposition of iron sulphide thin films. Before deposition, the microscope glass slide was degreased with ethanol for 15min. Then, ultrasonically cleaned with distilled water for another 15 min and dried in desiccators. Deposition of iron sulphide thin films was carried out using following procedure. 20ml of iron nitrate (0.1M) was complexed with 20ml of various concentrations of sodium tartrate (0.1M, 0.2M and 0.3M) in order to study the influence of complexing agent on the properties of thin films. Then 20ml of sodium thiosulfate (0.1M) was added slowly to the mixture. The cleaned glass slide was immersed vertically into beaker. The pH was adjusted to 1.5 by adding hydrochloric acid using pH meter. During deposition process, the beaker was kept undisturbed at 75°C. After the completion of deposition (1.5h), the glass slide was removed, washed several times with distilled water and dried naturally in desiccators for further characterization.

In order to investigate the crystallographic properties of the iron sulphide thin films, we carried out the X-ray diffraction analysis using Philips PM 11730 diffractometer with CuK_{α} (λ=1.5418 Å) radiation. The surface morphology was observed by a scanning electron

microscopy (JEOL, JSM-6400). All the samples taken at 20 kV with a 1000 X magnification. The elemental composition of the films was studied by scanning electron microscope attached with energy dispersive analysis of X-ray (EDAX) analyzer. The optical properties of the film were measured with a Perkin Elmer UV/Vis Lambda 20 Spectrophotometer in the wavelength range of 300 to 800nm. The film-coated microscope glass slide was placed across the sample radiation pathway while the uncoated microscope glass slide was put across the reference path. Thus, the absorbance measurement included only the contribution from FeS thin films.

RESULTS AND DISCUSSION

Table 1 indicates the X-ray diffraction (XRD) data for the films deposited at various concentrations of sodium tartrate. Five peaks at 2□ = 25.2°, 38.6°, 43.7°, 47.3° and 62.5° corresponding to *d*-spacing values of 3.5, 2.4, 2.1, 1.9 and 1.5 Å are attributed to the (110), (210), (202), (301) and (213) planes, which belong to FeS, are detected from the films deposited using 0.1M of sodium tartrate. All of the peaks are coincident well with the corresponding diffraction peaks of FeS (Keller-Besrest and Collin, 1990) compound (JCPDS reference code: 01-080-1028). The lattice parameter values for the dominant structure are: a=b=6.958 Å and c=5.824 Å. However, the number of hexagonal phase of FeS peaks decreased to four and three peaks as the concentration of sodium tartrate is increased to 0.2M and 0.3M, respectively. It is believed that the complexing reaction is complete with high concentration of complexing agent (0.2M and 0.3M) and therefore hinders the deposition of films. In this study, the position of several peaks is used to determine the iron sulphide as shown in table 1. The use of complexing agent is very common in the preparation of thin films through chemical bath deposition method. Iron sulphide thin films are deposited on microscope glass slides by the decomposition of iron nitrate and sodium thiosulphate in acidic medium containing sodium tartrate as complexing agent. Iron nitrate is the source to produce Fe^{2+} while sodium thiosulphate is the source to produce S^{2-}. Sodium tartrate played the important role on this study that is to react with Fe^{2+} ions to form Fe-tartrate complex. It is to release the Fe^{2+} ions on slowly and improved the lifetime of the deposition bath as well as adhesion of the deposition thin films on substrate.

The investigation of scanning electron microscopy (SEM) micrographs from figure 1 brings to a comparison of the surface morphologies from the deposited films under different concentrations of sodium tartrate. For the films deposited using 0.1M of complexing agent, the films indicate complete coverage of material over the surface of the substrate. In contrast, SEM micrographs show incomplete coverage of material over substrate surface for the films deposited using 0.2M and 0.3M of complexing agent. The number of grains decreased as the concentration of complex agent is increased to 0.2M and 0.3M, respectively. Furthermore, various grain sizes can be seen from SEM micrographs which indicating irregular growth rate of the grains. The distributions of grains are randomly throughout the substrate with certain sites only occupied by the grains. Therefore, we can conclude that the morphology of iron sulphide thin films is strongly dependent on the complexing agent.

Optical absorbance spectra of FeS thin films deposited under different concentrations of sodium tartrate are given in figure 2. As it can be observed that the absorbance spectrum of the films deposited using 0.1M sodium tartrate is very high in comparison with other samples in the visible region. The higher absorbance can be due to more FeS materials deposited (five prominent FeS peaks) and these materials are found to cover the surface of the substrate completely (Fig. 1a).

Table 1. Comparison of the JCPDS *d*-spacing data for iron sulphide thin films to experimentally observed values for the sample deposited at various concentrations of sodium tartrate.

Sodium tartrate (M)	20 / (°)	*hkl*	*d*-spacing (Å) Observed value	JCPDS value
0.1	25.2	110	3.5	3.5
	38.6	210	2.4	2.3
	43.7	202	2.1	2.1
	47.3	301	1.9	1.9
	62.5	213	1.5	1.5
0.2	25.2	110	3.5	3.5
	39.1	210	2.3	2.3
	43.5	202	2.1	2.1
	47.3	301	1.9	1.9
0.3	25.1	110	3.5	3.5
	43.6	202	2.1	2.1
	51.9	220	1.8	1.8

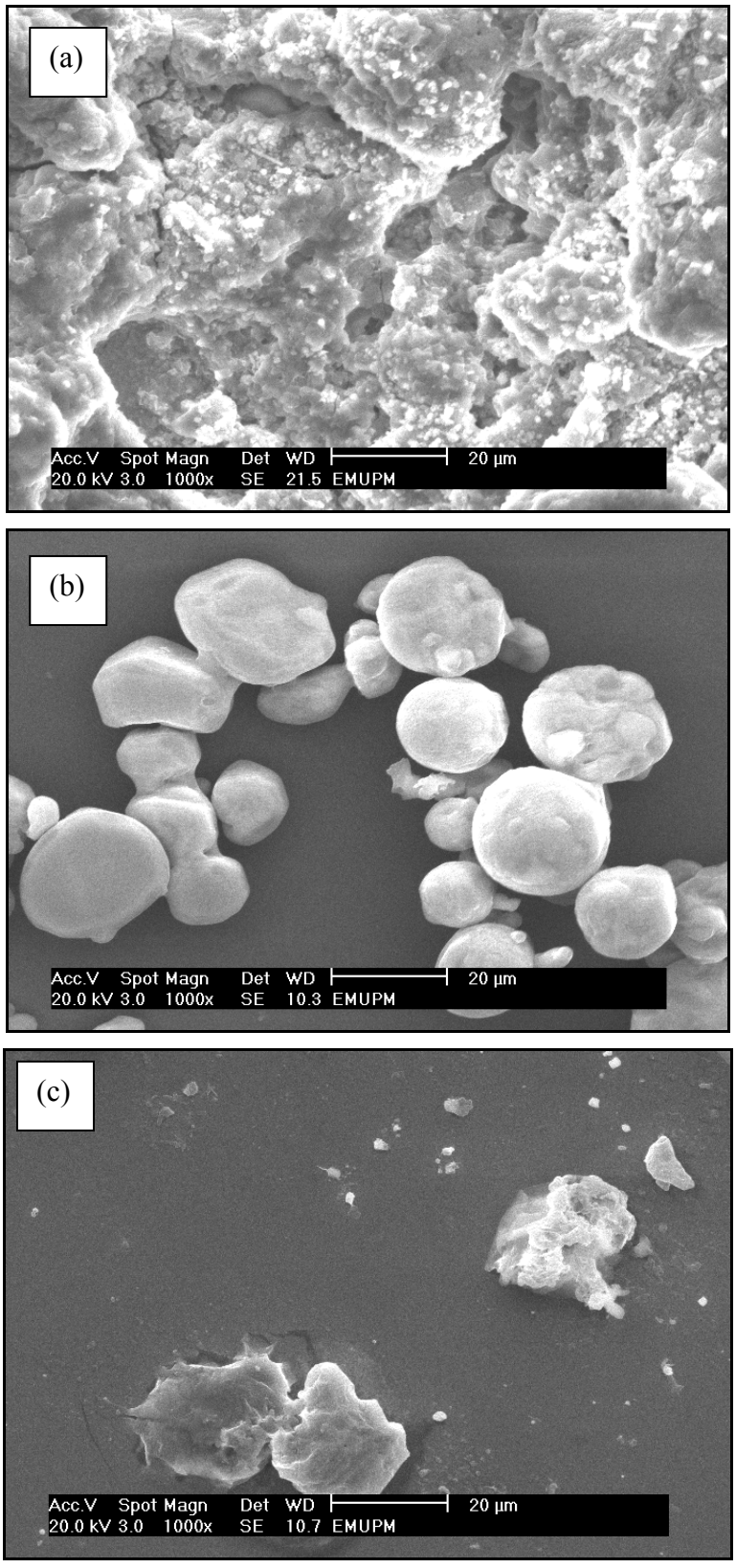

Fig. 1. The scanning electron microscopy (SEM) micrographs of FeS thin films deposited at various concentrations of sodium tartrate (a) 0.1M (b) 0.2M (c) 0.3M.

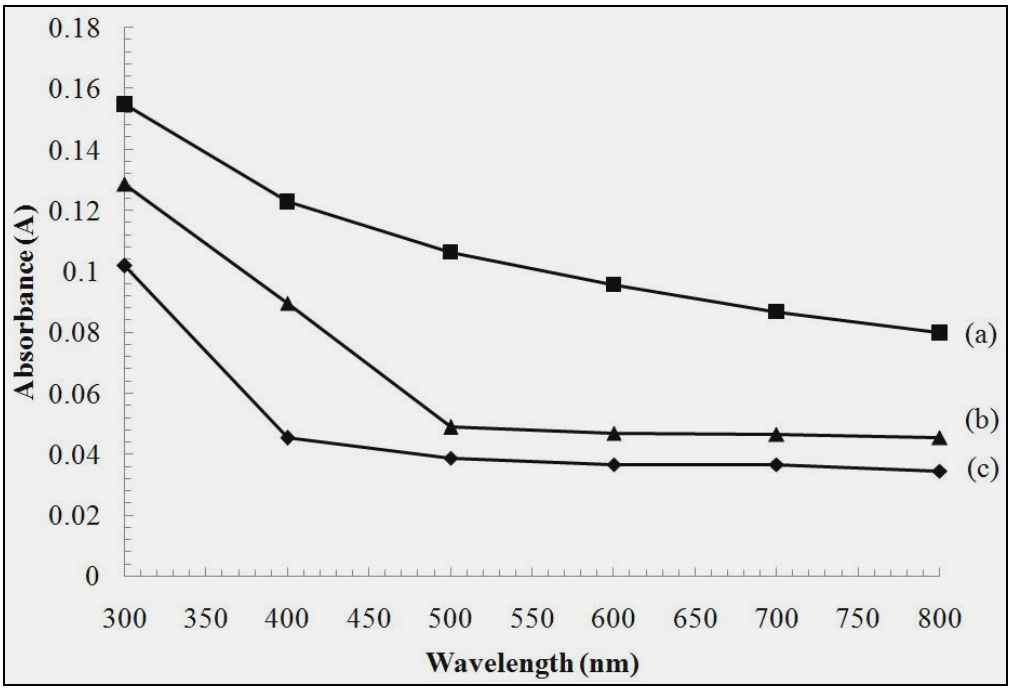

Fig. 2. Optical absorbance versus wavelength of FeS thin films deposited at various concentrations of sodium tartrate (a) 0.1M (b) 0.2M (c) 0.3M.

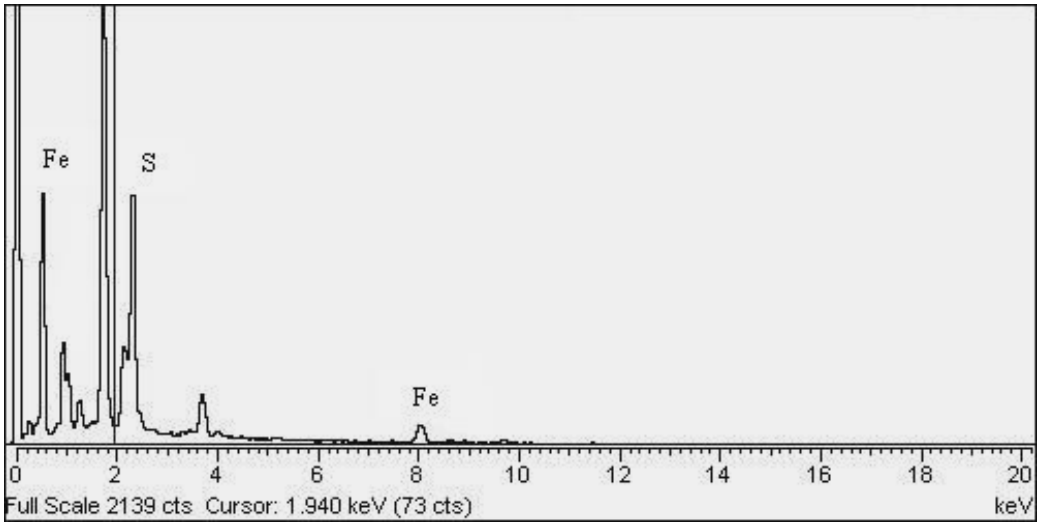

Fig. 3. EDAX spectrum of FeS thin films prepared using 0.1M of sodium tartrate as complexing agent.

The compositional analysis of the thin films was investigated by energy dispersive analysis of X-ray (EDAX) technique. The EDAX spectrum of FeS thin films prepared using 0.1M of sodium tartrate is shown in figure 3. The quantitative elemental analysis is carried out only for Fe and S. The atomic percentage (%) for these elements is 49.1% and 50.9%, respectively. The ratio of 1:1 of iron and sulphur has been confirmed by EDAX analysis.

CONCLUSION

In this paper, we presented the influence of complexing agent on the properties of FeS thin films. Overall, we concluded that 0.1M of sodium tartrate is the most favourable condition for growth of thin films. These films showed presence of higher number of FeS peaks and completely covered substrate surface based on X-ray diffraction and scanning electron microscopy results, respectively.

ACKNOWLEDGEMENTS

The authors would like to thank the Department of Chemistry, Universiti Putra Malaysia for the provision of laboratory facilities and MOSTI for the National Science Fellowship.

REFERENCES

Anuar, K., Tan, WT., Saravanan, N., Ho, SM. and Gwee, SY. 2009. Influence of pH values on chemical bath deposited FeS_2 thin films. Pacific Journal of Science and Technology. 10:801-805.

Anuar, K., Ho, SM, Tan, WT. and Ngai, CF. 2011. Influence of Triethanolamine on the Chemical Bath Deposited NiS Thin Films. American Journal of Applied Sciences. 8 :359-361.

Asenjo, B., Guillin, C., Chaparro, AM., Saucedo, E., Bermudez, V., Lincot, D., Herrero, J. and Gutirrez, MT. 2010. Properties of In_2S_3 thin films deposited onto ITO/glass substrates by chemical bath deposition. Journal of Physics and Chemistry of Solids. 71:1629-1633.

Birkholz, M., Lichtenberger, D., Hopfner, C. and Fiechter, S. 1992. Sputtering of Thin Pyrite Films. Solar Energy Materials and Solar Cells. 27:243-251.

Bronold, M., Kubala, S., Pettenkofer, C. and Jaegermann, W. 1997. Thin Pyrite (FeS_2) Films by Molecular Beam Deposition. Thin Solid Films. 304:178-182.

Ekuma, C., Nnabuchi, M., Nwabueze, A. and Owate, I. 2010. Optical characterization of chemically deposited SbCuS thin films. Ceramic Transactions. 222:243-249.

Ferrer, IJ., Nevskaia, DM., Heras, C. and Sanchez, C. 1990. About the Band Gap Nature of FeS as Determined from Optical and Photoelectrochemical Measurements. Solid State Communications. 74:913-916.

Gopakumar, N., Anjana, PS. and Vidyadharan, PK. 2010. Chemical bath deposition and characterization of CdSe thin films for optoelectronic applications. Journal of Materials Science. 45:6653-6656.

Goudarzi, A., Aval, GM., Sahraei, R. and Ahmadpoor, H. 2008. Ammonia-free chemical bath deposition of nanocrystalline ZnS thin film buffer layer for solar cells. Thin Solid Films. 516:4953-4957.

Hankare, PP., Jadhav, AV., Chate, PA., Rathod, KC., Chavan, PA. and Ingole, SA. 2008. Synthesis and characterization of tin sulphide thin films grown by chemical bath deposition technique. Journal of Alloys and Compounds. 463:581-584.

Keller-Besrest, F. and Collin, G. 1990. Structural aspects of the α transition in stoichiometric FeS: Identification of the high temperature phase. Journal of Solid State Chemistry. 84:194-210.

Moualkia, H., Hariech, S. and Aida, MS. 2009. Structural and optical properties of CdS thin films grown by chemical bath deposition. Thin Solid Films. 518:1259-1262.

Nakamura, S. and Yamamoto, A. 2001. Electrodeposition of Pyrite (FeS_2) Thin Films for Photovoltaic Cells. Solar Energy Materials and Solar Cells. 65:79-85.

Sonawane, PS., Wani, PA., Patil, LA. and Seth, T. 2004. Growth of $CuBiS_2$ thin films by chemical bath deposition technique from an acidic bath. Materials Chemistry and Physics. 84:221-227.

Thomas, B., Ellmer, K., Muller, M., Hopfner, C., Fiechter, S. and Tributsch, H. 1997. Structural and Photoelectrical Properties of FeS_2 (Pyrite) Thin Films Grown by MOCVD. Journal of Crystal Growth. 170:808-812.

Willeke, G., Blenk, O., Kloc, CH. and Bucher, E. 1992. Preparation and Electrical Transport Properties of Pyrite (FeS_2) Single Crystals. Journal of Alloys and Compounds. 178:181-191.

Received: June 7, 2011; Accepted: Oct 10, 2011

SENRA Academic Publishers, Burnaby, British Columbia
Vol. 6, No. 1, pp. 1869-1875, Feb 2012
Online ISSN: 1920-3853; Print ISSN: 1715-9997

Canadian Journal of pure&applied sciences

EFFECT OF A3[6]B$^{GLU \rightarrow LYS}$ MUTATION ON REACTIVITY OF THE CYSF9[93]B SULPHYDRYL GROUP OF HUMAN HAEMOGLOBIN C

*Jonathan Oyebamiji Babalola[1], Najeem Abiola Adesola Babarinde[2], Idowu Abideen Adeogun[3] and Titilola Stella Akingbola[4]
[1] Department of Chemistry, University of Ibadan, Nigeria
[2] Department of Chemical Sciences, Olabisi Onabanjo University, Ago Iwoye
[3] Department of Chemistry, University of Agriculture, Abeokuta, Nigeria
[4] Department of Haematology, University College Hospital, Ibadan

ABSTRACT

The pH dependence of the second order rate constant of the reaction of 5,5'-dithiobis(2-nitrobenzoate) (DTNB) with CysF9[93]β sulphydryl group of the oxy and carbonmonoxy derivatives of stripped haemoglobin C are complex while that of aquomet haemoglobins resembles the titration curve of a diprotic acid. However, in the presence of inositol hexakisphosphate, the profiles of oxy and carbomonoxy derivatives become simple while that of aquomet becomes bowl shaped. Increased ionic strength also simplified the complex profile. The pQs of the ionizable groups linked to the reactivity of DTNB with CysF9[93]β sulphydryl group range between 5.6 and 8.7 in stripped haemoglobin. The presence of inositol-P_6 decreases the pQ values to the range of 4.3 and 8.4. When compared with haemoglobins A and S, the reaction rate of heamoglobin C is lower than haemoglobin A but faster than haemoglobin S, implying that the net charge on the molecule has no direct relationship with the reaction rates.

Keywords: Haemoglobin C, Sulphyldryl group, Ionizable groups; Inositol-P_6; Ionic strength.

INTRODUCTION

Human haemoglobins A and C have identical α subunits, but differ from each other by one out of 146 amino acid residues on each of the β subunits. In haemoglobin A, the position A3[6]β is occupied by a negatively charged glutamic acid residue, while it is occupied by a positively charged lysine (an amino acid with relatively long side chain) residue in haemoglobin C. This mutation on the surface of haemoglobin molecule seems to be minor but it is of significant clinical consequence in individual with homozygous haemoglobin C (Hirsch *et al*., 1985).

The reactivity of CysF9[93]β sulphydryl group of hemoglobin has been employed as an indicator of both the tertiary and quaternary structural changes in relation to its immediate neighbourhood (Guidotti, 1965; Antonini and Brunori, 1969; Hensley *et al*., 1975; Okonjo *et al*., 2010). 5,5□-dithiobis(2-nitrobenzoate) (DTNB) is the most used sulphydryl reagents for this purpose because of its sensitivity to the electrostatic environment of haemoglobin and its stability at room temperature (Okonjo *et al*., 1996).

The reactivity DTNB with haemoglobin sulphydryl group has been used in determining tertiary transitions within haemoglobin (Okonjo *et al.,* 2008, 2010), tetramer dimer dissociation constants (Babalola *et al.*, 2005), Bohr effect (Babalola *et al.*, 2005) and the state of salt bridges within haemoglobin molecule (Okonjo and Nwozo, 1997; Babalola and Nwozo, 2002). Okonjo *et al.* (1995, 1996) has employed the sensitivity of DTNB to monitor the electrostatic environment of CysF9[93]β sulphydryl of human haemoglobins A and S. At 50 mmoldm^3 ionic strength, the pH dependence profiles of the second order rate constant are complex. The addition of inositolhexakisphosphate (inositol-P_6) simplified the profiles, reduced the second order rate constants and increased the pK_as of the ionizable groups linked to the reactivity of CysF9[93]β sulphydryl group. Increased ionic strength also simplified the profiles (Okonjo *et al.,* 1995, 1996).

Okonjo *et al.* (1996) had shown the effect of A3[6]β$^{glu \rightarrow val}$ mutation on the reactivity of CysF9[93]β sulphydryl group of human haemoglobin S compared to that of human haemoglobin A. The reactivity of CysF9[93]β sulphydryl group of human haemoglobin A is faster than that of haemoglobin S. This is contrary to expectation because the net charge on human haemoglobin S is more positive than that of haemoglobin A. Haemoglobin S was therefore expected to be more reactive towards the negatively charged DTNB. It would therefore be interesting to know what the reaction of negatively charged DTNB will be towards haemoglobin C which is known to have a greater net positive charge than both haemoglobins S and A. This is also special because the lysine which replaces valine in haemoglobin S or

*Corresponding author email: bamijibabalola@yahoo.co.uk

glutamic acid in haemoglobin A has a long side chain with a positively charged amino group end. Therefore, this study is aimed at comparing the effect of A3[6]$\beta^{glu \rightarrow lys}$ mutation on the reactivity of CysF9[93]β sulphydryl of human haemoglobin C with DTNB and those of human haemoglobins A and S.

MATERIALS AND METHODS

Haemoglobin Preparation

Fresh blood containing homozygous haemoglobin C was obtained from the Haematology Clinic of the University College Hospital, Ibadan into heparinized tubes. Haemoglobin was prepared from these blood samples using standard methods as previously described by Okonjo *et al.* (2008). Low molecular weight impurities contained in the haemoglobin were removed by dialysis using polyvinyl chloride dialysis tubing and subsequently deionized by passage through a Dintzis ion-exchange column (Dintzis, 1952).

Kinetic Experiment

The kinetics of the reaction of DTNB with haemoglobin C was monitored at 412nm on a Zeiss PMQ II UV-VIS spectrophotometer thermostatted with a Lauda 30D table Kryostat. The reactions were carried out in triplicate at 20^{o}C in phosphate (pH 5.6 to 8.0) and borate (pH 8.2 to 9.0) buffers. 10 cm^3 of haemoglobin with concentration 10μM haem (5μM in reactive sulphydryl group) was pipetted into the 2cm path length cuvette, the reaction was initiated by adding a predetermined volume of DTNB with stirring. The same conditions were used in the presence of inositol-P_6 except that 10 μmoldm^3 of inositol-P_6 was added. To determine the influence of high ionic strength, NaCl was added to the buffer to adjust the ionic strength to 200 mmoldm^3. The second-order rate constants were calculated from its rate equation after converting the transmittance reading to absorbance. The kinetic data were fitted using micromath scientist software package (Salt Lake City, Utah, USA) using the equation derived from the scheme of the reaction.

RESULTS AND DISCUSSION

The reaction of human haemoglobin C with DTNB showed that only CysF9[93]β is reactive just like we have haemoglobins A and S (Okonjo *et al.*, 1996) the change in absorbance with time is exponential across the pH ranges of the experiments.

Nature of the pH dependent profile of DTNB reaction with CysF9[93]β sulphydryl group of haemoglobin C

Ionic strength of 50 mmoldm^{-3}: Figures 1a, 1b, and 1c show the pH dependence profiles of the second order rate constants for reaction of DTNB with CysF9[93]β sulphydryl group of oxy, carbonmonoxy and aquomet derivatives of haemoglobin C respectively at ionic strength of 50 mM. The profiles for oxy (Fig. 1a) and carbonmoxy (Fig. 1b) have a peak each at around pH 7.2. The rate of reaction of oxy haemoglobin A and C are similar between pH 5 and 8 after which haemoglobin A reacts faster. The reaction of oxyhaemoglobin C is faster than that of S throughout the pH range of the experiment. In the case of the reaction of DTNB with carbonmonoxy haemoglobins the profiles are similar but with different rates. Haemoglobin A is at least about three times faster than haemoglobin C while that of haemoglobin S is lower. The profile of pH dependence of second order rate constant for aquomet derivative of haemoglobin C gave a simple profile resembling the titration curve of a diprotic acid (Fig. 1c). This is completely different from the profiles earlier obtained for haemoglobins A and S (Okonjo *et al.,* 1995, 1996). This is an indication that the electrostatic environment of CysF9[93]β is completely different in aquomet haemoglobin C compared to haemoglobins A and S. It can therefore be assumed that there is interaction between the iron III on the haem, LysA3[6]β and CysF9[93]β of haemoglobin C.

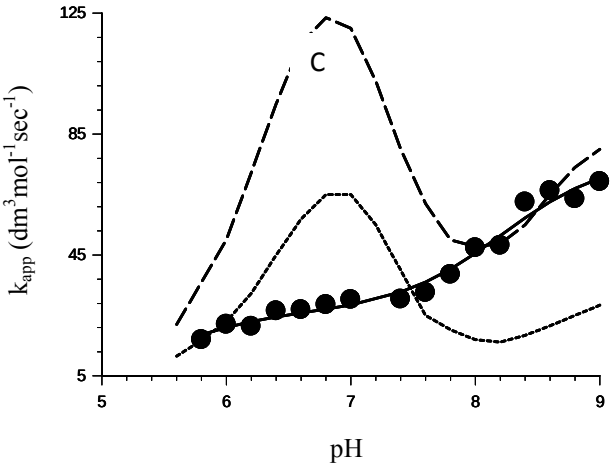

Fig. 1. Dependence of k_{app} on pH for the reaction of DTNB with CysF9[93]β sulphydryl group of haemoglobin C stripped of organic phosphate (filled circle). (a) oxy hemoglobin (b) carbonmonoxy hemoglobin (c) aquomet hemoglobin. The lines through the data points are the theoretical best-fit lines calculated with the parameters given in table 1. For comparison with the theoretical best fit lines for hemoglobin A (long dashes-lines) and S (short dashed-lines) drawn in full lines.

Naturally, the expectation would be that the reaction of DTNB with various haemoglobin would be in this order Haemoglobins C > S > A (according to their net positive charge. However this is not so except for aquomet haemoglobin between pHs 5.8 and 7.5. Going by the result obtained by Okonjo *et al.* (1996) that shows that haemoglobin A reacts faster than haemoglobin S with DTNB, one would expect that haemoglobin S would be faster than haemoglobin C but this is not so. This is an

indication that the net charge on the haemoglobin does not play a specific role on the overall rate of reaction of DTNB. The charges that would be probably important would be those of the amino acid residue that are electrostatically linked with CysF9[93]β sulphydryl group.

Ionic strength of 50 mmoldm^{-3} plus inositol –P$_6$: In the presence of organic phosphate, inositol-P_6, the pH dependence profile of k_{app} for haemoglobin C changes drastically in all the derivatives. The complex profile of oxy and carbonmonoxy haemoglobin C in the absence of organic phosphate became simple on addition of organic phosphate in figures 2a and 2b, respectively. The simple profiles resemble the titration curve of a diprotic acid, this result is similar to what was obtained when organic phosphate was added to haemoglobins A and S. This confirms that the binding of organic phosphate to ValNA1[1]β, HisNA2[2]β LysEF6[82]β and HisH21[143]β changes the conformation of CysF9[93]β, thereby changing its electrostatic environment and making it occluded below pH 7.8 for oxy haemoglobin C and between pH 6.4 and 8.2 for carbonmonoxy haemoglobin C. The most striking result in the reaction of DTNB with aquomet haemoglobin C in the presence of inositol-P_6 is the bowl shaped profile obtained for the pH dependence of $k_{app.}$ Such a shape has not been reported for CysF9[93]β sulphydryl group to the best of our knowledge. The presence of inositol-P_6 increases the rate of reaction in aquomet derivative in the pH range of this study. This is an indication the binding of organic phosphate to ValNA1[1]β, HisNA2[2]β LysEF6[82]β and HisH21[143]β change the conformation of the molecule. In most cases organic phosphate lowered the rate of reaction of DTNB with CysF9[93]β sulphydryl group (Okonjo *et al.,* 1995, 1996), the increased rates observed here could be attributed to the interaction of the side chain of LysA3[6]β, the haem and CysF9[93]β sulphydryl group.

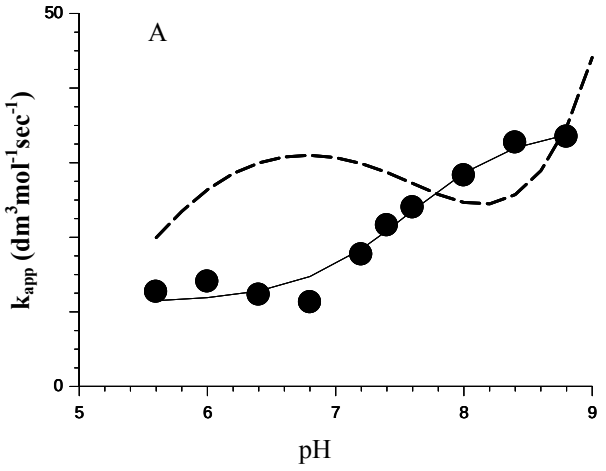

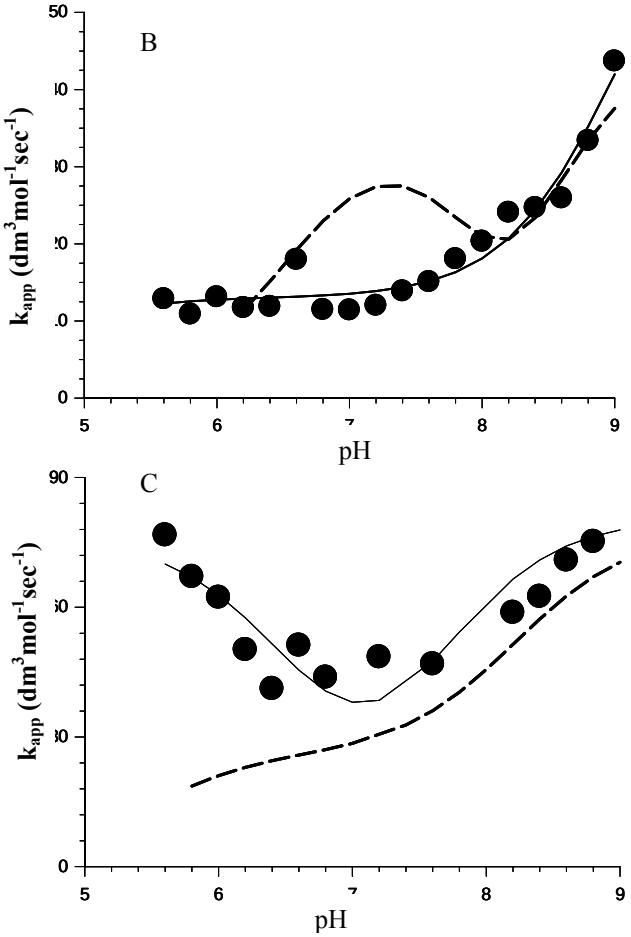

Fig. 2. Dependence of k_{app} on pH for the reaction of DTNB with CysF9[93]β sulphydryl group of haemoglobin C in the presence of organic phosphate (solid line). (a) oxy hemoglobin (b) carbonmonoxy hemoglobin (c) aquomet hemoglobin. For comparison with the theoretical best fit lines for stripped hemoglobin C (long dashed-lines).

Ionic strength of 200 mmoldm^{-3}: Haemoglobin tetramer dissociates to dimers under the influence of increasing ionic strength (Okonjo *et al.*, 1996), to this end a more stable derivative of haemoglobin (carbonmonoxy haemoglobin) was used to investigate the effect of increased ionic strength. The complex profile obtained at 50 moldm^{-3} NaCl become simplified when the ionic strength was increased to 200 moldm^{-3} (Fig. 3), this is in agreement with the earlier observations made for haemoglobins A and S (Okonjo *et al.*, 1996). The simplification is due to the fact that the added salt screened off the electrostatic environment and exposed CysF9[93]β sulphydryl group. When compared, the rates of reactions in the presence of 200 moldm^{-3} NaCl were higher than in the presence of organic phosphate, as expected this is because the increased ionic strength increased the proportion of the dimers which are known to react faster (Babalola *et al.,* 2005).

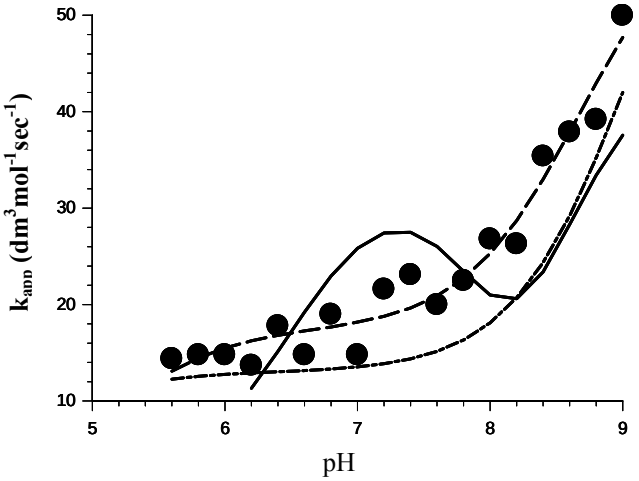

Fig. 3. Dependence of k_{app} on pH for the reaction of DTNB with CysF9[93]β sulphydryl group of carbonmonoxy haemoglobin C at 200 mM ionic strength. Full-line represents the best fit line for similar reaction with stripped haemoglobin at 50 mM while dotted-line represents the best fit line for the reaction in the presence of 10 μmoldm^{-3} inositol hexakisphosphate.

Analysis of pH dependence profiles

It has been suggested that the reactivity of sulphydryl group depends on its conformation and its electrostatic environment, particularly the number and nature of ionizable groups electrostatically linked to it (Okonjo *et al*., 1996). These factors determine the nature and shape of the pH dependence of $k_{app.}$

Simple profile:

It is known that in haemoglobin only the thiol anion reacts with DTNB (Robyt *et al.,* 1971; Hallaway *et al.,* 1980) for this reason we previously accounted for the profile similar to those reported for haemoglobin C in Figures 1c, 2a, 2b and 3 in term of the fraction of thiol anion form of sulphydryl (Okonjo *et al.,* 1995, 1996, 1997). Moreover, the salt bridge is formed in R state haemoglobin between HisHC3[146]β and AspFG1[94]β and this salt bridge hinders access to CysF9[93]β sulphydryl group. These considerations give rise to the two term equation 1 below (Okonjo and Aboluwoye, 1992):

$$k_{app} = k_1 \frac{Q_1}{Q_1 + [H^+]} + k_2 \frac{Q_2}{Q_2 + [H^+]} \qquad 1$$

In this equation, k_1 is the limiting apparent second-order rate constant at high pH for the DTNB reaction when the reactivity of the CysF9(93)β sulphydryl group is linked to the ionization of HisHC3(146)β, with ionization constant Q_1, k_2 is the limiting apparent second order rate constant at high pH when the sulphydryl reactivity is linked to the ionization of CysF9(93)β, with ionization constant Q_2. The analyses of the simple profiles in this study with equation (1) gave the best-fit parameters for oxy and carbonmonoxy in Table 1 and aquomet haemoglobin in Table 2 (the profile that resembles the titration curve of a diprotic acid). The mean pQ_1 and pQ_2 values are 4.33 ± 0.3 and 8.36 ± 0.7 respectively, these values are lower than the mean values of 6.6 and 8.8 obtained for pQ_1 and pQ_2 for both haemoglobins A and S (Okonjo *et al.*, 1995, 1996). However the values can still be attributed to the same ionizable residues electrostatically linked to the reactivity of CysF9[93]β sulphydryl group i.e. the pQ_1 of 4.33 is assigned to the HisHC3[143]β. The value pQ_1 value for Histidine should be around 6.0, but the presence of the positively charged LysA3[6]β (pQ_1 around 10.8) caused a repulsion that reduced the pQ_1 value of HisHC3[143]β. The 8.36 value obtained for pQ_2 is assigned to CysF9[93]β which normally has a pQ value of 8.3. The pQ_1 and pQ_2 values of 5.6 and 8.2 obtained for aquomet derivatives could not be compared with those obtained for haemoglobins A and S because of the difference in their profiles, however the value of pQ_2 can be assigned to the CysF9[93]β while the pQ_1 value of 5.6 is assigned to HisHC3[143]β. The value of pQ_2 is similar to what is expected for cysteine indicating that in aquomet haemoglobin in the absence of organic phosphate the LysA3[6]β do not affect its pQ_2 value while it increased that of pQ_1, this implies that the orientation of the positively charged lysine is towards the histidine group rather than the cysteine or the haem.

Bowl shaped profile:

Bowl shaped profile can be theoretically accounted for by assuming that there is an ionizable cationic group close to the sulphydryl group. The implication is that at low pH the cationic group is positively charged and the reaction with the negatively charged DTNB is fast. Bowl shaped profiles were previously analysed with equation 2 below:

$$k_{app} = k_1 \frac{[H^+]}{Q_1 + [H^+]} + k_2 \frac{Q_2}{Q_2 + [H^+]} \qquad 2$$

The terms in the equation 2 are similar except that the first fractional term is the fractional population of the cationic form of this group. The analyses of the bowl shaped profiles for aquomet haemoglobin C in the presence of inositol-P_6 figure 2c with equation (2) gave the best-fit parameters reported in table 1. This clearly explained that the binding of inositol-P_6 brings the

LysA3[6] closer to the sulphydryl as provided by the equation and the observed increase rate. The pQ_1 and pQ_2 values of 6.6 and 7.6 obtained for aquomet derivatives could not be compared with those obtained for haemoglobins A and S because of the difference in their profiles, however the value of pQ_1 can be assigned to the HisHC3[143]β while the pQ_2 value of 7.6 is assigned to CysF9[93]β. The value of pQ_1 is similar to what is

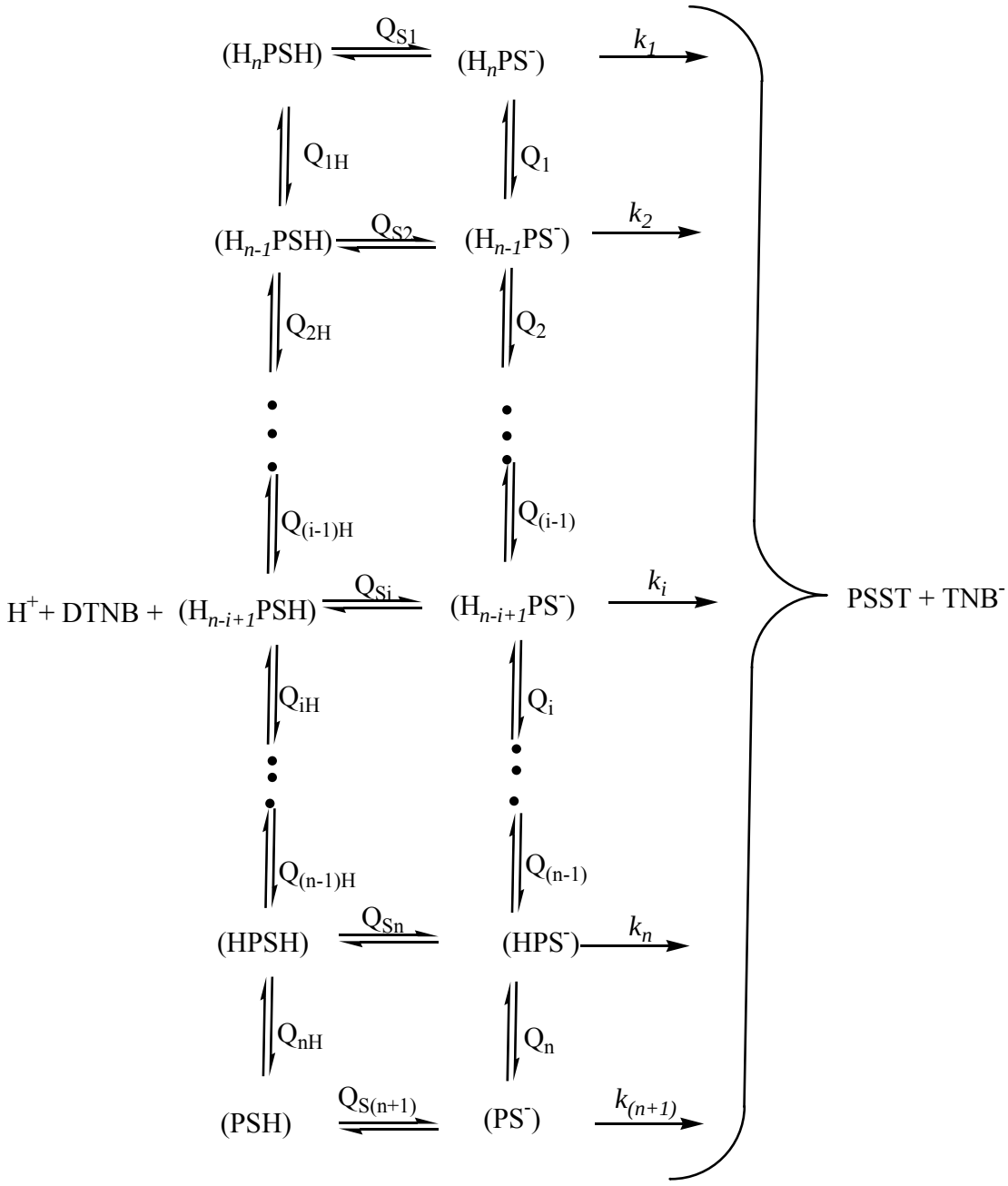

Scheme I

expected for Histidine indicating that in aquomet haemoglobin in the presence of organic phosphate the lysA3[6]β do not affect its pQ_1 while it reduce that of pQ_2 this implies that the orientation of the positively charged lysine is towards the sulphydryl group rather than the histidine or the haem and this clearly explain why the electrostatic environment of CysF9[93]β is affected and the profile is bowl shaped unlike those of oxy and carbonmonoxy.

Complex profile

However, the complex profiles in the figures 1a and b were analysed using equation 3 derived from scheme I.

Table 1. Reaction of DTNB with CysF9[93]β sulphydryl group of haemoglobin C in the presence of inositol-P_6

	$k_1(dm^3mol^{-1}s^{-1})$	$k_2(dm^3mol^{-1}s^{-1})$	pQ_1	pQ_2
Oxy	11.70	23.97	3.98	7.64
Carbon monoxy	14.50 (17.46)*	55.52 (44.29)*	4.67 (5.13)*	9.07 (8.67)*
Mean			4.33 ± 0.3	8.36 ± 0.7
Aquomet	76.13	80.62	6.60	7.60

*the values in the bracket are the parameters used for fitting the kinetic data for stripped carbonmonoxy derivatives in the presence of 200 $mmoldm^{-3}$ NaCl and were not used to find the mean values.

Table 2. Reaction of DTNB with CysF9[93]β sulphydryl group of Stripped Haemoglobin C.

	k_1 $(dm^3\,mol^{-1}s^{-1})$	k_2 $(dm^3\,mol^{-1}s^{-1})$	k_3 $(dm^3\,mol^{-1}s^{-1})$	pQ_1	pQ_2	pQ_{S3}	pQ_{1H}	pQ_{2H}
Oxy	38.29	2059.04	253.96	8.47	9.00	9.86	6.38	6.87
Carbon monoxy	43.12	2.90	52.66	7.93	8.48	8.08	8.00	6.98
Mean				8.20 ± 0.3	8.74 ± 0.3	8.97 ± 0.9	7.19 ± 0.8	6.93 ± 0.1
Aquomet	27.23	50.15	-	5.57	8.23	-	-	-

This was previously explained based on the assumption that the complex profile is a result of the electrostatic interaction of the ionizable groups with CysF9[93]β sulphydryl group in its reaction with DTNB. The best-fit parameters for the complex profiles for figures 1a and 1b are presented in table 2.

$$K_{app} = \frac{k_{n+1} + \sum_{i=1}^{n} k_i (H^+)^{n+1-i} \left(\prod_{j=i}^{n} Q_j \right)^{-1}}{\left\{ 1 + \sum_{i=1}^{n} k_i (H^+)^{n+1-i} \left(\prod_{j=i}^{n} Q_j \right)^{-1} + \frac{[H^+]}{Q_{s(n+1)}} \left[\sum_{i=1}^{n} k_i (H^+)^{n+1-i} \left(\prod_{j=i}^{n} Q_{jH} \right)^{-1} \right] \right\}} \quad 3$$

The mean pQ_1 and pQ_2 values for complex profiles are 8.2 ± 0.3 and 8.7 ± 0.3 respectively for stripped haemoglobin C, these two values are higher than those obtained for haemoglobins A and S (Okonjo *et al.,* 1995, 1996).

CONCLUSION

The replacement of glutamic acid at A3[6]β position of hemoglobin A with lysine in hemoglobin C is of structural consequence. Contrary to expectation, the rate of reaction of haemoglobin C with DTNB is lower than that of haemoglobin A despite increase net positive charge on haemoglobin C. Surprisingly, the aquomet derivative (both stripped and in the presence of organic phosphate) displayed some characteristic profiles that bring to the fore the effect of replacement of glutamic acid at A3[6]β position with lysine.

ACKNOWLEDGEMENT

The authors are grateful to Prof. K. O. Okonjo of Chemistry Department University of Ibadan for useful discussions. The work also benefitted from the support of the Alexander von Humboldt-Stiftung, Bonn, Germany, the International Centre for Theoretical Physics, Trieste, Italy and the Senate Research Grant (SRG/FSC/ 2006/16A) of the University of Ibadan.

REFERENCES

Antonini, E. and Brunori, M. 1969. On the rate of conformation change associated with ligand binding in hemoglobin. Journal of Biological Chemistry. 244:3909-3912.

Babalola, JO. and Nwozo, S. 2002. A new structure in the vicinity of HisHC3[146]β of pigeon haemoglobin induced by inositol hexakisphosphate. Scientia Iranica. 9:139-147.

Babalola, JO., Babarinde, NA. and Akingbola, TS. 2005. Varying apparent rate constant: determination of uptake and release of protons during tetramer-dimer dissociation in human hemoglobin A. Italian Journal of Biochemistry. 54:61-68.

Bettati, S., Viappiani, C. and Mozzarelli, A. 2009. Hemoglobin, an "evergreen" red protein. Biochimica et Biophysica Acta. 1794:1317-1324.

Dintzis, HM. 1952. Dielectric properties of human mercaptalbumin. Ph.D thesis, Harvard University, Cambridge, Mass.

Guidotti, G. 1965. The rates of reaction of the sulphydryl group of human hemoglobin. Journal of Biological Chemistry. 240:3924-3927.

Hensley, P., Edelstein, SJ., Wharton, DC. and Gibson, QH. 1975. Conformation and spin state in methemoglobin. Journal of Biological Chemistry. 250:952-960.

Hirsch, RE., Ravetos-Suarez, C., Olison, JA. and Nagel, RL. 1985. Ligand state of intraerythrocytic circulating HbC crystal in homozygote CC patient. Blood. 66:775-777.

Okonjo, KO. 1980. The effect of organic phosphates on the sulphydryl reactivities of oxyhemoglobins, A and S. Journal of Biological Chemistry. 255:3274-3277.

Okonjo, KO., Aken'ova, YA., Aboluwoye, CO., Nwozo, S., Akhigbe, FU., Babalola JO. and Babarinde, NA. 1996. Effect of A3[6]$\beta^{Glu\rightarrow Val}$ mutation on reactivity of CysF9[93]β sulfhydryl group of human hemoglobin S. Journal of the Chemical Society (Faraday Transactions). 92:1739-1746.

Okonjo, KO. and Nwozo, S. 1997. Ligand – dependent reactivity of the CysB5(23)β sulfhydryl group of the major haemoglobin of chicken. Journal of the Chemical Society (Faraday Transaction). 93:1361-1366.

Okonjo, KO., Bello, OS. and Babalola, JO. 2008. Transition of hemoglobin between two tertiary conformations: the transition constant differs significantly for the major and minor hemoglobins of the Japanese quail (*Cortunix cortunix japonica*). Biochimica et Biophysica Acta. 1784:464-471.

Okonjo, KO., Adeogun, IA. and Babalola, JO. 2010. Tertiary conformational transition in sheep hemoglobins induced by reaction with 5,5´-dithiobis(2-nitrobenzoate) and by binding of inositol hexakisphosphate. Journal of Biophysical Chemistry. 146:65-75.

Hallaway, BE., Hedlund, BE. and Benson, ES. 1980. Studies on the effect of reagent and protein charges on reactivity of the β93 sulfhydryl group of human hemoglobin using selected mutations. Archives of Biochemistry and Biophysics. 203:332-342.

Robyt, JF., Ackerman, RJ. and Chittenden, CG. 1971. Reaction of protein disulfide groups with Ellman's reagent: A Case study of the number of sulfhydryl and disulfidegroups in apergillus oryzea α-amylase, papain, and lysozyme. Archives of Biochemistry and Biophysics. 147:262-269.

Received: May 21, 2011; Accepted: Dec 9, 2011

SENRA Academic Publishers, Burnaby, British Columbia
Vol. 6, No. 1, pp. 1877-1881, Feb 2012
Online ISSN: 1920-3853; Print ISSN: 1715-9997

Canadian Journal of pure&applied sciences

KINETICS OF ANAEROBIC DIGESTION OF PALM OIL MILL EFFLUENT

*JT Nwabanne[1], AC Okoye[2] and HC Ezedinma[1]
[1]Department of Chemical Engineering
[2]Department of Environmental Management
Nnamdi Azikiwe University, PMB 5025, Awka, Nigeria

ABSTRACT

Globally, Nigeria is one of the largest producers of palm oil however the effluents generated from palm oil mills are usually discarded into the water bodies thereby causing environmental pollution. Serious efforts are made in the treatment before discharge into surface waters. This work is aimed at studying the kinetics of anaerobic digestion of palm oil mill effluent (POME) in a batch reactor at mesophilic condition. The digestion period lasted for 40 days. Maximum biogas production of 19.50% was obtained at hydraulic retention time of 10 days. Temperature has a significant effect, particularly on the performance of biogas-forming bacteria. Micro-organisms grew as temperature increased from 28 to 34^{o}C after which the growth started decreasing. The percentage total suspended solid (TSS) and the effluent substrate concentration decreased as hydraulic retention time increased. The kinetics of anaerobic digestion of palm oil mill effluent followed a first order kinetic model with a first order reaction constant of 1.306day^{-1}. The maximum rate of utilization (K), half velocity constant (K_s), endogenous decay constant (K_d), microbial growth yield (Y) and maximum specific growth rate μ_{max} were found to be 0.868day^{-1}, 97.66mg/l, 0.344day^{-1}, 0.550 and 0.477day^{-1} respectively. Values of K and K_s suggest that the digesting microbes require much retention time to regenerate and hence inoculation is needed for better performance.

Keywords: POME, anaerobic, digestion, kinetics.

INTRODUCTION

In Nigeria palm oil industry is the largest producer of palm oil mill effluent. The operation of palm oil mill requires large volume of water, which are subsequently discharged into the environment, either raw or treated. Palm oil mill effluent (POME) is a colloidal suspension of 95-96% water, 0.6-0.7% oil and 4-5% total solids including 2-4% suspended solids originating in the mixing of sterilizer condensate, separator sludge and hydrocyclone wastewater that are mostly debris from palm fruit mesocarp (Ahmad *et al*., 2003; Bek-Nielsen *et al*., 1999; Ahmad *et al*., 2005). Raw POME has a Biological Oxygen Demand value of around 25,000mg/l, making it about 100times more polluting than sewage (Mahaswaran and Singam, 1997). Due to high pollution load and environmental significance of POME, treatment of POME, is currently receiving attention in order to mitigate its effects on the environment. A number of treatment processes has been reported by several researchers for treatment of POME (Ahmad *et al*., 2003, 2005; Zinatizadeh *et al*., 2006). Biological treatment is a very common process used. A concentrated mass of micro-organism is used to break down organic material into stabilized wastes. Considering the highly organic character of POME, the anaerobic process is the most suitable approach for treatment (Perez *et al*., 2001).

Anaerobic digestion is a microbial process in which micro-organism breakdown biodegradable material in the absence of oxygen. It is widely used to treat wastewater, sludge and organic waste because it provides volume and mass reduction of the input material. The organic matter is decomposed and it generates a gas (called biogas which is highly energetic), a residual sludge, and a wastewater with less pollution (Mailleret *et al*., 2004). The process of anaerobic digestion occurs in three stages: (1) hydrolysis and acidogenesis (2) acetagenesis and (3) methanogenesis. Digestion is not complete until the substrate has undergone all three stages. Each stage has unique bacteria responsible for the process. The first group hydrolyses the organic matter into volatile fatty acids of low molecular weight and alcohol, and the second group converts them to methane and carbon dioxide. Biogas production is sensitive to digester temperature and pH (Angelidaki and Ahring, 1993; Angelidaki *et al*., 1999; Keshtkar *et al*., 2003; Yilmaz and Atalay, 2003). Methane-forming bacteria are most productive in either mesophilic conditions at 25-40^{o}C or in the thermophilic range at 50-65^{o}C.

Anaerobic digestion can be carried out either in batch or continuous process. In the batch process, the substrate is put in the reactor at the beginning of the digestion period. Retention time ranges from 30-60 days and only about 1/3 of the tank volume is used for the active digestion. Large

*Corresponding author email: joe nwabanne@yahoo.com

tank volume required for this type of operation is a problem. In the continuous process, fresh substrate is added and an equal amount of effluent is removed continuously, maintaining equilibrium. Reactions occur at a fairly consistent rate resulting in nearly constant biogas production. The purpose of the present work is to study the anaerobic digestion of POME effluent in a batch reactor in order to determine the kinetics of the process.

MATERIALS AND METHODS

Material collection and preparation

Palm oil mill effluent (POME) was collected from Mother Theresa palm oil processing mill, Awka South Local Government Area, Anambra State, Nigeria. Coarse and other particulates (solid materials) were removed from the sample using 100mm sieve prior to laboratory study.

Experimental procedure

Preliminary studies were taken immediately on delivery of the sample to the laboratory to determine such parameters as pH, Chemical Oxygen Demand (COD), microbial concentration (Bio-load) and Total Suspended Solid (TSS) according to the approved techniques by American Public Health Association (APHA, 2005). Five liter of the sample were poured into a bioreactor, stirred to ensure a homogenous mixture and subjected to anaerobic digestion. Digestion lasted for a period of 40 days. Periodic samples were collected every 5 days and analyzed for the above parameters. The biogas produced was measured after every 5 days by means of downward displacement of water by the biogas in an inverted measuring cylinder.

RESULTS AND DISCUSSION

Figure 1 shows the effect of time on biogas production during anaerobic digestion. From the figure, it can be seen that maximum biogas production of 19.50% was obtained at hydraulic retention time of 10 days, and started decreasing thereafter. This decrease in biogas production as time increase is as a result of gradual decrease in the

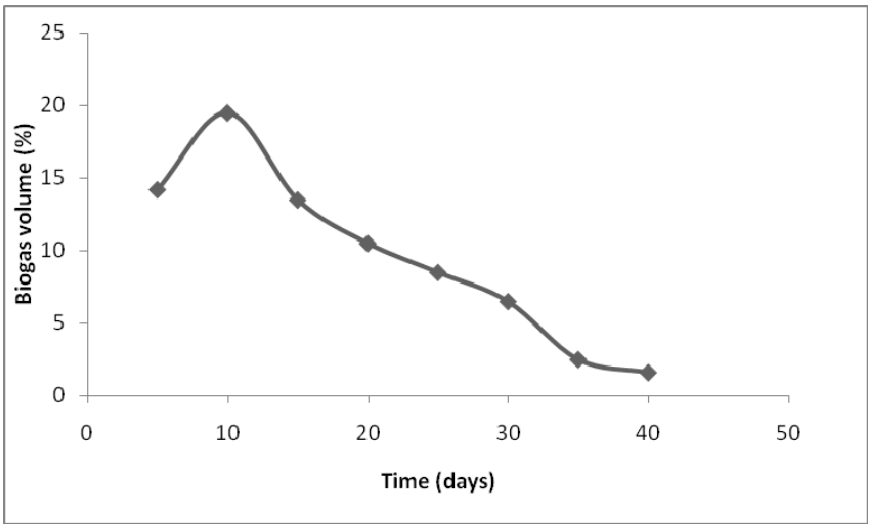

Fig. 1. A plot biogas volume against hydraulic retention time.

Table 1. Batch experimental data for determination of kinetic parameters.

t (day)	Temp (^oC)	pH	So (mg/l)	Se (mg/l)	Xo (mg/l)	Xe (mg/l)	X (mg/l)	Initial TSS (mg/l)	Effluent TSS (mg/l)
0	0	4.7	58000		1034.84			1050	
5	28.0	7.6		8437		5004.46	3019.65		960
10	34.0	7.8		5035		8322.94	4678.89		840
15	32.0	7.5		2248		4777.20	2906.02		720
20	34.5	7.2		730		3133.28	2084.06		630
25	35.0	6.9		537		2253.66	1644.25		500
30	35.5	6.8		410		1088.72	1142.59		430
35	36.4	6.7		207		934.76	834.67		300
40	37.0	6.6		109		780.59	526.34		110

X= average cell mass concentration = $\frac{X_o+X_e}{2}$ (Reynolds and Richard, 1996).

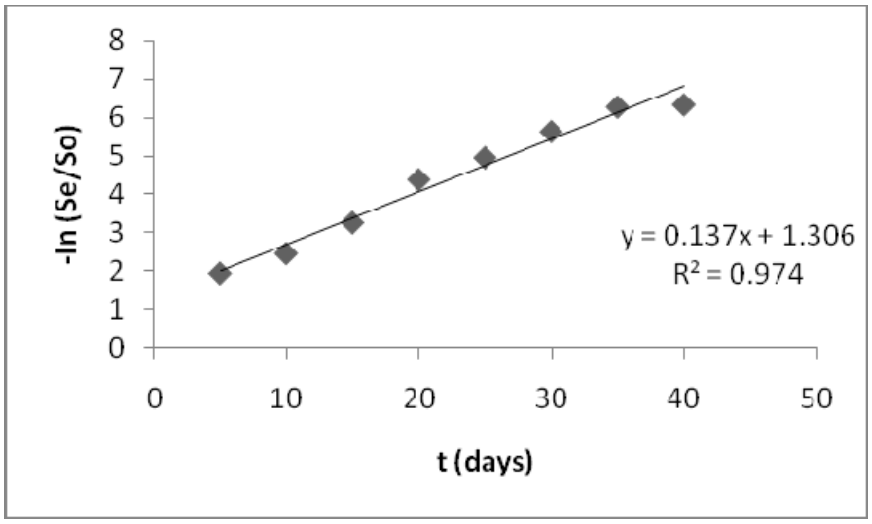

Fig. 2. First order kinetic plot for POME digestion.

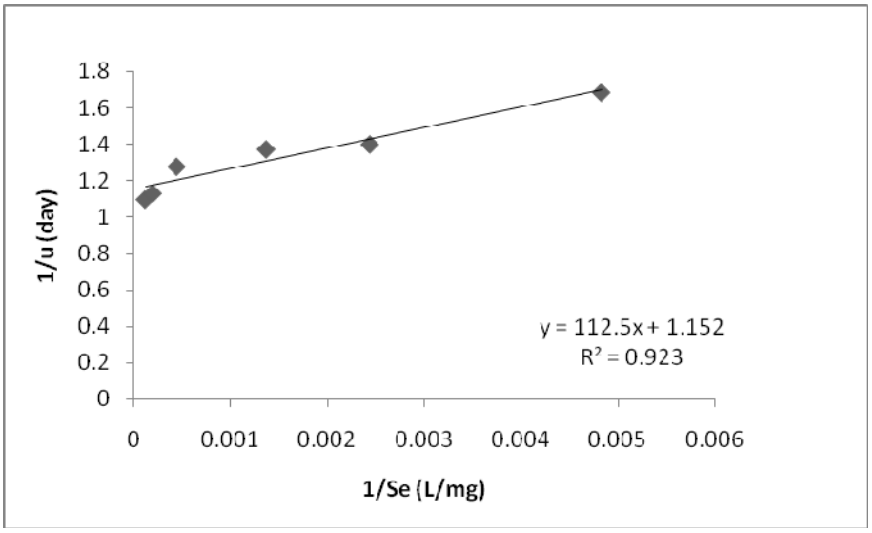

Fig. 3. Plot for determination of K and K_s

concentration of biodegradable substrate (Jose *et al*., 2009).

Temperature has a significant effect, particularly on the performance of biogas-forming bacteria. Table 1 shows the effect of temperature on microbial effluent concentration during anaerobic digestion. During the process, the temperature of the digester remained at mesophilic conditions (28 to 37^{o}C). It can be seen from the table that micro-organisms grew as temperature increased from 28 to 34^{o}C after which the growth started decreasing. This decrease in microbial effluent concentration was as a result of increase in temperature which made the condition unfavourable to the micro-organism. A mesophilic digester should be maintained between 30^{o}C and 35^{o}C for optimal functioning.

The pH of the effluent was between 6.6 and 7.8 during the digestion period, which indicates sufficient alkalinity of the reactor medium for the wastewater. A bioreactor should be operated at pH values between 6.7 and 7.4 because the methanogenic activity falls when the pH value decreases below 6.5. Another study Yadvika *et al*. (2004) reported a desired pH range of 6.8-7.2 for anaerobic digestion. Jash and Ghosh (1996) reported a favourable pH range of 6.6-7.8 for methanogenic bacteria. The percentage total suspended solid (TSS) decreased as hydraulic retention time increased.

Kinetic evaluation

The kinetics of the microbial process of anaerobic digestion may be divided into kinetics of growth and kinetics of food (or substrate) utilization. Some kinetics

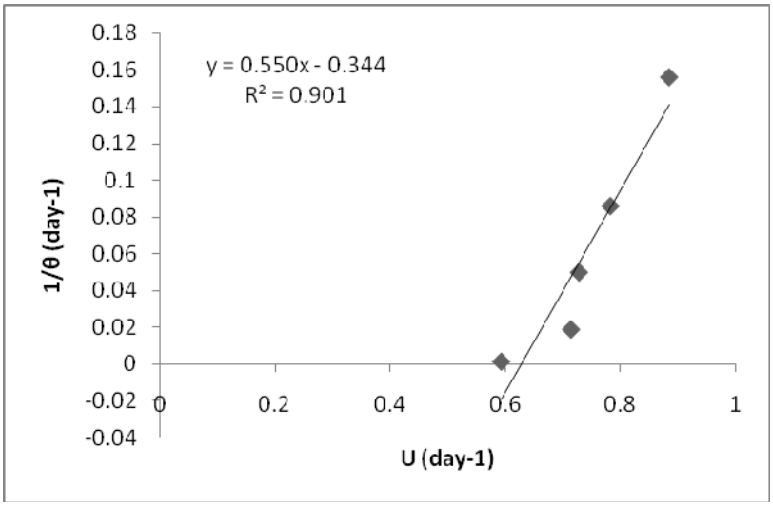

Fig. 4. Plot for determination of Y and K_d

models were investigated. A time-averaged cell mass (Reynolds and Richards, 1996) was used for COD determination.

According to Raj and Anjaneyulu (2005) limited substrate consumption is a first order reaction which can be expressed as:

$$\frac{-ds}{dt} = K'S \quad (1)$$

Where K' is the rate constant?

The above equation is characterized as exponential growth and the substrate concentration profile with respect to hydraulic retention time (HRT) as follows:

$$S = S_o \exp(-K_s t) \quad (2)$$

Where S_o is the influent substrate concentration (mg/l), S is the effluent substrate concentration (mg/l) and t is hydraulic retention time (days).

Equation (2) shows the exponential growth of the organism as the substrate is utilized. Rearranging and taking natural logarithm of both sides of Equation (2) gives equation (3)

$$In\left(\frac{S_e}{S_o}\right) = -K_s t \quad (3)$$

A plot of - $In(S_e/S_o)$ against t was linear as shown in Figure 2, with regression coefficient of 0.974. This confirmed that the kinetics of POME digestion followed a first order reaction.

The rate of substrate utilization (U) is related to effluent substrate concentration (Se) according to Equation (4) (Viessman and Hammer, 1993).

$$\frac{1}{U} = \frac{K_s}{KS_e} + \frac{1}{K} \quad (4)$$

Where K_s is half-velocity constant (mg/l), K is the maximum rate of substrate utilization (day^{-1}).

A plot of $\frac{1}{U}$ against $\frac{1}{S_e}$ was linear as shown in figure 3 with $\frac{K_s}{K}$ and $\frac{1}{K}$ as slope and intercept respectively. Values of K and K_s calculated from the intercept and slope of the graph were $0.868day^{-1}$ and 97.66mg/l respectively, suggesting that the digesting microbes requires much retention time to regenerate and hence inoculation for better performance.

The specific rate of substrate utilization is related o mean cell residence time according to Equation (5).

$$\frac{1}{\theta} = YU - K_d \quad (5)$$

Where θ is mean cell residence time (day), K_d is the endogenous decay coefficient (day-1) and Y is the biomass yield (mg/mg).

A straight line graph was obtained by plotting 1/θ against U as shown in figure 4. From the slope and intercept of the graph, the Y and K_d value was obtained as 0.550mg/mg and $0.344day^{-1}$ respectively.

The maximum specific rate of growth of micro-organism μ_{max} is related to biomass yield Y and maximum rate of substrate utilization K according to Equation (6).

$$K = \frac{\mu_{max}}{Y} \quad (6)$$

The maximum specific rate of growth of microorganism μ_{max} calculated from Equation (6) was $0.477day^{-1}$. Zinatizadeh *et al.* (2006) in their study on kinetic evaluation of palm oil mill effluent digestion in a high rate up-flow anaerobic sludge fixed film bioreactor obtained μ_{max} value of $0.207day^{-1}$. According to the

authors, the small value of μ_{max} implies relatively high amount of biomass in the reactor.

CONCLUSION

The results obtained from this research study reveal that palm oil mill effluent derived from palm oil production has a high level of anaerobic biodegradability and that substantial quantity of biogas can be obtained it. The kinetics of POME was well described by first order kinetic model. Biokinetic parameters K, K_s, K_d, Y and μ_{max} were found to be 0.868day^{-1}, 97.66mg/l, 0.344day^{-1}, 0.550 and 0.477day^{-1} respectively.

REFERENCES

Ahmad, AL., Isamail, S. and Bhatia, S. 2003. Water recycling from palm oil mill effluent (POME) using membrane technology, The European Conference on Desalination and the Environment: Fresh water for All, Malta.

Ahmad, AL., Bhatia, S., Ibrahim, N. and Samathi, S. 2005. Adsorption of residue oil from Palm oil mill effluent using rubber powder. Brazilian Jounal of Chemical Engineering. 22(3):371-379.

Angelidaki, I. and Ahring, BK. 1993. Thermophilic anaerobic digestion of livestock waste: The effect of ammonia. Applied Microbiology Biotechnology. 38:560-564.

Angelidaki, I., Ellegaard, L. and Ahring, BK. 1999. A comprehensive model of anaerobic bioconversion of complex substrates to biogas. Biotechnology and Bioengineering. 63:363-372.

APHA. 2005. Standard methods for the examination of water and wastewater (21st ed.). Washington, DC, USA.

Bek-Nielsen, C., Singh, G. and Toh, TS. 1999. Bioremediation of palm oil mill effluent. In: Processings Porim Inernational Palm Oil Congress, Kuala lumpur, Malaysia.

Jash, T. and Ghosh, DN. 1996. Studies on the solubilization kinetics of solid organic residues during anaerobic biomethanation. Energy. 21(7/8):725-730.

Jose, AL., Maria, AM., Artuor, FC. and Antonio, MM. 2009. Anaerobic digestion of glycerol derived from biodesiel manufacturing. Bioresource Technology. 100:5609-5615.

Keshtkar, A., Meyssami, B., Abolhamd, G., Ghaforian, H. and Asadi, MK. 2003. Mathematical modelling of non-ideal mixing continuous flow reactors for anaerobic digestion of cattle manure. Bioresource Technology. 87:113-124.

Maheswaran, A. and Singam, G. 1997. Pollution control in the palm oil industry-Promulgation of regulations: Planter. 53:470-476.

Mailleret, L., Bernard, O. and Steyer JP. 2004. Nonlinear adaptive control with unknown kinetics. Automatica. 40(8):1379-1385.

Perez, M., Ronero, LI. and Sales, D. 2001. Organic matter degradation kinetics in an anaerobic thermophilic fluidized bed bioreactor. Anaerobe. 25-35.

Raj, SSD. and Anjaneyulu, Y. 2005. Evaluation of biokinetic parameters for pharmaceutical wastewaters using aerobic oxidation integrated with chemical treatment process. Biochem. 40:165-175.

Reynolds, TD. and Richards, PA. 1996. Units operations and processes in environmental engineering (2nd ed.). PWA Publishing Co. Boston, USA. 798.

Viessman, WJr. and Hammer, MJ. 1993. Waste supply and pollution control. Happer Collins College Publishers. New York, USA. 513-679.

Yadvika, S., Sreekrishnan, TR., Kohil, S. and Rana, V. 2004. Enhancement of biogas production from solid substrates using different techniques: a review. Bioresourece Technology. 95:1-10.

Yilmaz, AH. and Atalay, FS. 2003. Modelling of the anaerobic decomposition of solid wastes. Energy Sources. 25:1063-1072.

Zinatizadeh, AAL., Mohamed, AR., Abdullah, AZ., Mashitah, MD., Hasnain Isa, M. and Njafpour, GD. 2006. Process modelling and analysis of palm oil mill effluent treatment in an up-flow anaerobi sludge fixed film bioreactor using response surface methodology (RSM). Water Res. 40:3193-3208.

Received: June 24, 2011; Accepted: Dec 28, 2011

SENRA Academic Publishers, Burnaby, British Columbia
Vol. 6, No. 1, pp. 1883-1895, Feb 2012
Online ISSN: 1920-3853; Print ISSN: 1715-9997

Canadian Journal of pure&applied sciences

INVESTIGATING CONCRETE STEEL REBAR DEGRADATION USING SOME SELECTED INHIBITORS IN MARINE AND MICROBIAL MEDIA

*Omotosho, O A[1], Loto, C A[1,2] and James, O O[3]
[1]Department of Mechanical Engineering, Covenant University
[2]Department of Chemical and Metallurgical Engineering
Tshwane University of Technology, Pretoria, South Africa
[3]Department of Chemistry, Covenant University, P.M.B 1023, Ota, Nigeria

ABSTRACT

Potential monitoring investigations were conducted on concrete steel rebar samples premixed with selected inhibitors accompanied by fixed amount of sodium chloride salt and partially immersed in sulphuric acid and sodium chloride solution. Varying concentration of potassium dichromate, potassium chromate and sodium nitrite inhibitors were used individually and synergistically in this study. The potential readings were taken in accordance with ASTM C 876 through the open circuit potential corrosion monitoring technique. Suppressive quality and dependability of the inhibitor was then assessed by the Weibull probability density distribution as an extreme value statistical modeling approach to study performance effectiveness and forecast the most effective inhibitor concentration in each media. Inhibitor effect on the compressive strengths of the reinforced concrete samples was also examined and reported. Results showed that 0.15M potassium chromate inhibitor had the best overall and individual performance in its inhibiting ability in the H_2SO_4 medium, while 0.68M sodium nitrite admixture was predicted as showing the lowest probability of corrosion risk in NaCl medium. Also, the best synergistic performance was shown by sample admixed with 0.06M $K_2Cr_2O_7$, 0.15M K_2CrO_4 and 0.27M $NaNO_2$ partially immersed in the NaCl medium. The compressive strength of concrete sample admixed with 0.03M $K_2Cr_2O_7$ and 0.10M K_2CrO_4 was the highest amongst samples admixed with inhibitor in both media, though the control sample partially immersed in the NaCl medium had the highest overall compressive strength value.

Keywords: Potential, concrete steel rebar corrosion, kolmogorov–smirnov statistics, compressive strength, Weibull distribution.

INTRODUCTION

Instances of building collapse have become an issue of concern in Lagos, South western-Nigeria with statistics from Lagos State Physical Planning and Development Authority showing Lagos Island has having the highest frequency of the incidences recorded. The high incidences of collapsed structures in Lagos Island may be connected with its proximity to the Atlantic where ample supply of salt is available (Omotosho, 2011). Corrosion of steel rebar in concrete is a phenomenon that has been linked to structural failure in concrete infrastructure. This phenomenon is prevalent in marine and sewage environments because of the presence of chloride and sulphate ions. These ions have the tendency of destroying the passive film on steel surface. The ever increasing Lagos population has also led to increased deposition of sewer waste in these water bodies, thereby increasing biogenic sulphuric acid attack (BSA) on concrete infrastructure.

The hydration reactions in cement components produce hydroxides which increase alkalinity within the pore structure of concrete by the formation of a passive film that protects the steel rebar from corrosion (Liu, 1996; Smith and Virmani, 2000). This buffer can be completely run-down by the entry of hostile electrochemical agents of corrosion in the form of carbonation, chloride contamination (Schiegg *et al*., 2000; Richard, 2002; NEA/CSNI, 2002 and Bertolini *et al*., 2004) and BSA on concrete in sewage environments (Hewayde *et al*., 2007). Carbonation hardens the concrete and reduces the alkalinity between steel and concrete, while the chloride ions breaks down the protective passive oxide layer which was originally produced by the passivating alkaline pore water on the embedded steel surface ((NEA/CSNI, 2002). The potency of BSA attack on concrete structure destroys hydration products of concrete changing it to gypsum and stimulates the formation of ettringite or hydrated calcium aluminium sulphate hydroxide. This is achieved through the dual mechanisms of sulphate reducing bacteria and sulphur oxidizing bacteria on concrete (Parande *et al*., 2006; Vollertsen *et al*., 2008).

However, several researchers Omotosho *et al*. (2010), Omotosho (2011), Omotosho *et al*. (2011) and Loto *et al*.

*Corresponding author email: olugbenga.omotosho@covenantuniversity.edu.ng

Table 1. Composition of steel rebar employed for the experiment.

Element	C	Si	Mn	P	S	Cu	Cr	Ni	Fe
Composition (%)	0.3	0.25	1.5	0.04	0.64	0.25	0.1	0.11	96.81

Table 2. List of Premixed Inhibitor Samples with fixed amount of NaCl in concrete.

S/N	Concrete Block Sample	Inhibitor Concentration
1	Concrete premixed with 0.1M NaCl (control sample).	None
2	Concrete premixed with 0.1M NaCl.	0.03M $K_2Cr_2O_7$
3	Concrete premixed with 0.1M NaCl.	0.06M $K_2Cr_2O_7$
4	Concrete premixed with 0.1M NaCl.	0.10M $K_2Cr_2O_7$
5	Concrete premixed with 0.1M NaCl.	0.13M $K_2Cr_2O_7$
6	Concrete premixed with 0.1M NaCl.	0.16M $K_2Cr_2O_7$
7	Concrete premixed with 0.1M NaCl.	0.19M $K_2Cr_2O_7$
8	Concrete premixed with 0.1M NaCl.	0.05M K_2CrO_4
9	Concrete premixed with 0.1M NaCl.	0.10M K_2CrO_4
10	Concrete premixed with 0.1M NaCl.	0.15M K_2CrO_4
11	Concrete premixed with 0.1M NaCl.	0.19M K_2CrO_4
12	Concrete premixed with 0.1M NaCl.	0.24M K_2CrO_4
13	Concrete premixed with 0.1M NaCl.	0.29M K_2CrO_4
14	Concrete premixed with 0.1M NaCl.	0.14M $NaN0_2$
15	Concrete premixed with 0.1M NaCl.	0.27M $NaN0_2$
16	Concrete premixed with 0.1M NaCl.	0.41M $NaN0_2$
17	Concrete premixed with 0.1M NaCl.	0.54M $NaN0_2$
18	Concrete premixed with 0.1M NaCl.	0.68M $NaN0_2$
19	Concrete premixed with 0.1M NaCl.	0.82M $NaN0_2$
20	Concrete premixed with 0.1M NaCl.	0.03M $K_2Cr_2O_7$, 0.10M K_2CrO_4
21	Concrete premixed with 0.1M NaCl.	0.06M $K_2Cr_2O_7$, 0.05M K_2CrO_4
22	Concrete premixed with 0.1M NaCl.	0.03M $K_2Cr_2O_7$, 0.41M $NaNO_2$
23	Concrete premixed with 0.1M NaCl.	0.03M $K_2Cr_2O_7$ 0.14M $NaNO_2$
24	Concrete premixed with 0.1M NaCl.	0.05M K_2CrO_4, 0.27M $NaNO_2$
25	Concrete premixed with 0.1M NaCl.	0.10M K_2CrO_4, 0.14M $NaNO_2$
26	Concrete premixed with 0.1M NaCl.	0.03M $K_2Cr_2O_7$, 0.10M K_2CrO_4, 0.41M $NaNO_2$
27	Concrete premixed with 0.1M NaCl.	0.06M $K_2Cr_2O_7$, 0.15M K_2CrO_4, 0.27M $NaNO_2$
28	Concrete premixed with 0.1M NaCl.	0.10M $K_2Cr_2O_7$, 0.05M K_2CrO_4, 0.14M $NaNO_2$

(2011) have identified the use of corrosion inhibitors as a practicable means of combating the challenges associated with protecting concrete steel rebar from corrosion. Some of these articles worked on the use of individual inhibitors (Omotosho *et al*., 2011; Loto *et al*., 2011) while others used two inhibitors in synergy (Omotosho *et al*., 2010; Omotosho, 2011) but none has worked on the use of three inhibitors in synergy amongst the studies conducted so far. Of the articles examined, none has used potassium dichromate, potassium chromate and sodium nitrite as inhibitors in combined synergy on concrete steel rebar partially immersed in saline and sulphate media. Aside from this there is paucity of articles that has used a statistical means to analyze data emanating from open circuit potential (OCP) monitoring experiments because of the fluctuations experienced in potential readings taken.

Therefore, this paper focuses primarily on investigating the individual and synergistic effects of potassium dichromate, potassium chromate and sodium nitrite on concrete steel rebar degradation in saline and sulphate simulating environments by using a two-parameter Weibull distribution function to analyze the varying or fluctuating potential readings in order to be able to clarify data appropriately and to identify the most effective inhibitor concentration. Weibull analysis was also used to categorize inhibitor admixtures according to ASTM C 876. In addition, the concrete test samples used in the experiments were also subjected to compressive strength tests.

MATERIALS AND METHODS

A mix ratio of 1:2:4 consisting of mixtures of Portland cement (320kg/m^3), sand (700kg/m^3) and gravel (1150

kg/m^3) were used for preparing the experimental concrete blocks. All these were mixed with water (140kg/m^3) (Omotosho *et al*., 2010; Omotosho, 2011).

The first of the two sets of blocks was prepared for the sodium chloride and sulphuric acid media. This first set was made up of twenty eight blocks for each media but a total of fifty six for the two media. The blocks were cast with different inhibitor concentration premixed with fixed amount of sodium chloride. For each of the premixed inhibitor and the NaCl the percentages quoted were estimated based on every 10kg weight of the concrete from which the blocks were prepared. All reagents used were AnalaR grade. The composition of steel rebar used in the concrete and the list of the concrete blocks with premixed inhibitors is shown in tables 1 and 2 respectively. The 10mm diameter steel rebar inserted in the concrete block was cut into numerous pieces each with a length of 160mm. An abrasive grinder was used to remove mill scale and rust stains on the specimens before it was inserted in each concrete block. Only 140mm of the steel rebar was inserted in the block, the remaining 20mm stuck out at one end of the block and it was coated to prevent atmospheric corrosion. This part was connected to the multimeter. The test solutions used for the experiment with their concentration were; 3.5% NaCl solution and 0.5M dilute sulfuric acid. The reference electrode used in the experiment was the copper sulphate electrode (CSE).

The second set was made up of two concrete block samples with no premixed inhibitor in their formulation. They were intentionally made for determining strength under diverse curing conditions. One of the concrete blocks in the second group was cured in air for two weeks, and the other was cured in water for the same period (Omotosho *et al*., 2011).

The schematic diagram of the experimental set up can be obtained elsewhere (Omotosho *et al*., 2011; Loto *et al*., 2011). Electrochemical potential readings were obtained by positioning a copper/copper sulfate electrode (CSE) securely on the concrete sample. The two terminals of the digital multimeter were connected to the copper sulfate electrode and the visible part of the embedded steel rebar respectively. This was done to make an absolute electrical circuit. Record of the readings was taken at three separate locations on each concrete block directly over the embedded steel rebar (Omotosho *et al*., 2010; Omotosho *et al*., 2011). The mean of the three readings obtained was estimated as the potential reading for the steel rebar in two-day intervals for 32 days. The experiments were conducted under free corrosion potential and at ambient temperature of 25^{o}C. The immersion of the sample blocks in the test medium was partial; the level of the test solution was just beneath the visible part of the steel rebar to prevent contact. Data examination and analysis of experimental readings was performed using the technique employed elsewhere (Omotosho *et al*., 2010; Omotosho *et al*., 2011) which involved the use of a two-parameter Weibull distribution function given by Equation 1.

$$F(x)=1-\exp\left(-\left(\frac{x}{j}\right)^{l}\right) \quad (1)$$

Where l and j is the shape and scale parameter respectively.

The quality of the data was also measured by a Weibull prediction of the mean μ (Omotosho *et al*., 2010):

$$\nu = j\Gamma\left(1+\frac{1}{l}\right) \quad (2)$$

Where Γ ( ) is the gamma function of ( )

In a bid to ascertain the consistency of the OCP data to Weibull distribution, a goodness of fit test was conducted using the Kolmogorov-Smirnov (K-S) test (Omotosho *et al*., 2010; Omotosho *et al*., 2011). The K-S test was used to determine the contrast the empirical F^* and the theoretical distribution function F(x) (Omotosho *et al*., 2010; Omotosho *et al*., 2011).

$$d = d(x_1,...,x_n) = \sqrt{n}\sup_{-\infty<x<\infty}\left|F^*(x) - F(x)\right| \quad (3)$$

Where n is the number of the analyzed data points.

Subsequently, at a significant level of α = 0.05, the P-value of the K-S test is subjected to the hypothesis test:

$$\begin{aligned} S_o &: P \geq \alpha \\ S_A &: P \geq \alpha \end{aligned} \quad (4)$$

Where S_o and S_A is the null and alternative hypothesis such that the OCP data follow and does not follow the two-parameter Weibull distribution respectively (Omotosho *et al*., 2010; Omotosho *et al*., 2011). The influence of the inhibitors on the compressive strength of the test samples was established using the concrete samples in the second set of samples alluded to earlier. The completion of the electrochemical potential monitoring process was followed by the removal of steel-reinforced test samples from their test medium for the purpose of air-hardening them for seven days. Each block was subsequently subjected to weighing and compressive fracture test (Omotosho *et al*., 2011).

RESULTS AND DISCUSSION

Concrete samples premixed with potassium dichromate in sulfuric acid and sodium chloride medium

The plots of mean corrosion potential versus time for the control specimen in both sulphuric acid and NaCl medium are presented in figure 1. Potential reading of steel in the control specimen moved from the active region at -

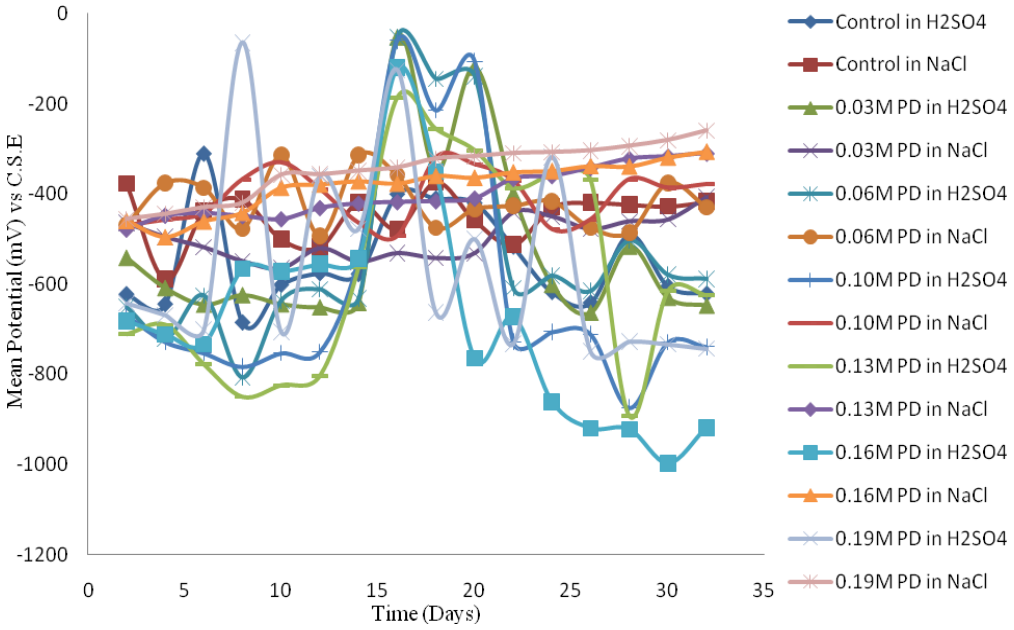

Fig. 1. Relationship of corrosion potential with time for test sample admixed with varying concentration of $K_2Cr_2O_7$ and 0.1M NaCl in H_2SO_4 and NaCl media.

620mV (CSE) to the passive region at -315mV (CSE) on the 7th day. This was because the sulphate ions in the medium had not reached the steel surface as a result of the protection provided by the alkaline pore solution of the concrete. Starting from the 8th to the 15th day, potential reading was in the active region, it then moved towards the passive region until the 20th day. The sulphate ions in the medium may have succeeded in destroying the alkaline barrier resulting in the active corrosion potential observed. Subsequently, the corrosion products suppressed the corrosion reaction and this led to the passive potential. Steel potential that became active after the 20th day is attributable to the dissolution of the corrosion products which exposed steel rebar surface.

The corrosion potential of the control test sample in the NaCl medium as shown in figure 1 drifted from the passive region of -348mV(CSE) to the active region of -605mV(CSE) in the first 5 days of the experiment. After the 5th day, potential readings increased gradually to -400mV (CSE) on the 14th day indicating that the alkaline barrier between steel rebar and the chloride ions in the matrix was capable of reducing corrosion. This trend was sustained until the experiment ended except for the fluctuation on the 25th day.

The potential versus time curves for concrete steel rebar admixed with varying amounts of potassium dichromate partially immersed in H_2SO_4 and NaCl media are presented in the figure 1. An observation of the potassium dichromate potential curves for the two media shows that the inhibitor was more effective in the NaCl environment. Generally, a decrease in the negative potential of steel was shown by the NaCl medium throughout the experiment. It was also observed that higher inhibitor concentration produced improved inhibition for both media but it was not prolonged in the H_2SO_4 medium. The phenomenon of passsivation (surface film formation), depassivation and repassivation was fluctuating throughout the experiment in both media, but was milder in the H_2SO_4 medium. In addition, it was observed that the inhibitor did not totally prevent corrosion but only reduced or delayed its commencement in a corrosive environment. The inhibition effectiveness observed in the NaCl medium as concentration increased may be as a result of anions becoming inhibitive or acting in such a way as to seal holes in the passive film. The sulphate ions in the H_2SO_4 media did not permit the anions to become effectual rather it stifled their action which may have resulted in the fluctuating depassivation and repassivation phenomenon that was observed throughout the experiment.

Samples premixed with potassium chromate in sulfuric acid and sodium chloride medium

The plots of potential readings against time obtained for the concrete test samples partially immersed in sulphuric acid and sodium chloride are presented in figure 2. It is obvious from the curves obtained that the potential readings demonstrated upward and downward shift from the beginning of the experiment to the end in the two test media, though this incessant spikes and unsteadiness of

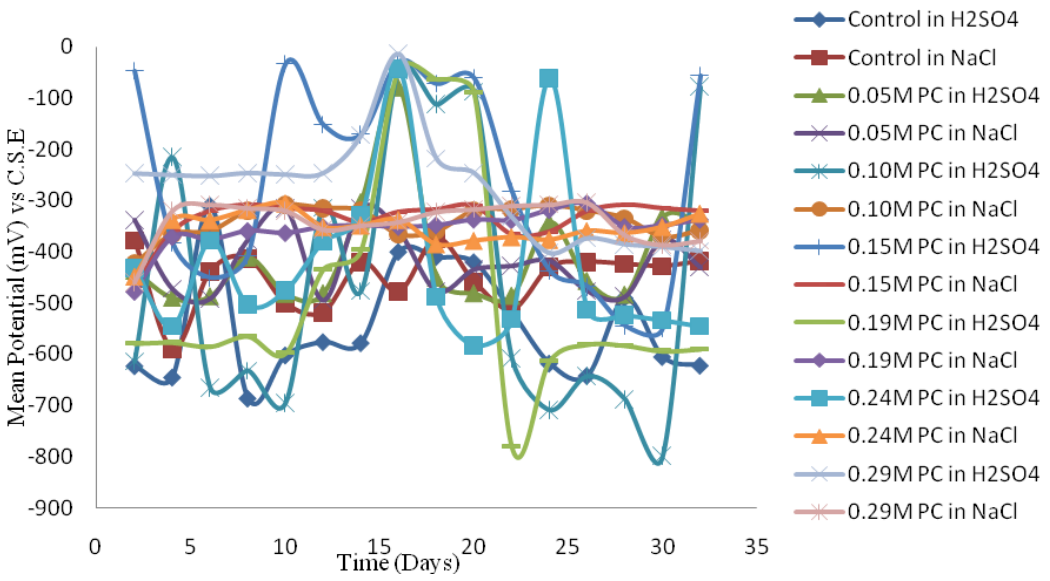

Fig. 2. Relationship of corrosion potential with time for test sample admixed with varying concentration of K_2CrO_4 and 0.1M NaCl in H_2SO_4 and NaCl media.

the readings were less in the NaCl medium indicating that there may be a correlation between the OCP readings and action of NaCl environment. Fundamentally, the shift of the readings towards the passive region infers that the inhibitors were able to protect steel rebar from corrosion through the formation of a thin passive film on the surface of the steel whereas the drift into the active region shows that the aggressive ions present in the medium succeeded in destroying the passive film on the steel rebar as was the case for most of the samples in the sulphuric acid medium. In certain instances, as observed in the curves in figure 2 the destruction of the film was short-lived, while in other instances it was prolonged. This phenomenon of repeated destruction and repair of the passive film on the steel rebar led to persistent and frequent fluctuations. This unsteadiness of the readings may have occurred because of the continued contest between the alkaline environment around steel rebar in the concrete test samples and the acidic environment of the sulphuric acid or the chloride ions in the NaCl medium. The complex steel-concrete-inhibitor-media reaction may be another reason for these fluctuations. Hence, the H_2SO_4 medium was more aggressive because of the presence of sulphate ions and therefore fluctuations became more repeated, continuous, erratic and apparent, whereas the samples in the NaCl medium showed fewer fluctuations.

Samples premixed with sodium nitrite in sulfuric acid and sodium chloride medium

The curves of potential versus time for concrete steel rebar premixed with varying concentration of sodium nitrite partially immersed in NaCl and H_2SO_4 media are presented in figure 3. Clearly the $NaNO_2$ inhibitor was not so effective in the H_2SO_4 medium. Throughout the experimental period fluctuating corrosion potential was displayed and most of the potential reading was in the active corrosion region. In the NaCl medium, it is observed that the $NaNO_2$ inhibitor is more effective as more passivating potential was experienced showing that the H_2SO_4 medium produced sulphate ions that suppressed the activity of the inhibitor throughout the experimental period. Nitrite is an anodic inhibitor that offers only single action inhibitive effect on the steel as revealed in figure 3 in the case of concrete steel rebar in the NaCl medium. The inhibitive effect also increased with increase in nitrite additions in the NaCl medium which indicates that a higher amount of this inhibitor is required to promote anodic passivity. However, the phenomenon of fluctuating corrosion potential was more pronounced in the sulphuric acid medium throughout the duration of the experiment.

Samples premixed with synergetic combination of inhibitors in sulfuric acid and sodium chloride medium

Figures 4 and 5 show the curves of potential against time for concrete steel rebar premixed with synergetic combination of two and three inhibitors respectively in sulphuric acid and sodium chloride medium. The behavior displayed by these synergetic combinations is not so different from the individual use of the inhibitors. Worthy of note is the fact that some of the synergetic combinations showed improved performance in the NaCl medium when compared to the sulphuric acid medium. It

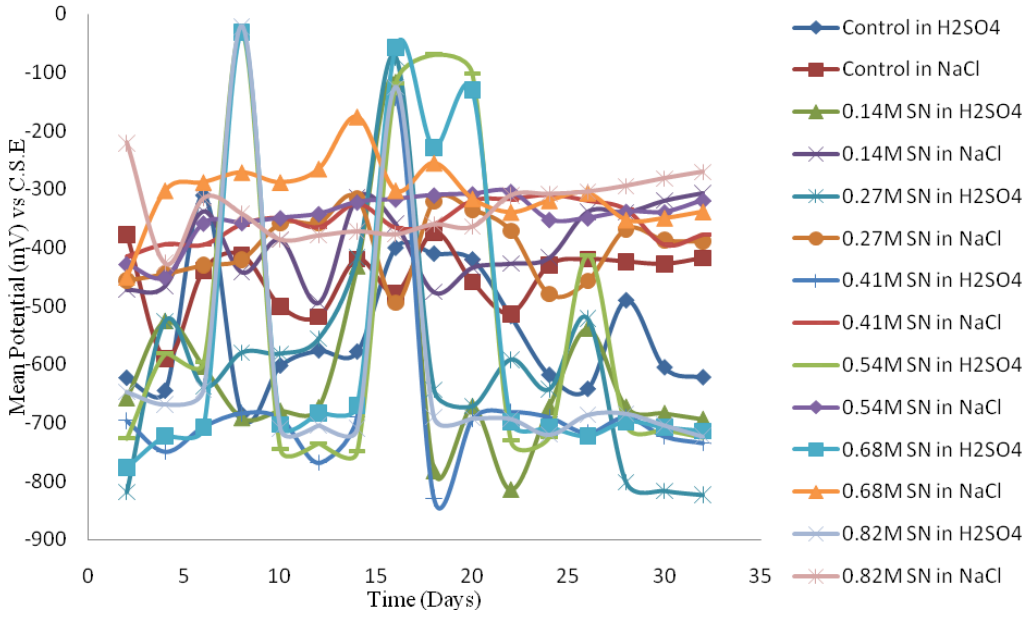

Fig. 3. Relationship of corrosion potential with time for test sample admixed with varying concentration of $NaNO_2$ and 0.1M NaCl in H_2SO_4 and NaCl media.

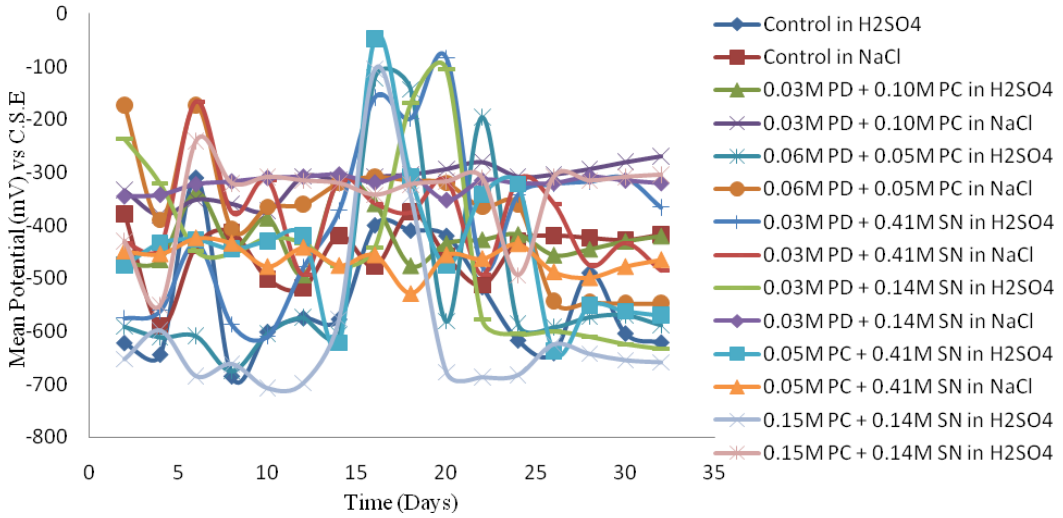

Fig. 4. Relationship of corrosion potential with time for test sample admixed with varying concentration of two inhibitors per sample and 0.1M NaCl in H_2SO_4 and NaCl media.

was also observed that fluctuations also reduced when the inhibitors were synergistically combined and in fact reduced more in the NaCl medium, but these fluctuations did not disappear.

However, the inference that could be drawn from figures 1 to 5 is that data became difficult to understand and it also became almost impossible to identify the most efficient inhibitor concentration. Therefore, it became imperative that a tool having the capacity to analyze data satisfactorily would be needed to interpret and establish the most effective inhibitor concentration. A two-parameter Weibull distribution function was therefore utilized to perform the task. By engaging a statistical tool to determine the quality and the reliability of inhibitions in the respective media, a clear interpretation of the inhibitions in the test media could be obtained irrespective of the fluctuations displayed by the admixed inhibitors. Subsequently, Weibull distribution fittings to the OCP measurements for the premixed inhibitor were made. The aptness and dependability of the fittings were then investigated using the K–S goodness of fit test in a bid to

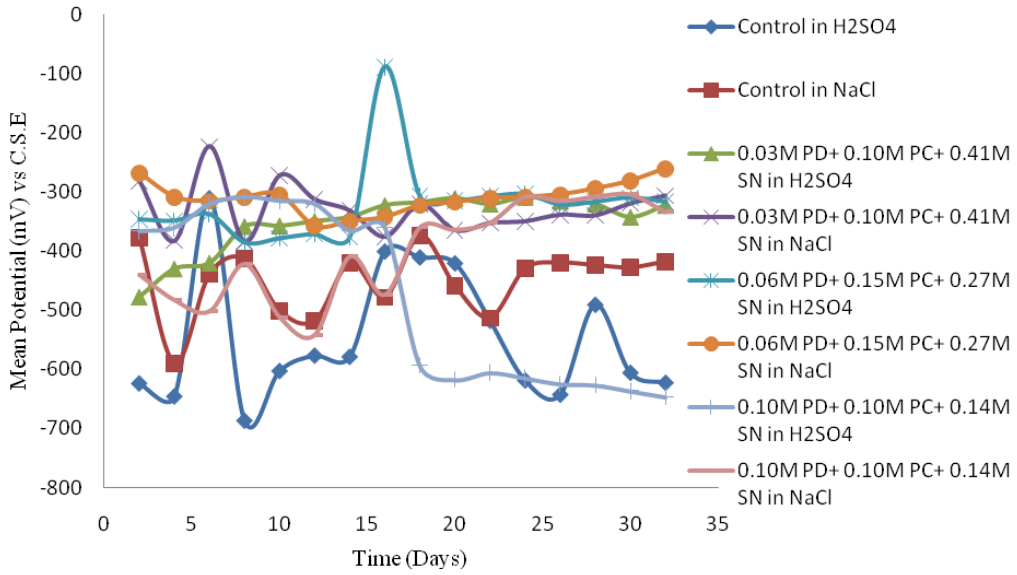

Fig. 5. Relationship of corrosion potential with time for test sample admixed with varying concentration of three inhibitors per sample and 0.1M NaCl in H_2SO_4 and NaCl media.

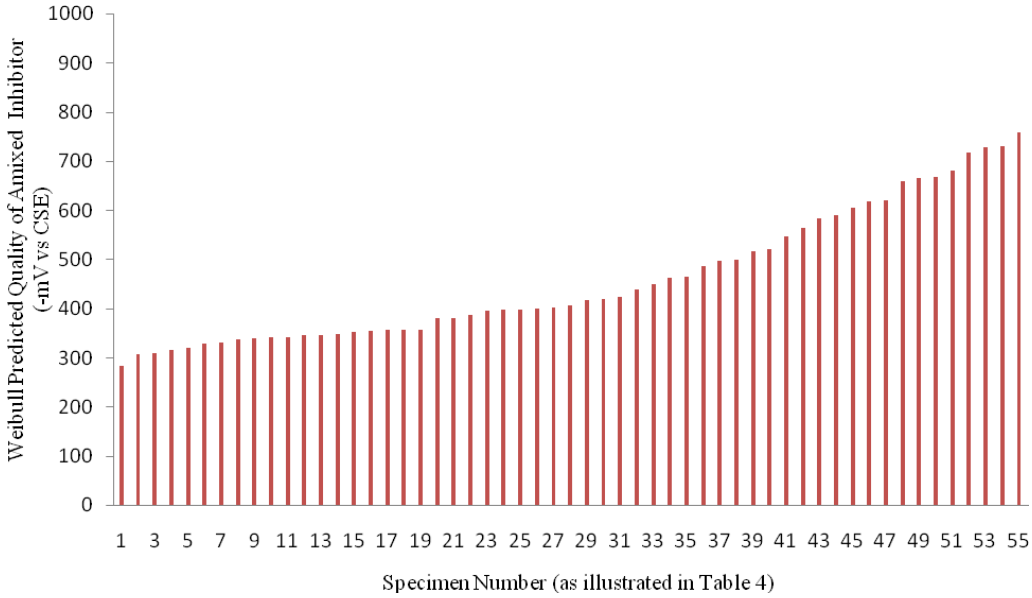

Fig. 6. Performance ranking of inhibiting quality of premixed inhibitor based on prediction by the Weibull distribution.

determine the consistencies of the OCP measurements for each admixed inhibitor with the Weibull distribution fittings. The results obtained are shown in table 3.

Weibull result and evaluation

In table 3 the value of l for all inhibitor amounts show that the data spread exhibits good consistency with relatively small scatter. Most of the samples comply with the null hypothesis which shows that the OCP data came from a two-parameter Weibull distribution based on the P-value of the K-S test from ($P \geq 0.05$). The null hypothesis was not satisfied by certain samples in table 3, this samples identified with their numbers are 25, 30, 36, 40, 44, 46, 47, 49, 53 and 55.

The sudden increase in the negative corrosion potential in the first 12 days of the experiment may have been the reason why the specimen did not satisfy the null hypothesis. The increased negative potential could also have led to pitting corrosion because of the presence of sulphate and chloride ions in which the specimens were partially immersed.

Table 3. Weibull distribution fitting results of inhibitor admixtures in reinforced concrete samples.

S/N	Admixture	Medium	l	j	ν	Prob (μ)	P-value (K-S) test
1	Control	NaCl	8.723	475.482	449.621	0.459	0.356
2	0.03M $K_2Cr_2O_7$	NaCl	11.628	518.347	496.135	0.452	0.936
3	0.06M $K_2Cr_2O_7$	NaCl	7.593	446.035	418.971	0.463	0.896
4	0.10M $K_2Cr_2O_7$	NaCl	7.643	432.697	406.577	0.463	0.552
5	0.13M $K_2Cr_2O_7$	NaCl	7.821	423.742	398.616	0.462	0.787
6	0.16M $K_2Cr_2O_7$	NaCl	7.688	405.138	380.792	0.463	0.263
7	0.19M $K_2Cr_2O_7$	NaCl	6.415	372.313	346.669	0.469	0.495
8	0.05M K_2CrO_4	NaCl	7.049	445.544	416.931	0.465	0.852
9	0.10M K_2CrO_4	NaCl	11.290	357.148	341.455	0.452	0.277
10	0.15M K_2CrO_4	NaCl	7.969	357.002	336.141	0.461	0.059
11	0.19M K_2CrO_4	NaCl	9.841	374.249	355.799	0.456	0.164
12	0.24M K_2CrO_4	NaCl	11.893	371.702	356.077	0.451	0.816
13	0.29M K_2CrO_4	NaCl	8.574	361.505	341.570	0.459	0.259
14	0.14M $NaN0_2$	NaCl	6.573	423.549	394.890	0.468	0.755
15	0.27M $NaN0_2$	NaCl	7.829	423.156	398.083	0.462	0.816
16	0.41M $NaN0_2$	NaCl	11.898	371.516	355.904	0.451	0.955
17	0.54M $NaN0_2$	NaCl	9.020	365.539	346.188	0.458	0.089
18	0.68M $NaN0_2$	NaCl	5.544	332.708	307.296	0.475	0.594
19	0.82M $NaN0_2$	NaCl	6.802	354.613	331.222	0.467	0.914
20	0.03M $K_2Cr_2O_7$, 0.10M K_2CrO_4	NaCl	10.358	331.764	316.090	0.454	0.253
21	0.06M $K_2Cr_2O_7$, 0.05M K_2CrO_4	NaCl	3.120	425.566	380.698	0.507	0.674
22	0.03M $K_2Cr_2O_7$, 0.41M $NaNO_2$	NaCl	3.966	426.939	386.792	0.491	0.587
23	0.03M $K_2Cr_2O_7$, 0.14M $NaNO_2$	NaCl	22.941	327.499	319.851	0.441	0.075
24	0.05M K_2CrO_4, 0.27M $NaNO_2$	NaCl	19.090	476.672	463.494	0.443	0.799
25	0.10M K_2CrO_4, 0.14M $NaNO_2$	NaCl	4.550	379.141	346.216	0.484	0.024
26	0.03M $K_2Cr_2O_7$, 0.10M K_2CrO_4, 0.41M $NaNO_2$	NaCl	8.018	347.528	327.319	0.461	0.984
27	0.06M $K_2Cr_2O_7$, 0.15M K_2CrO_4, 0.27M $NaNO_2$	NaCl	13.065	321.094	308.648	0.449	0.683
28	0.10M $K_2Cr_2O_7$, 0.05M K_2CrO_4, 0.14M $NaNO_2$	NaCl	5.342	435.931	401.786	0.476	0.659
29	Control	H_2SO_4	4.985	595.688	546.846	0.479	0.572
30	0.03M $K_2Cr_2O_7$	H_2SO_4	1.378	662.188	605.050	0.586	0.027
31	0.06M $K_2Cr_2O_7$	H_2SO_4	1.311	670.344	618.112	0.593	0.087
32	0.10M $K_2Cr_2O_7$	H_2SO_4	0.365	515.080	2251.364	0.820	0.049
33	0.13M $K_2Cr_2O_7$	H_2SO_4	2.338	658.847	583.803	0.529	0.925
34	0.16M $K_2Cr_2O_7$	H_2SO_4	2.056	808.576	716.289	0.541	0.360
35	0.19M $K_2Cr_2O_7$	H_2SO_4	1.475	686.007	620.583	0.578	0.076
36	0.05M K_2CrO_4	H_2SO_4	2.115	494.230	437.718	0.539	0.022
37	0.10M K_2CrO_4	H_2SO_4	1.142	545.374	520.091	0.612	0.316
38	0.15M K_2CrO_4	H_2SO_4	1.009	283.942	282.882	0.631	0.691
39	0.19M K_2CrO_4	H_2SO_4	1.104	611.594	589.469	0.617	0.103
40	0.24M K_2CrO_4	H_2SO_4	1.254	555.679	517.198	0.599	0.044
41	0.29M K_2CrO_4	H_2SO_4	1.171	373.278	353.410	0.609	0.054
42	0.14M $NaN0_2$	H_2SO_4	2.079	752.258	666.323	0.540	0.098
43	0.27M $NaN0_2$	H_2SO_4	1.664	760.920	679.979	0.564	0.075
44	0.41M $NaN0_2$	H_2SO_4	1.932	854.119	757.543	0.548	0.008
45	0.54M $NaN0_2$	H_2SO_4	0.995	657.743	659.043	0.633	0.075
46	0.68M $NaN0_2$	H_2SO_4	0.980	723.070	729.378	0.635	0.036
47	0.82M $NaN0_2$	H_2SO_4	0.915	898.800	937.469	0.646	0.004

continued..

Table 3 continue…

S/N	Admixture	Medium	l	j	ν	Prob (μ)	P-value (K-S) test
48	0.03M $K_2Cr_2O_7$, 0.10M K_2CrO_4	H_2SO_4	8.878	446.556	422.611	0.458	0.745
49	0.06M $K_2Cr_2O_7$, 0.05M K_2CrO_4	H_2SO_4	1.713	631.568	563.233	0.560	0.020
50	0.03M $K_2Cr_2O_7$, 0.41M $NaNO_2$	H_2SO_4	2.100	448.440	397.180	0.539	0.667
51	0.03M $K_2Cr_2O_7$, 0.14M $NaNO_2$	H_2SO_4	2.147	522.428	462.667	0.537	0.415
52	0.05M K_2CrO_4, 0.27M $NaNO_2$	H_2SO_4	1.594	556.566	499.171	0.569	0.142
53	0.10M K_2CrO_4, 0.14M $NaNO_2$	H_2SO_4	1.877	748.442	664.410	0.551	0.010
54	0.03M $K_2Cr_2O_7$, 0.10M K_2CrO_4, 0.41M $NaNO_2$	H_2SO_4	7.223	374.595	350.978	0.465	0.115
55	0.06M $K_2Cr_2O_7$, 0.15M K_2CrO_4, 0.27M $NaNO_2$	H_2SO_4	2.549	381.087	338.295	0.522	0.027
56	0.10M $K_2Cr_2O_7$, 0.05M K_2CrO_4, 0.14M $NaNO_2$	H_2SO_4	3.198	542.575	485.944	0.505	0.259

Table 4. Predicted Corrosion Condition.

S/N	Admixture	Medium	ν	Predicted Corrosion condition
1	0.15M K_2CrO_4	H_2SO_4	282.882	Intermediate corrosion risk
2	0.68M $NaN0_2$	NaCl	307.296	Intermediate corrosion risk
3	0.06M $K_2Cr_2O_7$, 0.15M K_2CrO_4, 0.27M $NaNO_2$	NaCl	308.648	Intermediate corrosion risk
4	0.03M $K_2Cr_2O_7$, 0.10M K_2CrO_4	NaCl	316.090	Intermediate corrosion risk
5	0.03M $K_2Cr_2O_7$, 0.14M $NaNO_2$	NaCl	319.851	Intermediate corrosion risk
6	0.03M $K_2Cr_2O_7$, 0.10M K_2CrO_4, 0.41M $NaNO_2$	NaCl	327.319	Intermediate corrosion risk
7	0.82M $NaN0_2$	NaCl	331.222	Intermediate corrosion risk
8	0.15M K_2CrO_4	NaCl	336.141	Intermediate corrosion risk
9	0.06M $K_2Cr_2O_7$, 0.15M K_2CrO_4, 0.27M $NaNO_2$	H_2SO_4	338.295	Intermediate corrosion risk
10	0.10M K_2CrO_4	NaCl	341.455	Intermediate corrosion risk
11	0.29M K_2CrO_4	NaCl	341.570	Intermediate corrosion risk
12	0.54M $NaN0_2$	NaCl	346.188	Intermediate corrosion risk
13	0.10M K_2CrO_4, 0.14M $NaNO_2$	NaCl	346.216	Intermediate corrosion risk
14	0.19M $K_2Cr_2O_7$	NaCl	346.669	Intermediate corrosion risk
15	0.03M $K_2Cr_2O_7$, 0.10M K_2CrO_4, 0.41M $NaNO_2$	H_2SO_4	350.978	Intermediate corrosion risk
16	0.29M K_2CrO_4	H_2SO_4	353.410	High (>90% risk of corrosion)
17	0.19M K_2CrO_4	NaCl	355.799	High (>90% risk of corrosion)
18	0.41M $NaN0_2$	NaCl	355.904	High (>90% risk of corrosion)
19	0.24M K_2CrO_4	NaCl	356.077	High (>90% risk of corrosion)
20	0.06M $K_2Cr_2O_7$, 0.05M K_2CrO_4	NaCl	380.698	High (>90% risk of corrosion)
21	0.16M $K_2Cr_2O_7$	NaCl	380.792	High (>90% risk of corrosion)
22	0.03M $K_2Cr_2O_7$, 0.27M $NaNO_2$	NaCl	386.792	High (>90% risk of corrosion)
23	0.14M $NaN0_2$	NaCl	394.890	High (>90% risk of corrosion)
24	0.03M $K_2Cr_2O_7$, 0.27M $NaNO_2$	H_2SO_4	397.180	High (>90% risk of corrosion)
25	0.27M $NaN0_2$	NaCl	398.083	High (>90% risk of corrosion)
26	0.13M $K_2Cr_2O_7$	NaCl	398.616	High (>90% risk of corrosion)
27	0.10M $K_2Cr_2O_7$, 0.05M K_2CrO_4, 0.14M $NaNO_2$	NaCl	401.786	High (>90% risk of corrosion)
28	0.10M $K_2Cr_2O_7$	NaCl	406.577	High (>90% risk of corrosion)
29	0.05M K_2CrO_4	NaCl	416.931	High (>90% risk of corrosion)
30	0.06M $K_2Cr_2O_7$	NaCl	418.971	High (>90% risk of corrosion)
31	0.03M $K_2Cr_2O_7$, 0.10M K_2CrO_4	H_2SO_4	422.611	High (>90% risk of corrosion)
32	0.05M K_2CrO_4	H_2SO_4	437.718	High (>90% risk of corrosion)
33	Control	NaCl	449.621	High (>90% risk of corrosion)
34	0.03M $K_2Cr_2O_7$, 0.14M $NaNO_2$	H_2SO_4	462.667	High (>90% risk of corrosion)

continued..

Table 4 continue…

S/N	Admixture	Medium	ν	Predicted Corrosion condition
35	0.05M K_2CrO_4, 0.27M $NaNO_2$	NaCl	463.494	High (>90% risk of corrosion)
36	0.10M $K_2Cr_2O_7$, 0.05M K_2CrO_4, 0.14M $NaNO_2$	H_2SO_4	485.944	High (>90% risk of corrosion)
37	0.03M $K_2Cr_2O_7$	NaCl	496.135	High (>90% risk of corrosion)
38	0.05M K_2CrO_4, 0.27M $NaNO_2$	H_2SO_4	499.171	High (>90% risk of corrosion)
39	0.24M K_2CrO_4	H_2SO_4	517.198	Severe corrosion
40	0.10M K_2CrO_4	H_2SO_4	520.091	Severe corrosion
41	Control	H_2SO_4	546.846	Severe corrosion
42	0.06M $K_2Cr_2O_7$, 0.05M K_2CrO_4	H_2SO_4	563.233	Severe corrosion
43	0.13M $K_2Cr_2O_7$	H_2SO_4	583.803	Severe corrosion
44	0.19M K_2CrO_4	H_2SO_4	589.469	Severe corrosion
45	0.03M $K_2Cr_2O_7$	H_2SO_4	605.050	Severe corrosion
46	0.06M $K_2Cr_2O_7$	H_2SO_4	618.112	Severe corrosion
47	0.19M $K_2Cr_2O_7$	H_2SO_4	620.583	Severe corrosion
48	0.54M $NaN0_2$	H_2SO_4	659.043	Severe corrosion
49	0.10M K_2CrO_4, 0.14M $NaNO_2$	H_2SO_4	664.410	Severe corrosion
50	0.14M $NaN0_2$	H_2SO_4	666.323	Severe corrosion
51	0.27M $NaN0_2$	H_2SO_4	679.979	Severe corrosion
52	0.16M $K_2Cr_2O_7$	H_2SO_4	716.289	Severe corrosion
53	0.10M $K_2Cr_2O_7$	H_2SO_4	728.907	Severe corrosion
54	0.68M $NaN0_2$	H_2SO_4	729.378	Severe corrosion
55	0.41M $NaN0_2$	H_2SO_4	757.543	Severe corrosion
56	0.82M $NaN0_2$	H_2SO_4	937.469	Severe corrosion

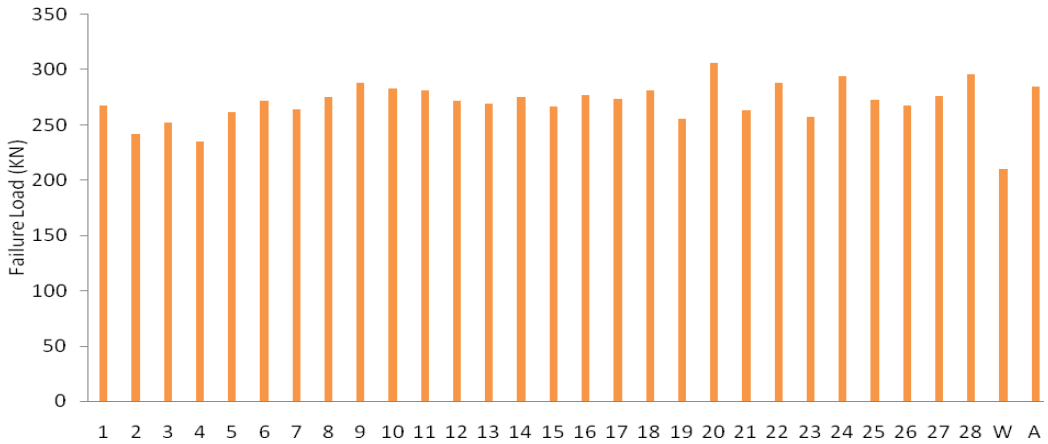

Fig. 7. Histogram of the compressive failure load for the reinforced concrete specimens immersed in sulfuric acid. W=concrete specimen cured in water, A= concrete specimen cured in air. Numbers 1 to 7 represents the list of concrete specimen described previously in table 2.

In addition, the mean values obtained from the Weibull assessment are suitable for appraising the level of corrosion according to ASTM C 876 standard of classification with reference to CSE as presented in table 4.

The performance ranking based on the prediction by the Weibull mean of inhibiting quality of admixed inhibitor in the reinforced concrete samples is presented in figure 6. From figure 6, specimen number 1 as shown in table 4 with 0.15M K_2CrO_4 admixture partially immersed in the H_2SO_4 medium has a maximum Weibull mean evaluation of -282.882 mV (CSE). The dependability of this predicted mean value stands at a probability of 69.1%. Directly at the rear of specimen 1 are specimens admixed with 0.68M $NaN0_2$ and the synergetic admixtures of 0.06M $K_2Cr_2O_7$, 0.15M K_2CrO_4, 0.27M $NaNO_2$ and 0.03M $K_2Cr_2O_7$, 0.10M K_2CrO_4 all partially immersed in

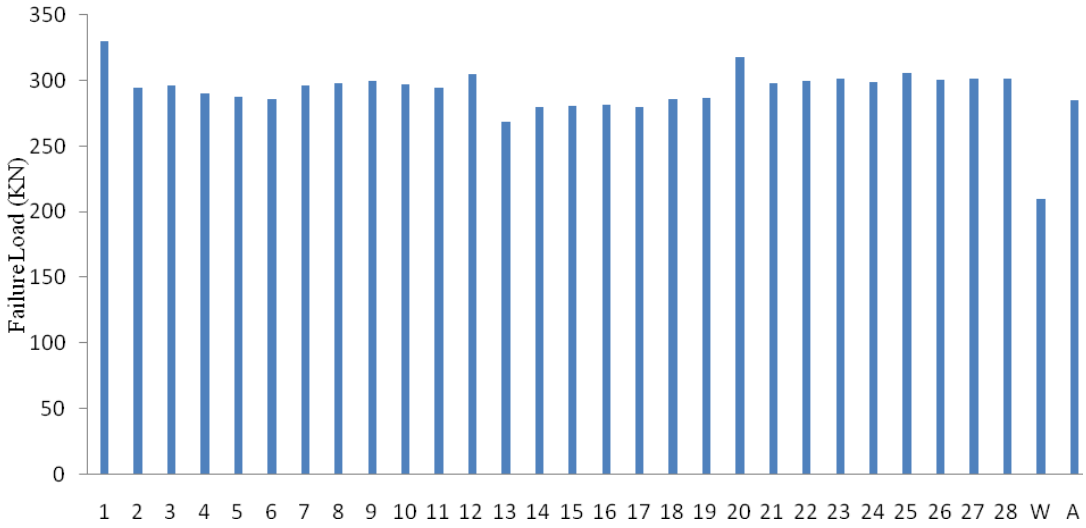

Fig. 8. Histogram of the compressive failure load for the reinforced concrete specimens immersed in sodium chloride medium. W=concrete specimen cured in water, A= concrete specimen cured in air. Numbers 1 to 28 represents the list of concrete specimen described previously in table 2.

NaCl medium having Weibull mean values of 307.296, 308.648 and 316.090 mV (CSE). The reliability of this predicted mean value stands at a probability of 59.4, 68.3 and 25.3% respectively. Though the synergetic admixtures did not show optimal performance, it clearly indicated that using the inhibitors in synergy in this particular case improved the inhibiting performance. Despite the fact that the first fifteen samples that exhibited optimal inhibiting qualities in table 4 are in the intermediate corrosion risk range according to ASTM C 876, yet their inhibiting performances was still better than that of the control samples in the NaCl and sulphuric acid medium.

Moreover, by examining table 4 and figure 6, the predicted Weibull mean values can be used to clearly identify specimens 1 to 32 and 34 to 40 as exhibiting positive and negative inhibiting qualities respectively when compared to the control sample in the NaCl medium (specimen 33). However, samples 34 to 40 and 42 to 56 exhibited positive and negative inhibiting qualities respectively when compared to the control in sulphuric acid medium.

Compressive strengths of concrete test sample

Compressive fracture load data evaluation for concrete steel rebar samples immersed in NaCl and H_2SO_4 medium are presented in figures 7 and 8 respectively. The strengths of all reinforced concrete specimens used in the experiments and partially immersed in H_2SO_4 and NaCl media were higher than those of the specimen cured in water for two weeks. This indicates that the admixed inhibitor had no adverse effect on the concrete samples used. The reason for the higher compressive strength in the admixed samples than in the sample cured in water could probably be due to the consolidation effect of the inhibitors on the concrete because of the chemical reactions. The exposure of the concrete samples partially to the air and the media might also have led to the dual hardening mechanism linked to the samples.

After examining the compressive strength values obtained for the samples immersed in the H_2SO_4 and NaCl media it was discovered that no precise trend was established. Increasing inhibitor concentration did not lead to increase in compressive strength values and vice-versa when compared to the concrete specimens cured in air. However, in the H_2SO_4 medium specimens 1, 2, 3, 4, 5, 6, 7, 8, 10, 11, 12, 13, 14, 15, 16, 17, 18, 19, 21, 23, 25, 26 and 27 (as depicted in Table 2) gave a loss in compressive strength while specimen 9, 20, 22, 24 and 28 gave an increase when compared to the specimen cured in air. On the other hand, in the NaCl medium specimens 13, 14, 15, 16 and 17 (as depicted in Table 2) showed losses in compressive strength, whereas specimens 1, 2, 3, 4, 5, 6, 7, 8, 9, 10, 11, 12, 18, 19, 20, 21, 22, 23, 24, 25, 26, 27 and 28 was observed to show increases in compressive strength when compared to the sample cured in air. The result of the compressive strength test also indicated that more samples showed losses in compressive strength in the H_2SO_4 medium than the NaCl medium indicating that the sulphate ions in the sulphuric acid medium had a deleterious effect on the concrete sample. Therefore, the inhibitor admixtures that resulted in an increase in the compressive strength of the concrete samples could become useful formulations in concrete block making for construction in the various media.

CONCLUSION

The effect of three inhibitors, namely potassium dichromate, potassium chromate and sodium nitrite on concrete steel rebar corrosion, individually and synergistically in saline and sulphate media using the OCP technique was investigated in this study. The subsequent fluctuating corrosion potential readings were statistically evaluated using the Weibull probability distribution. The study also determined the compressive strength of concrete test samples in order to ascertain the effect of the inhibitor on the compressive strength of the samples. The experimental results showed potassium chromate (0.15M) as having the best overall and individual performance in its inhibiting ability in the H_2SO_4 medium. Furthermore, Weibull distribution has modeled statistical-based performance evaluation of three inhibitors (individually and synergistically) on concrete steel rebar corrosion. Forty six of the samples were well fitted based on K–S goodness of fit test, while ten had outliers. Rebar concrete samples admixed with 0.15M potassium chromate inhibitor with Weibull ν = -282.882 mV (CSE) at a probability of 69.1% is predicted as exhibiting optimum inhibiting quality in H_2SO_4 medium, while 0.68M sodium nitrite admixture with Weibull ν = -307.296 mV (CSE) and probability of 59.4% was pr`edicted as showing the lowest probability of corrosion risk in NaCl medium. Also, the best synergistic performance was shown by sample admixed with 0.06M $K_2Cr_2O_7$, 0.15M K_2CrO_4 and 0.27M $NaNO_2$ partially immersed in the NaCl medium with Weibull ν = -308.648 mV (CSE) and probability of 68.3%. Thus, Weibull mean values of corrosion potential obtained for all samples made the interpretation of the data using ASTM C 876 achievable despite the fluctuations. The compressive strength of concrete sample admixed with 0.03M $K_2Cr_2O_7$ and 0.10M K_2CrO_4 (specimen 20 in Table 2) was the highest amongst samples admixed with inhibitor in both the sulfuric acid (306KN) and NaCl media (318KN). However, the control sample had the highest overall compressive strength value of 330KN when it was partially immersed in the NaCl medium. Therefore, from the results potassium chromate with concentration of 0.15 M is suggested as an inhibitor for concrete structures in sulphate environment, while 0.68 M sodium nitrite is recommended for concrete structures in NaCl medium, since they both showed highest resistance to corrosion in their respective medium. The performance of concrete sample admixed with the synergistic combination of 0.03M $K_2Cr_2O_7$, 0.10M K_2CrO_4 in NaCl medium is also quite impressive because apart from ranking number four on table 4 it ranked number one in compressive strength value amongst samples admixed with inhibitors. Consequently, it is also suggested as a construction formulation for concrete infrastructure.

REFERENCES

Bertolini, L., Elsener, B., Pedeferri, P. and Polder, RP. 2004. Corrosion of Steel in Concrete: Prevention, Diagnosis, Repair. WILEY-VCH Verlag GmbH & Co, Weinheim.

Hewayde, E., Nehdi, ML., Allouche, E. and Nakhla, G. 2007. Using concrete admixtures for sulphuric acid resistance. Proceedings of the Institution of Civil Engineers, Construction Materials. 160:25-35.

Liu, Y. 1996. Modeling the Time to Corrosion Cracking of the Cover Concrete in Chloride Contaminated Reinforced Concrete Structures. Ph.D thesis, Virginia Polytechnic Institute and State University, Blacksburg, Virginia, USA.

Loto, CA., Omotosho, OA. and Popoola, API. 2011. Inhibition effect of potassium dichromate on the corrosion protection of mild steel reinforcement in concrete. Int. Journal of Physical Sciences. 6 (9):2275-2284.

Nuclear Energy Agency/Committee on the Safety of Nuclear Installations (NEA/CSNI). 2002. Electrochemical techniques to detect corrosion in concrete structures in nuclear installations. Organisation for Economic Co-operation and Development (OECD). [Technical note].

Omotosho, OA. 2011. Assessing the Performance of Potassium Dichromate and Aniline on Concrete Steel Rebar Deterioration in Marine and Microbial Media. Research Journal of Applied Science. 6(3):143-149.

Omotosho, OA., Loto, CA., Ajayi, OO. and Okeniyi, JO. 2011. Aniline effect on concrete steel rebar degradation in saline and sulfate media. Agricultural Engineering International: The CIGR E journal. 13(2): Inpress

Omotosho, OA., Okeniyi, JO. and Ajayi, OO. 2010. Performance evaluation of potassium dichromate and potassium chromate inhibitors on concrete steel rebar corrosion. J Fail. Anal. and Preven.10 (5):408-415.

Parande, AK., Ramsamy, PL., Ethirajan, S., Rao, CRK. and Palanisamy, N. 2006. Deterioration of reinforced concrete in sewer environments. Proceedings of the Institution of Civil Engineers, Municipal Engineer. (159):11-20.

Richard, RL. 2002. Leading the Way in Concrete Repair and Protection Technology. Concrete Repair Association, Costa Rica. 1.

Schiegg, Y., Hunkeler F. and Ungricht, H. 2000. The Effectiveness of Corrosion Inhibitors - a Field Study. 16th Congress of IABSE Paper 234, Lucerne.

Smith, JL. and Virmani, YP. 2000. Materials and Methods for Corrosion Control of Reinforced and Prestressed Concrete Structures in New Construction. US Department of Transportation – Federal Highway Administration. Publication No. 00- 081.

Vollertsen, J., Nielsen, AH., Jensen, HS., Wium-Andersen, T. and Hvitved- Jacobsen, T. 2008. Corrosion of concrete sewers – The kinetics of hydrogen sulfide oxidation. Science of the Total Environment. (394):162-170.

Received: August 30, 2011: Accepted: Jan 7, 2012

SENRA Academic Publishers, Burnaby, British Columbia
Vol. 6, No. 1, pp. 1897-1900, Feb 2012
Online ISSN: 1920-3853; Print ISSN: 1715-9997

Canadian Journal of pure&applied sciences

Short Communication

CONFORMAL MAPPING TECHNIQUE FOR STUDYING FLUID FLOW IN CONTRACTION GEOMETRY

Mohamed M Allan
Department of Mathematics, Faculty of Science, Zagazig University, Zagazig, Egypt

ABSTRACT

In this paper, fluid flow over contraction geometry with a moving lower edge is studied by using conformal mapping techniques. Using elliptic integral is presented. The resulting streamlines are very much convenient and acceptable.

2000 AMS: Subject classification 65M12**,** 65M50, 76-08

Keywords: Conformal mapping, elliptic integral, streamlines, lower edge.

INTRODUCTION

In many engineering applications, lubrication, channel flows, pipe flows etc, the contraction appears frequently, which makes it necessary to study thoroughly the distribution of the streamlines and its values along the geometry of the flow with different contraction ratios. In this paper we restrict ourselves to domains which can be broken up into a union of smi-infinit rectangles. In particular we consider the contraction geometry which is an infinite channel whose diameter changes abruptly. In this paper we used the conformal mapping for studying the flow of a fluid in contraction geometry by computing its streamlines through transformed it to a flow on rectangle, (Ismail and Allan, 1995). This transformations are determined by using Schwarz-Christoffel (S-C) transformation which its numerical computations have been carried out by different methods in recent years. For example, the conformal mapping of unit disk onto a prescribed polygon has been studied successfully by Davis (1979). The mapping from a straight channel to a channel of arbitrary shape and periodic channel has been investigated by Floryan (1985). We define a Laplace's equation with mixed boundary conditions on contraction geometry and transform the whole problem onto a definite rectangle by means of the upper half plane .we use the fact that: if the fluid is following Laplace's equation, then under (S-C) transformation its form is unaltered. But if the flow is obeying Poisson's equation, the change is only in the source function (Dorr, 1970).

Schwarz-Christoffel transformation.
Consider the Schwarz-Christoffel integral

$$z=c\int_0^t (t-a_1)^{\alpha_1-1}(t-a_2)^{\alpha_2-1}\ldots(t-a_{N-1})^{\alpha_{N-1}-1}\,dt+c_1 \quad (1)$$

$$=c\int_0^t \prod_{j=1}^{N-1}(t-a_j)^{\alpha_j-1}\,dt+c_1 \quad (2)$$

which maps the upper half of the t-plane to interior of open polygon in the z-plane. There are a total of $2N+2$ parameters

$\alpha_1,\alpha_2,\ldots,\alpha_N$, $a_1,a_2,\ldots,a_N$, c and c_1 where $a_1,a_2,\ldots,a_N$ are points on the real axis whose images are to be vertices of the polygon and the inequality relations:

$$a_1 < a_2 < \ldots < a_{N-1} < a_N \quad (3)$$

are taken as the constraints of the system. The parameters $\alpha_1\pi$, $\alpha_2\pi,\ldots,\alpha_N\pi$ denote interior angles of the polygon with N vertices such that

$$\alpha_1\pi + \alpha_2\pi + \ldots + \alpha_N\pi = (N-2)\pi \quad (4)$$

It is noted that the Nth parameters α_N and a_N don't appear explicity in the integral since the last one of the vertices of the polygonal region is mapped to a point at infinity on the real axis of the ζ-plane. Vertices of the polygon on the z-plane and these corresponding mapping points along the real axis on the ζ-plane satisfy the relation

*Corresponding author email: m_m_allan@hotmail.com

$$z_k = c\int_0^{a_k}\prod_{j=1}^{N-1}(t-a_j)^{\alpha_j-1}dt + c_1, k = 1,2,...,N \qquad (5)$$

Mathematical formulation of the problem

The problem mathematically amounts to the solution of Laplace's equation $\nabla^2\psi = 0$ with mixed boundary conditions as given in figure 1 below

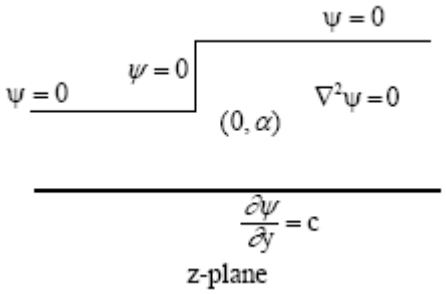

Fig. 1. Contraction geometry and boundary conditions.

where ψ represent the stream function of the fluid that is moving from right to left through some contraction of specified width. We here assume that the fluid is irrotational non-viscous, bearing in mind that the same method of solution which be described here. Below can be used also in the case of rotational non-viscous flow.

Transformation from the upper half plane to the contraction geometry

The contraction geometry, Ω of figure 1 can be mapped conformally onto the rectangle , Ω'' defined by

$$\Omega'' = \{(u,v): -a < u < a,\ 0 < v < b\}.$$

This transformation is performed in two stages:

1- Let $z = x + iy$ (contraction geometry) defined on the z-plane and $t = \xi + i\eta$ (upper-half), then Ω can be mapped conformally onto the upper half plane by means of the transformation

$$\frac{dz}{dt} = \frac{-1}{\pi t}\left[\frac{t-1}{t-\left(\frac{1}{\alpha^2}\right)}\right]^{\frac{1}{2}} \qquad (6)$$

where α is contraction ratio. If we write $w = u + iv$ then Ω' is mapped conformally onto Ω'' y means of the transformation

$$\frac{dt}{dw} = -\pi t \qquad (7)$$

2-Given a point w w in the region Ω'' it is a simple task to write down the point in z in Ω to which it corresponds

$$z = i - \frac{1}{\pi}\left\{\log\left[\frac{\sqrt{w-1}+\sqrt{w-\beta}}{\sqrt{w-1}-\sqrt{w-\beta}}\right] - \alpha\log\left[\frac{\sqrt{w-1}+\alpha\sqrt{w-\beta}}{\sqrt{w-1}-\alpha\sqrt{w-\beta}}\right]\right\} \qquad (8)$$

where $t = -\exp(-\pi w)$ and $\beta = \frac{1}{\alpha^2}$.

One cannot, in a straightforward manner, write down the analytic solution in Ω. One would need to find analytically $w(z)$ given above. What we have done is to take a point w in Ω'' n which the analytic solution is known, then find z in contraction.

Finding the points of mapping from the upper half-plane to rectangle.

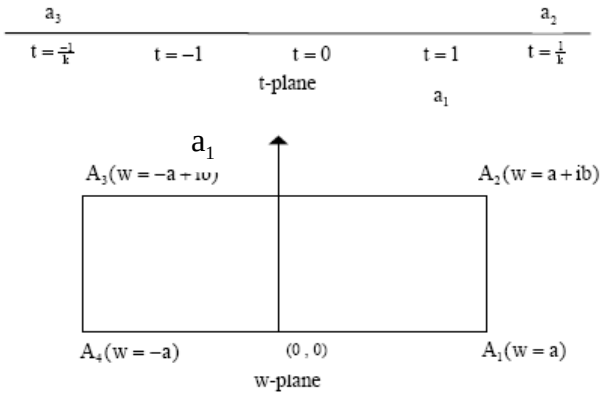

Fig. 2. Mapping from upper plane to rectangle.

By using (S-C) transformation, the function which defines a conformal mapping of the upper half plane onto a given rectangle may be represented in the form

$$w = c\int_{t_0}^{t}(t-1)^{\frac{1}{2}-1}(t-\frac{1}{k})^{\frac{1}{2}-1}(t+\frac{1}{k}1)^{\frac{1}{2}-1}(t+1)^{\frac{1}{2}-1}dt + c_1 \qquad (9)$$

$$w = c\int_{t_0}^{t}\frac{dt}{\sqrt{(1-t^2)(1-k^2t^2)}} + c_1 \qquad (10)$$

by using the correspondence points, we get $c_1 = 0$ and

$$a = c\int_0^1\frac{dt}{\sqrt{(1-t^2)(1-k^2t^2)}}, 0 < k < 1 \qquad (11)$$

The integral on the right is the so-called complete elliptic integral of the first kind which does not have a closed form. In order to be able to perform the mapping, we have to find the value of the above integral at each chosen point of the upper half-plane. The above integral written in the form

$$F(k,\phi)=\int_0^{\phi}\frac{d\phi}{\sqrt{(1-k^2\sin^2\phi)}} \tag{12}$$

By using Landen's transformation,

$$\tan\phi=\frac{\sin 2\phi_1}{k+\cos 2\phi_1} \quad or\ k\sin\phi=\sin(2\phi_1-\phi) \tag{13}$$

we get

$$F(k,\phi)=\int_0^{\phi}\frac{d\phi}{\sqrt{(1-k^2\sin^2\phi)}}=\frac{2}{1+k}\int_0^{\phi_1}\frac{d\phi_1}{\sqrt{1-k_1^2\sin^2\phi_1}}\ where, k_1=\frac{2\sqrt{k}}{1+k}. \tag{14}$$

This can be written $\mathrm{F}(\mathrm{k},\phi)=\frac{2}{1+\mathrm{k}}\mathrm{F}(\mathrm{k}_1,\phi_1)$

It is seen that $\mathrm{k}<\mathrm{k}_1<1$. By, successive application of Landen's transformation a sequence of moduli $\mathrm{k}_n, \mathrm{n}=1,2,3,\ldots$ is obtained such that $\mathrm{k}<\mathrm{k}_1<\mathrm{k}_2\ldots<1$ and we can prove that $\lim_{\mathrm{n}\to\infty}\mathrm{K}_\mathrm{n}=1.$ From this it follows that

$$F(k,\phi)=\sqrt{\frac{k_1k_2k_3\ldots}{K}}\int_0^{\phi}\frac{d\theta}{\sqrt{(1-\sin^2\theta)}}=\sqrt{\frac{k_1k_2k_3\ldots}{K}}-\ln\left(\tan\left(\frac{\pi}{4}+\frac{\phi}{2}\right)\right) \tag{15}$$

where

$$\mathrm{K}_1=\frac{2\sqrt{\mathrm{k}}}{1+\mathrm{k}},\quad \mathrm{K}_2=\frac{2\sqrt{\mathrm{k}_1}}{1+\mathrm{k}_1},\quad \mathrm{K}_3=\frac{2\sqrt{\mathrm{k}_2}}{1+\mathrm{k}2}, \tag{16}$$

$$\text{and}\quad \phi=\lim_{\mathrm{n}\to\infty}\phi_\mathrm{n}$$

By using this result, $F(k,\phi)$ can be computed.

Finding the values of ψ over the rectangle

This is equivalent to solving Laplace's equation with mixed boundary conditions as in figure 3.

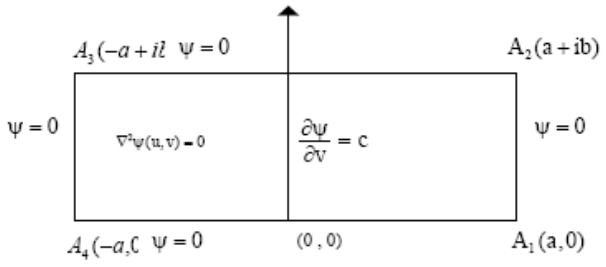

Fig. 3. Rectangle geometry and boundary conditions.

The final solution of this problem on the above rectangle given by

$$\psi(u,v)=\sum_{n=odd}\frac{8ac}{n^2\pi^2\cosh\left(\frac{n\pi b}{2a}\right)}\sin\frac{n\pi(u+a)}{2a}\sinh\frac{n\pi v}{2a} \tag{17}$$

RESULTS AND DISCUSSION

We have designed a program written in FORTRAN to calculate the streamlines of the solution ψ of the entire problem at every points of a rectangle. The results show that the method described in this paper gives accurate results in the whole domain of contraction geometry. The streamlines of Laplace's equation on the rectangle is given in figure 4 and the solution over the contraction geometry shown in figures 5,6 at different contraction ratios which provides the streamlines of some contraction with a base that is moving with a constant velocity. This results is very acceptable compared to those obtained by Phillips and Davies **(**1988) and Chuang and Hsiung **(**1993).

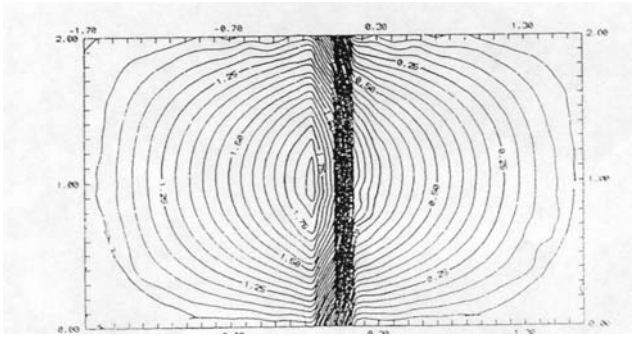

Fig. 4. Contours of ψ in the rectangle.

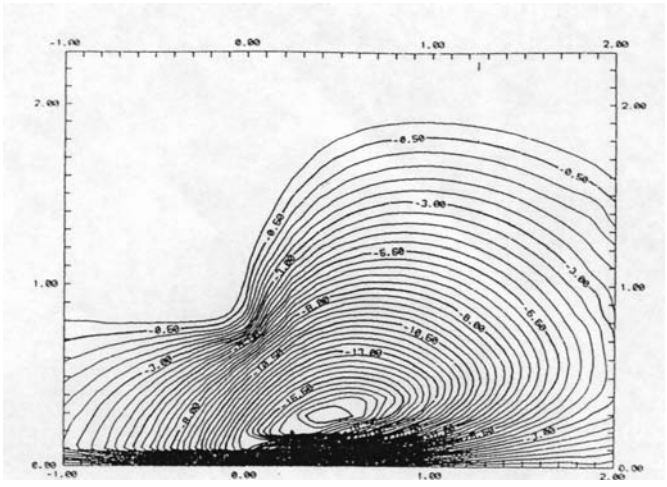

Fig. 5. Contours of ψ in the contraction with $\alpha=.5$

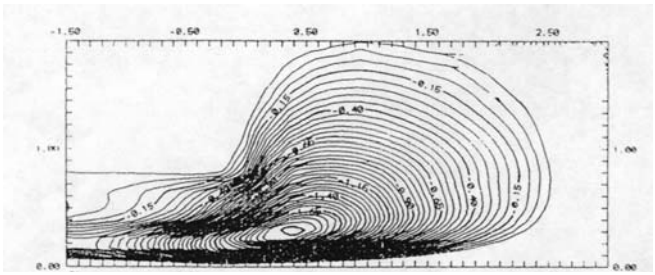

Fig. 6. Contours of ψ in the contraction with $\alpha = .25$

REFERENCES

Chuang, JM. and Hsiung, CC. 1993. Numerical computation of schwartz-christoffel transformation for simply connected unbounded domain." Computer method in App. Mech. and Eng. J. 105:93-109.

Davis, RT. 1979. Numerical method for coordinate generation based on the Schwarz-Christoffel transformation. 4th computational fluid dynamics Conference. AIAA paper. No. 19-1463.

Dorr, FW. 1970. The Direct solution of the discrete Poisson equation on a rectangle. SIAM Rev. 12:248-263.

Floryan, JM. 1985. Conformal-Mapping-Based coordinate Generation Method for Channel Flows. Comput. Phys. 58:229-245.

Ismail, IA. and Allan, MM**.** 1995. A Conformal Mapping Method for Studying the fluid Flow in L-geometry". [Accepted for publication in AL-AZHAR Engineering Fourth Int. Conf. (AEIC'95-EGYPT)].

Phillips, TN. and Davies, AR. 1988. On Semi-infinite Spectral elements for Poisson problems with re-entrant boundary singularities. comp. and appl. Math. 21:173-188.

Received: June 7, 2011; Revised: Dec 4, 2011; Accepted: Dec 5, 2011

SENRA Academic Publishers, Burnaby, British Columbia
Vol. 6, No. 1, pp. 1901-1904, Feb 2012
Online ISSN: 1920-3853; Print ISSN: 1715-9997

Canadian Journal of pure&applied sciences

Short Communication

A NEW PVC-GLASS MATERIAL TO BE USED IN MULTIPURPOSE APPLICATIONS

Safwan M. Al-Qawabah
Department of Mechanical Engineering, Tafila Technical University
PO Box: 13720, Amman 11942

ABSTRACT

In the present study, a mixture of two waste materials glass and PVC were used with three different percentages (namely: 30% glass 70% PVC, 50% glass 50% PVC, and 70% glass 30% PVC), hardness, macrostructure, density, and thermal conductivity were investigated. Based on results, it was revealed that as the glass content increased, there is an enhancement in the hardness, where the thermal conductivity was decreased as the glass percentage increased this lead to use the new material as an insulator material.

Keywords: PVC, glass, thermal conductivity, microstructure, microhardness.

INTRODUCTION

A composite material is basically a combination of two or more materials, each of which retains it own distinctive properties. Composite structures, such as fibre-reinforced plastic laminates and sandwich panels made with laminate skins and light-weight cores, are widely used in the aerospace, marine, aeronautical, automotive and recreational industries (Imielinska and Guillaumat, 2004; Li and Weitsman, 2004; Bull and Edgren, 2004). Their superior bending stiffness, low weight, excellent thermal insulation, acoustic damping, ease of machining, corrosion-resistance and stability offers advantages over traditional metallic materials. However, shortcomings of fibre-reinforced plastics are their low translaminar (through thickness) mechanical properties and susceptibility to failure by impact loading – by hard objects or wave slamming. Wood fibres were initially used for reducing and disposing of large amounts of natural fibre waste materials and for cost reduction. But, they are now preferably used as reinforcing materials in polymers, and offer low cost and low density products (Imielińska *et al*., 2008).

Beirnes and Burns (1986), Scandola *et al*. (1982), Fried and Lai (1982), Mauritz (1990) and Ceccorulli *et al*. (1987) reported that the improvement of mechanical properties for structural engineering applications can be obtained if the wood fibers are properly blended with the polymers.

The most significant monomeric plasticizer family is the phthalates, which constitute about 70% of the plasticizers used. There have been many studies on the glass transition temperature of PVC phthalate mixtures. The objective in this study is to produce a new composite material from waste materials, then investigate its hardness, strength, and its thermal conductivity.

MATERIALS AND METHODS

Materials

A set of materials was used throughout this study namely; waste glass, waste PVC.

1- Waste glass is shown in figure 1, thickness of glass that was used 4 mm (broken cups, waste glass bottles).

Fig. 1. Waste glass.

2- Waste plastic (PVC)

The plastic waste is shown in figure 2.

Corresponding author email: safwan_q@yahoo.com

Fig. 2. Waste plastic bottle.

Equipment

The following set of equipment was used in this study:

1- Electric furnace carbolite 1450 ˚C
3- Electronic balance
4- Microscope type NIKON 108.
5- Digital micro hardness tester

Experimental procedures

The material was prepared through these steps:

1. Crashing the glass to small pieces as shown in figure 3.

Fig. 3. Crashed glass.

2. Cutting PVC bottles to small pieces.
3. Mixing PVC pieces with glass pieces at percentage of mixing (30%: glass, 70% PVC) 5 grams glass with 15 gram PVC.
4. Heating the mixture at temperature 1400˚C for three minutes in electric furnace.
5. Mixture will melted as shown in figure 4.

Fig. 4. Mixture of melted composites.

6. Filling the mixture of glass and PVC in special die.
7. Repeating this procedure with different composition

Three specimens were performed with different glass composition as shown table1.

Table1. The composite composition

Specimen #	% Composition
1	30 glass + 70 PVC
2	50 glass + 50 PVC
3	70 glass + 30 PVC

The produced three composites are shown in figure 5.

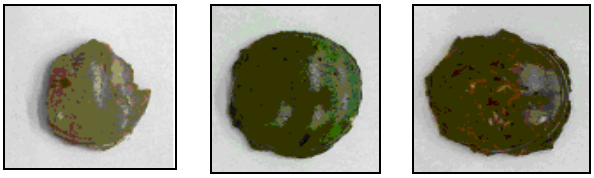

1 2 3

Fig. 5. The produced composites percentages (1-30% glass, 2-50% glass, 3-70% glass).

RESULTS AND DISCUSSION

The effect of different glass percentages on the hardness of new composite materials

These specimens were test by using brinell hardness tester in order to obtain the hardness of each specimen as shown in Table 2, by comparing these results with glass and PVC hardness which are 1550 HB, 12 HP respectively (CES software), there is a large different between them, where the value of hardness was reduced under glass hardness and over PVC.

Table 2. Hardness of the three composites.

% Composition	Hardness (HB)
30 % glass + 70 % PVC	52
50 % glass + 50 % PVC	73
70 % glass + 30 % PVC	97

Hardness values give an indication about the magnitude of yield strength by using CES software Tables the yield strength for each specimen (approximately) is shown in Table 3.

Table 3. Yield strength of the three composites.

% Composition	Yield strength MPa
30 glass + 70 PVC	125
50 glass + 50 PVC	200
70 glass + 30 PVC	250

The effect of different glass percentages on the compression modulus of new composite materials

It can be seen from figure 6 the compression modulus increased as the glass content was increased. The maximum enhancement was 62.5% which achieved at 70 % glass addition. This can be attributed to the general increase in the mechanical behavior as the glass increases, however the glass have a high hardness values compared to PVC materials.

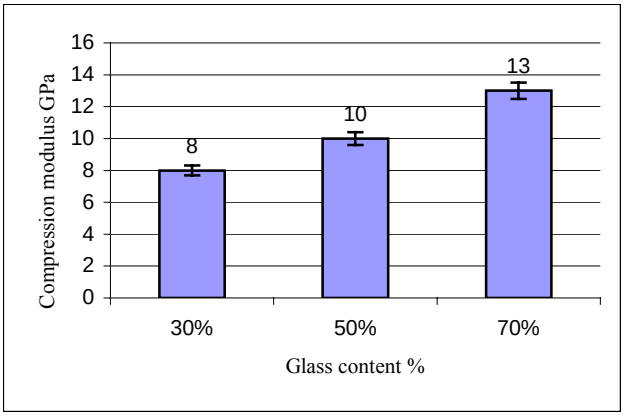

Fig. 6. The compression modulus of the new glass polymer composite.

The effect of different glass percentages on the microstructure of new composite materials

The photomicroscan were taken for the three percentages as shown in figure 7.

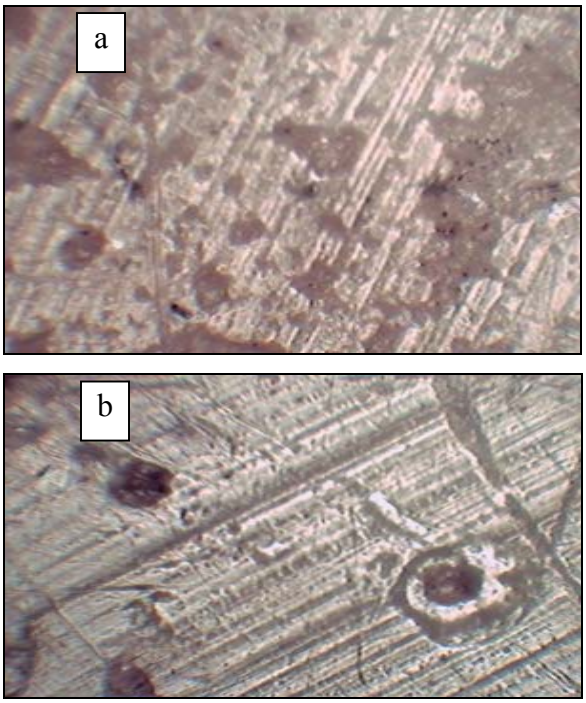

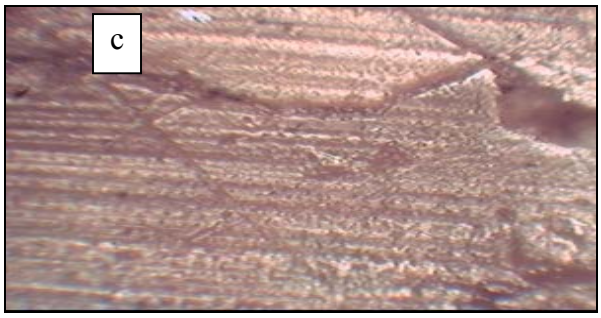

Fig.7. Photomicroscan of **a**) 30% glass **b**) 50% glass and **c**) 70% glass additions at 200x.

The effect of different glass percentages on the thermal conductivity of new composite materials

Thermal conductivity was obtained based on simple experiment as following:

Thermal conductivity can be measured referring to heat transfer equations which are:

$Q = k * \Delta T / \Delta X$

Where,

Q: Amount of heat

Where, K: thermal conductivity, ΔT: difference in temperature, and ΔX: Material thicknesses, the difference in temperature at each specimen are shown in table.4.

Table 4. The difference in temperature for the composite materials.

% Composition	Difference in temperature (˚C)
30 glass + 70 PVC	31
50 glass + 50 PVC	28
70 glass + 30 PVC	24

However,

$Q = m * cp * \Delta T$

m: mass of heated water which is 0.2 kg

cp: water specific heat which is 1.004 kj / kg

$\Delta T = 32$

So

$Q = 6.4256$ W / m^2

The magnitude of thermal conductivity at each spacemen are shown in Table 5

Table 5. Thermal conductivity of three composite

% Composition	Thermal conductivity ($w/(m^2.k)$)
30 glass + 70 PVC	0.001004
50 glass + 50 PVC	0.001147
70 glass + 30 PVC	0.00133

Where the thermal conductivity of glass and PVC are 1.75 , 0.2 respectively (CES software), all values in Table are less than these values , which means this polymer can be used as insulter material with low thermal conductivity.

The effect of different glass percentages on the density of new composite materials

Density of each specimen can be calculated as following:
Specimen density = glass percentage * glass density + PVC percentage * PVC density
Where:
Glass density: 2510 kg/m^3
Specimen 1 density = 0.30 * 2510 + 0.7 * 1240
Specimen 1 density = 1621 kg/m^3
Specimen 2 density = 0.50 * 2510 + 0.5 * 1240
Specimen 2 density = 1875 kg/m^3
Specimen 3 density = 0.70 * 2510 + 0.3 * 1240
Specimen 3 density = 2129 kg/m^3
The Specimen's density increased as the glass content increased as shown in figure 8.

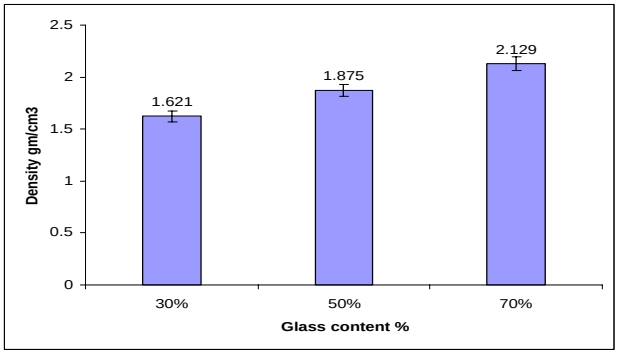

Fig. 8. The effect of glass addition on the density of new composite materials.

CONCLUSION

Based on present study, it can be conclude that the hardness and the thermal conductivity were increased as the glass percentage increase, while yield stress and the density were increased as the glass percentage increased.

ACKNOWLEDGEMENT

This work has been supported by IFRAD Company which is acknowledged. The efforts of the technical staff at IFRAD Company are highly appreciated. Special thanks to Eng. Mahmood Al-Rababah

REFERENCES

Beirnes, KJ. and Burns, CM. 1986. Thermal analysis of the glass transition of plasticized poly (vinyl chloride). J. Appl. Polym. Sci. 31:2561-557.

Bull, PH. and Edgren, F. 2004. Compressive strength after impact of CFRP foam core sandwich panels in marine applications. Compos Part B. 35:535-541.

Ceccorulli, G., Pizzoli, M. and Scandola, M. 1987. Polymer Effect of a low MW plasti- cizer on the thermal and viscoelastic properties of miscible blends of bacter-ial poly(3-hydroxybutyrate) with cellulose acetate butyrate. Macromolecules. 28:2077-084.

Fried, JR. and Lai, SY. 1982. Experimental assessment of the thermodynamic theory of the ompositional variation of Tg. J. Appl. Polym. Sci . 27:2869-883.

Imielinska, K. and Guillaumat, L. 2004. The effect of water immersion ageing on low-velocity impact behaviour of woven aramid–glass fibre/epoxy composites. Compos Sci. Technol. 64:2271-2278.

Imielińska, K., Guillaumat, L., Wojtyra, R. and Castaings, M. 2008. Effects of manufacturing and face/core bonding on impact damage in glass/polyester–PVC foam core sandwich panels. Composites Part B: Engineering. 39(6):1034-1041.

Li X, Weitsman J. 2004. Sea-water effects on foam-cored composite sandwich lay-ups. Compos Part B. 35:451-59.

Mauritz, KA., Storey, RF. and George, SE. 1990. A general free volume- based theory for the diffusion of large molecules in amorphous polymers above Tg. 1 Application to di-n-alkyl phthalates in PVC. Macromolecules. 23:441-50.

Mauritz, KA., Storey, RF. and Wilson, BS. 1990. Efficiency of plasticization of PVC by higher-order di-alkyl phthalates and survey of mathematical models for prediction of polymer/diluent blend*Tg*'s. J. Vinyl Technol. 12(3):165-73.

Scandola, M., Ceccorulli, G., Pizzoli, M. and Pezzin G.1982. Density of Elastin-Water System. In Water in Polymers. Polym Bull. 653-60.

Accepted on Dec 29, 2011